Application of a Human Primary Epithelial-Fibroblast co-culture system to study Fibrosis

---

Jaineeta Richardson, BSc. and MSc.

Division of Respiratory Medicine

Thesis submitted to the University of Nottingham for the degree of Doctor of Philosophy

September 2017

For my loving and supportive husband Edward and my two beautiful children Dhani and Jaya.

Abstract

Idiopathic Pulmonary Fibrosis (IPF) is a chronic, progressive lung disease which manifests over several years with an unknown aetiology. The current paradigm suggests that reoccurring injury to the lungs results in damage to the alveolar epithelial cells, progressing to the destruction of the alveolar-capillary basement membrane. Although little is known about how the alveolar epithelium is injured, it is thought that repeated epithelial injury releases a wide variety of soluble factors which can initiate a series of events such as migration, differentiation and activation of mesenchymal cells i.e. fibroblasts into myofibroblasts. Myofibroblasts are proliferative, protected from apoptosis and produce extra-cellular matrix (ECM) in IPF. In turn it is likely these mesenchymal cells modify epithelial behaviour, producing a pro-fibrotic environment. Dysregulation of the normal processes in the lung results in abnormal communication between epithelial and mesenchymal cells which prevents resolution of the wound-repair response leading to tissue fibrosis and eventual organ failure.

In this project a 3D co-culture model was designed to investigate the interactions between epithelial cells and fibroblasts. This type of method enabled a non-contact approach between epithelial cells and fibroblasts in collagen mimicking the *in vivo* micro-environment. In the model, repetitive epithelial injury resulted in increased fibroblast proliferation, ECM synthesis and decreased apoptosis, similar to the biology of IPF. Affymetrix analysis revealed up regulation of fibroblast genes involved in cell cycle, proliferation, differentiation and in regulation of transcription in response to epithelial injury. Potential mediators of epithelial-fibroblast cross-talk were identified and revealed endothelin-1 to be involved in increased fibroblast proliferation and ECM gene expression. Treatment with bosentan against endothelin receptors resulted in the inhibition, in which there was reduced proliferation and matrix synthesis in the co-culture fibroblasts. Using the 3D co-culture model revealed that injury to epithelial cells can influence the response to fibroblasts *in vitro.* This then can be used with further antagonists, to study various mediators and block different pathways. We suggest that this model can be reliably used as a tool to investigate the interactions between various cell types.

Abstracts and Oral Communications

Richardson, J., Clements, D. and Johnson, S.R (2011). "Development of a repetitive epithelial injury co-culture model in Idiopathic Pulmonary Fibrosis". Poster presentation: GSK, CRAFT annual meeting Stevenage, UK 2011.

Richardson, J., Clements, D., *Blanchard, A.* and Johnson, S.R (2012). "Validation of an *in-vitro* human primary epithelial-mesenchymal co-culture system to study fibrosis. Poster presentation: GSK, CRAFT annual meeting Stevenage, UK 2012.

Richardson, J., Clements, D., Blanchard, A. and Johnson, S.R (2013). "Validation of an *in-vitro* human primary epithelial-mesenchymal co-culture system to study fibrosis. Poster presentation: American Thoracic Society (ATS) International Conference, Philadelphia, USA, 2013.

Richardson, J., Clements, D., Blanchard, A. and Johnson, S.R (2013). "Validation of an *in-vitro* human primary epithelial-mesenchymal co-culture system to study fibrosis. Oral communication: British Association for Lung Research, Summer Meeting, Nottingham, UK, 2013

Richardson, J., Clements, D., Blanchard, A. and Johnson, S.R (2013). "Validation of an *in-vitro* human primary epithelial-mesenchymal co-culture system to study fibrosis. Oral communication: Young investigator Meeting *(YIM),* Groningen, Holland, *2013*

Publications

Boorsma, C.E., Dekkers, B.G., van Dijk, E.M., Kumawat, K., **Richardson, J.**, Burgess, J.K. and Alice, J.E (2014). "Beyond TGFbeta — novel ways to target airway and parenchymal fibrosis". Pulm Pharmacol Ther 29:166–180.

Acknowledgements

I'd firstly like to thank Professor Simon Johnson for giving me the opportunity to start my research career and helping me to achieve a long-lived goal. I'm thankful for his support and guidance through-out this PhD. I am thankful to Dr. Debbie Clements for her constant support, teaching me to question, and for giving me the skills required for a career in research. I would like to thank Prof. Anna Grabowska for her guidance and advice.

I am enormously grateful to the University of Nottingham staff and students for technical assistance: Colin Nicholson assisting me with Bioanalyser, Vidya Navaratnam and Richard Hubbard for donating serum samples, Amanda Tatler, Suzanne Miller, Emily Hodge for locating IPF and normal lung tissue slides as well Andrea Greener for her amazing support for administration. I would like to thank, Dr William Coward, Dr Natasha Dovlatova, Jo Zuranska, Dr William Chang, Dr Mariel Slater, Dr Jenny Cane, Jamie Patel, Amy Root, Mohammad Algahtani, Jane and Gordon May, Julie Hawley, Helen Naylor, and Dr Shahideh Safavi for their support throughout the PhD years.

Thank you to all my friends you have supported me emotional and listening to me over the years; Shelley, Kristy, Josie, Dawn, Faye, Carmen, Emma L, Charlotte L, Melissa, Perveen, Lida, Deborah, Cath R, Sasha, Nicola, Jo B, Anna W, Shivani and Michelle C.

I am especially indebted to Jeanne Ransom the manager at Wollaton Village Nursery as well as her remarkable staff including Sarah, Sara, Emma, Rachel for being so supportive and understanding with childcare.

The invaluable support from my family, mum and dad, my brothers Lalit and Josh, my in-laws Joan and Malcolm and my sister in law Jennifer, whom have stood by my side and been so understanding. My two amazing children Dhani and Jaya, whom have been my inspiration and strength to continue this PhD. Also, finally thank you to my wonderful husband Edward, you whom I couldn't have done this PhD without. Over the years you have been just so brilliant and supportive through this journey. Our journey. We did it!

Table of Contents

Chapter One 1

1.1 Pulmonary fibrosis and Idiopathic Pulmonary Fibrosis 2

1.1.1 Idiopathic Pulmonary Fibrosis 3

1.1.2 The Prevalence of Idiopathic Pulmonary Fibrosis 3

1.1.3 Epidemiology and Risk Factors 4

1.1.4 The Pathogenesis of IPF 4

1.2 Injury Response and Remodelling 5

1.2.1 Alveolar Epithelial Cells 7

1.2.2 Characteristics of Fibroblasts and Myofibroblasts 7

1.2.3 Extracellular Matrix 9

1.2.4 Apoptosis 10

1.3 Soluble Mediators involved in epithelial fibroblast interaction 14

1.3.1 Role of growth factors 15

1.3.3 Role of cytokines 18

1.3.4 Role of Alarmins 20

1.3.5 Role of MMPs 21

1.4 Epithelial-Mesenchymal 'Crosstalk' 24

1.4.1 Pro-fibrotic Role of Transforming Growth Factor - β 24

1.4.2 Notch Pathway 26

1.4.3 Sonic Hedgehog Pathway 27

1.4.4 WNT pathway 28

1.5 IPF models 28

1.5.1 In Vitro Models 28

1.5.2 Animal Models 29

1.6 Gene Expression 31

1.6.1 Microarray Analysis of Pulmonary Fibrosis 32

1.7 A novel therapeutic target in IPF 33

1.8 Approved oral therapies 34

1.9 Aims and Hypothesis 39

Chapter Two 40

2.1 Materials 41
2.1.2 Reagents/Chemicals 41
2.1.3 Antibodies 42
2.2 Methods: Cell Culture 43
2.2.1 Recovery of cryo-preserved Primary Human Cells 43
2.2.2 Harvesting of Primary Human Cells 45
2.2.3 Maintenance of Primary Human Cells 45
2.2.4 Determination of cell counts 45
2.2.5 Cryopreservation of cells 46
2.3 Optimising Primary Human cells 46
2.3.1 Optimising fibroblasts in 3 dimensional gels 46
2.3.2 Optimising Small Airway Epithelial Cell in Transwells® 47
2.3.3 CellTracker Probes 47
2.4 Co-culture of NHLFs and SAEs 48
2.4.1 Scratch wound Injury 49
2.4.2 Bleomycin administration on epithelial cells 49
2.4.3 Carbon Particles addition 49
2.4.4 Releasing the Cells from Collagen the Gel Environment 50
2.5 Low Grade Injuries on SAEs 50
2.5.1 Enzyme-Linked Immuno-Sorbent Assay (ELISA) 50
2.5.2 Zymography 52
2.6 Cell Proliferation 54
2.6.1 Immunostaining 54
2.6.2 Fluorescence Staining with DAPI 55
2.6.3 MTT Reduction Assay 55
2.7 Apoptosis and cell death 56
2.7.1 TUNEL 56
2.7.2 Western Blotting 57
2.8 Quantitative PCR 60
2.8.1 RNA Extraction 60
2.8.2 cDNA synthesis 61

2.8.3 SYBR green ® Real time Polymerase Chain Reaction 61
2.8.4 Analysis of PCR 64
2.9 Bioanalyser 64
2.9.1 Preparation of gel matrix 64
2.9.2 Cleaning the electrodes 64
2.9.3 Preparation of Gel-dye matrix 64
2.9.4 Loading chip with the gel matrix and RNA 6000 Nano Marker 65
2.9.5 Loading the RNA sample and the RNA 6000 ladder 65
2.9.6 Running the chip 65
2.9.7 Clean the electrodes 66
2.10 Slide preparation and Immunohistochemistry 66
2.10.1 Generation of tissue and tissue processing 66
2.10.2 Histology 66
2.11 Statistical Analysis 69
Chapter Three 70
3.1 General Introduction 71
3.2 Aim and Objectives 73
3.3 Methods 74
3.3.1 Co-culture of epithelial cells and fibroblasts cells in Transwells® 74
3.3.2 Low-Grade-injury on epithelial cells 74
3.3.3 Dual staining of fibroblasts with anti-Ki-67 and DAPI 74
3.3.4 Apoptosis 75
3.3.5 Quantitative analysis 75
3.3.6 Statistical Analysis 75
3.4 Results 76
3.4.1 Optimising primary human cells 76
3.4.2 Optimising cell number for normal human lung fibroblasts 76
3.4.3 Determining Proliferation of Fibroblasts in collagen gel 79
3.4.4 Cell Concentration of Small Airway Epithelial cells 82
3.4.5 Validation of Low Grade injury on Epithelial Cells 84
3.4.6 Effect of low grade injury on epithelial cells 84

3.4.7 The effect of epithelial injury on fibroblast proliferation..... 90

3.4.8 The effect of epithelial injury on extracellular matrix gene expression by fibroblasts. 95

3.4.9 The effect of epithelial injury on apoptosis of fibroblast cells..... 97

3.5 Discussion 105

3.6 Summary 113

Chapter Four 114

4.1 General Introduction 115

4.2 Aim and Objectives 117

4.3 Methods 118

4.3.1 Regulatory approvals for the serum samples 118

4.3.2 Study participants.....118

4.3.3 3D co-culture model.....120

4.3.4 MMP activity assay 120

4.3.5 Gelatin zymography 121

4.3.6 Quantitative analysis 121

4.3.7 Enzyme-Linked Immuno-Sorbent Assay (ELISA) 121

4.3.8 Statistical Analysis 121

4.4 Results: Expression of MMPs in 3D Co-Culture Model.....122

4.4.1 MMP-1 expression in 3D co-culture model 122

4.4.2 MMP-7 expression in 3D co-culture model 125

4.4.3 MMP-2 expression in 3D co- culture model 128

4.4.4 MMP-9 expression in the 3D co-culture model 130

4.4.5 Expression of MMP-3 and TIMP-1 in co-cultured fibroblast cells.....137

4.4.6 Expression of MMP-9 on IPF tissue 139

4.5 MMP-9 expression in IPF serum samples.....142

4.5.1 MMP-9 expression pro and active in serum samples 142

4.5.2 Total MMP-9 expression in serum samples 147

4.5.3 Lung function and MMP-9 expression in IPF serum samples.....149

4.6 Discussion 154

4.7 Summary 162

Chapter Five **163**

5.1 Introduction 164

5.2 Aims 165

5.3 Methods 166

5.3.1 RNA isolation of fibroblasts and epithelial cells 166

5.3.2 Agilent Bioanalysor Analysis 166

5.3.3 Microarray analysis of fibroblasts and epithelial cells using Affymetrix GeneChip Systems 167

5.3.5 Normalisation 168

5.3.6 Summarisation 170

5.3.6.3 Validating gene expression of microarray data by Quantitative RT-PCR 171

5.3.7 Statistical Analysis 172

5.4 Results 172

5.4.1 Array Studio Gene database 172

5.4.2 Principal Components Analysis 175

5.4.3 Hierarchical clustering and Differential signature expression 187

5.4.4 Pathways involved in epithelial cells and fibroblasts 189

5.4.5 Validation of house-keeping genes via Quantitative RT-PCR 194

5.4.6 Validation of the gene dataset 197

5.5 Discussion 200

5.6 Summary 204

Chapter Six **205**

6.1 Introduction 206

6.2 Aims 207

6.3 Methods 208

6.3.1 Selection of candidate genes from the gene dataset 208

6.3.2 Validation of selected microarray genes by Quantitative RT-PCR analysis. 208

6.3.3 Quantitative real-time PCR (Q-PCR) 212

6.3.4 Generation of tissue and tissue processing 212

6.3.5 Histology 212

6.3.6 Determining the expression of Endothelin-1 in the 3D co-culture model 213

6.3.7 Statistical Analysis 214

6.4 Results 215

6.4.1 Gene expression changes measured by using quantitative RT-PCR analysis..215

6.4.2 Immunohistochemistry of selected candidate genes 227

6.4.3 The validation of upstream mediators in the IFN pathway 234

6.4.4 The Effect of Endothelin-1 *in vitro* 238

6.4.4.3 To determine the expression of ECM genes with the addition of bosentan in co-culture model 245

6.5 Discussion 248

6.5.1 Selection of candidate genes from the microarray dataset 248

6.5.2 Pathway Analysis 250

6.5.3 The expression of IL-6 in the 3D co-culture model 251

6.5.4 The expression of Endothelin-1 in the 3D co-culture model 253

6.5.5 Effect of Bosentan on matrix gene expression 254

6.5.6 The role of IFN α/β, Endothelin-1 and BIRC5 in the 3D co-culture model 254

6.6 Summary 256

Chapter Seven 257

7.1 Discussion 258

7.1.1 The type of injuries used in the 3D co-culture model 260

7.1.2 The effect of epithelial cell injury on fibroblasts 262

7.1.3 Fibroblasts in response to epithelial cell injury 263

7.1.4 The expression of MMPs in the 3D Co-culture model.....264

7.1.5 Data analysis of DNA Microarray 271

7.1.6 Pathway analysis 273

7.1.7 The effect of Bosentan on Endothelin-1 in 3D co-culture model 278

7.1.8 Epithelial-fibroblast crosstalk in the 3D co-culture model 280

7.2 Recent understanding and advances of IPF 281

7.2.1 Current paradigm of IPF: 281

7.2.2 Underlying mechanisms: 281

7.2.3 IPF models to understand IPF mechanisms 284

7.3 Future work 288

7.4 Summary 290

Appendices..... 293

Appendix 1: Websites and On-line resources**..... 294**

Appendix 2: List of suppliers.....295

Appendix 3: Buffer and Reagent Information 297

Appendix 4: KiCqStart® SYBR® Green Primers 299

Appendix 5: Bioanalyser results 302

Appendix 6: Serum samples from study 306

Appendix 7: MicroArray Database CD 307

Appendix 8: Epithelial cells in Transwell® insert. 308

8.1 Migration of epithelial cells in a Transwell® insert 308

Bibliography..... 309

List of Figures

Chapter 1

Figure 1-1: A diagram to show in pathogenic events in IPF..... 6
Figure 1-2: Activation of bleomycin 30
Figure 1-3: Signalling pathways involved in pulmonary fibrosis and idiopathic pulmonary fibrosis 36

Chapter 2

Figure 2-1: Haemocytometer grid layout..... 46
Figure 2-2: A diagram to represent a co-culture model of epithelial and fibroblast cells..... 48
Figure 2-3: A representative standard curve for IL-α..... 51
Figure 2-4: A zymogram to demonstrate enzyme activity 52
Figure 2-5: Standard Curve for MMP-2 activity..... 53
Figure 2-6: The Thermal Profile Cycle..... 63
Figure 2-7: The Bioanalyser Electropherogram..... 66

Chapter 3

Figure 3-1: Fibroblasts in collagen at 1, 4 and 7 days..... 77
Figure 3-2: MTT assay of fibroblasts in collagen over 7 days in serum-free medium to determine cell viability..... 78
Figure 3-3: Confocal images of fibroblasts..... 80
Figure 3-4: Effect of cell numbers on proliferation..... 81
Figure 3-5: The optical density measured by MTT assay..... 83
Figure 3-6: Confocal images of epithelial cells..... 83
Figure 3-7: Small Airway Epithelial Cells in 24 well plates and Cultured in serum free DMEM..... 86
Figure 3-8: MTT assay showing optical density of control vs injuries inflicted to epithelial cells..... 87
Figure 3-9: IL-1α response of control vs injuries inflicted to epithelial cells..... 89
Figure 3-10: MTT showing optical density of fibroblasts in co-culture on day 6..... 93
Figure 3-11: Ki 67 +ve Fibroblasts in co-culture inflicted with epithelial injury 93
Figure 3-12: Fibroblast α-*SMA* gene expression in the 3D co-culture model. 94
Figure 3-13: Quantitative RT-PCR analysis used to determine gene expression showing ECM components..... 96
Figure 3-14: The effect of various apoptotic inducers on fibroblasts..... 100
Figure 3-15: Expression of Caspase 3 in co-cultured fibroblasts..... 102
Figure 3-16: Expression of PARP with western blot..... 103
Figure 3-17: Measurement of PARP cleavage expressed as a percentage of total PARP cleavage in fibroblasts..... 104

Chapter 4

Figure 4-1: Total MMP-1 expression by ELISA..... 123
Figure 4-2: Quantitative RT-PCR analysis to determine *MMP-1* expression..... 124
Figure 4-3: Total MMP-7 expression..... 127
Figure 4-4: Quantitative RT-PCR analysis to determine expression of MMP-7..... 127
Figure 4-5: Gelatin zymogram of co-cultured supernatants taken from fibroblasts..... 129
Figure 4-6: Expression of active MMP-2..... 129

Figure 4-7: Gelatin zymogram of co-cultured supernatants taken from fibroblasts..... 131
Figure 4-8: Gelatin zymogram of supernatants taken from epithelial monolayer cell model (without co-cultured fibroblasts)..... 131
Figure 4-9: Expression of pro-MMP-9 in the co-culture supernatants..... 133
Figure 4-10: Expression of MMP-9 in the epithelial monolayer model..... 133
Figure 4-11: Expression of active-MMP-9 in the epithelial monolayer model..... 134
Figure 4-12: MTT activity in fibroblasts..... 136
Figure 4-13: MTT in epithelial cells..... 136
Figure 4-14: Quantitative RT-PCR analysis to determine gene expression of MMP-3..... 138
Figure 4-15: Quantitative RT-PCR analysis to determine gene expression of TIMP-1..... 138
Figure 4-16: Immunohistochemistry of MMP-9 in lung tissue..... 140
Figure 4-17: Immunohistochemistry of Alpha smooth muscle actin (α-SMA) in lung tissue..... 140
Figure 4-18: Representative gelatin zymography showing gelatinase activity of individual control and IPF serum samples..... 143
Figure 4-19: MMP-9 expression using Gelatin Zymography..... 145
Figure 4-20: Pro-MMP-9 expression using Gelatin Zymography..... 146
Figure 4-21: Total MMP9 expression in gelatin Zymography..... 148
Figure 4-22: Total MMP-9 expression using ELISA..... 148
Figure 4-23: Lung function of lung capacity carbon monoxide transfer factor (TLCO) and Forced Vital capacity (FVC) of patients with IPF (alive and dead)..... 151
Figure 4-24: Linear regression of %TLCO and active-MMP-9..... 153

Chapter 5

Figure 5-1: Tukey's Biweight Estimate..... 168
Figure 5-2: MicroArray Database print screen..... 174
Figure 5-3: Principal Component Analysis of epithelial cells and fibroblasts..... 177
Figure 5-4: Principal Component Analysis of each batch..... 177
Figure 5-5: Principal component analysis of individual treatments for epithelial cells for each experiment batch..... 179
Figure 5-6: Principal component analysis of individual experiments in epithelial cell with relevant treatments..... 179
Figure 5-7: Venn diagram outlining differentially expressed genes of epithelial cells..... 180
Figure 5-8: Principal component analysis of individual treatments..... 183
Figure 5-9: Principal component analysis of individual experiments..... 183
Figure 5-10: Venn diagram outlining differentially expressed in fibroblasts..... 184
Figure 5-11: Hierarchical clustering of the differentially over-expressed genes in both cell types..... 188
Figure 5-12: Interferon α/β Pathway in epithelial cells..... 190
Figure 5-13: Fibroblasts treated bleomycin Upstream Mediators..... 192
Figure 5-14: Measurement of expression of house-keeping genes by quantitative RT-PCR analysis..... 195
Figure 5-15: Measurement of expression of house-keeping genes by quantitative RT-PCR analysis in epithelial cells..... 196

Figure 5-16: The expression of selected genes from the co-cultured fibroblasts from the microarray database analysed by RT-PCR analysis…… 199

Chapter 6

Figure 6-1: Candidate epithelial cells from microarray database…… 220
Figure 6-2: The IFN genes expressed in the epithelial cells…… 222
Figure 6-3: Fibroblast genes selected from the microarray database…… 224
Figure 6-4: Fibroblast mediators predicted by the IPA…… 226
Figure 6-5: Expression of CCAAT/enhancer protein (C/EBP-α) in normal and IPF lung…… 229
Figure 6-6: Expression of IRF-9 in normal and IPF lung…… 231
Figure 6-7: Expression of ET-1 in normal and IPF lung…… 233
Figure 6-8: The IFN genes and IL-6 expression in 3D co-culture fibroblasts…… 236
Figure 6-9: The expression of gene in injured epithelial cells…… 237
Figure 6-10: Addition of different concentrations of bosentan on fibroblasts and epithelial cells…… 240
Figure 6-11: A MTT reduction assay on fibroblasts in 3D co-culture model…… 242
Figure 6-12: ELISA: The expression of endothelin-1 measured by ELISA in the co- cultured supernatants…… 244
Figure 6-13: Addition of bosentan in 3D co-culture model and gene expression of fibroblasts over 6 days…… 246
Figure 6-14: Gene expression of *Collagen I, III* and α-*SMA* in the absence presence (BT) of bosentan…….. 247

Chapter 7

Figure 7-1: Proposed mechanism of inflammation in pulmonary fibrosis …… 283

List of Tables

Chapter 1

Table 1-1: Summary of growth factors involved in pathogenesis of IPF..... 17
Table 1-2: Summary of cytokines involved in pathogenesis of IPF..... 19

Chapter 2

Table 2-1: The components of FGM-2 bulletkit..... 44
Table 2-2: The components of SAGM bulletkit..... 44
Table 2-3: Addition of low grade injuries on SAEs..... 49
Table 2-4: Antibodies for Immunohistochemistry..... 55
Table 2-5: Preparation of resolving gels for SDS-PAGE..... 58
Table 2-6: Preparation of stacking gels for SDS-PAGE..... 58
Table 2-7: Primary antibodies used to detect apoptosis..... 59
Table 2-8: Conditions for cDNA synthesis..... 61
Table 2-9 Reagents for quantitative PCR reaction mixture..... 62

Chapter 3

Table 3-1: The addition of bleomycin to epithelial cells 91
Table 3-2: A table of apoptotic inducers and suppressors which were added to cultured fibroblasts for 24 hours..... 99
Table 3-3: Table of treatments selected for the addition on cultured fibroblasts..... 101

Chapter 4

Table 4-1: High resolution computed tomography (HRCT) diagnostic criteria for usual interstitial pneumonia (UIP)..... 120
Table 4-2: Clinical characteristics of patients with idiopathic Pulmonary fibrosis and the control group..... 143
Table 4-3: Ratios for pro and active MMP-9 expression in the groups for alive and dead compared to control patients..... 147
Table 4-4: Baseline characteristics of serum sample subjects..... 150

Chapter 5

Table 5-0 Identification of experiments conducted for microarray 166
Table 5-1: This table shows the number of genes detected in each group set of fibroblasts and epithelial cells..... 175
Table 5-2: A list of top 25 genes expressed in bleomycin and scratch injuries in epithelial cells..... 181
Table 5-3: The top 25 genes expressed in both bleomycin and scratch injuries in co-cultured fibroblasts..... 185
Table 5-4: Selection of genes based on the role they play in IPF 186
Table 5-5: Function of IFN α/β pathway gene altered in epithelial response to bleomycin which was upregulated..... 191
Table 5-6: Function of mediators involved in fibroblast which may be contribute in IFN α/β pathway..... 193
Table 5-7: A selection of genes was chosen on the assumption of the relevance of the fold change in co-cultured fibroblasts..... 197

Table 5-8: 2-δCt values of the primers with house-keeping gene β-actin..... 199
Table 5-9: 2-δCt values of the primers with house-keeping gene GAP-DH..... 199

Chapter 6

Table 6-1: Genes were selected for quantitative RT-PCR for validation from the ingenuity pathway analysis..... 209
Table 6-2: Candidate genes which were selected for quantitative RT-PCR for validation from the microarray dataset..... 210
Table 6-3: Primers and house-keeping genes used to validate the candidate genes..... 211
Table 6-4: Tissue samples obtained from tissue bank..... 212
Table 6-5: Antibodies used for immunohistochemistry experiments and dilutions..... 213
Table 6-6: Different concentration of bosentan used in the 3D co-culture model..... 213
Table 6-7: The selection of genes obtained from the ingenuity pathway and microarray database for epithelial cells and fibroblasts..... 216
Table 6-8: IFN genes and candidate genes which were obtained from the microarray gene database..... 218
Table 6-9: The comparison of the fold change of candidate epithelial cells (bleomycin vs no-injury) 220
Table 6-10: The comparison of the fold change of candidate epithelial cells (scratch vs no-injury) 220
Table 6-11: The IFN α/β pathway gene predicted by IPA (bleomycin vs no-injury)..... 222
Table 6-12: The comparison of the fold change of IFN genes (scratch vs no-injury)..... 222
Table 6-13: The comparison of the fold change fibroblast genes (bleomycin vs no-injury) 224
Table 6-14: The comparison of the fold change fibroblast genes (scratch vs no-injury) 224
Table 6-15: The comparison of the fold change of fibroblast mediators (bleomycin vs no-injury) 226
Table 6-16: The comparison of the fold change of fibroblast mediators (scratch vs no-injury) 226

Abbreviations

A	Adenine
AECs	Alveolar Epithelial Cells
ATI	Alveolar Type I
ATII	Alveolar Type II
Apaf	Apoptotic protease activating factor 1
ATP	Adenosine triphosphate
BALF	Bronchoalvelolar lavage fluid
Bcl-2	B-cell lymphoma 2
BM	Basement Memebrane
C	Cytosine
cAMP	Cyclic adenosine monophosphate
CFA	cryptogenic fibrosing alveolitis
CTGF	Connective Tissue Growth Factor
dATP	Deoxyadenosine triphosphate
DAPI	4,6-diamidino-2-phenylindole
DMEM	Dulbecco's modified eagle's media
DMSO	Dimethyl Sulfoxide
DNA	Deoxyribonucleic acid
DPLD	Diffuse parenchymal lung diseases
DRR	Discoidin domain *receptor*
ECL	Enhanced chemiluminescence
ECM	Extraceullar Matrix
EDTA	Ethylenediaminetetraacetic
EGF	Epithelial Growth Factor
ELISA	Enyzme Linked Immunosorbent Assay
EMT	Epithelial Mesenchymal Transition
FCS	Fetal Calf Serum
FGF	Fibroblast Growth Factor
FGM	Fibroblast Growth Medium
FITC	Fluorescein Isothiocyanate

GCRMA	Gene Chip Robust Multiarray Averaging
HGF	Hepatocyte Growth Factor
HFL-1	Human Fetal Lung Fibroblasts
NHLFs	Normal Human Lung Fibroblasts
HMGB	High-Mobility-Group-Box
HSP	Heat Shock Proteins
HRCT	High-Resolution Computerised Tomography
IIP	Idiopathic Interstitial Pneumonia
IL	Interleukin
ILD	interstitial lung diseases
IGF-1	Insulin-like Growth Factor -1
IPA	Ingenuity Pathway Analysis
IPF	Idiopathic Pulmonary Fibrosis
LAP	Latency-Associated Protein
MAPK	Mitogen-Activated Protein Kinase
MMP	Matrix Metalloproteinase
MAS	Microarray Suite
MM	MisMatch
PBS	Phosphate Buffered Saline
PDGF	Platelet Derived Growth Factor
PF	Pulmonary Fibrosis
PGE_2	Prostaglandin-E2
PM	Perfect Match
PVDF	Polyvinyl Difluoride
RIN	RNA Integrity Number
RMA	Robust Multi-Array
RT-PCR	Real Time Polymerase Chain Reaction
SABM	Small Airway Epithelial Cell Basal Media
SAEs	Small Epithelial Cells
SAGM	Small Airway Epithelial Cell Growth Media
SEM	Standard Error Mean

SHH	Sonic hedgehog
SMA	Smooth Muscle Actin
SSc	Systemic Sclerosis
T	Thymine
TBST	Tris-Buffered Saline
TGF	Transforming Growth Factor
Th2	T-helper cell, type 2
TNF	Tumour Necrosis Factor
TUNEL	TdT-mediated X-dUTP nick end labeling
UIP	Usual Interstitial Pneumonia
WISP	WNT1-inducible Signalling Protein
ZO	Zonula Occludens
α	Alpha
β	Beta
γ	Gamma

Chapter One

Introduction

1.1 Pulmonary fibrosis and Idiopathic Pulmonary Fibrosis

Pulmonary fibrosis (PF) and Idiopathic Pulmonary Fibrosis (IPF) are diseases that result in lung scarring (fibrosis), characterised by known or unknown causes. Pulmonary fibrosis is usually a result of a secondary effect of other diseases, such as autoimmune disorders i.e. rheumatoid arthritis or systemic sclerosis, viral infections and bacterial infection i.e. tuberculosis. Pulmonary fibrosis can also appear without any known cause. In this case, it is termed "idiopathic". Most pulmonary fibrosis cases are diagnosed as idiopathic pulmonary fibrosis.

Idiopathic Pulmonary Fibrosis (IPF) is a progressive lung disease characterised by inflammation and fibrosis. This results in thickening and hardening of the lungs and results in scar tissue. The thickening is due to an excessive amount of collagen deposition around the alveoli which results in a reduction in elastic recoil and impaired gas exchange. Clinically, this presents as exertional dyspnoea, a dry cough and breathlessness (Gross and Hunninghake 2001).

The characteristic histological pattern of IPF is usual interstitial pneumonia (UIP) and is confirmed by high-resolution computerized tomography (HRCT) scanning. UIP is defined by a combination of patchy interstitial fibrosis with alternating areas of normal lung. Heterogeneity of fibrosis is characterised by scattered fibroblastic foci in the background of dense acellular collagen and loss of lung architecture due to chronic scarring or honeycomb change (Meltzer and Noble 2008).

Histopathologically, IPF shows interstitial inflammation, patchy collagen fibrosis, fibroblastic foci, and microscopic honeycombing (Copley, Wells et al. 2003). Whereas pulmonary fibrosis, as the secondary effect of other diseases such as systemic sclerosis (SSc), demonstrates a pattern of nonspecific interstitial pneumonia in HRCT (de Lauretis, Veeraraghavan et al. 2011). However, despite histopathological similarities, the etiologies and biological behaviours of the two conditions are different. Therefore, is it necessary for a diagnosis with HRCT scanning.

1.1.1 Idiopathic Pulmonary Fibrosis

IPF was previously known as cryptogenic fibrosing alveolitis (CFA) belonging to a family of lung disorders known as interstitial lung diseases (ILD) or more accurately, the diffuse parenchymal lung diseases (DPLD). Within this broad category of diffuse lung diseases, IPF is the most common and severe form of Idiopathic Interstitial Pneumonia (IIP) (Meltzer and Noble 2008), which is irreversible with a poor prognosis. The unpredictable and variable diagnosis can be associated with the pathological pattern known as usual interstitial pneumonia (UIP). IPF can often be referred to as IPF/UIP (Raghu, Collard et al. 2011).

The diagnosis of IPF can be confirmed in two ways; 1) high-resolution computerised tomography (HRCT) scanning which shows characteristic features of basal subpleural honey-combing (Katzenstein and Myers 1998) and 2) a specific lung biopsy.

1.1.2 The Prevalence of Idiopathic Pulmonary Fibrosis

The incidence and prevalence of IPF varies widely according to methodology and population studies with estimates the incidence ranging from 0.6 to 17.4 per 100,000 person years and estimates the prevalence ranging from 0.7 to 63.0 per 100,000 (Mazzei, Richeldi et al. 2015). In a recent study, the incidence and prevalence of IPF were assessed in the epidemiological study idiopathic pulmonary fibrosis clinical syndrome (IPF-CS). There was an increase across the study period from 0.92 per 100,000 in the 1968-1972 calendar periods to 5.10 per 100,000 in the 2006-2008 calendar periods and was higher in men and the older age groups. The incidence of IPF-CS increased by 35% from 2000 to 2008 with an overall incidence rate of 7.44 per 100 000 person-years (95% CI 7.12 to 7.77). Incidence was higher in men, predominantly in Northwest England (Navaratnam, Fleming et al. 2011).

IPF is ultimately a fatal disease with a median survival time of 3 years (Meltzer and Noble 2008). The natural course of IPF is highly variable including some patients experiencing a rapid decline, others progressing relatively slowly and some patients having periods of relative stability punctuated by acute deteriorations in respiratory function (Ley and Collard 2013). There is no identifiable cause in the deteriorations of

the condition which are known as acute exacerbations (Collard, Moore et al. 2007).These can occur in up to a third of patients with IPF per year and are associated with substantial morbidity and mortality (Mazzei, Richeldi et al. 2015).

1.1.3 Epidemiology and Risk Factors

As the name suggests, 'idiopathic' means there is no specific cause for IPF. Epidemiologic studies have demonstrated associations of exposure to inhaled environmental agents and the development of IPF. This includes exposure to cigarette smoke (Baumgartner, Samet et al. 1997), wood dust and metal dust (Hubbard, Lewis et al. 1996), fumes, smoke and silica particles (Vallyathan, Shi et al. 1988), viral infections such as the Epstein-Barr virus which causes glandular fever and the hepatitis C virus may both contribute to fibrosis. (Lung, Lam et al. 1985). Gastroesophageal reflux disease causes the reflux of stomach contents into the oesophagus and may then be inhaled into the lungs (Tobin, Pope et al. 1998). Age; 50 and 70 (approximately 2/3 of patients are older than 60 at the time of diagnosis) (Coultas, Zumwalt et al. 1994). Gender; more men are diagnosed with the disease than women, perhaps because more men are smokers (Coultas, Zumwalt et al. 1994). Other possible causes may include working in agriculture, farming, and with livestock (Taskar and Coultas 2006).

1.1.4 The Pathogenesis of IPF

The pathogenesis of IPF is not well understood. There is no particular mechanism that can explain the complexity of the disease. The current paradigm suggests that repeated injury to the lung causes epithelial damage with subsequent destruction of the alveolar capillary basement membrane. Destruction of the basement membrane causes infiltration of fibroblasts into the alveolar space. Some fibroblasts differentiate into myofibroblasts which secrete collagen and lay down a matrix promoting wound contraction (Selman and Pardo 2002). It is considered likely that the disease may involve the epithelial-mesenchymal interactions which result in abnormal communication between epithelial and mesenchymal cells and prevent the resolution of the wound-repair response, leading to tissue fibrosis and eventually organ failure (Trelstad, Hayashi et al. 1982).

1.2 Injury Response and Remodelling

IPF is characterised by alveolar epithelial injury and activation, followed by migration/proliferation and activation of mesenchymal cells with the formation of fibroblasts/myofibroblasts foci, and finally by the accumulation of ECM with the subsequent destruction of the lung architecture (Selman and Pardo 2004). In the normal wound healing process, alveolar injury results in the epithelial cells (ECs), which consist of alveolar epithelial type I and II (ATI & II) being damaged. This initiates the recruitment of inflammatory and mesenchymal cells. Myofibroblasts secrete collagen and other ECM components which provide a provisional matrix for the epithelial cells to migrate over to regenerate the damaged areas of the lung (Wynn 2008). To restore normal tissue homeostasis, apoptosis takes place by removing inflammatory cells and myofibroblasts. The ECM is partially absorbed allowing epithelial cell migration and re-epithelialization with complete tissue repair of the lung (Shi, Xu et al. 2009).

However, in IPF these processes become dysregulated either through persisting injury or aberrant repair. The failure of repair results in the apoptotic process being impaired, accumulation of myofibroblasts and excessive ECM synthesis. This results, in abnormal re-epithelialization, which then leads to impaired gas exchange with progressive deterioration of the lung, (Figure 1-1) (Kim, Kugler et al. 2006).

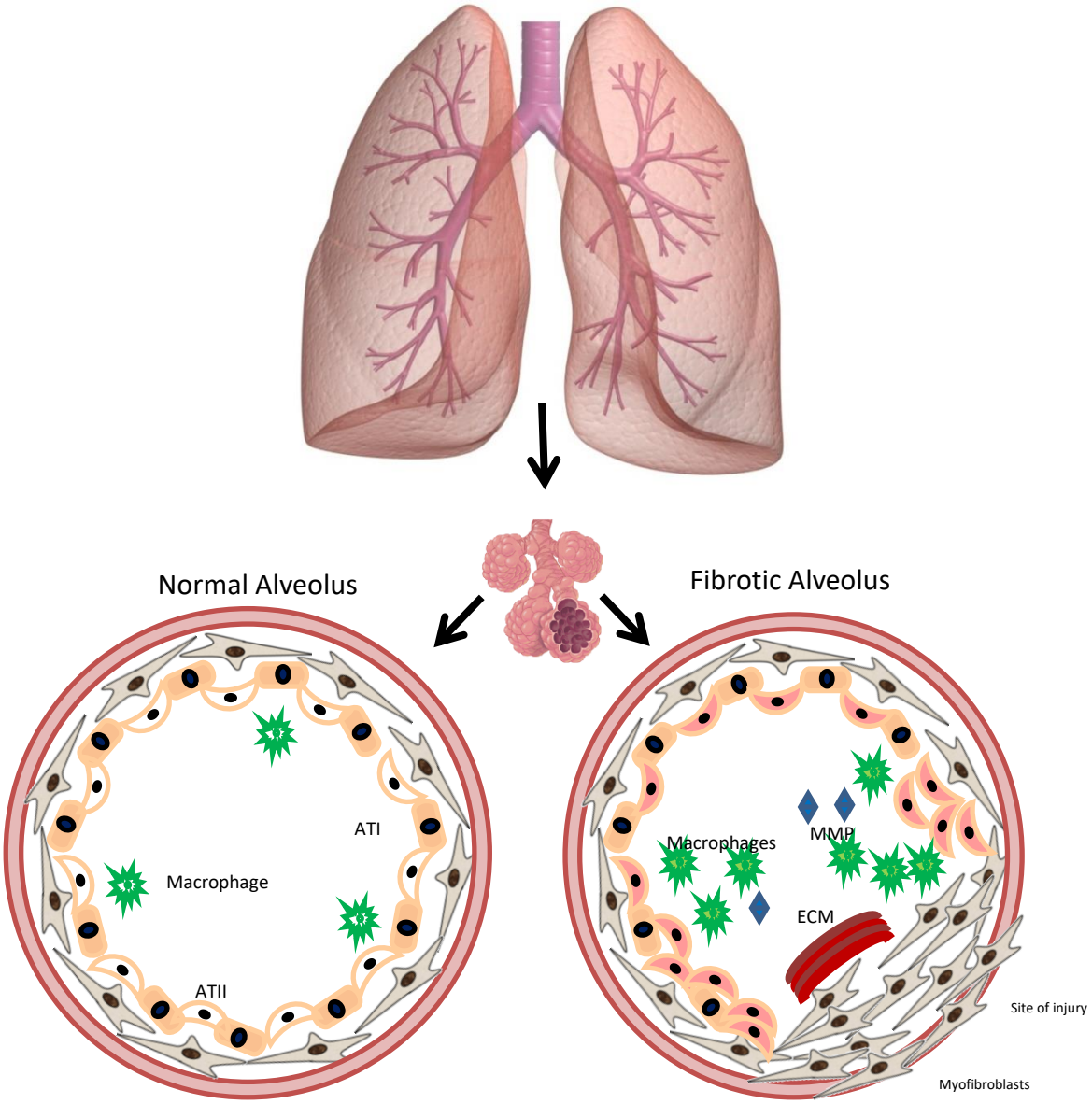


Figure 1-1: A diagram to show the main elements in IPF.
Unknown injury to the alveoli leads to epithelial disorganisation of alveolar epithelial type I and II cells (ATI & II cells). The epithelial cells release a variety of soluble mediators such as transforming growth factor (TGF-β), matrix metalloproteinases (MMPs) and platelet-derived growth factor (PDGF). This leads to degrade the basement membrane, with progression of fibroblasts and myofibroblasts which secrete excessive extracellular matrice (ECM) and leading to fibrosis.

1.2.1 Alveolar Epithelial Cells

There are two types of alveolar epithelial cells in the lung, alveolar type I (ATI) and alveolar type II (ATII). ATI are flat cells covering more than 90-95% of the alveolar surface area of the peripheral lung. ATI cells are highly attenuated and form an interface with pulmonary capillaries that are involved in gas exchange. These cells are unable to divide and are susceptible to injury (Selman and Pardo 2006). ATI cells are important in maintaining the normal cellular composition and function of the alveolar epithelium (Huiping 2009). Recently, ATI cells have been shown to be important in the transportation of water and sodium across the lungs (Sartori and Matthay 2002).

ATII cells are cuboidal shaped cells covering only 5% of the alveolar surface. They are found in the corners of alveoli and are in close proximity to mesenchymal cells lying beneath them (Huiping 2009). ATII cells are more resistant to injury and are capable of self-renewal and differentiation. They can function as progenitor cells for regeneration of the alveolar epithelium after injury (Selman and Pardo 2006). ATII cells are the main site of metabolism for arachidonic acids in the lungs which causes the release of lipid mediators such as Prostaglandins E_2 (PGE_2). PGE_2 has anti-proliferative effects on the epithelial cells and fibroblasts, i.e. inhibition of collagen synthesis and inhibition of epithelial cell and promotion of fibroblast apoptosis. PGE_2 is released when ATII cells are injured. The accumulation of PGE_2 can contribute to vascular permeability in the lung and result in large amounts of plasma proteins in the alveolar space which can contribute to pulmonary fibrosis (Cott, Westcott et al. 1990).

1.2.2 Characteristics of Fibroblasts and Myofibroblasts

Fibroblasts are mesenchymal cells which are the resident structural cells of the lung and play a key role in matrix homeostasis. Fibroblasts differentiate into myofibroblasts which are the key effector cells in pulmonary fibrosis (Desmouliere 1995). The exact origin of fibroblasts during pulmonary fibrosis is not well defined but there are three current theories. Firstly, there are resident fibroblasts within the lung. Secondly, fibroblasts known as fibrocytes which emerge from the bloodstream after the release from the bone marrow and thirdly, fibroblasts originate from epithelial cells through epithelial-mesenchymal transition (EMT) (Kalluri and Neilson 2003).

A key mesenchymal feature of pathological fibrosis is the increased number of fibroblasts differentiating into myofibroblasts. Myofibroblasts are contractile cells possessing morphologic and biochemical features which are intermediate between fibroblasts and smooth muscle cells (Phan 2008) that express markers such as vimentin and α-smooth muscle actin (α-SMA) (Allan, Beattie et al. 2008). They are present in all tissues in the body and play an important role in remodelling after injury. The key properties of myofibroblasts are; firstly, their ability to multiply after injury and secondly, the ability to secrete matrix proteins i.e. collagens (types I and III) which alters the local environment within the tissue (Singh and Hall 2008). Current evidence suggests that at least three local events are needed to generate α-SMA-positive differentiated myofibroblasts; firstly, accumulation of TGF-β. Secondly, the presence of ECM proteins i.e. fibronectin and thirdly, cell remodelling activity (Hinz, Phan et al. 2007).

The source of fibroblasts in the lung remains unclear but a popular explanation is that fibroblasts may derive from local epithelial cells in the lungs via EMT. A study by Greenburg and Hay 1982 first described EMT in cultured epithelial cells. The evidence was the direct outgrowth and movement of fibroblasts from epithelial-rich notochord and corneal epithelium embedded in an extracellular matrix (Hay 1995). Further studies since then have shown that fibroblasts differentiate into myofibroblasts and secrete collagen, altering the matrix which causes fibrotic lesions. These fibrotic lesions include fibroblasts, myofibroblasts and fibrocytes, known as the 'fibroblast foci', which are present in pulmonary fibrosis.

The activation of fibroblasts promotes proliferation, migration and transdifferentiation into activated myofibroblasts in response to growth factors such as TGF-β, Platelet-derived growth factor (PDGF) and Connective tissue growth factor (CTGF). PDGF is a potent mitogen for fibroblasts and myofibroblasts which promotes fibroblast differentiation and matrix synthesis (Coward, Saini et al. 2010). TGF-β has an indirect effect on the fibroblast proliferation via the induction of fibroblast growth factor (FGF) and activation of MAP kinase pathway. Moreover, fibroblasts are induced by TGF-β to

differentiate into myofibroblasts which represents the main source of excessive ECM during pulmonary fibrosis (Agostini and Gurrieri 2006).

1.2.3 Extracellular Matrix

The extracellular matrix is a complex structure that plays a key role in lung architecture and homeostasis. The ECM has multiple functions such as providing support and anchorage for cells, forming a tissue scaffold, and regulation of intracellular communication (Shi, Xu et al. 2009). ECM is comprised of the interstitial matrix and the basement membrane. The interstitial matrix is composed of polysaccharides and fibrous proteins within the intercellular spaces, while the basement membranes are sheet-like components of ECM on which various epithelial cells are present (Shi, Xu et al. 2009). The protein components of the basement membrane include collagens (predominantly type IV), laminin, elastin, proteoglycans, and fibronectin (Selman and Pardo 2002). These structural proteins play a role in the modulation of cell proliferation and differentiation in lung development (Shi, Xu et al. 2009).

Lung fibrosis is characterised by remodelling of the ECM which results in major alterations in both the quantity and composition of the ECM. There are at least two important disorders in fibrotic lungs; firstly, accumulation of ECM in the interstitial and alveolar spaces and secondly, disruption of the basement membrane (Pardo and Selman 2006). In the fibrotic lung, there are approximately two to three times more ECM than normal, including collagens (I and III,), tenascin c and proteoglycans i.e. versican (Estany, Vicens et al. 2010).

Recent evidence from *in vivo* and *ex vivo* experimental studies have demonstrated that the abnormal ECM in fibrotic lungs alters the behaviour of epithelial and mesenchymal cells (Shimbori, Gauldie et al. 2013). The profibrotic microenvironment of the ECM is characterised by altered biochemical and biomechanical properties. The ECM stores an abundant amount of growth factors such as transforming growth factor (TGF)β1 (Todd, Luzina et al. 2012). This excessive amount of ECM can promote progressive fibrogenesis in the lungs without any further initiation from other cells.

The ECM seems to play a more complex and dynamic role than previously thought (Blaauboer, Boeijen et al. 2014).

1.2.4 Apoptosis

Apoptosis plays a major role in tissue homeostasis to maintain a balance between cell survival and death (Kuwano 2007). The term "apoptosis", referred by *Kerr et al*. (Kerr 1999), describes cell death characterised by defined morphological changes including cell shrinkage, chromatin condensation, loss of nuclear membrane integrity, plasma membrane blebbing and apoptotic body formation, which helps regulate cellular proliferation. (Drakopanagiotakis, Xifteri et al. 2008). There are two signalling pathways of apoptosis called the Extrinsic and Intrinsic pathways.

The *Extrinsic pathway* also known as the 'Death receptor pathway' is mediated by the sub group of Tumour Necrosis Factor Receptors (TNF-R) super family that includes TNF-R, Fas and Tumour Necrosis Factor receptor is related to apoptosis inducing ligand (TRAIL). Activation of the initiator caspase, caspase-8 activates caspase-3 or amplifies caspase-3 activation by cleaving the B-cell lymphoma 2 (Bcl-2) family member BH3 interacting-domain death agonist (Bid). Bid cleavage leads to cytochrome c leakage, the formation of a protein complex called the apoptosome and activation of caspase-9 (Sakamaki and Satou 2009). The *extrinsic pathway* can be triggered in response to proliferative and inflammatory signalling pathways in which the Fas ligand and Fas system is initiated via the death domain (DD) and the cascade of events begin (Kalimuthu and Se-Kwon 2013).

The *Intrinsic (mitochondrial) pathway* involves members of the Bcl-2 family that regulate cytochrome c release from the mitochondria. Once released from the mitochondria, cytochrome c can interact with Apoptotic protease activating factor 1 (Apaf-1), deoxyadenosine triphosphate (dATP) and procaspase-9 to form the apoptosome. As part of the apoptosome, caspase-9 is processed and activated and proceeds to activate caspase-3 (Martin, Allan et al. 2005).

The intrinsic apoptotic pathway involves mitochondrial swelling, rupture of the outer membrane and release of proapoptotic factors from the intermembranous space. The

intrinsic signalling pathway mediating apoptosis involves the absence of certain growth factors, hormones and cytokines. The intrinsic stimuli can be triggered either by radiation, drugs, toxins, hypoxia, hyperthermia, viral infections or free radicals (Kim, Cheresh et al. 2015).

The intrinsic stimuli cause changes in the inner mitochondrial membrane. This results in an opening of the mitochondrial permeability transition (MPT) pore and release of two main groups of normally sequestered pro-apoptotic proteins from the intermembrane space into cytosol. Cytochrome c binds and activates Apaf-1 forming an "apoptosome complex", which in turn activates procaspase-9 into active caspase-9 and activates caspase 3. (Kalimuthu and Se-Kwon 2013).

1.2.4.1 Caspases

One of the earliest and most consistently observed characteristics of apoptosis is the activation of a series of cytosolic proteases called caspases (Sakamaki and Satou 2009). When apoptosis is activated, caspases cleave multiple protein substrates which leads to the loss of cellular structure and function and ultimately results in cell death. In particular, caspases -3, -8, and -9, have been implicated in apoptosis: caspase-9 in the mitochondrial pathway, caspase-8 in the Fas/CD95 pathway, and caspase-3 more downstream, activated by multiple pathways (Los, Mozoluk et al. 2002).

Caspase-3 performs the bulk of the cleavage events during apoptosis. Biochemical studies have shown that this caspase is highly active and is present at the highest concentration among all caspases in most cells (Kuwano 2007). For these reasons, caspase-3 supersedes other caspases in most biochemical events.

1.2.4.2 PARP

Poly (ADP ribose) polymerase 1 (PARP) was the first caspase substrate identified. **PARP-1** is a nuclear enzyme involved in DNA repair, DNA stability, and transcriptional regulation (Los, Mozoluk et al. 2002). This is a particularly interesting death substrate and its cleavage is now recognized as a hallmark of apoptosis. Caspases, in particular, caspase-3 and -7, cleave the 116-kDa form of PARP-1 at the DEVD site to generate an 85- and a 24-kDa fragment. The sequence DEVD is based on caspase-3 cleavage site in poly (ADP-ribose) polymerase (PARP). Previous work has suggested that in particular, caspase-7 is responsible for PARP activation during apoptosis (Kuwano, Hagimoto et al. 2004).

1.2.4.3 Alveolar Epithelial cells

The lung epithelium is composed of various different cell types. The lung epithelium is the first barrier of defence against environmental insults and infection. This barrier not only provides a mechanical and physical barrier but also prevents entry of foreign particles. The alveolar surface is mainly covered by two types of alveolar epithelial cells namely alveolar type I epithelial cells (ATI) and Alveolar type II epithelial cells (ATII). AT1 cells cover 90% of the airway surface. The AT1 structure consists of large flattened phenotype whose function is gas interchange. ATII are the most abundant epithelial cell type. The ATII cells help to maintain the alveolar space by secretion of several types of surfactant proteins and other ECM components (Serrano-Mollar 2012). The production of surfactant by ATII cells enables gas exchange to occur by lowering surface tension within the alveoli (Rackley and Stripp 2012).

Once the epithelium is injured, the epithelial/fibroblastic pathways of wound healing become activated. There is a loss of integrity of the alveolar epithelium with disruption of basement membrane integrity, collapse of the alveolar structure and the number of ATI cells is reduced. The progenitor cells are unable to differentiate to ATI cells and therefore, the site of injury is not repaired by AT1 re-epithelialisation (Chapman 2011). In IPF this has serious implications for the progression of the disease.

Studies have shown that epithelial cells, predominantly ATI, in apoptosis may be a key profibrotic event in lung fibrogenesis. Apoptosis of AECs are found both in the lungs of patients with IPF and in animal models of the disease (Uhal 2008). Fragmented DNA, a hallmark of apoptosis, was found in bronchiolar cells and AECs within lung biopsies from patients with IPF (Harari and Caminati 2010) and in the lungs of mice and rats with bleomycin-induced lung fibrosis (Kuwano, Kunitake et al. 2001). These finding were confirmed by simultaneous double labelling of fragmented DNA and α-smooth muscle actin, a marker for myofibroblasts, in biopsies from patients with IPF. Fragmented DNA in the alveolar epithelium was found frequently and immediately adjacent to α-smooth muscle actin-positive interstitial cells and foci of collagen. Thus epithelial apoptosis co-localises with myofibroblasts where collagen deposition is severe in patients with IPF (Li, Shu et al. 2004).

In addition to altered mesenchymal cells, abnormalities of the alveolar epithelium in patients with pulmonary fibrosis have shown loss of normal type I alveolar epithelium and replacement by hyperplastic type II cells, or bronchiolar cuboidal cells. This is a consistent finding in patients with IPF (Fujino, Kubo et al. 2011). In addition to these observations, more studies have focused on the mechanism or crosstalk between damaged epithelial cells and lung mesenchymal cells. This epithelial-mesenchymal crosstalk contributes to pulmonary fibrosis, in which altered lung mesenchymal cells along with alveolar epithelial cell injury result in the accumulation of ECM and remodelling of the lung architecture (Todd, Luzina et al. 2012).

1.2.4.4 Fibroblasts

In the normal wound healing process, excessive numbers of fibroblasts/myofibroblasts are removed by apoptosis. In contrast, myofibroblasts expressing α-SMA persist in regions where there is excessive scarring and in fibrotic conditions. As wound healing progresses, there is an increase in *in situ* end labelling of fragmented DNA. This is a marker of apoptosis, in myofibroblasts and vascular cells. This apoptosis is thought to be due to the combined effects of reduced growth factor expression, increased extracellular matrix turn-over and nitric oxide generation (Ramos, Montano et al. 2001).

As mentioned above, in lung biopsies from patients with IPF, cells showing strong nuclear labelling were only seen in the epithelium overlying myofibroblasts foci not in the myofibroblasts themselves suggesting resistance to apoptosis in these cells. This resistance to apoptosis has been demonstrated *in vitro* where myofibroblasts isolated from fibrotic lung were found to be more resistant to Fas-ligand-induced apoptosis than normal controls (Uhal 2008). One mechanism for this reduced susceptibility may be lower expression of cell surface Fas together with higher levels of apoptosis-inhibiting soluble Fas by these cells. These studies suggest that mesenchymal cells in IPF develop an apoptosis-resistant phenotype which contributes to persistent or progressive fibrosis (Harari and Caminati 2010).

1.3 Soluble Mediators involved in epithelial fibroblast interaction

Injury to lung epithelium releases a wide variety of soluble factors from fibroblasts, endothelial cells, macrophages and the injured epithelial cells as well as from the underlying matrix. These soluble factors that participate in epithelial repair include proteases, interleukins, growth factors, cytokines, chemokines and matrix components (Crosby and Waters 2010). Even though the pathogenesis of the disease is poorly understood, the presence of these soluble growth factors can possibly outline processes and mechanisms which can help to understand the pathogenesis of the disease.

1.3.1 Role of growth factors

Growth factors are proteins that bind to receptors on the cell surface with the primary result of activating cellular proliferation and/or differentiation. Many growth factors are quite versatile, stimulating cellular division in numerous different cell types, while others are specific to a particular cell-type (Allen and Spiteri 2002).

Individual growth factors are involved in the development of pulmonary fibrosis and regulate other cell functions as well as cell proliferation (Table1-1). They may originate from a variety of sources including immune cells, endothelial cells, epithelial cells, fibroblasts, platelets and smooth muscle cells. It is therefore, the interactions of growth factors with these epithelial and fibroblast cell types that are most critical in determining whether the ultimate outcome of wound-healing responses to lung injury is IPF.

The growth factor which has predominately been described in fibroblasts is TGF-β. TGF-β is activated by epithelial and fibroblast cells during the development of pulmonary fibrosis. The mechanism of TGF-β is known to be involved in recruitment, proliferation, myofibroblast differentiation and extracellular matrix production (Sheppard 2006). The pro-fibrotic effect of TGF-β causes the fibroblasts to be resistant to apoptosis and by contrast epithelial cells are not resistant (Kuwano, Hagimoto et al. 2004). Studies have shown that TGF-β promotes apoptosis of lung epithelial cells *in vitro* (Solovyan and Keski-Oja 2006).

Lung fibroblasts produce TGF-β latent complexes and studies have shown that these complexes are activated by the αvβ5 integrins which mediate fibroblast differentiation (Zhou, Hagood et al. 2010). TGF-β is involved in multiple mechanisms to mediate pro-fibrotic fibroblast-to-epithelial cell interactions. TGF-β is produced and activated by lung fibroblasts which mediate epithelial cell apoptosis. TGF-β thus could be an important mediator of different interactions between epithelial cells and fibroblasts in pulmonary fibrosis (Sakai and Tager 2013).

It is becoming increasingly apparent that 'injured' alveolar epithelial cells both secrete and respond to growth factors, which contribute to the outcome of the profibrogenic processes. Fibroblasts directly influence fibrogenesis which promotes the function of enhancing or inhibiting ECM protein synthesis, chemotaxis, production of MMPs and their inhibitors, expression of adhesion molecules and angiogenesis. Much less is known about growth factors which regulate the alveolar epithelial cell (AEC) function to modulate fibrogenesis. However, in AECs obtained from IPF patients, growth factors are potentially responsible for secretion of MMPs and paradoxically, inhibit proliferation through enhancement of apoptosis (Sakai and Tager 2013).

Table 1-1: Summary of growth factors involved in pathogenesis of IPF
Taken from (Allen and Spiteri 2002)

Growth Factors	**Source**	**Functional Effect**
Connective Tissue Growth Factor (CTGF)	Vascular endothelial cells	cell adhesion, migration, proliferation, angiogenesis
Epidermal Growth Factor (EGF)	Epithelial cells	Enhanced epithelial repair via stimulation of mitosis, migration, spreading
Fibroblast Growth Factor (FGF)	Fibroblasts	Stimulated mitogenesis
Platelet Derived Growth Factor (PDGF)	Mesenchymal origin	involvement in mesenchymal cell accumulation
Transforming Growth Factors-α (TGF-α)	Epithelial cells	induces epithelial development
Transforming Growth Factors -β (TGF-β)	Macrophages	Stimulation of migration of fibroblasts. Stimulation on wound healing Induction of EMT Activation of other growth factors.

1.3.3 Role of cytokines

Cytokines are a class of signalling proteins that are used extensively in cellular communication, immune function, and embryogenesis (Agostini and Gurrieri 2006). Cytokines are produced by a variety of hematopoietic and non-hematopoietic cell types and can exert autocrine, paracrine and endocrine effects. Therefore, cytokines can be related more to hormones than to growth factors in their overall functions. Cytokines and Chemokines also play an important role in the pathogenesis of fibrosis. Evidence has suggested that important stimuli to collagen deposition in pulmonary fibrosis are polypeptide mediator cytokines (Agostini and Gurrieri 2006). Released by resident lung cells and recruited inflammatory cells, cytokines are thought to stimulate fibroblast proliferation and increased synthesis of extracellular matrix proteins, including collagen. An early feature in the pathogenesis of IPF is alveolar epithelial and/or capillary cell injury. This promotes recruitment into the lung of circulating immune cells, such as monocytes, neutrophils, lymphocytes and eosinophils.

These effector cells, together with resident lung cells, such as macrophages, alveolar epithelial and endothelial cells, release cytokines, which stimulate target cells, typically fibroblasts, to replicate and synthesize increased amounts of collagen. Breakdown of extracellular matrix protein may also be inhibited thereby contributing to the fibrotic process. Numerous growth factors and cytokines have been implicated in the pathogenesis of lung fibrosis including tumour necrosis factor-α (TNF-α), platelet- derived growth factor (PDGF), insulin-like growth factor-1 (IGF-1), endothelin-1 (ET-1) and the interleukins, (IL)-1 and IL-8 (Table1-2), (Crosby and Waters 2010).

Table 1-2: Summary of cytokines involved in pathogenesis of IPF
Taken from (Agostini and Gurrieri 2006)

Cytokines/Chemokines	**Source**	**Functional Effect**
CCL2, CCL3, CCR2	Macrophages, fibroblasts, epithelial cells, and endothelial cells	Stimulates wound closure ECM turnover
CCL22	Dendritic cells and macrophages	May play a role in the trafficking of activated/effector T-lymphocytes to inflammatory sites
Endothelin-1 (ET-1)	Endothelial cells	Acts with other profibrotic mediators to recruit fibroblasts and allow for their differentiation to contractile myofibroblasts
Interleukin-1β (IL-1β)	Macrophages, neutrophils, epithelial cells, and endothelial cells	Inflammatory response, and is involved in a variety of cellular activities, including cell proliferation, differentiation, and apoptosis.
Tumour Necrosis Factor-α (TNF-α)	lymphoid cells, mast cells, endothelial cells, cardiac myocytes, adipose tissue, fibroblasts, and neurons	Activates NF-κB, MAPK and induction of death signalling

1.3.4 Role of Alarmins

Alarmins are endogenous mediators that are released in response to danger signals initiated by infection and /or tissue damage (Oppenheim and Yang 2005). These 'danger signals' initiate an inflammatory response which is capable of activating innate and adaptive immunity (Oppenheim, Tewary et al. 2007). Alarmins can include high-mobility-group box-1 (HMGB1) protein, interleukins such as IL-1α and heat-shock proteins (HSPs).

HMGB1 protein is a member of a superfamily of nucleosome-binding proteins and is released from injured necrotic cells or from activated monocytes, macrophages, dendritic cells and NK cells (Yang, Tewary et al.). A recent study has shown how HMGB1 plays an important role in tissue repair after injury. It has shown that when the tissue is damaged, bone marrow cells are recruited. In particular, Lin-/PDGFRα, a subpopulation of bone marrow cells, are mobilised by HMBG1. HMGB1 directs the Lin-/PDGFRα cells to the site of injury, which enables them to promote the recruitment and migration of these cells within the injury, thus contributing to wound healing (Tamai, Yamazaki et al. 2011).

Interleukin-1α is a well-known and established cytokine which is involved in the initiation and persistence of inflammation (Lappalainen, Whitsett et al. 2005). The macrophage-monocyte is a primary source of IL-1α, but many other cells, including fibroblasts, T cells, neutrophils, and bronchial and alveolar epithelial cells, also produce IL-1α (Dinarello 1996).

Studies have shown that an increased production of IL-1α can appear to mediate disease progression in IPF patients (Adegunsoye and Balachandran 2015.). *Suwara et al*, had reported IL-1α released from damaged epithelial cells is sufficient and essential to trigger inflammatory responses in human lung fibroblasts (Suwara, Green et al. 2014).

1.3.5 Role of MMPs

Matrix Metalloproteinases are zinc-dependent proteolytic enzymes that cleave the protein components of the extracellular matrix and thereby play a central role in tissue remodelling (Stamenkovic 2003). MMPs have additional roles in the release of matrix-bound growth factors, cell proliferation, angiogenesis, cellular invasion and migration (Henderson, Markwick et al. 2007).

MMPs can be divided into three groups: collagenases (MMP-1, -8, -13), gelatinases (MMP-2, -9), and stromelysins (MMP-3, -7, -10). These MMPs are constitutively expressed in various types of cells such as parenchymal, connective tissue, and inflammatory cells. The majority of the MMPs are secreted in the extracellular space and some of them are expressed as cell –surface enzymes. The MMPs of interest in pulmonary fibrosis are MMP-1, -2, -7 and -9.

MMP-1 is also known as collagenase-1 ~ 57kDa. MMP-1 is the prototype of the MMPs capable of degrading fibrillar collagens types I, II, and III. It is produced by a wide variety of normal cells such as fibroblasts, macrophages, endothelial and epithelial cells *in vitro* (Pardo and Selman 2005). MMP-1, like many other MMPs is undetectable in normal resting tissues and is mainly expressed during physiological and pathological tissue remodelling *in vivo* (Checa, Ruiz et al. 2008). Studies of the transcriptional behaviour of lung genes in IPF have shown a strong up-regulation of MMP-1 in pulmonary fibrosis. *Rosas et al*, reported an increase in MMP-1 in serum, BALF and lung tissue in IPF patients but not in chronic obstructive pulmonary disease or sarcoidosis patients (Rosas, Richards et al. 2008). Whereas *Zhou et al*, had performed a similar study using serum and BALF in IPF patients with sarcoidosis and had reported that MMP-1 may be increased in the inflammatory phase rather than matrix remodelling phase of lung fibrosis

The findings of both studies of Rosas and Zhou were somewhat contradictory. Rosas states that MMP-1 levels are higher in IPF and aid in the degradation of the extracellular matrix and contribute to the remodelling. As Zhou states, MMP-1 may be increased in the inflammatory phase as compared to the matrix remodelling phase of lung fibrosis.

The main characteristic of a fibrotic disorder is the exaggerated deposition of fibrillar collagens which are major substrates of this enzyme. Rosas' findings were to suggest that MMP-1 aids the degradation of the extracellular matrix and aberrant tissue remodelling. However, in IPF there is exaggerated deposition of fibrillar collagens and if MMP-1 was present in the area of the fibrillar collagens then they would be degraded. Pardo and Selman suggested that MMP-1 is absent from the interstitial compartment where collagen is being accumulated (Pardo and Selman 2006). Zhou's findings are MMP-1 levels increase in the inflammatory phase of fibrosis and regulate an injury response.

Overall, it can be stated that MMP-1 is primarily localised in alveolar epithelial cells and bronchiolar epithelial cells. During an injury response, these cells are involved in the inflammatory phase. MMP-1 then progresses to the lining of the honeycomb cystic spaces and is absent from the interstitial compartment where collagen is being accumulated (Pardo and Selman 2006).

MMP-2 is a 72-kDa gelatinase A. It is known to degrade a broad range of matrix and non-matrix substrates and is more effective against collagen type IV. MMP-2 is known to be produced by fibroblasts, endothelial cells and alveolar epithelial cells (Chakrabarti and Patel 2005).

Studies in bleomycin-induced pulmonary fibrosis have shown that the activity of MMP-2 provokes the disruption of basement membranes and may have a major role in the invasion of fibroblasts into the alveolar spaces. In addition, the disruption of the basement membrane may also contribute to the failure of an orderly repair of the damaged ATI epithelial cells, affecting normal reepithelialisation and may play an additional role by inducing epithelial apoptosis (Pardo and Selman 2006).

MMP-7 is also known as matrilysin. MMP-7 is prominently expressed by alveolar epithelium in pulmonary fibrosis (Li, Park et al 2002). MMP-7 is known to degrade several ECMS including collagen IV, laminin, fibronectin, tenascin and ostepontin. A recent study has shown the involvement of MMP-7 in epithelial repair. *McGuire et al,* have shown that MMP-7 is highly expressed in lungs of patients with pulmonary

fibrosis. MMP-7 mediates the shedding of E-cadherin from injured lung epithelium. Epithelial (E)-cadherin is a transmembrane glycoprotein which is localised at adherent junctions and mediates calcium-dependant cell-cell adhesion in most epithelial cells. E-cadherin is thought to regulate cell differentiation and morphogenesis in epithelial cells (McGuire, Li et al. 2003).

Alveolar epithelial cells from bleomycin-induced mice have shown to activate matrilysin which results in shedding of E-cadherin and accelerated cell migration. Matrilysin is co-localised with E-cadherin at the basolateral surfaces of migrating tracheal epithelium, and the reorganisation of cell-cell junctions was seen in wild-type mice. In bronchoalveolar lavage fluid (BALF) from bleomycin-induced wildtype mice, results showed E-cadherin ectodomain was shed but was not shed in matrilysin-null mice. It would suggest that E-cadherin is a substrate for MMP-7 and indicate that shedding of E-cadherin is required for epithelial repair (McGuire, Li et al. 2003).

MMP-9 is a 92-kDa gelatinase B. MMP-9 is produced mainly by inflammatory cells such as neutrophils, monocytes, macrophages, eosinophils and lymphocytes (Corbel, Belleguic et al. 2002). MMP-9 gene expression and protein levels have also been shown to be elevated in BALF from patients with IPF. Studies have shown that the enzyme has been localised in epithelial cells, neutrophils and macrophages with some staining in subepithelial fibroblasts (Pardo and Selman 2006). Likewise, in bleomycin-induced pulmonary fibrosis, an increase of MMP-9 and disruption of the alveolar epithelial basement membrane has been reported (Yaguchi, Fukuda et al. 1998).

1.4 Epithelial-Mesenchymal 'Crosstalk'

Epithelial-mesenchymal interactions are characterised by epithelial and mesenchymal cell communication during wound repair which leads to normal function of the lung tissue (Selman and Pardo 2002). Persistent injury is likely to cause dysregulation of the normal wound healing processes, resulting in abnormal communication between epithelial and mesenchymal cells. This prevents resolution of the wound-repair response leading to tissue fibrosis and eventual organ failure. It is likely that signalling pathways that are involved in these processes become disrupted, leading to the aberrant 'crosstalk' and failure in the repair process (Coward, Saini et al. 2010). Studies have revealed that dysregulation in the repair process can lead to abnormal communication in the signalling pathways, in particular, in IPF. These pathways can include TGF-β, Notch, Shh and Wnt.

1.4.1 Pro-fibrotic Role of Transforming Growth Factor - β

The transforming growth factor-β (TGF-β) superfamily is composed of a group of diverse polypeptides responsible for many cellular activities including proliferation, differentiation, migration, adhesion, extracellular matrix (ECM) synthesis, and cell death (Aschner and Downey 2016).

The TGF-β superfamily includes three TGF-β isoforms (TGF-β1, -β2 and -β3), activins and inhibins, growth differentiation factors (GDFs), bone morphogenetic proteins (BMPs), and anti-mullerian hormone (AMH). These ligands are involved in biological responses, based on their cell/tissue-specific expression, their interactions with inhibitory molecules and the unique combinations of receptors with which they complex. TGF-β ligands form receptor complexes with one of seven type I receptors (also termed activin-like kinase or ALK receptors) along with either one of five type II receptors (ActRIIA, ActRIIB, TGFBRII, BMPRII and AMHRII). For TGF-β1, ligand contact with the type II receptor TGFBRII leads to recruitment and phosphorylation of the type I receptor ALK-5 (Walton, Johnson et al. 2017).

In all occurrences, ligand receptor complex formation leads to the activation of kinase

domains within the receptors, which potentiate phosphorylation cascades involving SMAD transcription factors. The TGF-β isoforms and activins converge to induce intracellular signalling via SMAD-2/3 transcription factors. Activation of SMAD-2/3 regulates to the expression of several profibrotic genes, including collagens i.e. COL1A1, COL3A1, COL5A2, COL6A1, COL6A3, COL7A1, (Verrecchia, Chu et al. 2001) plasminogen activator inhibitor-1 (PAI-1) (Hua, Liu et al. 1998), integrins (Margadant and Sonnenberg 2010), connective tissue growth factor (Chen, Goldschmeding et al. 2002), and matrix metalloproteases (Yuan and Varga, 2001).

In Idiopathic pulmonary fibrosis, TGF-β is believed to be fundamental to the pathogenesis of the disease (Aschner and Downey 2016). In the lung, TGF-β is expressed by multiple cell types including epithelial cells, macrophages, and fibroblasts, and levels are elevated in animal models and in patients with IPF (Bergeron, Soler et al, 2003).

In vitro, TGF-β can induce myofibroblast differentiation of fibroblasts (Kim, Wei. et al 2009) and mesenchymal transition of epithelial cells (Willis and Borok 2007.). Myofibroblasts isolated from patients with IPF exhibit a durable invasive phenotype in culture. Myofibroblasts also secrete their own TGF-β, inducing further transcriptional activation of collagens and other ECM components via Smad-dependent pathways, as well as inducing further ATII cell apoptosis, which perpetuates the aberrant wound-healing process (Parker, Rossi et al. 2014). Targeted ATII cell deletion of TβRII provides protection from bleomycin-induced fibrosis (Li, Krishnaveni et al. 2011). As noted previously, TGF-β activation can occur via integrins, particularly, αvβ6, and this process is of critical importance in the development of tissue fibrosis (Walton, Johnson et al 2017).

Integrins are a large family of heterodimeric cell surface receptors, consisting of a single α and β subunit, which bind to ECM proteins. They act as mechanotransducers by generating information from the ECM to the cell interior or vice versa and have diverse roles in mediating cell adhesion, shape, migration, proliferation, survival, differentiation, and invasion (Hynes, 2009).

Expression of the αvβ6 integrin is low in normal lung epithelium but significantly increased in injured epithelium (Xu, Porte et al. 2009). The reason for this could be that the avβ6 integrin is constitutively bound to TGF-β, where injurious stimuli are detected. The adverse effect of the injury can transmit the signal through the lung epithelium to the αvβ6 integrin via a G-protein coupled receptor–mediated pathway (Jenkins, Su et al. 2006). It has been shown that thrombin, and synthetic nonproteolytic agonists of protease-activated receptor 1 (PAR1), are able to induce αvβ6 integrin–mediated TGF-β activation via the PAR1 receptor (Jenkins, Su et al. 2006). Epithelial cells require an intact cytoskeleton to activate TGF-β via the αvβ6 integrin and signal to the cytoskeleton via activation of RhoA and rho kinase (Jenkins, Su et al. 2006)

TGF-β activation is ubiquitous; however, the αvβ6 integrin is restricted to the epithelium and thus can only activate latent TGF-β in direct association with epithelial cells. In the presence of injury, overexpression of the αvβ6 integrin can promote the development of tissue fibrosis (Sheppard 2006). In the event of an injury, epithelial cells secrete increased levels of IL-1β which acts as a paracrine factor on the airway fibroblasts. Airway fibroblasts respond to IL-1β by up-regulating β8 expression and αvβ8-mediated TGF- β activation. Increased activation of TGF- β by the fibroblasts causes autocrine effects on the fibrogenic fibroblast phenotype, in turn, up-regulates collagen I and α-smooth muscle actin (α-SMA) along with paracrine effects on adjacent airway epithelium. This decreases fibroblast secretion of human growth factor and inhibits epithelial proliferation. Airway epithelial wounding also causes increased αvβ8-mediated activation of TGF- β, which inhibits airway epithelial migration. Increased levels of active TGF-β contribute to the increased expression of β6 by airway epithelial cells because the gene encoding β6 integrin is TGF-β responsive, thus forming a self-amplifying loop of TGF- β activation (Nishimura 2009).

1.4.2 Notch Pathway

Notch Signalling was first discovered in 1993, in a fruit fly, *Drosophila,* which revealed that this pathway is essential for cell fate decision and development (Fortini, 2009). Further studies have shown that Notch signalling may play a vital role in EMT.

EMT may be involved in the development of the myofibroblast population that contributes to fibrogenesis. While TGF-β is seen as the main driving force for EMT, recent studies have demonstrated the importance of the Notch receptor signalling pathway in EMT. This pathway regulates the cell fate specification and siRNA targeting of components of the Notch pathway, which has shown to block TGF-β induced EMT in kidney tubule epithelial cells (Zavadil and Bottinger 2005). Another study has shown that Notch signalling plays a role in EMT, both upstream and downstream of TGF-β in rat AECs *in vitro*, and in the inhibition of Notch receptor activation of TGF-β-induced α-SMA expression (Aoyagi-ikeda, 2010). This would suggest that inhibition of the Notch signalling pathway could be a therapeutic opportunity in pulmonary fibrosis (Datta, Scotton et al. 2011).

1.4.3 Sonic Hedgehog Pathway

Sonic Hedgehog (Shh) plays an important role in embryonic development, tissue patterning and organogenesis (Bolanos, Milla et al. 2012). There are three hedgehog homologs in mammals, 1) Sonic hedgehog (Shh), 2) Indian Hedgehog (IHH) and 3) Desert Hedgehog (DHH). All these hedgehog signalling responses are mediated by Patched-1 (PTCH1), a 12-pass integral membrane protein and Smoothened (SMO), a seven-pass integral membrane protein (King, Pardo et al. 2011) . Shh is highly expressed in the distal epithelium and diffuses from there to activate signalling in the nearby mesenchyme via PTCH1, SMO and their transcriptional effectors glioma oncogene homolog GLI1, GLI2 and GLI3 (Bolanos, Milla et al. 2012).

Shh is the most broadly expressed and has shown to be responsible for branching morphogenesis in the lung. Studies in human adult IPF lungs have shown over-expression of Shh and GLI2 localised to epithelial cells, whereas Patched-1, Smoothened, and GLI1 have been observed mainly in fibroblasts and inflammatory cells but not in normal lung (Stewart, Hoyne et al. 2003). *In vitro,* studies have revealed that Shh is released by human AEC type II cells when stimulated by oxidative injury and inhibited by TGF-β (Bolanos, Milla et al. 2012) and also protected lung fibroblasts from TNF-α/IFN-γ/Fas-induced apoptosis (Pongracz and Stockley 2006).

Shh pathway is activated in IPF lungs and may contribute to the pathogenesis of fibrosis by increasing the proliferation, migration, extracellular matrix production, and survival of fibroblasts (Kugler, Joyner et al. 2014). This pathway may be a promising therapeutic approach for IPF.

1.4.4 WNT pathway

WNT signalling pathway plays an important role in normal cellular differentiation and proliferation. This pathway is also critical for the development of many organs including the lung. Studies in mouse models of pulmonary fibrosis have revealed that a WNT target gene, WNT1-inducible signalling protein (WISP1), was increased in ATII cells, which led to increased proliferation EMT. In addition, this resulted in enhanced deposition of ECM components (Konigshoff, Kramer et al. 2009). In the same model, neutralising monoclonal antibodies specific for WISP1 reduced the expression of genes characteristic of fibrosis and reversed the expression of genes associated with EMT; hence this led to decreased collagen deposition and improved lung function and survival. It can be stated that WISP1 may be a key regulator of ATII cells suggesting that this pathway may be important in fibrosis (Konigshoff, Kramer et al. 2009).

1.5 IPF models

1.5.1 In Vitro Models

The use of *in vitro* models is often favoured to *in vivo* and subsequent clinical studies. *In vitro* models provide useful information regarding the development and progression of the disease, in particular, the development of fibrosis. Usually the model is heavily dependent on human cells and tissues to ensure many of the physiological parameters are maintained in the *in vitro* model systems. Typical *in vitro* system modelling involves explants of lung tissue or cultures of inflammatory and mesenchymal cells obtained from animal models or patients with pulmonary fibrosis and from the lungs of control subjects without pulmonary fibrosis.

Primary cell cultures are obtained from either a healthy or diseased lung tissue allowing the cells to keep their functional differentiated state for a short period (days to weeks). The use of fibroblast cultures has allowed assessment of the characteristics of fibroblasts or myofibroblasts in IPF and other interstitial diseases

(Marshall, Gohlke et al. 2004). Another important cell type used is the type II alveolar epithelial cells. These cells are difficult to obtain from human tissue. However, they can be derived by biological manipulation, such as the A549 cell lines which are tumour derived. (Prasad, Hogaboam et al. 2014). Macrophages also participate in the fibrotic process and are obtained from bronchoalveolar lavage in patients or in animals in which pulmonary fibrosis has been induced (Drakopanagiotakis, Xifteri et al. 2008).

Another method which is used to simulate the environment that could occur in the lung tissue of patients with pulmonary fibrosis is the use of cell co-cultures. Usually a Transwell® system is used to allow 2 types of cells to be cultured together in a non-contact method. This method can be used to analyse the effect of various individual cell types and can allow identification of diverse mediators that are secreted and involved in fibrogenesis. Using this type of method has allowed others to the study the interaction between alveolar epithelial cells and fibroblasts or myofibroblasts in culture, (Prasad, Hogaboam et al. 2014) or to observe the interaction between macrophages, epithelial cells, and fibroblasts (Prasse, Pechkovsky et al. 2006).

The development of pulmonary models using *in vitro* models began in the 1990s (Sporty, Horalkova et al. 2008) and despite the large number of pulmonary *in vitro* models, currently there are no validated *in vitro* models of pulmonary fibrosis. However, using this co-culture method does provide an insight into the phenomena that occur in patients with fibrosis.

1.5.2 Animal Models

Animal models play an important role in the study of diseases, and many models have been established to examine pulmonary pathology. The situation with IPF is even more complicated, as the aetiology and natural history of the disease is uncertain and no single cause is known to induce IPF in animals (Moeller, Ask et al. 2008).

Numerous animal models of pulmonary fibrosis have been developed over the years to mimic features of IPF. These models include fluorescein isothiocyanate (FITC),

radiation damage, instillation of bleomycin, silica or asbestos and transgenic mice or gene transfer of human fibroblasts into immunodeficient mice. However, the best method for bleomycin-induced pulmonary fibrosis are murine models (Moore and Hogaboam 2008).

Bleomycin (BLM) is a chemotherapeutic antibiotic used to treat lymphoma, squamous cell carcinomas, germ cell tumours and malignant pleural effusion. This drug was discovered in 1962 and was reported by *Umezawa et al,* (Umezawa, Ishizuka et al. 1967). BLM is a water-soluble glycopeptidic antibiotic and is isolated from bacterium *Streptomyces verticillus* (Moeller, Ask et al. 2008).

Bleomycin is thought to cause single and double-strand DNA breaks in a process dependent on the presence of both molecular oxygen and a metal ion. In the presence of a reducing agent, Fe (III) is substituted by Fe (II). BLM forms a complex with Fe(II), which is subsequently oxidized to Fe(III) in presence of O_2, resulting in the reduction of oxygen to free radicals. A ternary complex BLM–Fe (II)–O_2 is formed with a nucleophilic bond (Figure 1-2). Depending on the presence or absence of oxygen, a nucleophilic attack on the bond results in a break in the DNA strand and as a consequence, free radicals are produced that ultimately lead to cell death (Della Latta, Cecchettini et al. 2015).

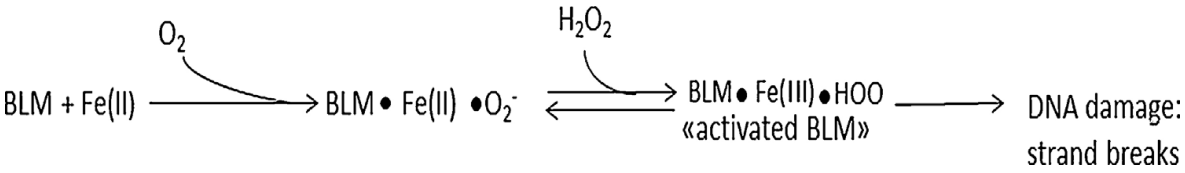


Figure 1-2: Activation of BLM by oxgyen and iron (Della Latta, Cecchettini et al. 2015)

Bleomycin-induced pulmonary fibrosis in murine model is the best described inducer of experimental pulmonary fibrosis. The model involves a single intratracheal or intranasal delivery of bleomycin to the lung. This insult is based on a dose-dependent damage to the lung, characterised by inflammatory cell infiltrates, collagen deposition, and parenchymal consolidation similar to human IPF. The mice lungs are generally studied 7–14 days following a single insult to study the resolution phase of the initial inflammatory phase, and 21-28 days following insult to investigate the fibrotic phase. Using the bleomycin model, there are several obvious and substantial differences compared to human idiopathic pulmonary fibrosis (IPF). The most relevant limitation is that the progression and rate of the disease development is different from human disease. IPF is a chronic disease that develops over a long time span, whereas the conventional single insult bleomycin model is generally studied less than a month following an acute lung insult (Chung, Monick et al. 2003).

Nevertheless, the bleomycin induced pulmonary fibrosis model is very useful to illustrate pathogenesis *in vivo* and to identify cell–cell interactions, mediators and signalling pathways that can contribute to fibrotic changes in mice. The murine model (using different insults) can provide an insight to understand the similarities and differences between pulmonary fibrosis of known etiology and Idiopathic pulmonary fibrosis. However, in humans it is difficult to identify these changes until the last stages of the disease and this limits the use of treatment available (Walters, Cho et al. 2008).

1.6 Gene Expression

IPF is a lethal interstitial lung disease, which is poorly understood (Katzenstein and Myers 1998). Expression profiling can provide information on a genome-level, which has been applied successfully to multiple diseases (Kaminski and Rosas 2006). This type of information can generate thousands of candidate genes, key regulators and protein networks which can identify the involvement of particular pathways in various diseases. Another important application of gene expression is that it can generate and verify new hypotheses, which can be critical to the development of new diagnostic and therapeutic approaches. Despite the fact that expression profiling is a useful tool to understand lung fibrosis, the amount of data available is limited.

1.6.1 Microarray Analysis of Pulmonary Fibrosis

Murine bleomycin-induced models are commonly used to study the mechanism of IPF, but with limitations. To study IPF on a gene expression level, techniques have been developed where RNA and microRNA extracts from IPF lung samples can be analysed. The analysis can be complex, but this strategy contributes to identifying genes that are up regulated or down regulated. This can suggest possible future targets (du Bois 2010). An example of this approach was the MMP-7 gene. This gene was shown to be up-regulated in IPF and the protein encoded by this gene was found to be localised in IPF epithelial cells of IPF patients (Rosas, Richards et al. 2008). Transgenic Wnt reporter mice were used to characterise the expression pattern of cyclin Dl, MMP-7, and TGF-β determined by the activation of Wnt/ β-catenin signalling pathway, in bleomycin-induced lung fibrosis (Liu, Carron et al. 2009).

Another example is insulin-like growth factor (IGF-I). Using microRNA profiling of mouse bleomycin-induced pulmonary fibrosis, combined with gene expression profiling data, has enabled identification of the IGF-1 pathway in pulmonary fibrosis. This pathway is involved in directly stimulating proliferation and collagen synthesis of fibroblasts hence promoting fibrosis (Honeyman, Bazett et al. 2013). In comparison to patients with IPF, *Krein et al* 2003, had shown using immunohistochemistry of 8 patient biopsy specimens that IGF-I and CD68 immunoreactivities correlate positively in the lung specimens. Previous reports have shown that macrophages secrete enhanced levels of IGF-I protein in fibrotic lung diseases. In addition, macrophages have been shown to possess mRNA for IGF-I (ref), implying that macrophages might be an important source of IGF-I in IPF patients (Krein and Winston 2002).

Taken together with the microarray data for bleomycin-induced mice and immunohistochemistry/ RT-PCR data from human patients, neither of the methods provides a full picture of the processes and identification of growth factors or pathways. However, both approaches are important to get as many answers as possible.

1.7 A novel therapeutic target in IPF

While the pathogenic mechanisms involved in IPF are not well understood, studies have suggested that repetitive lung injury can initiate a series of events which can lead to the activation of myofibroblasts, accumulation and remodelling of the ECM (Fernandez and Eickelberg 2012).

TGF –β is the most researched potential mediator known in IPF. In the lungs, TGF-β is produced by a wide variety of cell types, including alveolar macrophages, neutrophils, activated alveolar epithelial cells, endothelial cells, fibroblasts, and myofibroblasts. In these cells, TGF-β also stimulates expression of a number of pro-inflammatory and fibrogenic cytokines, including TNF-α, PDGF, IL-1β, EGFR or IL-13, thereby further enhancing the fibrotic response (Fernandez and Eickelberg 2012)

Studies have shown 'crosstalk' of TGF-β with developmental pathways (Wnt, Sonic Hedgehog, and Notch) and the implication in the pathogenesis of IPF. *Aoyagi-Ikeda et al*, showed that Notch signalling induces increased myofibroblast differentiation via TGF-β–induced EMT in a rat model. The data also indicated that Notch is required for α-SMA overexpression via TGF-β/Smad3 signalling and gene transcription in ATII cells (Aoyagi-Ikeda, Maeno et al. 2011). *Konnigshoff et al*, showed Wnt/β-catenin activation in IPF which may play a key role in epithelial injury and epithelial–mesenchymal crosstalk. A Wnt target gene, Wnt-1–inducible signalling protein-1 (WISP-1) was blocked with a monoclonal specific antibody and the amount of bleomycin-induced fibrosis was attenuated (Konigshoff and Eickelberg 2010). *Zhou et al*, reported that gene induction of α-SMA was mediated by Wnt/ β-catenin, CREB binding protein, and TGF-β in a Smad3 dependant manner. These data revealed that the inhibition and knockdown of Smad3, knockdown of β-catenin and overexpression of inhibitor of β-catenin and TCF (ICAT), can terminate the effects of TGF-β1 on α-SMA transcription/expression, indicating a requirement for β-catenin in these Smad3-dependent effects. This could provide a new target to develop efficient therapies for IPF (Zhou, Liu et al. 2012).

Another study revealed that TGF-β1 mediates a response to epidermal growth factor receptor (EGFR) signalling by induction of amphiregulin, a ligand of EGFR, which may be a potential therapeutic target for idiopathic pulmonary fibrosis associated with TGF-β1 activation (Zhou, Lee et al. 2012). In addition, chitotriosidase (Chit1), a true chitinase in humans, was associated with TGF-β1 signalling, and sensitised TGF-β1 signalling by enhancing TGF-β1 receptor expression and activation of mitogen-activated protein kinase (MAPK)-Erk signalling. This could be a new biomarker and therapeutic target of scleroderma-associated pulmonary fibrosis (Lee, Park et al. 2014).

TGF-β is a pleiotropic growth factor with chemotactic and proliferative properties, suggesting it plays a major role in in the fibrotic process in pulmonary fibrosis and is a potential therapeutic target. Studies in mice and humans have shown to inhibit TGF-β and can be evaluated by a list of ongoing trials investigating the efficacy of new molecules in IPF (https://clinicaltrials.gov). Pirfenidone has been proven to have an antifibrotic and anti-inflammatory effect by attenuating TGF-β production and action (Cottin 2012). STX-100X is a monoclonal antibody blocking αVβ6. STX-100X inhibits TGF-β activation at the site of injury. This therapy proved to be effective in blocking αvβ6-mediated TGF-β activation and successfully prevented the development of pulmonary fibrosis in two different mice models of fibrotic injury (Horan, Wood et al. 2008), (Puthawala, Hadjiangelis et al. 2008). Evidence suggests that TGF-β is a central player in fibrosis and an attractive therapeutic target to control fibroproliferation in IPF (Fernandez and Eickelberg 2012).

1.8 Approved oral therapies

IPF is an age-related condition with approximately 0.2% of patients older than 75 (Raghu, Chen et al. 2014). The nature of the stimuli that triggers the fibrotic process in IPF is still unknown. Several factors have been associated with an increased risk of developing the disease, including cigarette smoking, environmental/ occupational pollutants, microbial agents, chronic microaspiration secondary to gastroesophageal reflux, and genetic abnormalities (Spagnolo, Rossi et al. 2014). The disease is severely progressive with approximately a 5-year survival (King, Schwarz et al.

2001). IPF is characterised as a highly variable and heterogenic clinical disease which makes the natural history of the disease largely unpredictable in individual patients (Ley, Collard et al. 2011).

The understanding of IPF pathobiology has significantly improved over time, and approach to treatment has shifted. Previous IPF treatment hypothesis were based on inflammation, recommending corticosteroids in addition to cytotoxic agents, such as Prednisone, Azathioprine, and *N*-Acetylcysteine. However, few patients responded to anti-inflammatory therapies and the prognosis remained poor (clinical trial; PANTHER-IPF), (Raghu, Anstrom et al. 2012).

Current concepts suggested that persistent micro-injury to alveolar epithelial cells induces a fibrotic response. The growth factors and cytokines secreted by the injured epithelial cells promote fibroblast recruitment, proliferation, and differentiation to invasive myofibroblasts (Selman and Pardo 2014). In turn, actively proliferating fibroblasts and myofibroblasts organize into *fibroblastic foci* and are responsible for the excessive collagen production that results in scarring of the lung and architectural distortion (Selman and Pardo 2014), (Spagnolo, Sverzellati et al. 2015).

More recently, clinical trials have shifted their focus from anti-inflammatory and immunosuppressant drugs to anti-fibrotic drugs. Recent advances have shown a number of mediators, growth factors, and signalling pathways involved in the fibrotic process in IPF (Figure 1-3). Therefore, there may be other pharmacological treatments of IPF to target before lung transplantation (Raghu, Collard et al. 2011).

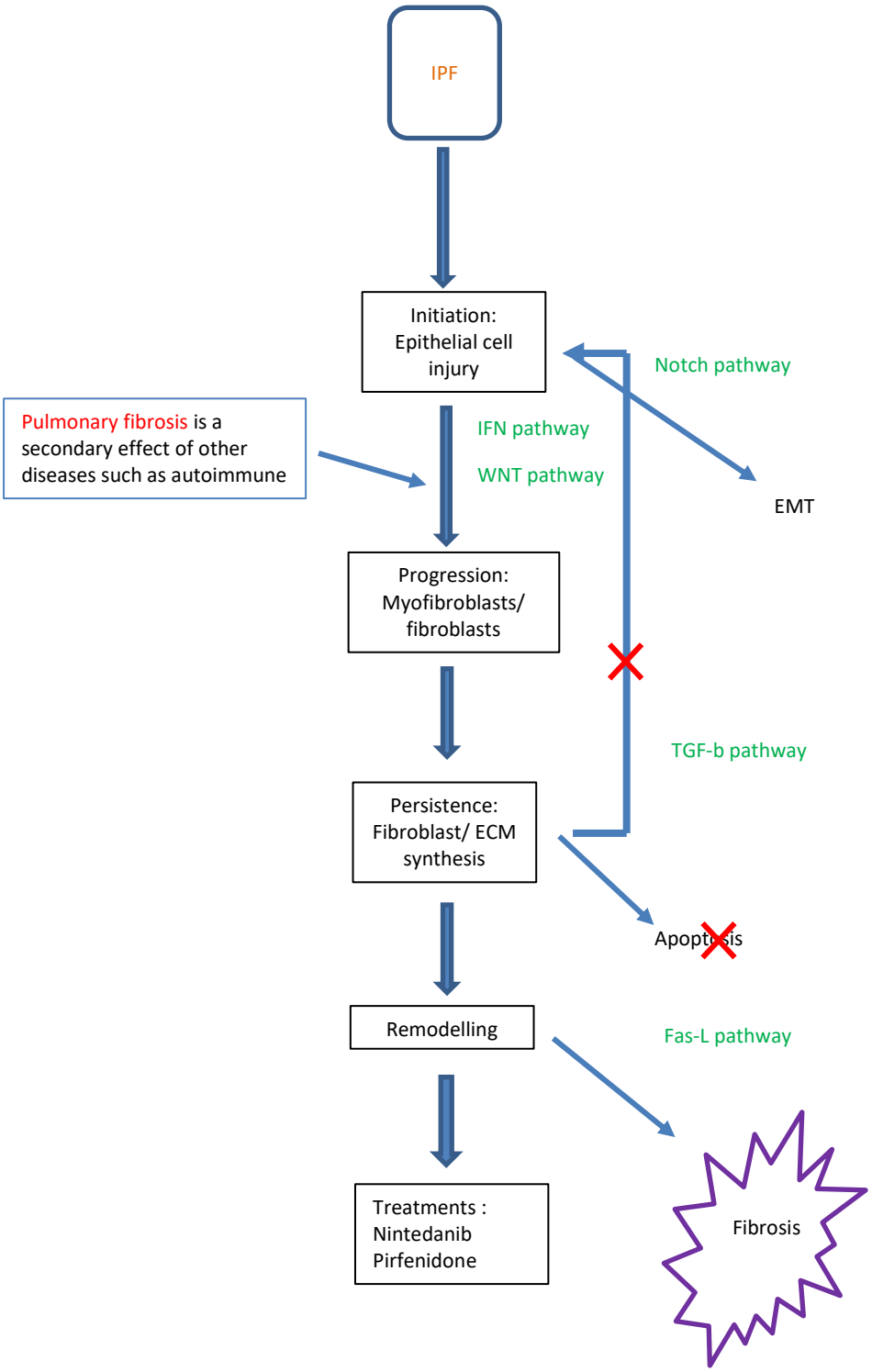


Figure 1-3: Signalling pathways involved idiopathic pulmonary fibrosis. In Idiopathic pulmonary fibrosis (IPF), the cause of injury unknown; however, it can be triggers by environmental exposures, viruses, smoking or acid reflux. All these can initiate a cascade of events and activate pathways. The initiation occurs when there is epithelial injury by an unknown cause. The injury response can triggers pathways such as IFN pathway or WNT pathway. The WNT pathway is involved in the progression of the fibroblasts. The fibroblasts differentiation into myofibroblasts. The TGF-β pathway is involved in the persistence of the myofibroblasts in which ECM is synthesized and remodelling of the lung occurs. Apoptosis is inhibited. Pulmonary fibrosis is a secondary effect of other diseases such as SSc. In both cases the end result is very similar as are the drugs used to slow down the progression of the disease.

Nintedanib is licensed for the treatment of mild to moderate IPF. Nintedanib is an indolinone derivative and is an intracellular inhibitor of tyrosine kinases, including fibroblast growth factor receptor 1, 2 and 3, platelet-derived growth factor receptor α and β, and vascular endothelial growth factor receptor 1, 2 and 3 (Wollin, Maillet et al. 2014). Nintedanib competitively binds to the adenosine triphosphate inhibiting a number of downstream signalling cascades such as fibroblast proliferation, migration and differentiation and the secretion of extracellular matrix (Wollin, Wex et al. 2015). Studies in bleomycin mouse models and silica-induced lung fibrosis have demonstrated antifibrotic and anti-inflammatory activity of nintedanib. The effect is the reduction in numbers of lymphocytes and neutrophils in bronchoalveolar lavage fluid, reducing levels of inflammatory cytokines in lung tissue, and diminishing lung inflammation, granuloma formation and fibrosis (Wollin, Maillet et al. 2014).

Pirfenidone is a medication used for the treatment in IPF. The drug has anti-fibrotic, anti-inflammatory and anti-oxidant properties. *In vivo* studies have shown Pirfenidone was able to attenuate BLM-induced lung fibrosis and to reduce PDGF and TGF- β levels in the lungs. The anti-inflammatory properties of the drug are manifested by attenuation in TNF- α and IFN- γ levels in experimental models of inflammation. *In vitro*, it has been demonstrated to inhibit fibroblast proliferation and collagen synthesis, as well as TGF-β expression (Datta, Scotton et al. 2011). Another study explored the role of Pirfenidone in the suppression of fibrocyte accumulation in the lungs in response to systemic administration of BLM in a murine model. The drug was able to decrease the fibrocyte content via the attenuation of Chemokine Ligand-2 (CCL2) and Chemokine Ligand-12 (CCL12) production (Inomata, Kamio et al. 2014) . *Hisatomi et al.* also studied the role of Pirfenidone in BLM-induced lung fibrosis, showing that this drug inhibited the over-expression of collagen type I and HSP47, a collagen-specific molecular chaperone that is always expressed in and around the fibrotic lesions (Hisatomi, Mukae et al. 2012). Following these studies on animal models, Pirfenidone was the subject of several trials in IPF, and it is now commercially available for the treatment of IPF.

The use of experimental animal models has allowed the identification of specific patterns and mechanisms of BLM-induced lung fibrosis, such as the role of

inflammation (Ward and Hunninghake 1998), epithelial–mesenchymal transition (Chapman 2011), the activation of fibroblasts to myofibroblasts (Tanjore, Xu et al. 2009), the formation of fibroblastic foci (Cool, Groshong et al. 2006), basement membrane damage (Singer, Kawka et al. 1986), injury and apoptosis of alveolar epithelium (Plataki, Koutsopoulos et al. 2005), turnover and remodelling of extracellular matrix (ECM) components (Cox and Erler 2011). Animal studies have shown the importance of the initial development of fibrosis (Della Latta, Cecchettini et al. 2015), as well as studying the effects of potential drugs against IPF. In recent years, animal studies have been used to investigate two oral therapies, Nintedanib and Pirfenidone which have been approved for clinical trials (ASCEND ClinicalTrials.gov), so far they have only been able to slow the progression of the disease (Raghu and Selman 2015). The usages of *in vivo* models have limitations, usually caused by the species-specificity of many molecules. Thus, using an *in vitro* model system may enable us to understand cell-cell contact, the crosstalk of epithelial cells and fibroblasts.

1.9 Aims and Hypothesis

The hypothesis is that epithelial injury will affect fibroblast behaviour to generate a profibrotic response which will increase fibroblast proliferation, promote ECM synthesis and inhibit apoptosis in a 3D co-culture system.

The aim of the project was to develop a human epithelial and fibroblast 3D co-culture system to study epithelial-mesenchymal interactions which contribute to the development of fibrosis after chronic epithelial injury. Epithelial mediators were to be identified by transcriptional profiling and therefore, would enable the identification of any novel mediators released during epithelial-mesenchymal interactions. This 3D model could reduce the need for animal models in research and be used in fibrosis research to identify potential therapeutic interventions.

The specific aims of the thesis were:

1. To develop an epithelial /mesenchymal 3D co-culture system to mimic an *in vivo* microenvironment.
2. To examine the effect of epithelial wounding on fibroblast proliferation, apoptosis and ECM synthesis in the 3D co-culture model.
3. To examine the effect of epithelial wounding on fibroblasts by transcriptional profiling.
4. To manipulate epithelial mediator release in response to injury and study the effect on fibroblast behaviour.

Chapter Two

Materials and Methods

2.1 Materials

All materials used throughout this thesis are listed below.

2.1.1 Consumables

- Haemocytometer — Fisher Scientific
- 25 and T75 cell culture flasks — Costar, Corning, Netherlands
- 24 well plates — Fisher Scientific
- 24 Transwell® plates with 0.4um pore — Fisher Scientific

2.1.2 Reagents/Chemicals

- Bleomycin — Kyowa,
- β-mercaptoethanol — Sigma-Aldrich, M6250
- Bovine Serum Albumin (BSA), protease-free — Sigma-Aldrich, A3059
- Carbon black particles (90) — Degussa Corp, Germany
- Celltracker Probes (Green-CMFDA) — Invitrogen, C7025
- Collagen Type 1 — Sigma-Aldrich, C7761
- Citrate Buffer, pH 6.0, 10× — Sigma-Aldrich, C9999
- Coomassie blue stain — BDH, 443283M
- DAPI — Sigma-Aldrich, D9542
- DEPC-treated water — Invitrogen, 75-0024
- Developer and replenisher, — Sigma-Aldrich, P7042
- Donkey Serum — Immunocruz, 12710
- Dulbecco's Modified Eagle's medium (DMEM) — Sigma-Aldrich, D5796
- Dulbecco's Modified Eagle's medium (DMEM/F12) — Invitrogen, 11039-021
- Dimethyl Sulphoxide (DMSO) — Sigma-Aldrich, 154958
- ECL — GE Healthcare, RPN-2209
- Eosin Y solution — Sigma-Aldrich, T115
- Fetal Calf Serum (FCS) — Sigma-Aldrich, F-7524
- Filter paper — Biorad, 1703965
- Fixer and replenisher, — Sigma-Aldrich, P8307
- Formaldehyde (37 wt. % solution in H2O) — Sigma-Aldrich, 533998
- Gel: Mini-PROTEAN TGX, 4-15% — Bio-Rad Labs 4561084S
- Glacial acetic acid — Fisher Scientific,A/0400/PB17
- Goat serum — Sigma-Aldrich, G6767
- Hematoxylin — Sigma-Aldrich, 51275
- HEPES — Sigma-Aldrich, H3784
- Human IL-1α — R&D systems, DY200
- Human Total MMP-1 Duoset — R&D, DY901
- Human Total MMP-2 Duoset — R&D, DY902
- Human Total MMP-7 Duoset — R&D, DY907
- Human Total MMP-9 Duoset — R&D, DY909
- Hydrogen peroxide — Sigma-Aldrich, H1009
- Impact DAB — Vector Lab, SK4105
- *In Situ* Cell Death Detection Kit, Fluorescein — Roche, 11684795910
- Interferon α rat (IFN-a) — Sigma-Aldrich, I8657
- Methanol — Fisher Scientific, M/4000/17
- MTT — Sigma-Aldrich, M5655
- Penicillin streptomycin — Sigma-Aldrich, P4333
- Phosphate Buffered Saline (PBS) — Oxoid, BR0014
- Photographic film (Hyperfilm) — GE Healthcare, 28906837
- Platelet Derived Growth Factor (PDGF) — PeproTech, 100-14B
- Precision Plus Protein Standards (kaleidoscope marker) — Bio-Rad, 161-0375
- PVDF membrane — GE Healthcare, RPN303F
- Restore stripping Buffer. — Fisher scientific, 21059
- RNeasy® Mini Kit — Qiagen, 74104
- SeeBlue Plus 2 prestained standard — Invitrogen, LC5925
- Small Airway Epithelial Cell Basal Media — Lonza, CC2547

- Small Airway Epithelial Growth Media — Lonza, CC331
- Spectra Protein ladder — Thermo scientific, 26634
- Staurosporine from Streptomyces — Sigma-Aldrich, S5921
- Superscript™ First-Strand Synthesis System for RT-PCR kit — Invitrogen, 11904-018
- Triton X-100 — Sigma-Aldrich, 9002-93-1
- Tris-Gly SDS zymogram running buffer — Invitrogen, LC2675
- Tris-Gly SDS zymogram sample buffer — Invitrogen, LC2676
- Trypsin-EDTA — Sigma-Aldrich,
- Tween® 20 — Sigma-Aldrich, P7949
- VectaMount Permanent Mounting Medium — Vector Labs, H-5000
- Zymogram renaturing buffer — Invitrogen, LC2670
- Zymogram developing buffer — Invitrogen, LC2671
- Zymogram pre-cast gelatin gels — Invitrogen, VXEC6175BOX

2.1.3 Antibodies

- Anti-Ki-67 — Dako,
- Anti-mouse Alexa-488 (FITC) — Invitrogen,
- Anti CEBP-Alpha (raised in Mouse) — Abcam, ab128482
- Anti-α smooth muscle actin clone 1A4 — Sigma-Aldrich, A2547
- Anti-Endothelin 1 (raised in Rabbit) — Abcam, 117757
- Anti-IRF9 (raised in Rabbit) — Sigma-Aldrich,HPA0001862
- Anti-mouse Ig — Vector Labs, MP-7402
- Anti-rabbit Ig. — Vector Labs, MP-7401
- Anti-rabbit IgG (PGAR) — Sigma-Aldrich, A5045
- Caspase 3 (Total) — Cell signalling tech, 9664
- Caspase 3 (Uncleaved) — Cell signalling tech, 9662
- Caspase 7 (Uncleaved) — Cell signalling tech, 9492
- Caspase 9 (Uncleaved) — Cell signalling tech, 7237
- Fas-Ligand — R&D, 126-FL-010/CF
- PARP (Total) — Cell signalling tech, 9542
- PARP (Uncleaved) — Cell signalling tech, 5625
- Recombinant Human TNF-alpha Carrier Free — R&D, 210-TA-010/CF
- Recombinant Mouse IFN-gamma Carrier Free — R&D, 485-MI-100/CF
- Recombinant IL-6 — R&D, 206-IL-01

2.2 Methods: Cell Culture

2.2.1 Recovery of cryo-preserved Primary Human Cells

Normal Human Lung Fibroblasts (NHLFs) were used through-out the project. These were primary human cells established from normal lung tissue of a 61 year old male, non-smoker, and were obtained commercially from Lonza (CC-2512, Lot no: 0000204947) at passage 2.

The epithelial cells used in this project were Small Airway Epithelial cells (SAEs), which were primary human cells established from normal lung tissue of a 61 year old male, non-smoker, and were obtained commercially from Lonza (CC-2547, Lot no: 0000105938) at passage 2. Both primary cells were from the same donor.

The frozen cells were introduced back into culture by thawing the cryovials at 37^{o}C. The cells were thawed, using their own specific media. NHLFs were diluted in FGM (Fibroblast Growth Media) with bulletkit from Lonza, which was prepared by adding the singlequots® supplements (Table 2-1). The SAEs cells were diluted in SABM (Small Airway Basal Media) with bulletkit from Lonza, which was prepared by adding the singelquots® supplements (Table 2-2), making up SAGM (Small Airway Growth Medium). The cells were seeded into a T-25 flask and medium was changed after 24 hours.

Table 2-1: The components of FGM-2 bulletkit (Lonza; Cat no: CC-3132)

Singelquot	**Amount**
hFGF	0.5ml
Insulin	0.5ml
Fetal Bovine Serum (FBS).	10ml

Table 2-2: The components of SAGM bulletkit (Lonza; Cat no: CC-3118)

Singlequot	**Amount**
Bovine Pituitary Extract (BPE)	2ml
Hydrocortisone	0.5ml
hEGF	0.5ml
Epinephrine	0.5ml
Transferrin	0.5ml
Insulin	0.5ml
Retinoic Acid	0.5ml
Triiodothyronine	0.5ml
Fatty Acid Free (BSA-FAF).	5ml

2.2.2 Harvesting of Primary Human Cells

Cells were cultured in T-25 cell culture flasks. When the cells reached confluency, they were dissociated by rinsing with 500μl of warm 1x Trypsin-EDTA solution for 30 seconds which was aspirated off. This was followed by adding 2ml of fresh trypsin to the T-25 flask or 5ml to a T-75 flask and left until cell-substrate attachments were loosened. The flask was slightly tapped to loosen the cells from the plastic. Trypsin was then neutralised by adding 4mls of trypsin inhibitor; and cells were re-suspended in fresh SAGM and collected by centrifugation at 200 *g* for 5 minutes at room temperature. The cell pellet was then re-suspended in the desired media at the appropriate cell density required and seeded into appropriate new cell culture flasks or plates. All cells were incubated at 37^{o}C in humidified 5% CO_2 incubator.

2.2.3 Maintenance of Primary Human Cells

Normal human lung Fibroblasts and Small Airway Epithelial cells were cultured in their specific bullet kits, (refer to section 2.2.1). Gentamicin-1000 was not added as it can affect the growth of cells and therefore, was substituted with 1%v/v Penicillin Streptomycin. Cells were passaged when they reached 80-90% confluency. The cells were harvested (refer to section 2.2.2) and seeded into plates depending on the experiment to be carried out or cryopreserved.

2.2.4 Determination of cell counts

Cell counts were routinely determined prior to seeding cells into fresh media as required in order to maintain a constant cell number for each experiment. After harvesting and re-suspending, 20μl aliquot of cells were placed in the chambers of a Neubauer Haemocytometer (Figure 2-1). Cells in one quadrant of the grid were counted and multiplied by 10^4 to give the number of cells per ml. Volumes of cells were then adjusted to give the desired seeding densities.

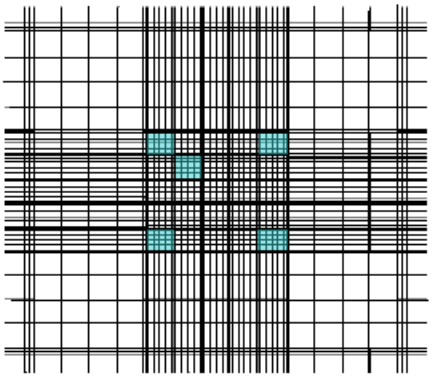


Figure 2-1: Haemocytometer grid layout

2.2.5 Cryopreservation of cells

Approximately $3x10^6$ cells per ml were harvested (refer to section 2.2.2). The cells were centrifuged at 200 *g* for 5 minutes at 37°C and re-suspended in ice-cold Freezing Medium (FCS+10% DMSO). Cells were placed in a sterile cryovial and immediately stored at -80°C for 48 hours and then transferred for storage in liquid nitrogen (-179°C).

2.3 Optimising Primary Human cells

2.3.1 Optimising fibroblasts in 3 dimensional gels

Collagen I is an extracellular matrix component derived from rat tail tendon, mainly consisting of collagen type I which is commercially available from Roche. The stock concentration of collagen was 3.3 mg/ml. The collagen was dissolved in sterile 0.2%v/v acetic acid and left to dissolve overnight at room temperature on a rocker. The collagen was neutralised with sterile 10x DMEM with sodium bicarbonate pH7.4, 0.2M Hepes and 10N sodium hydroxide, giving a final concentration of 2.4mg/ml kept at 4°C.

The cells were optimised using a range of concentrations from $5x10^4$, $2.5x10^5$, $5x10^5$ and $7.5x10^5$ cell numbers. This was to determine which concentration of cells would produce a confluent layer of cells without contracting the collagen after 7 days. The cells were harvested and counted for each cell number (ref to section 2.2.2 and 2.2.4). Cells at different concentrations were placed in a 5ml bijoux container, containing 500µl of collagen, vortexed and kept on ice. Approximately 400µl of

collagen with cells was pipetted in the 24 well plate in triplicate for each cell concentration and allowed to set in the incubator at 37°C + 5%v/v CO_2 for an hour. Once the collagen had set, 500µl of DMEM F/12 was added and the plate returned to the incubator at 37°C + 5% CO_2 for 7 days. The gels were observed using a light microscope at day 1, day 4 and day 7.

2.3.2 Optimising Small Airway Epithelial Cell in Transwells®

To examine how the SAEs behave, various cell numbers were inserted into a 24 well Transwell® plate. The epithelial cells were seeded on the 24 well insert in triplicate at various cell numbers with serum free SAGM added to the top and bottom of the well and placed in the incubator at 37°C + 5% CO_2 for 24 hours to adhere. The wells were observed using a light microscope at day 1, day 4 and day 7.

2.3.3 CellTracker Probes

To investigate whether epithelial cells were migrating through the pores, a celltracker green CMFDA dye was added to the cells. The Celltracker probes are reagents that are fluorescent chloromethyl derivatives that freely diffuse through the membranes of live cells. Once inside the cell, the thiol-reactive probe undergoes a glutathione *S*-transferase–mediated reaction to produce membrane-impermeant glutathione–fluorescent dye within the cells.

Cells were added to the insert of the Transwell® with serum-free medium and left to adhere for 24 hours in the incubator at 37°C + 5% CO_2. After 24 hours, prewarmed celltracker green CMFDA dye at 20µM was added to the cells and left for 30 minutes in the incubator at 37°C + 5% CO_2. The plate was replaced with fresh medium and was observed every day for 7 days without replacing fresh medium. Images were observed using a Nikon Diaphot 300 with epifluorescence.

2.4 Co-culture of NHLFs and SAEs

To investigate the effect of epithelial cells and fibroblast cells in 3D co-culture system. The cells were individually harvested and counted (refer to section 2.2.2, 2.2.3 and 2.2.4). Fibroblasts mixed in with the collagen were plated at $5x10^5$ cells onto the bottom of the wells with serum free DMEM/F12 and allowed to polymerize in the incubator at 37°C + 5% CO_2 for an hour. After an hour, DMEM/F12 was added and incubated 37°C + 5% CO_2 for 24 hours. Epithelial cells were seeded on the insert with 0.4μm pore size and allowed to adhere for 24 hours before adding the insert on the fibroblasts. After 24 hours, inserts containing epithelial cells were added to the fibroblasts in collagen with serum free DMEM/F12 (Figure 2-2). Images were taken at day 1, day 4 and day 7 with a Nikon Diaphot 300 inverted phase contrast microscope.

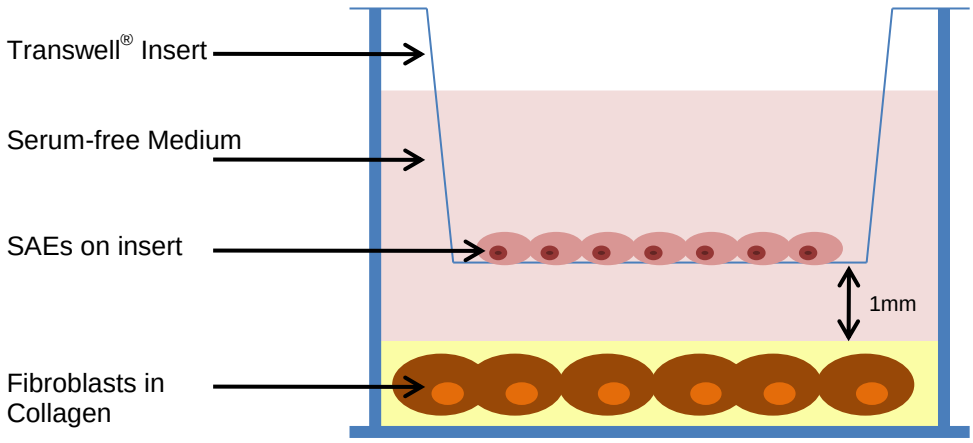


Figure 2-2: A diagram to represent co-culture model of epithelial and fibroblast cells. Small Airway Epithelial cells (SAEs) on a 0.4μm pore insert and Fibroblasts in the well below. Cultured *in vitro* in Transwell® plate with serum free medium for 7 days.

2.4.1 Scratch wound Injury

Epithelial cells in the inserts had adhered and were of confluent state after 24 hours of seeding. The epithelial monolayer was then subsequently scratched with a p200 pipette tip to one scratch wound in the middle of the insert. After 48 hours, supernatants were removed and kept at -80^{o}C. Fresh serum free medium was added and scratch wounding was repeated. This was done over 6 days.

2.4.2 Bleomycin administration on epithelial cells

Bleomycin was prepared in serum-free DMEM/F12. Bleomycin was not added directly onto the fibroblasts. Bleomycin was only added to epithelial cells in the inserts, every 24 hours for 6 days. A series of inserts were set up, in which epithelial cells were exposed to bleomycin, (Table 2-3).

After 24 hours, the bleomycin was washed off with PBS and replaced with DMEM/F12. The insert was then placed on the fibroblast-collagen gel and left for 48 hours. After 48 hours, supernatants were removed and kept at -80^{o}C. Fresh serum free medium was added and bleomycin inserts were added on the fibroblast/collagen gels. This was done over 6 days. The experiments were carried out in triplicate; (n=3).

2.4.3 Carbon Particles addition

Carbon black particles were prepared (2mg/ml) in serum-free SABM. The carbon black particles were added to the epithelial inserts at various concentrations (Table 2-3). After 48 hours, supernatants were removed and kept at -80^{o}C. Fresh serum-free medium was added. This was done for 6 days. The wells were observed using a light microscope at day 6.

Table 2-3: Addition of low grade injuries on epithelial cells

Bleomycin Concentration – Addition every 24 hours	Carbon Black Concentration- Addition once
0.5mU/ml	5μg/ml
2mU/ml	25μg/ml
5mU/ml	50μg/ml
25mU/ml	100μg/ml

2.4.4 Releasing the Cells from Collagen the Gel Environment

Type I Collagenase (Sigma) was diluted to a concentration of 200units/ml with serum free DMEM. The gels where then exposed to the collagenase for 1 hour, until the gel had completely dissolved and the resultant media was spun down in the bench top centrifuge at 12,000 rpm for 5 minutes to form a cell pellet. The resultant supernatant was aspirated and discarded leaving the cell pellet.

2.5 Low Grade Injuries on SAEs

The effect of low-grade injury was investigated on epithelial cells in the absence of fibroblasts. The injuries included mechanical and chemical methods (refer to section 2.4). The model was to mimic an *in vitro* response in relation to injury in IPF. In order to determine an inflammatory response from SAEs, IL-1α was measured.

2.5.1 Enzyme-Linked Immuno-Sorbent Assay (ELISA)

For the quantitative determination of human IL-1-α concentrations in cell culture supernatants from low-grade injury samples of SAEs, a commercially available ELISA kit was used. Briefly, this assay involves an analyte-specific monoclonal antibody pre-coated onto a microplate. After the sample had been added, the relevant protein present binds to the antibody. An enzyme-linked analytic-specific detection antibody is added and a substrate solution develops colour (through its digestion by the enzyme) in proportion to the amount of protein present in the sample.

The Human IL-1α Duoset ELISA was used following the manufacturer's protocol in a 96-well microplate. All reagents and equipment were provided with the kit and prepared according to the manufacturer's protocol. Briefly, after reagents, samples, and standards were prepared, 100μl capture antibody was added to each well and incubated overnight at room temperature. Standard controls or samples were then added, and incubated at room temperature for 2-3 hrs according to the specific assay carried out. The wells were washed four times with Wash Buffer (400 μl, 25x concentrated solution of buffered surfactant with preservatives), and desired conjugate was added for 1 hr at room temperature. The wells were washed again, and Substrate Solution was added and incubated for 20-30 min at room temperature

protecting it from the light. Finally, Stop Solution (2 N sulphuric acid) was added to each well and the absorbance was read on a plate reader (Flexstation 3, Molecular Devices, with Softmax pro software) at 450 nm within 30 min. Wavelength correction was done at 540 nm or 570 nm in order to avoid optical imperfections which might occur if the readings were made at only 450. Data analysis was carried out using the ELISA plate reader Softmax pro software. Values for data analysis were done by first creating a standard curve from the standards (Figure 2-3). The standards included using a 4 parametric logistic fitting and which was used to determine the concentration (ng/ml) of IL-1α in the samples and statistical analysis was done using Prism 5.0 software with two-way ANOVA with the Bonferroni post-hoc test.

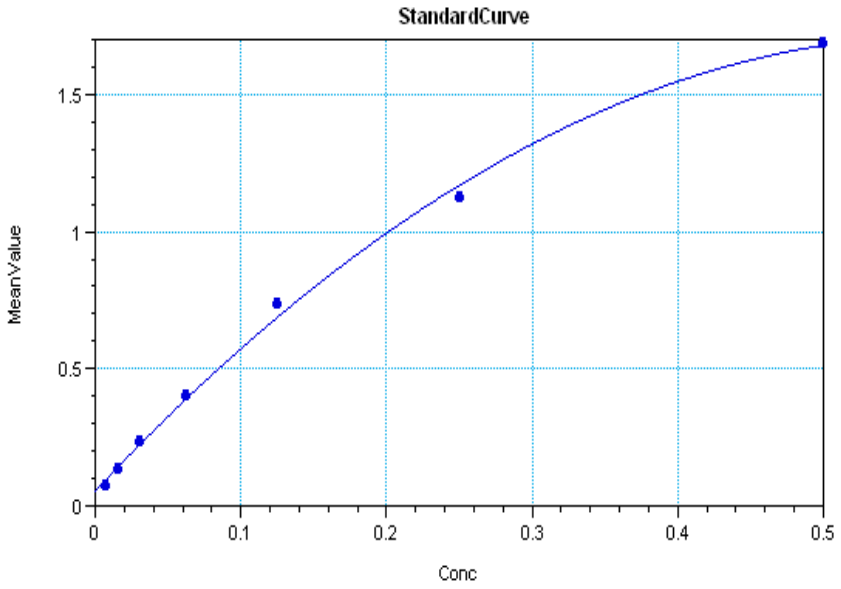


Figure 2-3: A representative standard curve for IL-α.
A standard curve was created from the standards included, using a 4-PL curve fit (4-parameter logistic).

2.5.2 Zymography

Zymography can be used to detect and characterise proteases such as matrix metalloproteinases (Henderson, Markwick et al. 2007). In order, to investigate the presence of a specific protease activity in low grade injury supernatants, the protein is dissolved in a buffer, loaded onto a pre-cast zymogram gel containing the relevant substrate (e.g. gelatin in the case of MMP 2 and MMP 9) and separated by gel electrophoresis. The gels are then incubated overnight at 37^{o}C to allow enzymatic digestion of the substrate and then stained with Coomassie blue, and destained to reveal areas of protease activity as clear bands (Figure 2-4).

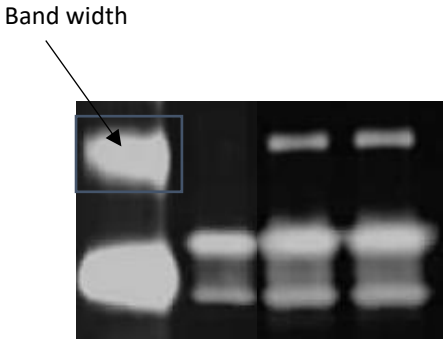


Figure 2-4: A zymogram to determine enzyme activity.
The enzyme activity is measured in the individual bands as demonstrated by a box around the band. Each band is measured and the band width is calculated.

2.5.2.1 Preparing the Samples

Cell culture samples (supernatants) were used undiluted. 10µl sample (diluted as necessary) was mixed with 10µ sample buffer (4% SDS, 0.15M Tris (pH 6.8), 20% (v/v) glycerol, 0.5 % (w/v) bromophenol blue and allowed to stand for 10 minutes at room temperature. 15µl of the sample buffer mix was then loaded onto a pre-cast 15 well Novex polyacrylamide gel supplemented with 0.1% gelatine and run with 1x tris-glycine SDS zymogram running buffer at 125V for 100 minutes.

2.5.2.2 Renaturing and Developing the Gels

The gels were then incubated at room temperature with gentle agitation with 1x zymogram renaturing buffer for 30 minutes. The gels were then equilibrated for 30 minutes with 1x zymogram developing buffer at room temperature and incubated overnight at 37^{o}C with fresh developing buffer. The gels were then stained for 15-30

minutes with 0.5% Coomassie Blue in acetic acid, methanol and water (1:4:5) and destained in acetic acid, methanol and water (1:4:5). The images were photographed and analysed using Syngene GeneSnap 6.0 for densitometry.

2.5.2.3 Recombinant MMP 2 standard

Recombinant MMP 2 (R&D systems) was used as a standard for zymography. To convert the pro–MMP 2 into the activated form, the recombinant MMP 2 was incubated with APMA (4-Aminophenylmercuric Acetate) for 1 hour at 37^{o}C. APMA was used at a working concentration of 1mM. The stock solution was 20mM. This was made by dissolving 35.2mg of APMA in 200µl of DMSO and making up a solution to 5mls with 100 mM Tris HCl. The MMP 2 standard was initially assessed by running a standard curve analysis with increasing concentrations of the standard (Figure 2.5).

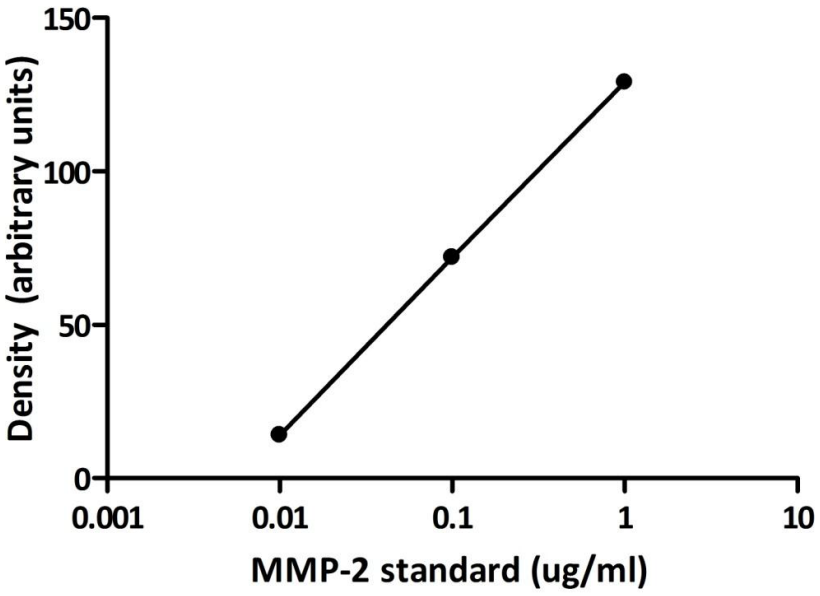


Figure 2-5: Standard Curve for MMP-2 activity

2.5.2.4 Imaging the gels

The gels were imaged and digitally recorded using Gene Genius Bio-Imaging System with GeneSnap 6.00.22 software (Gene Tools; Syngene, Cambridge, UK). The images were saved in TIFF format.

2.5.2.5 Densitometry

The bands were examined with ImageJ 1.46 software (download http://rsbweb.nih.gov/ij/), to measure the density of the bands. The largest destained area was selected using the region of interest with a rectangular selection tool. The same region of interest was then applied to all other bands and the mean density was again determined. Results were plotted as mean $\pm$ SEM and are comparable within experiments.

2.6 Cell Proliferation

2.6.1 Immunostaining

The cells were cultured in a 24 well plate for 2 hours, 1 day, 4 days and 7 days using phenol red free DMEM/F-12 medium. At each timepoint the supernatants were aspirated and the cells in each well were fixed for a minimum of 24 hours at 4^{o}C with 500μl 4% formaldehyde in PBS. A minimum time point of 24 hours was set as lower time points exhibited a comparatively high failure rate with staining failure occurring at 4 hours and 6 hours. After the 24 hours the formaldehyde was removed and the wells were washed 3 times with 500μl of PBS. Triton X-100 solution diluted to 0.5%v/v in PBS was then added to the wells for 20 minutes in order to permeabilise the cells' membranes, after which the cells were washed again with PBS three times.

Non-specific binding sites were blocked by incubating the cells in a 1% w/v bovine serum albumin (BSA)/ 10%v/v goat serum/ PBS mix for 30 minutes at room temperature. This was then aspirated off and the primary antibody added (Table 2-4). The cells were incubated in the primary antibody overnight at 4°C.

Table 2-4: Antibodies for Immunohistochemistry

Antibody	Dilution	Type	Supplier
Anti Ki-67 clone MIB -1	1 : 75	Monoclonal mouse	Dako®
FITC Alexa 488 Anti mouse	1 : 200	Polyclonal goat	Invitrogen®
DAPI (4,6-diamidino-2-phenylindole dihydrochloride)	1 : 600	Stain	Sigma®

After 24 hours the primary antibody was removed, the cells were washed well in PBS three times, the secondary antibody was then added (Table 2-4). The cells were incubated in the secondary antibody for an hour at room temperature, after which they were washed 3 times more in PBS. DAPI was then added to the wells for five minutes to stain the nucleus before the cells were washed for the final time in PBS. The cells were then imaged using a Nikon Diaphot 300 inverted microscope with epifluorescence.

2.6.2 Fluorescence Staining with DAPI

The cells were cultured in a 24 well plate for 2 hours, 1 day, 4 days and 7 days using DMEM/F-12. At each time point the supernatant was aspirated from each well and cells were fixed for a minimum of 20 minutes with 500μl 4%v/v formaldehyde at room temperature. The formaldehyde was then removed and the wells were washed 3 times with 500μl of PBS. DAPI was added and incubated for 5 minutes. The cells washed in PBS again and imaged using a Nikon Diaphot 300 with epifluorescence. Cell counts were done manually.

2.6.3 MTT Reduction Assay

The MTT assay is based on the ability of a mitochondrial dehydrogenase enzyme from viable cells to cleave the tetrazolium ring of the pale yellow MTT [3-(4,5-dimethylthiaaol-2-yl)-2,5-diphenyltetrazolium bromide) and form dark blue formazan crystals. These are largely impermeable to cell membranes, thus resulting in an accumulation of these crystals within healthy cells. The crystals are then solubilised using isopropanol. The number of surviving cells is directly proportional to the level of formazan created and the colour can be quantified using a multiwall scanning

spectrophotometer at 570 nm. At a specific time point, the supernatant was aspirated from the cells and 500μl of warm 0.5mg/ml MTT in DMEM was added. After a 4 hour incubation at 5%v/v CO_2 and 37°C, the MTT solution was aspirated off and 250μl/well of isopropanol was added to dissolve the formazan blue crystals. 100μl of the blue solution was transferred into a 96 well plate and absorbance was measured at 570nm using a plate reader.

2.7 Apoptosis and cell death

2.7.1 TUNEL

Fibroblasts were seeded in collagen for 6 days during which injuries were inflicted (refer to section 2.6). On day 6, treatments were added to induce apoptosis to the fibroblasts in collagen and incubated for 24 hours. Fibroblasts in collagen were then fixed in 3.7% paraformaldehyde, and rinsed twice with PBS. After washing, cells were permeabilised with PBS with 0.1% Triton-x100 (sigma) and 0.1% sodium citrate (sigma) for 10 minutes on ice and then washed again.

Following permeabilisation, wells were incubated with the Fluorescein *in situ* Cell Death Detection Kit (Roche), according to manufacturer's instructions. For each experimental well, 5μl vial 1 (enzyme solution) and 45μl vial 2 (substrate solution) were combined and allowed to equilibrate over ice.

The wells were rinsed twice with PBS and the surrounding area dried. For the negative control, one well of fixed and permeabilised cells were incubated with 50μl well label solution (vial 2) only. For the positive control, fixed and permeabilised cells were incubated with RNAse free DNAse (Qiagen) for 10 minutes to induce DNA strand breaking prior to labelling. For the experimental well, 50μl per well of combined solution was added to each well and the wells covered with parafilm to prevent drying. The wells were then incubated in a humid atmosphere for 60 minutes at 37°C in the dark. Subsequently, wells were counterstained with DAPI (1μg/ml), and rinsed three times with PBS. Fluorescence images were obtained as detailed above and fluorescent cells were counted using ImageJ 1.46.

2.7.2 Western Blotting

2.7.2.1 Protein determination

Sample protein content was determined by combination of 10ul sample with 500ul of Bio-Rad reagent pre-diluted 1:5 with distilled water. Optical density at 595nm was established by a plate reader in pairs of 200ul aliquots in a 96 well plate (Multiskan with Ascent Software, Thermofisher, Loughborough, UK). Protein content was calculated by comparison with a standard curve created using serial dilutions of 200mg/ml BSA.

2.7.2.2 Gel preparation, protein separation and blotting

Equal quantities of protein were established by further dilution with cell lysis buffer. Equal volumes of sample or control and 2x sample buffer were then mixed, heated to 95^{o}C for 5 minutes and then centrifuges at 13 000rpm for 5 minutes. Gels were prepared (Table 2-5 and 2-6) and run for 90 minutes on a bio-Rad-proten III system (BioRad, Hemel Hempstead) using 1x running buffer, prepared as in Appendix I. The gels were blotted using the Bio-Rad wet blotting system (buffer prepared as in Appendix I), with methanol-activated PVDF membrane. Blotting was performed in an ice-cooled gel tank for an hour.

Table 2-5: Preparation of resolving gels for SDS-PAGE

Solution components	**Volume for 1 x 10% gel (μl)**
Distilled water	4000
30% (w/v) acrylamide (Severn Biotech)	3300
10% SDS (Sigma)	100
1.5M Tris-HCL (pH 8.8)	2500
10% ammonium persulphate (Sigma)	100
Temed (Sigma)	4

Table 2-6: Preparation of stacking gels for SDS-PAGE

Solution components	**Volume for 1 x 1.5mm gel gel (μl)**
Distilled water	3400
30% (w/v) acrylamide (Severn Biotech)	830
10% SDS (Sigma)	50
1.0M Tris-HCL (pH 8.8)	630
10% ammonium persulphate (Sigma)	50
Temed (Sigma)	5

2.7.2.3 Membrane blocking, antibodies and detection

Membranes were blocked with 10% goat serum (serum) in Tris-Buffered Saline and Tween 20 (TBST), and anti-DDR-1 antibody (polyclonal rabbit anti-human, Santa Cruz Biotechnology, Heidelberg, Germany) was applied for one hour at room temperature (1:1000 dilution in blocking buffer, see appendix I). After three 15 minute washes with Phosphate Buffered Saline (PBS) solution with Tween 20 (PBS-T), the HRP-conjugate secondary polyclonal goat anti rabbit antibody (Santa Cruz Biotechnology) (Table 2-7), was applied for 45 minutes (1:10000 dilution in blocking buffer) followed by three further washes, Detection was achieved using Enhanced chemiluminescence (ECL) reagents and ECL hyperfilm (GE Healthcare, Amersham): Reagents A&B were combined in equal volumes and incubated for 5 minutes. 1ml of the mixture was applied to the surface of each membrane and incubated for a further minute. Each hyperfilm was then developed under dark room conditions until bands appeared using develop and fixer (Fidgeon, peterlee).

Table 2-7: Primary antibodies used to detect apoptosis

Primary antibodies	**Dilution**
Cleaved Caspase 3 – rabbit mAB – cell signalling #9664	1:1000
Cleaved Caspase 7 - rabbit mAB - cell signalling #9492	1:1000
Cleaved Caspase 9 - rabbit mAB- cell signalling #7237	1:1000
Cleaved PARP - rabbit mAB - cell signalling #5625	1:1000

2.7.2.4 Stripping and re-probing for loading control

The polyvinyl difluoride (PVDF) membrane was incubated for 50 minutes at 50°C in 10ml stripping buffer (see appendix I), agitated every 10-15 minutes. The membrane was then washed thoroughly with distilled water, and the presence of protein bands confirmed by staining with Ponceau-S solution. The membrane was reblocked, exposed to the new primary antibody (Table 2-6), secondary antibody (HRP-conjugate polyclonal anti- rabbit 1:10000), sigma) and ECL reagent.

2.8 Quantitative PCR

2.8.1 RNA Extraction

Medium was aspirated from the well until dry. The Qiagen RNeasy kit (Qiagen, Crawley) was then used to prepare RNA. 600 μl RLT buffer was added to each pair of wells in a 12 well plate. The buffer was pipetted up and down twice to ensure lysis and the products transferred to a 1.5ml eppendorf tube. The lysate transferred to a QIAshredder spin column in a 2ml collection tube and centrifuged for 3 minutes at 10 000rpm. One volume of 70% ethanol was added to the homogenized lysate and mixed well by pipetting. The sample was transferred to an RNeasy spin column in a 2ml collection tube and centrifuged for 15 s at 10 000rpm. The flow-through was discarded. DNA digested as follows: 350 μl of buffer RW1 was added to the RNeasy spin column, and then centrifuged for 15 s at 10 000 rpm. The flow-through was discarded.

DNase was prepared by the addition of 10ul DNase stock to 70 μl RBB buffer per column. The DNase incubation mix was added to the RNeasy spin column and incubated at room temperature for 30 minutes. 350 μl of buffer RW1 was added to wash the column and was centrifuged for 15 s at 10 000rpm. The flow-through was discarded and 500 μl buffer RPE was added to the column. This was centrifuged for a further 15 s at 10 000. The flow-through was discarded and a further 500 μl buffer RPE added to the column which was further centrifuged for 2 minutes at 10 000rpm. The flow-through was discarded. The spin column was placed in a new eppendorf and 40 μl RNase-free water was added to the membrane. This was centrifuged for 1 minute at 10 000rpm and the products stored at -80°C.

2.8.2 cDNA synthesis

In a 0.5ml microfuge tube the following were mixed together: 4μl random hexamers (50 ng/ml), 4 μl dNTPs (5mM stock), 10 μl RNA sample and 8 μl sterile distilled water. The tube was then heated at 65°C for 5 minutes, incubated briefly on ice, and then return to room temperature. The tube was spun briefly to collect condensation. Subsequently 8 μl 5 x FS was added per tube, followed by 4 μl 0.1M DTT and 2 μl Superscript II. A control sample without Superscript II was also prepared. The sample was then heated on a PCR block using the conditions (Table 2-8). Each tube was spun briefly to collect condensation and all products were stored at -20°C.

Table 2-8: Conditions for cDNA synthesis

Temperature	Time
25°C	10 mins
42°C	5-60 mins
70-75°C	10-15 mins
4°C	pause

2.8.3 SYBR green ® Real time Polymerase Chain Reaction

PCR (polymerase chain reaction) is a technique used for the exponential amplification of a specified region of DNA. Complementary oligonucleotides are designed to bind on opposite strands to the 5“ and 3“ ends of the sequence to be amplified, and a DNA polymerase enzyme synthesises new DNA from these sites in the 5“ to 3“ direction, using the original fragment as a template. Successive rounds of amplification produce the fragment of interest on an exponential scale.

Primers used for standard PCR throughout this thesis are detailed in Table A4.1 (*Appendix 4*). In general, primers were 17-28bp long, consisted of 50-60% of the GC base pair, and did not contain significant nucleotide repetition, particularly of the G and C bases, to avoid stable mispriming in GC-rich regions. Primers were purchased from Sigma-Aldrich using the KiCqStart® SYBR® Green Primers website which is for predesigned primers for gene expression analysis (http://www.sigmaaldrich.com/catalog/product/sigma/kspq12012?lang=en&region=GB)

Quantitative PCR was undertaken using the SYBR green technique on a Stratagene MX3005P real-time PCR system. cDNA samples were diluted 1:25, and the mixture (Table 2-9) was added to each well of a 96-well plate. All samples created in triplicate.

Table 2-9 Reagents for quantitative PCR reaction mixture

Reagent	Each reaction per well
SYBR Mastermix	12.5
Water	6.5
5uM primer Forward	1
5uM primer reverse	1
cDNA (1:25 dilution of stock with water)	5
Total volume	25μl per sample/well

A heated lid thermocycler was used for this PCR on the following program. The program uses 3 segments,

Segment 1 (Initial denaturation):		95°C for 10 minutes
Segment 2:	95°C for 30 seconds	40 cycles
	60°C for 30 seconds	
	72°C for 1 minute	
Segment 3 (melting point for primers):		95°C for 1 minute
		55°C for 30 seconds
		95°C for 30 seconds

4°C pause

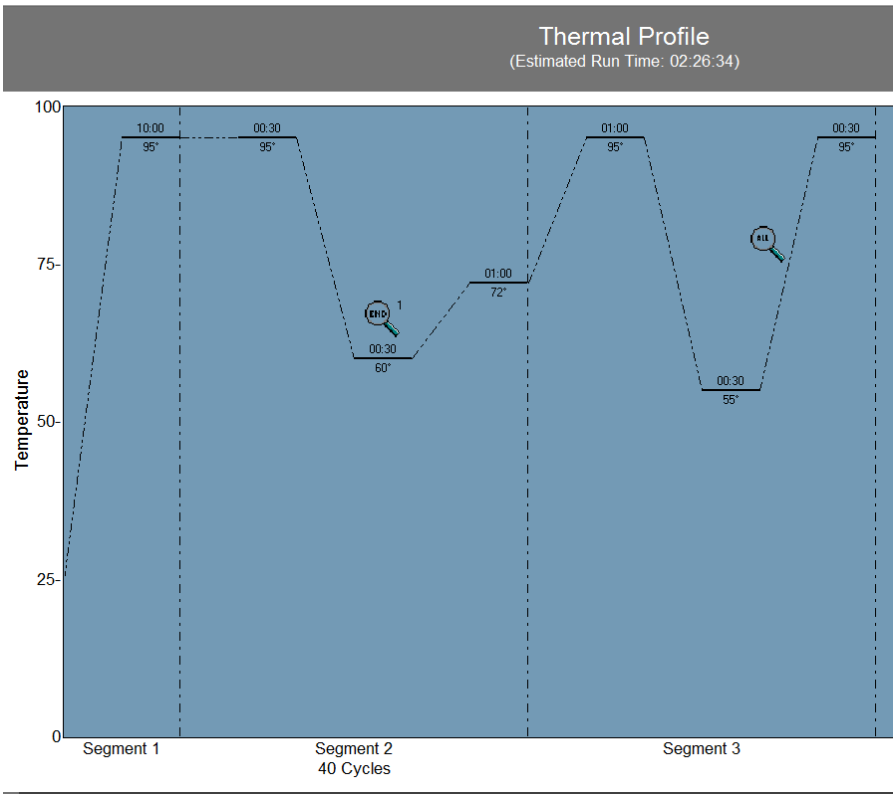


Figure 2-6: The Thermal Profile Cycle.
This consists of three segments, which will allow a disassociation curve to be produced. This curve will provide information about primer dimers.

2.8.4 Analysis of PCR

Data were examined after each experiment. Data were considered valid if Ct values varied by less than 0.25 within triplicate. In order to compare data thresholds were added automatically by the software and validated visually, The software then calculated Ct values which were normalised with a respect to a 'housekeeping gene' for each sample. Data points were plotted as $2^{-\Delta Ct}$ (Livak and Schmittgen 2001), and statistical analysis undertaken using one-way ANOVA.

2.9 Bioanalyser

All reagent and reagent mix (exclude RNA ladder) were kept in 4°C. Reagents were taken out of the fridge to warm at room temperature for at least 30 minutes. The dye and gel-dye mix were wrapped in aluminium foil and put in the drawer to protect from light. The heat block was set at 70°C.

2.9.1 Preparation of gel matrix

550 ul of gel matrix was added to the spin filter and spun for 10 min at 4000 rpm (1500g+-20%). 65 ul of filtered gel was added to 0.5ml RNase free microfuge tubes which is included in the kits. The aliquot was stored at 4°C.

2.9.2 Cleaning the electrodes

Two electrodes were cleaned. One electrode cleaner was added with 350ul RNase free water and the other one with 350ul RNase Zap. Place the electrode cleaner with RNase Zap in the Aligent **Bioanalysor** for 1 minute. The electrode cleaner was placed in water, in the machine for 10 seconds. Leave the machine open for 10 seconds for water to dry.

2.9.3 Preparation of Gel-dye matrix

The dye was vortexed for 10 seconds and spun down. 1ul of dye was added to 65μl of gel matrix. These were vortexed thoroughly for 10 seconds and visually inspected to ensure the proper mixing of gel and dye. The gel and dye were then centrifuged at maximum speed (13000g or 14000rpm for eppendorf microcentrifuge) for 10 minutes.

2.9.4 Loading chip with the gel matrix and RNA 6000 Nano Marker

The new chip was placed on priming station and loaded with 9μl of gel-dye matrix into the well marked G. The plunger was set at the 1ml mark of the syringe. The chip priming station was closed and the plunger was pressed down until it had clicked into place. After 30 seconds, the plunger was released using the clip release mechanism. 9μl of the gel dye matrix was pipetted into the two additional wells marked G (fourth column, first and second rows). 5μl of marker was pipetted into the well-marked ladder and each of the 12 RNA wells. 6ul marker was loaded into each unused sample.

2.9.5 Loading the RNA sample and the RNA 6000 ladder

The RNA sample and RNA ladder were put in the 70° C heating block for 2 minutes and put on ice for 5 minutes. They were centrifuged to clear any condensate from the tube's walls and cap. 1ul of ladder was loaded into the well-marked "ladder" and 1ul of RNA loaded into each of the 12 wells. The chip was placed in the adapted vortex and mix for 1 minute at 2400rpm.

2.9.6 Running the chip

Place the loaded Chip in the Bioanalyser. The Assay was selected for 'RNA' and the press 'start'. The files were automatically saved at the end of the run of the chip.

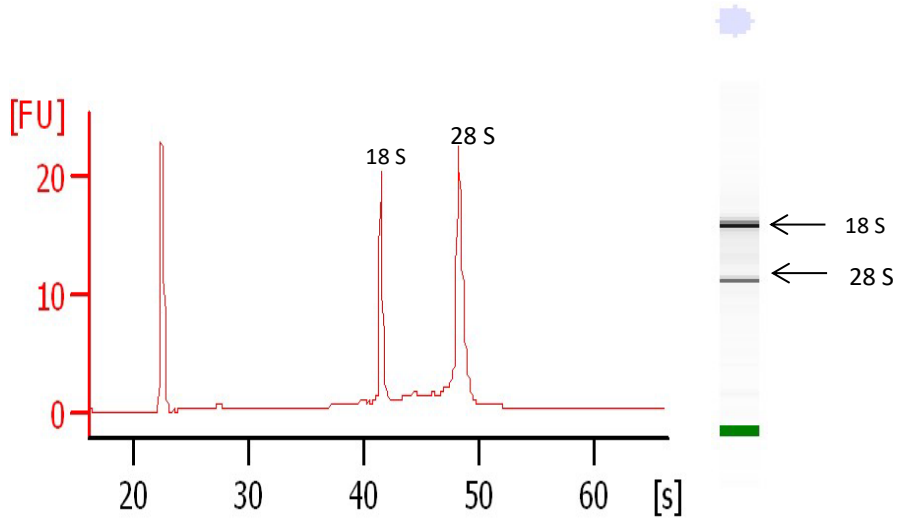


Figure 2-7: The Bioanalyser Electropherogram.
This diagram shows the total RNA assay, the RNA fragments 18S and 28S for eukaryotic RNA are detected and are an indication of RNA integrity /quality.

2.9.7 Clean the electrodes

Once the samples on the chip had finished, the machine was cleaned. The chip with samples was removed from Bioanalyser, and the cleaning was repeated.

2.10 Slide preparation and Immunohistochemistry

2.10.1 Generation of tissue and tissue processing

IPF tissues were obtained from The Nottingham Health Science Biobank (NHSB), University of Nottingham. This was approved by the Nottingham Research and Ethics Committee (REC ref: 08/H0407/01). The paraffin embedding and sectioning was done by Dr Emily Hodge, University of Nottingham.

2.10.2 Histology

2.10.2.1 Haematoxylin and eosin (H&E) staining

Haematoxylin and eosin (H&E) staining is a commonly used technique to allow visualisation of the cell structure and organisation of tissue. H&E were used to assess quality of tissue fixation/ processing. Sections were de-waxed in histoclear for 15 mins before being rehydrated through a series of alcohols, 100% (2 x 5 mins), 90% (2 mins), 70% (2 mins), and running tap water (5 mins). Sections were immersed in a water based haematoxylin solution (Sigma, U.K.) for 35 secs and then quickly washed in running tap water or until turned blue which identified the nuclei. Slides

were then submerged in undiluted alcoholic Eosin Y solution (Sigma UK) for 2 mins followed by a rinse in running tap water and then dehydrated through a series of alcohols, 70% (2 mins), 90% (2 mins), 100% (2 x 5 mins) and histoclear (15 mins) before being mounted with coverslips using Vectamount (vector labs, UK), slides were left for 24 hours before visualisation under light microscope.

2.10.2.2 Immunohistochemistry on IPF tissue

Immunohistochemistry was used to identify candidate genes which were of interest in the IPF tissue sections. Positive control tissue was used initially to optimise the antibodies. The positive control tissues were chosen from the human protein atlas http://www.proteinatlas.org/, for the desired antibody to be optimised.

Immunohistochemisty is a commonly used technique to investigate cell structure and organisation of tissue. It exploits the basic principles of immunology i.e. the specific interaction of an antibody with its antigen, to allow the visualisation of specific cell or tissue constituents. All immunohistochemistry conducted in studies reported in this thesis utilised the immunoperoxidase method of staining. Sections were dewaxed in histoclear for 10 minutes followed by submersion in 100% alcohol (2 x 5mins), 90% (2 minutes), 70% (2 minutes), and running tap water (5 minutes).

Sections were then immersed in 10% H_2O_2 methanol solution for 10 minutes to block any endogenous peroxidase activity then washed twice in PBS for 10 minutes. Slides were then blocked with 2.5% RTU normal horse serum for 15 minutes. The appropriate concentration of primary antibody solution (made in blocking solution) was added to sections which were then incubated overnight at 4^{o}C.

After 24 hours sections were washed in PBS (2 x 5 mins) and then incubated with biotinylated secondary antibody (1:100) for one hour at room temp. Following this, sections were washed in PBS and then incubated with an avidin-biotin-peroxidase complex solution (Vector Laboratories, UK) at room temp for a period of one hour.

Sections were washed in PBS (2 x 5 mins) and then incubated with 3’3’-

diaminobenzidene solution to visualise antibody binding. The colour reaction was stopped after 3 mins by immersion of sections in running water (10 mins). Sections were then dehydrated through a series of alcohols; 70% (2 mins), 90% (2 mins.), 100% (2 x 5 mins) and then xylene (10 mins) before being mounted and cover slipped in Vectamount (vector labs, UK), slides were left for 24 hours before visualisation under light microscope.

2.10.2.3 Avidin-biotin-peroxidase Complex (ABC) immunostaining

The ABC method of staining was used for all immunohistochemistry experiments reported in this thesis. The method was first reported by *Hsu et al, 1981* (Hsu et al., 1981) and is based on the high affinity of the protein avidin to bind biotin. Briefly, sections are incubated with a primary antibody to the antigen of interest (Table 6-4). A secondary biotin-conjugated antibody is then introduced which binds the primary antibody and causes the localisation of many biotin molecules to the site of the antigen. Following this, an avidin/ biotinylated peroxidase complex is added to the section which binds to the biotinylated secondary antibody thus amplifying the signal. Finally a chromogen (diaminobenzidene) is added to the section which reacts with the peroxidase forming a brown deposit which is readily visible via light microscopy.

2.10.2.4 Optimisation of antibodies

Prior to conducting immunostaining on full studies the optimal concentration for each antibody was established. Secondary antibodies against the species in which the primary antibody was raised were used; these in turn determined the species of normal sera which was added to the blocking solution. All immunohistochemistry experiments conducted included a negative control which received identical treatment with the exception of the addition of primary antibody. This ruled out the possibility of non-specific binding causing the generation of false positive results.

2.11 Statistical Analysis

All statistical analysis was performed using GraphPad Prism version 6.0.
The statistical analysis performed were either one-way analysis of variance (ANOVA) followed by Tukey's post-hoc test or two-way ANOVA with the Bonferroni post-hoc test.

A one-way ANOVA is used to determine whether the mean of a dependent variable is the same in two or more unrelated, independent groups. A two-way ANOVA is used to determine multiple comparisons.

Post-test analysis was used once the data was analysed using appropriate the ANOVA for each data set. Tukey's post-hoc test was used for a single-step multiple comparison statistical test. It can be used to determine the means of the data, which are significantly different from each other. The Bonferroni post-hoc test is a multiple-comparison correction used when several dependent or independent statistical tests are being performed simultaneously.

All the data was analysed in GraphPad Prism version 6.0. The P values which were significant were shown with asterisks. The asterisks; *** represents $p<0.001$, ** represents $p<0.01$ *and* * represents $p<0.05$.

All experiments were performed in triplicate. Comparisons between treatments, the data were expressed as mean $\pm$ SEM. Independent biological experiments were conducted as > n=3.

Chapter Three

The development and validation of the small airway epithelial and normal human lung fibroblasts in a three dimensional co-culture model

3.1 General Introduction

Idiopathic pulmonary fibrosis is a disease with an unknown cause and a poor prognosis (Nicholson, Fulford et al. 2002). Attempts to understand the pathogenesis of the disease have been based on various animal models of lung fibrosis. Commonly used models include exposure to bleomycin, silica, fluorescein isothiocyanate, irradiation or expression of specific genes through a viral vector or transgenic system (Moore and Hogaboam 2008). A popular model to characterise IPF is the bleomycin induced murine model, which involves the intratracheal administration of bleomycin in mice to induce pulmonary fibrosis (Adamson and Bowden 1974). The bleomycin induced murine models have been an important part in the study of the evolution of fibrotic responses and have led to the identification of key cells, mediators, and mechanisms that may likely be involved in the progression of the disease (Moeller, Ask et al. 2008).

The 3D co-culture model was developed using a Transwell® system consisting of small airway epithelial cells, which would mimic the alveolar epithelium, and normal human lung fibroblasts in collagen, which would mimic the *in vivo* environment. Using this approach, the cells were separated by a porous membrane through which soluble factors were able to diffuse freely in a non-direct cell interaction. A previous *in vitro* study has shown that, direct cell-cell contact in collagen consisting of dermal fibroblasts with HKC-8 cells in co-culture, may have limitations such as extraction of a specific cell type from the model (Moll, Ebeling et al. 2013). Recently, it has been shown that the non-direct interaction between IPF fibroblasts and A549 in the Transwell® model involves distinct phenotypic changes in response to epithelial injury (Prasad, Hogaboam et al. 2014).

In this study, human small airway epithelial cells (SAEs) were used throughout as these were commercially available from Lonza. Ideally alveolar type II cells would have been a better cell type for the study. However, as these cells are located in the alveoli, these were difficult to retrieve and culture. Normal human lung fibroblasts (NHLFs) were also used throughout the study and were available from Lonza. Both

cell types were obtained from the same donor and the numbers of batches were reserved to maintain the same cell type usage through-out the project.

The advantage of culturing the fibroblasts in collagen, is that collagen is a major component of the ECM complex and this will mimic the basement membrane for the cells as well as initiate signalling events between matrix and cells (Schuliga, See et al. 2009). The collagen gel provides an environment similar to that of *in vivo* conditions providing a natural substrate for cellular attachment, growth and differentiation, and also promoting cellular proliferation and differentiation (Ruszczak 2003). Fibroblasts cultured in a collagen gel (3D) have distinct characteristics compared to those cultured without collagen (2D) (Mio, Adachi et al. 1996). The fibroblasts cultured in gels acquire a bipolar spindle form, while fibroblasts without manifest a disordered membrane that possess one or more broad, flattened features (Mio, Adachi et al. 1996).

The objective of this study was to develop a model of repetitive injury utilising various injury methods. This would aid understanding of the mechanisms underlying the crosstalk between epithelial cells and fibroblasts. A 3D co-culture system was established in which epithelial cells were able interact with fibroblasts to mimic similar epithelial-mesenchymal interaction *in situ* in pulmonary fibrosis.

This 3D co-culture model aims to demonstrate the response of epithelial injury on fibroblasts, in a non-cell-cell interaction and can identify the soluble mediators driving the pathologic fibrotic remodelling. A better understanding of soluble mediators and pathways in experimental models could provide a critical approach to identify novel targets to assess and validate in IPF. Also the development of the model could aim to reduce animal models such as bleomycin-mouse models, be reproducible and provide high throughput to screen for soluble mediators.

3.2 Aim and Objectives

The aim of the project was to develop a human epithelial and fibroblast *in vitro* 3D co-culture system to study epithelial-mesenchymal interactions, which contribute to the development of fibrosis after epithelial injury. A co-culture system was developed to model the *in vivo* interactions between injured epithelial cells and fibroblasts in the absence of cell contact.

In order to achieve this first aim, the following was done:

I. Optimise the cell concentration individually for fibroblasts in collagen and epithelial cells in Transwell® inserts.
II. Examine fibroblast proliferation in collagen over seven days, in the absence of epithelial cells.
III. To examine the effect of wounding on epithelial cells by measuring an injury response.
IV. Observe the effect of epithelial and fibroblast cells in a co-culture model.

3.3 Methods

Primary human small airway epithelial cells (cat no: CC2547) and normal human lung fibroblasts (cat no: CC2512) were purchased from Lonza. They were cultured in their specific bullet kits (refer to section 2.2). For the culturing of fibroblasts in rat tail collagen refer to section 2.3. For the culturing of epithelial cells on Transwell® refer to section 2.4. Measurements of cell viability was performed by MTT assay (refer to section 2.6.3).

3.3.1 Co-culture of epithelial cells and fibroblasts cells in Transwells®

To develop the 3D co-culture model, fibroblasts at $5x10^5$ were mixed with 3mg/ml rat tail collagen type I in DMEM/F12 in the absence of serum. The mixture of cells and collagen were seeded and incubated at 37°C + 5% CO_2 for one hour allowing the collagen to set. After an hour, a Transwell® insert with 0.4μm pore size containing cultured $1x10^5$ epithelial cells was laid on top of the well. In the Transwell® and insert, fresh serum free DMEM/F12 was added and left for 24 hours before injury.

3.3.2 Low-Grade-injury on epithelial cells

A low grade injury model was set up to investigate the effect of various injuries on the epithelial cells in the absence of fibroblasts. The injuries included mechanical i.e. scratch and chemical i.e. bleomycin methods (refer to section 2.4). An inflammatory response from SAEs was measured by expression of IL-1α by ELISA (refer to section 2.5.1).

3.3.3 Dual staining of fibroblasts with anti-Ki-67 and DAPI

To determine cell proliferation in the 3D co-culture model, fibroblasts were fixed after 6 days post wounding and were studied using a proliferative marker Ki-67 (refer to section 2.6.1) and dual stained with DAPI, a nuclear counterstain (refer to section 2.6.2). For DAPI stained wells, ~250 cells were counted, averaged and compared to anti-Ki67 cell counts on the same image as the DAPI stained cell. The anti-Ki67/DAPI percentage was calculated. Confocal microscopy was performed using a Zeiss Axio Observer D1, Hamamatsu electron multiplier CDD Camera C9100-13, with a Yokogawa spinning disk system. Images were captured in slices of 0.1um thickness.

Volocity software 4.2.1 analysis software and Improvision were used to analyse the images.

3.3.4 Apoptosis

The 3D co-culture model was set up as described in section 2.4 with the addition of various injuries. The fibroblasts were fixed after 6 days post wounding and a TUNEL assay was performed (refer to section 2.7.1). Fluorescence images were obtained as detailed above and fluorescent cells were counted using ImageJ 1.46.

The second approach was to measure the PARP cleavage by western blotting (refer to section 2.7.2). The 3D co-culture model was set up as described in section 2.4; with the addition of injuries. ImageJ 1.46 was used to analyse the images.

3.3.5 Quantitative analysis

Protein quantification was determined by densitometry analysis, using computer imaging software (ImageJ 1.38x; W. S. Rasband, National Institutes of Health, Bethesda, MD; http://rsbweb.nih.gov/ij/). The largest destained area was selected using the region of interest with rectangular selection tool. The same region of interest was then applied to all other bands and the mean density was again determined. Results were plotted as mean $\pm$ SEM and are comparable within experiments.

3.3.6 Statistical Analysis

Data were analysed using GraphPad Prism 6.0 software (GraphPad Software, Inc.). Continuous data from independent experiments which were considered to follow a normal distribution were displayed as the mean value ± SEM. The statistical significance was assessed by one-way ANOVA followed by Tukey's post-hoc test when comparing multiple conditions to a control or two-way ANOVA with the Bonferroni post-hoc test when comparing multiple conditions with one another. The P values which were significant were shown with asterisks. The asterisks; *** represents $p<0.001$, ** represents $p<0.01$ *and* * represents $p<0.05$. n=3 (refer to section 2.11).

3.4 Results

3.4.1 Optimising primary human cells

The 3D co-culture model consisted of small airway epithelial cells (SAEs) and normal human lung fibroblasts (NHLFs). The SAEs were optimised in the Transwell® insert to achieve the correct cell number so that the cells would form a confluent layer over 7 days. The NHLFs were optimised in the rat tail collagen type I at 3mg/ml, to obtain the correct cell number without the collagen contracting over 7 days.

It was important to establish the correct seeded cell number for the fibroblasts in collagen, so the fibroblasts remained confluent in the 3D environment and would not contract during the 7 days of culture. Previous studies have demonstrated that cells plated at a higher density would reach confluence much sooner than expected, which then consequently led to cell loss and/or cessation of proliferation (Masur, Dewal et al. 1996). Therefore, adjusting the initial cell number permits the balance between the cell number and collagen which is necessary for cell to cell contact to occur in the 3D co-culture model.

3.4.2 Optimising cell number for normal human lung fibroblasts

The aim of this experiment was to establish a suitable cell number of fibroblast cells plated in a collagen gel without the collagen contracting. Cell densities of $2.5x10^5$, $5x10^5$ or $7.5x10^5$ cells per ml in phenol red-free serum-free medium and were mixed with 3mg/ml rail tail collagen type I.

The results demonstrated for all cell numbers in collagen after 24 hours (day 1), the cells had elongated in the collagen and the collagen was intact (Figure 3-1). At day 4 the cells had changed shape and with a developed spindle like morphology. At day 7 the cells seeded at $2.5x10^5$ cells per ml, which showed that the cells had maintained a connection and had not formed a confluent layer with large gaps between the structures, (Figure 3-1). Wells seeded at $5x10^5$ cells per ml had formed a confluent 3D layer with the collagen intact during 7 days. The collagen gel plugs with $7.5x10^5$ cells per ml had contracted when observed at day 7 and therefore, this cell number was not suitable.

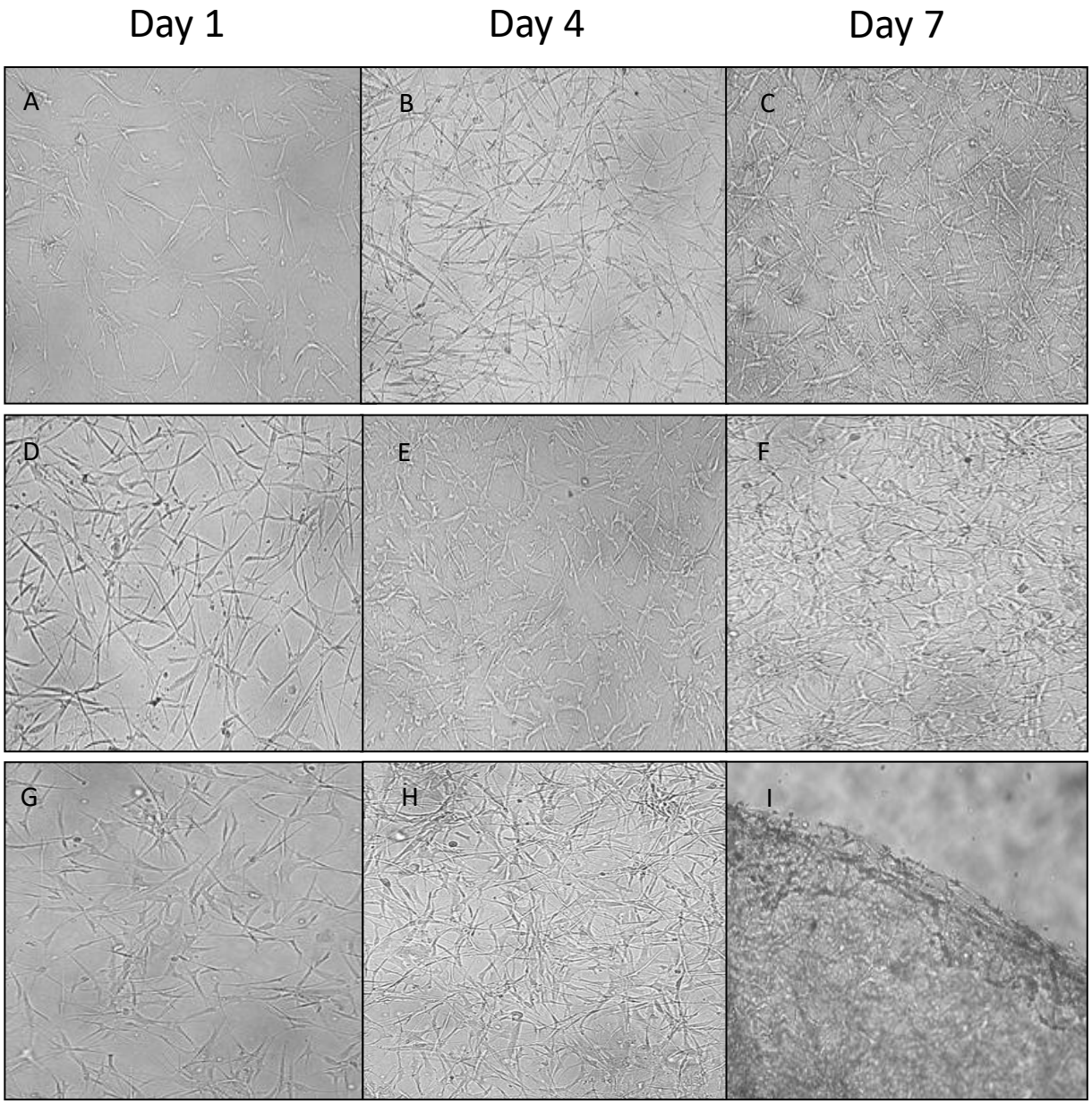


Figure 3-1: **Fibroblasts in collagen at 1, 4 and 7 days**. This was to establish a suitable cell number of fibroblast cells plated in a collagen gel without the collagen contracting. The fibroblasts were observed over 7 days. All cells were cultured with serum free DMEM. Images were taken using a phase contrast microscope at x10 magnification on day 1 (column 1), day 4 (column 2) and day 7 (Column 3). The cells were set up in triplicate. A-C, $2.5x10^5$ cells per ml. D-F, $5x10^5$ cells per ml and G-I, $7.5x10^5$ cells per ml.

An MTT assay was performed in triplicate for each cell number $2.5x10^5$ and $5x10^5$ cells per ml in collagen. These cells in collagen did not contract over 7 days. The assay revealed that, for both cell numbers, the cells were viable over the 7 days (Figure 3-2). An MTT assay was not performed on $7.5x10^5$ cells per ml as the collagen had contracted suggesting that the cells had increased too much in cell number and the collagen gel was not able to support the number of cells. For this reason, the cell number $7.5x10^5$ cell per ml was discarded.

$5x10^5$ cells per ml were chosen for further experiments as in culture the cells were confluent without collagen contraction. Also, the fibroblasts appeared to have a spindle shape with cytoplasmic projections coming from all directions. The observations demonstrated that the cells were variable with a uniform structure over the 7 days. Statistical analysis was performed using GraphPad Prism version 6.0 (refer to section 2.11). A two-way ANOVA with the Bonferroni post-hoc test was used to determine the viability for the two cell numbers over the 7 days. Two-way ANOVA was used to determine multiple comparisons i.e. cell number over the number of days. The analysis demonstrated that the cells were viable from day 1 to day 7 ($p<0.05$) for both cell numbers.

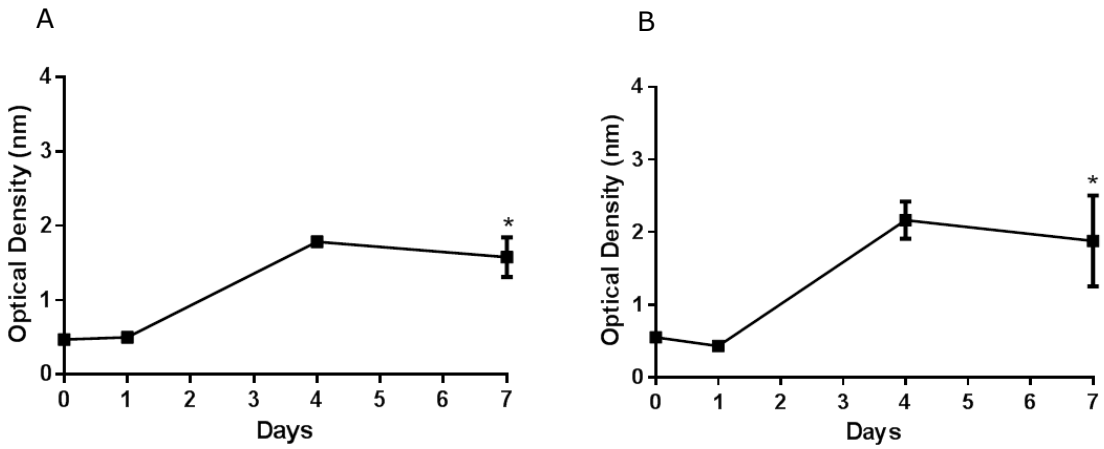


Figure 3-2: MTT assay of fibroblasts in collagen over 7 days in serum-free medium to determine cell viability. A; cell number $2x10^5$ cells per ml and B; cell number $5x10^5$ cells per ml. Both cell numbers remained viable over 7 days. Using statistical analysis two-way ANOVA with the Bonferroni post-hoc test. The asterisk * represents $p<0.05$. Experiments were conducted in triplicate. n=3 independent biological experiments.

3.4.3 Determining Proliferation of Fibroblasts in collagen gel

Proliferation of fibroblasts was measured in the absence of serum. This was to determine a baseline proliferation prior to inflicting different injuries in the 3D co-culture model. Fibroblasts in collagen were seeded on a 24 well glass bottom plate at the cell number of $5x10^5$ cells per ml serum free DMEM/F12 in triplicate (refer to section 3.4.2).

Positive controls were set up using fetal calf serum 10% (FCS) and Platelet derived growth factor at 10ng/ml (PDGF), which were added individually to the medium. Fetal calf serum is an essential component in culture medium providing cells with nutrients necessary for them to grow and proliferate. Platelet derived growth factor helps maintain the proliferative precursor phenotype of fibroblasts in cell culture (Nakagawa, Pawelek et al. 1989). A serum-free medium was used as a negative control.

Cell proliferation was determined using two methods anti-Ki67, a nuclear marker of cell proliferation (Bullwinkel, Baron-Luhr et al. 2006) and DAPI, fluorescent DNA stain to detect live and dead cells (Kapuscinski 1995), (refer to section 2.6). For each condition, ~250 cells (fibroblasts) DAPi stained cells were counted, averaged and compared to anti-Ki67 cell counts on the same image as DAPI stained cells. The anti-Ki67/DAPI percentage was calculated. The cells were imaged using a Nikon Diaphot 300 with epifluorescence and counted manually on day 1, day 4 and day 7 (Figure 3-3).

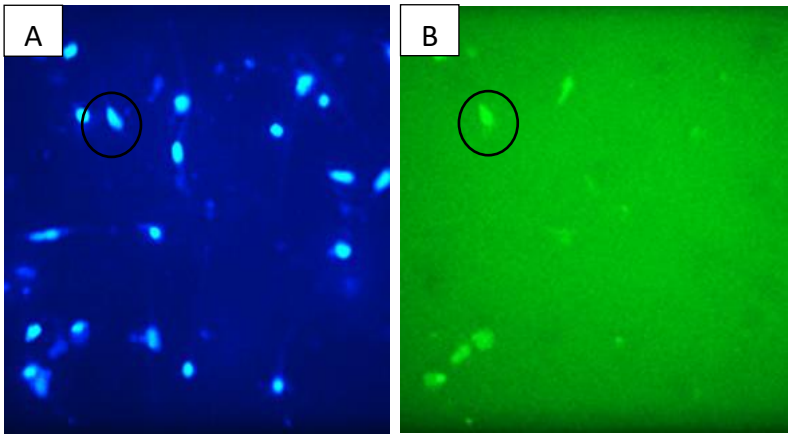


Figure 3-3: Confocal images of fibroblasts after 7 days in co-culture. (A), Fibroblasts stained with DAPI (appears as blue dots) and (B), fibroblasts counter stained for Ki-67 after 7 days of co-culture. Images are representative of the same field of view. Images at magnification x10.

The statistical analysis was performed using a two-way ANOVA with the Bonferroni post-hoc test (refer to section 3.3.5). The results revealed the DAPI count and number of anti-Ki67 positive cells increased over 7 days (Figure 3-4) in the positive control. The cell number also increased in the serum free ($5x10^5$ per ml) cell population. The anti-Ki67/DAPI percentage demonstrated that from day 0 to day 7, the cells seeded at $5x10^5$ per ml in serum-free media had proliferated 37% compared to cells with PDGF with an increase of 41% over 7 days.

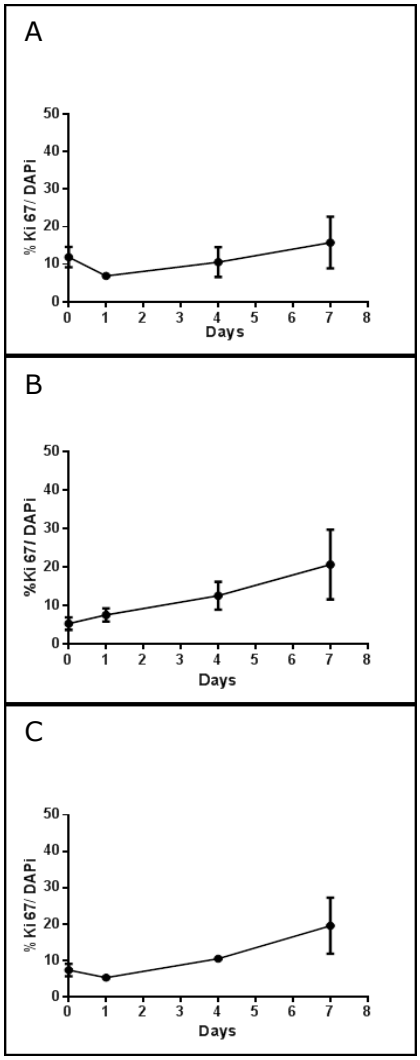


Figure 3-4: The effect of different soluble factors on the cell number of fibroblasts. Fibroblasts were seeded at a cell number $5x10^5$ per ml and grown in collagen for 7 days. The cells were examined using dual labelling with anti-Ki-67 and DAPI. **A**: Cells with addition of FCS; **B**: Cells with addition of PDGF and **C**: cells in serum free medium. Fibroblasts in serum-free showed a reduced proliferative response compared to the positive control and PDGF. Statistical analysis was performed using GraphPad Prism version 6.0. A two-way ANOVA with the Bonferroni post-hoc test was performed. There was no significant difference in cell number with using positive control. Experiments were conducted in triplicate. n=3 independent biological experiments.

3.4.4 Cell Concentration of Small Airway Epithelial cells

The aim of this experiment was to optimise the cell number for small airway epithelial cells so that when the cells were seeded they remained in a confluent layer during 7 days in the Transwell® inserts. Cells were seeded on a 24 well Transwell® insert with a 6.5mm insert and a 0.4μm pore size. The cells were cultured in SAGM (refer to section 2.3.2) in triplicate at cell density $5x10^4$, $1x10^5$ and $5x10^5$ cells per ml. For epithelial cells, cell number was determined by staining the cells with DAPi (refer to sections 2.6.2) and cell viability for both cell types was measured by MTT (refer to section 2.6.3); both methods were used to determine live cells. The cells were observed at day 1, 4 and 7 using a phase contrast microscope.

The statistical analysis was performed using a two-way ANOVA with the Bonferroni post-hoc test (refer to section 3.3.5). The analysis for each cell number revealed there was an increase in cell viability over 7 days (Figure 3-5). The percentage increase for each cell number seeded was calculated from day 1 to day 7. Cells seeded at $5x10^4$ increased 58% from day 1 to day 7. Cells seeded at $1x10^5$ cells per ml increased by 60% and cells seeded at $5x10^5$ cells per ml increased 62%, all with a significance of $p<0.05$.

To determine which cell number was suitable in the co-culture model, epithelial cells were stained with DAPI on day 7 for each cell number (Figure 3-6). The images show that $1x10^5$ cells per ml resulted in an even monolayer with no clumping and therefore, this cell number was used for the co-culture model. To determine whether the cells migrated through the pores into the well below, a cell tracker probe was added to the epithelial cells. The observations clarified that the cells did not migrate through the pores and remained in the insert as expected. (These results were not shown).

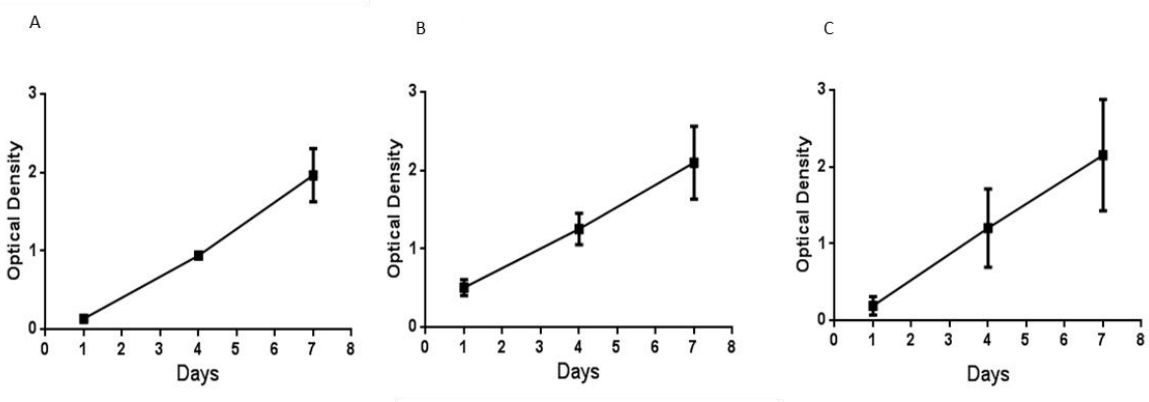


Figure 3-5: **The optical density measured by MTT assay to determine cell viability of epithelial cells.** Cell viability for individual cell numbers for epithelial cells in monolayer from day 1 to day 7. A; $5x10^4$, B; $1x10^5$ and C; $5x10^5$ cell number. Percentage increase was calculated on day 1, day 4 and day 7. Using statistical analysis two-way ANOVA with the Bonferroni post-hoc test. There was no significant difference in cell viability for the individual cell number. The experiments were conducted in triplicate; n=3, independent biological experiments.

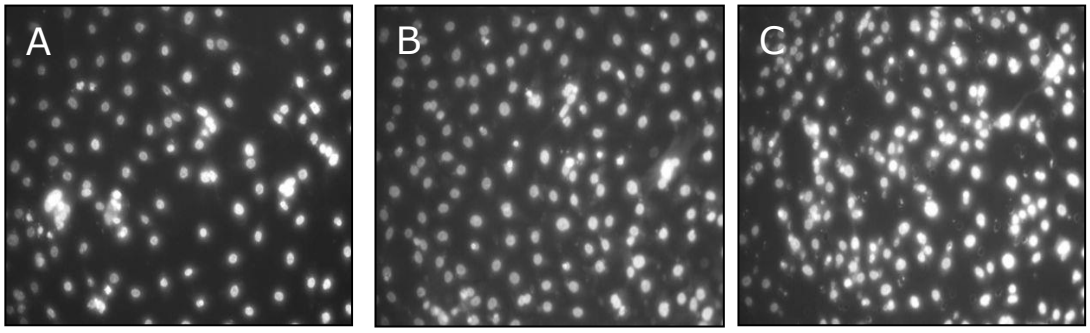


Figure 3-6: Confocal images of individual cell numbers of epithelial cells on day 7. Epithelial cells were stained with DAPI at day 7, to determine cell number. A; cells at $5x10^4$ cells per ml, B; cells at $1x10^5$ cells per ml, and C; cells at $5x10^5$ cells per ml. Image magnification x10.

3.4.5 Validation of Low Grade injury on Epithelial Cells

Epithelial damage was quantified by the release of IL-1α. IL-1α is an alarmin which are endogenous molecular 'danger signals' released by cells that can contribute to the innate immune response by activating immune cells via multiple receptors including Toll-like receptors (TLR), Nod-like receptors (NLR) and the receptor for advanced glycation end products (RAGE) (Tracy, Bowman et al. 2012). Pulmonary fibrosis is associated with the up-regulation of alarmins such as Interleukin 1-alpha (IL-1α) and High mobility group box 1 (HMGB1) (Bianchi 2007).

The aim of this experiment was to inflict a variety of injuries on small airway epithelial cells alone and measure an injury response. Epithelial cells were wounded by either mechanical or chemical injuries and the effect of cell injury was assessed by measuring the level of IL–1α response by ELISA.

3.4.6 Effect of low grade injury on epithelial cells

The low grade injuries were only inflicted on the epithelial cells. The injuries used were a *scratch-wound* using a sterile p200 pipette tip. This technique was used because it was an established technique for repeated injury (Wadsworth, Nijmeh et al. 2006). Chemical injuries were inflicted using *bleomycin*, as this a recognised agent to induce lung fibrosis in mice (Hamilton, Li et al. 1995). The addition of ultrafine *carbon black* particles (Pigment black Printex 90) obtained from Degussa Corporation (Frankfurt, Germany) were used to mimic carbon particles present in air pollution (Doornaert, Leblond et al. 2003).

The injuries were selected on the basis of a physical injury (scratch), chemical (bleomycin) and environment (carbon black). As where mentioned, the causes of IPF are unknown. Therefore, in using three different injuries would demonstrate a general injury response in the epithelial cells. The aim was to inflict various injuries on the epithelial cells, with techniques as described above. The assessment of the epithelial injury was determined by measuring IL-1α in supernatants.

Epithelial cells were seeded at $1x10^5$ per ml in a 24 well plate with serum-free medium for all conditions. Scratch-wound and bleomycin were inflicted on epithelial cells every 24 hours over 7 days, whereas carbon black was only added at day 1 and left for the duration of the experiment (Figure 3-7). Supernatants were removed for IL-1α analysis from each well and replaced with fresh serum free medium every day. Controls were set up, where no-injury was inflicted and all conditions were set up in triplicate. Cell number was not determined through-out the experiments. However, MTT reduction assay was performed after 7 days to determine cell viability of the epithelial cells. The MTT reduction assay results revealed that the cell viability for scratch-wound injury had decreased as compared to the no-injury ($p<0.001$, unpaired t-test), (Figure 3-8). The conditions which represented the same decrease in cell viability as the control vs scratch-wound were bleomycin 5mU/ml ($p<0.001$, one-way ANOVA followed by Tukey's post-hoc test) and carbon black 25 μg/ml ($p<0.001$, one-way ANOVA followed by Tukey's post-hoc test). IL-1α was measured as a marker for cell injury (refer to section 2.5) over 7 days in supernatants.

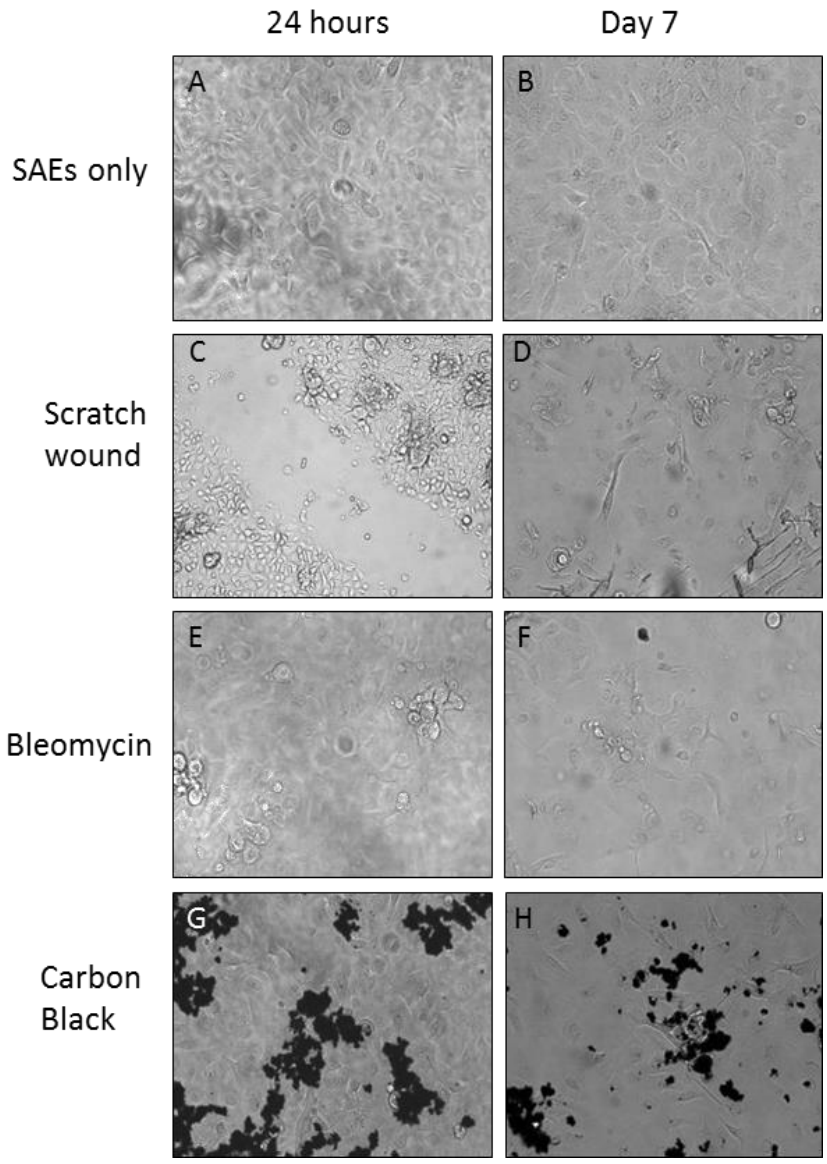


Figure 3-7: Small Airway Epithelial Cells in 24 well plates and cultured in serum free DMEM till day 7. The epithelial cells were inflicted with various injuries; scratch, addition of bleomycin and carbon black. This was to observe any visual effect on the cells. These images represent 24 hours after injury and injury on day 7. A-B, Control (non-injured); C-D, Scratch-wounding; E-F, Bleomycin 5mU/ml and G-H, Carbon Black 25ug/ml (appear as black clumps).

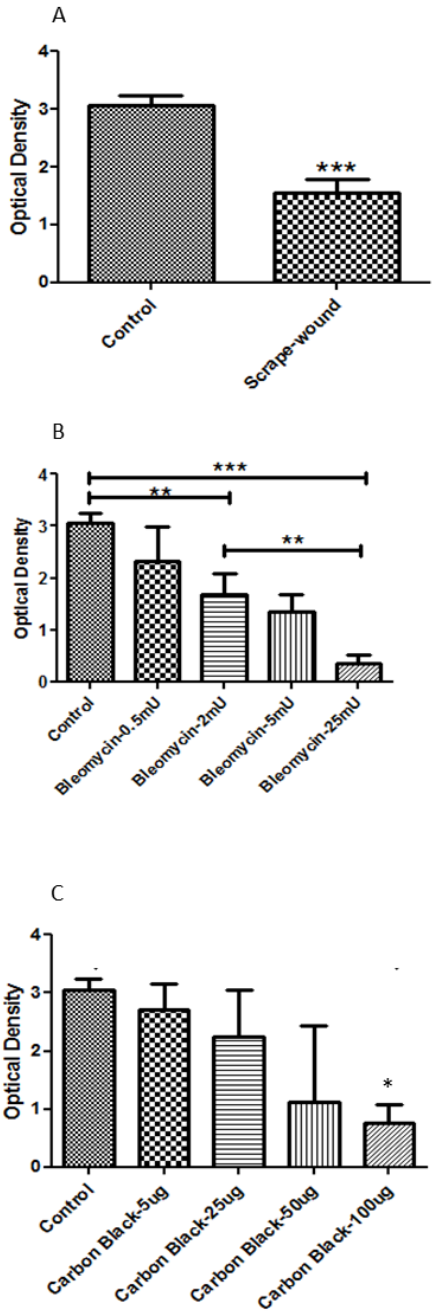


Figure 3-8: **MTT reduction assay showing cell viability in response to injuries inflicted on epithelial cells at day 7**. **A**: Epithelial cells inflicted with scrape wound, **B**: epithelial cells with the addition of bleomycin and **C**: epithelial cells with the addition of carbon black. These injuries were inflicted over 7 days. The data shown is the optical density on day 7. The graphs show the average cell viability by MTT reduction assay of the control and injuries. The experiments were conducted in triplicate. Statistical analysis was done by t-test and one-way ANOVA with a Tukey's post-hoc test in GraphPad prism V.6. The asterisks; *** represents $p<0.001$, ** represents $p<0.01$ *and* * represents $p<0.05$. n=3, independent biological experiments.

To determine the injury response of scratch-wound, bleomycin 5mU/ml and carbon black 25μg/ml in epithelial monolayer culture, IL-1α was measured as a marker for cell injury (refer to section 2.5). The results suggested that for control vs scratch-wound (0.0057ng/ml vs 0.1580ng/ml) on day 7, there was a significant increase in IL-1α production over 7 days ($p<0.001$) (Figure 3-9).

Control vs bleomycin 5mU/ml, had shown an increase in IL-1α production from day 4 to day 7. The results for day 7, for conditions control vs bleomycin 5mU/ml (0.0057ng/ml vs 0.0327ng/ml), was borderline significant $p<0.0315$.

Control vs carbon black 25μg/ml, there was an increase of IL-1α response from day 2 to day 7. The results on day 7 were (0.0363ng/ml vs 0.0.673ng/ml) which was not significant. As there was no significance in the IL-1α response, carbon black injury was discarded from future experiments.

The cell viability of the epithelial cells reduced with the various injury techniques on day 7 (refer to section 3.4.6); however, there was an increase response of IL-1α in the epithelial supernatants over 7 days. The reason for this could be the IL-1α response was accumulating over the 7 days rather than the epithelial cells releasing more IL-1α. For further *in vitro* experiments only scratch and bleomycin injuries were used. All statistical analysis was performed with two-way ANOVA with the Bonferroni post-hoc test, (refer to section 3.3.6).

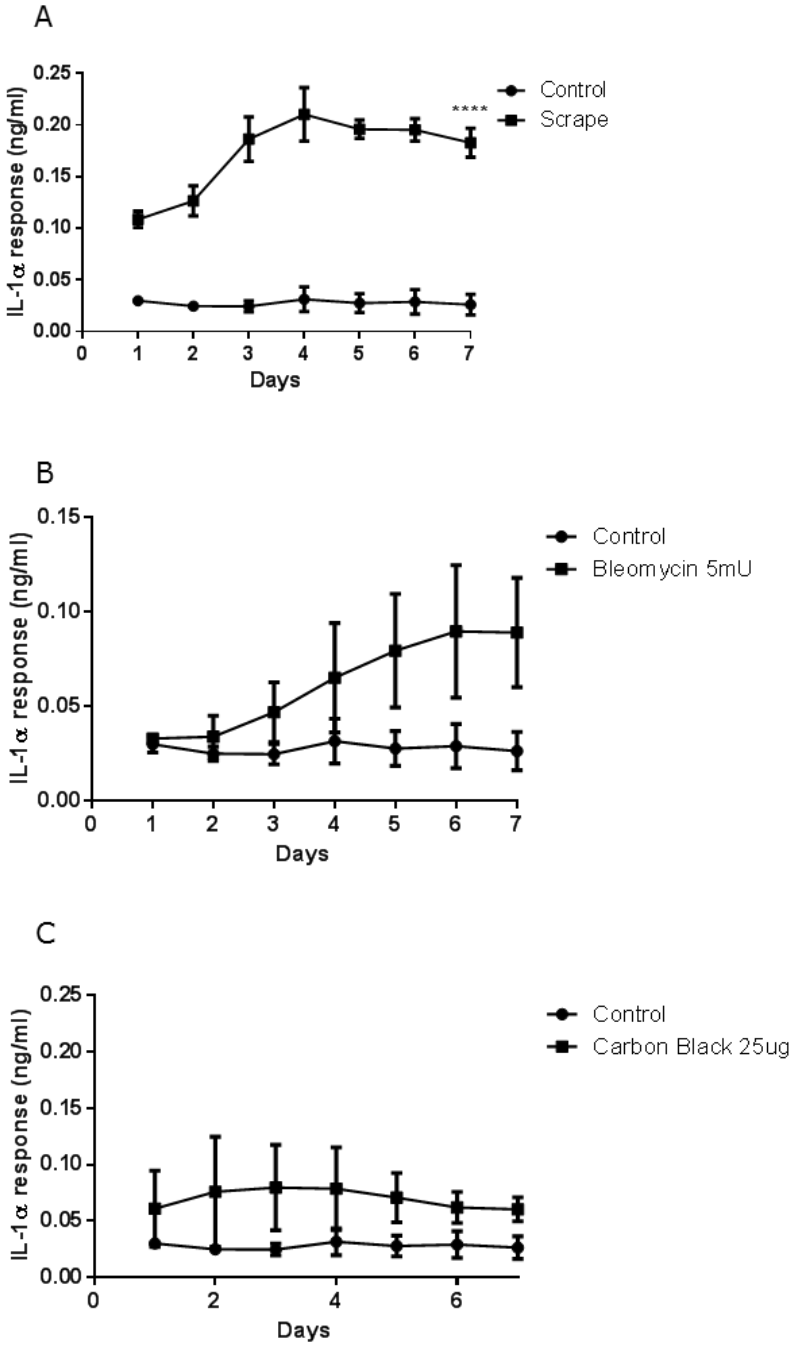


Figure 3-9: IL-1α response of epithelial cells after various injuries over 7 days. ELISA was performed to determine expression of IL-1α response in epithelial cell supernatants. All the graphs show mean concentration (ng/ml) conducted in triplicate n=3. A); scratch-wound vs Control with a significance of $p<0.001$, two-way ANOVA with the Bonferroni post-hoc test). B); Bleomycin vs Control with a borderline significance of $p<0.0315$, two-way ANOVA with the Bonferroni post-hoc test). C); Carbon Black vs Control with no significance. The asterisk *** represents $p<0.001$. Experiments were conducted in triplicate. n=3 independent biological experiments.

3.4.7 The effect of epithelial injury on fibroblast proliferation

IPF is a heterogeneous disease represented by a histologic feature known as the fibroblast foci which consists of resident lung fibroblasts, differentiated fibroblasts and fibrocytes (Selman and Pardo 2002). When epithelial cells are injured, this initiates an inflammatory cascade effect and exaggerated pro-fibrotic cytokine expression which contributes to the development of the fibroblast foci and increased extracellular matrix deposition (Ramos, Montano et al. 2001) and leads to the extensive wound repair in the lungs.

The origin of the lung fibroblasts during pulmonary fibrosis is unknown, but recurrent injury of the epithelial cells is thought to contribute to the recruitment and proliferation of fibroblasts (Tanjore, Xu et al. 2009). The potential sources of fibroblasts can include resident lung interstitial fibroblasts, differentiated progenitor cells from bone marrow known as fibrocytes and transition of epithelial cells to a fibroblast phenotype through a process known as epithelial–mesenchymal transition (EMT) (Kalluri and Neilson 2003).

Animal studies have demonstrated that *in situ* proliferation contributes to the lung fibroblast population (Zhang, Rekhter et al. 1994). Animal studies have also demonstrated that during bleomycin-induced pulmonary fibrosis, multiple origins of fibroblasts are involved in the fibroblast population in the disease and in particular, the epithelial cells undergo EMT (Tanjore, Xu et al. 2009).

The aim of this study was to determine whether injured epithelial cells have an effect on the fibroblast proliferation in collagen. The rationale was that lung fibroblasts are key mediators of fibrosis resulting in accumulation of excessive interstitial collagen and extracellular matrix due to increased proliferation of fibroblasts. The fibrotic triggers in IPF are unknown but it is believed that persistent epithelial injury leads to accumulation of fibroblasts leading to fibroblast foci (Habiel and Hogaboam 2014).

The co-culture model was set-up in the Transwell® system with epithelial cells and fibroblasts in collagen (refer to section 2.3). Bleomycin was prepared in serum-free DMEM/F12. Bleomycin was not added directly onto fibroblasts. Bleomycin was only added to epithelial cells in the inserts every 24 hours for 6 days. A series of inserts were set up in which epithelial cells were exposed to bleomycin (Table 3-1).

After every 48 hours, the bleomycin was washed off the epithelial cells (a set) with PBS and replaced with DMEM/F12. The insert/set was then placed on the fibroblast - collagen gel and left for 48 hours. After 48 hours, supernatants were removed and kept at -80°C. Fresh serum free medium was added to the well consisting of fibroblasts and bleomycin inserts were added on the fibroblast/collagen gels. This was done every 48 hours over 6 days. The experiments were carried out in triplicate; (n=3).

Table 3-1: A table to explain the addition of bleomycin on the epithelial cells

Addition of bleomycin on epithelial cells	**Fibroblasts in collagen**
Day 0: Addition of bleomycin to Insert set **A** Insert set B Insert set C	No addition to fibroblasts
Day 1: Addition of Bleomycin to Insert set B Insert set C	Insert A added to fibroblasts
Day 2: Addition of Bleomycin to Insert set B Insert set C	No addition to fibroblasts
Day 3: Addition of Bleomycin to Insert set C	Insert set A removed Insert B added to fibroblasts
Day 4: Addition of Bleomycin to Insert set C	No addition to fibroblasts
Day 5:	Insert set B removed Insert C added to fibroblasts
Day 6:	Samples analysed.

Epithelial cells in the inserts were injured either by scratch-wounding or bleomycin administration. Carbon black addition was discarded as an injury because there no IL-1α response over 7 days (Figure 3-9). During the validation stage (section 3.4.5), the injuries (bleomycin or scratch) were performed every 24 hours over 7 days. However, in the following experiments, the injuries were performed every 48 hours over 6 days in order to limit the disturbance of the co-culture model. After 6 days, an MTT reduction assay was performed to determine cell viability of the fibroblasts. The cells were also stained for anti-Ki67 and DAPI to determine cell number and cell proliferation (refer to section 2.6.2).

The MTT assay results revealed that the cell viability of the fibroblasts had increased with both scratch and bleomycin injury, as compared to fibroblasts which were not exposed to epithelial cells and non-injured fibroblast cells (Figure 3-10), with a significance of $p<0.01$ using one-way ANOVA followed by Tukey's post-hoc test, (refer to section 3.3.6).

The Ki-67 positive percentage of cells showed a very similar trend as to the MTT reduction assay results (Figure 3-11). The Ki-67 results revealed that in the epithelial cells exposed to bleomycin, the fibroblasts had proliferated by 11%. Using statistical analysis, the results were insignificant compared to the non-injured fibroblast cells (control).

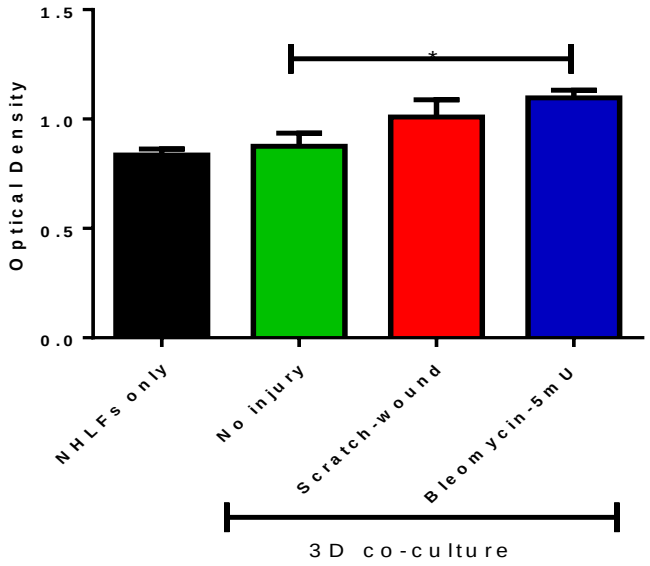


Figure 3-10: **MTT reduction assay showing optical density of fibroblasts in co-culture on day 6 after epithelial injury.** The epithelial cells were inflicted with various injuries and no-injury. The MTT reduction assay was used to determine the cell viability of the fibroblasts after epithelial injury. Administration of bleomycin vs no-injury with a significance of $p<0.05$, one-way ANOVA with Tukey's post-hoc test. The asterisk * represents $p<0.05$. Experiments were conducted in triplicate. n=3 independent biological experiments.

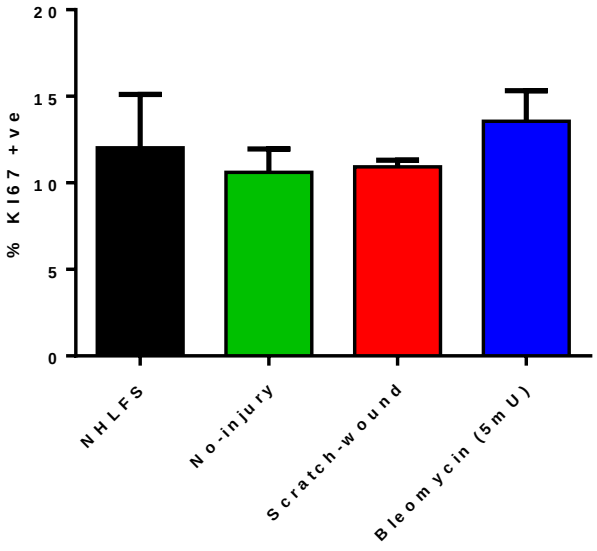


Figure 3-11: Ki 67 +ve Fibroblasts in co-culture inflicted with epithelial injury. Ki-67 positive cells were counted in different wells and the percentage difference between the various injuries on day 6 was calculated. Statistical analysis was performed using one-way ANOVA. Experiments were conducted in triplicate. n=3 independent biological experiments.

The expression of α-*SMA* was measured in co-cultured fibroblasts to determine fibroblast differentiation i.e. the differentiation to myofibroblasts in response to epithelial cell injury. There is no specific marker to identify fibroblast differentiation, nevertheless α-*SMA* is the classic marker for myofibroblasts (Phan 2008). Quantitative RT-PCR (refer to section 2.8) was performed to determine the expression of α-*SMA* in fibroblasts. The analysis revealed that there was a significant increase of α-*SMA* in response to bleomycin injury compared with uninjured controls ($p < 0.0021$), (Figure 3-12). All statistical analysis was performed with one-way ANOVA followed by Tukey's post-hoc test (refer to section 3.3.6).

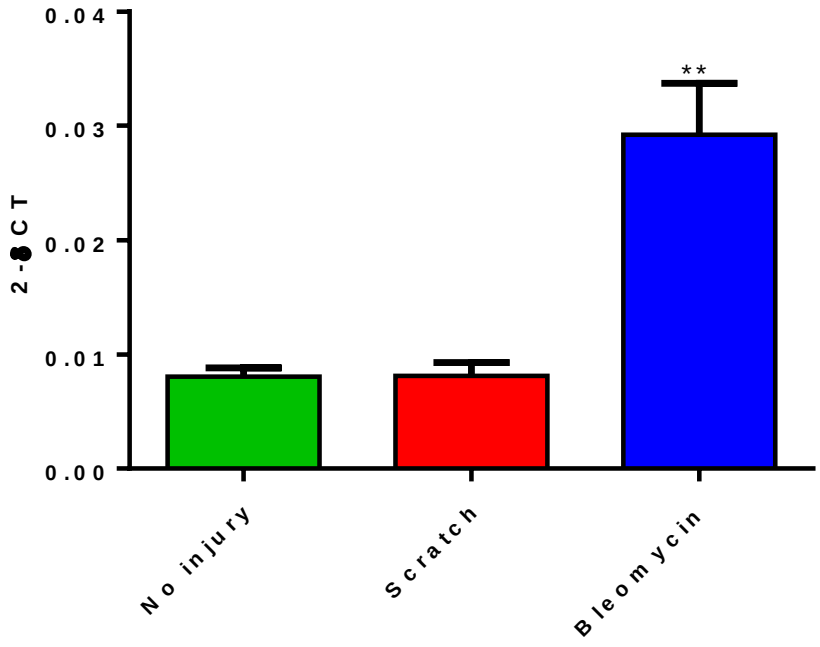


Figure 3-12: **Gene expression of *α-SMA* in co-cultured fibroblasts.** Gene expression of α-*SMA* in co-cultured fibroblasts in response to epithelial cell injury after six days. Administration of bleomycin vs no-injury with a significance of $p<0.01$, one-way ANOVA with Tukey's post-hoc test. The asterisk ** represents $p<0.01$. Experiments were conducted in triplicate. n=3 independent biological experiments

3.4.8 The effect of epithelial injury on extracellular matrix gene expression by fibroblasts.

In the human lung, ECM consists primarily of collagen I and collagen III, which provides tensile strength (Schuliga, See et al. 2009). Elastins provide elasticity and other ECM proteins can include fibronectin, glycosaminoglycans and proteoglycans such as Versican, which serve to maintain lung cell polarity and survival (Booth, 2012). ECM components, such as Collagen I and III which are the most predominantly increased components in the matrix after injury (Choe, Sporn et al. 2006).

The aim of this experiment was to determine if there was an up regulation of the expression of certain ECM components in fibroblasts in response to epithelial cell injury. The co-culture model was set up in the Transwell® system in triplicate (n=3) (refer to section 2.4) and gene expression was assessed using quantitative RT-PCR analysis in triplicate (refer as section 2.8). The data were normalised to *β-actin* house-keeping gene (n=3).

There was a significant increase in *Collagen I and III* gene expression but not *Versican*, in fibroblasts in response to epithelial cell injury (Figure 3-13). The *Collagen I* expression revealed that in addition of bleomycin vs no-injury, there was no significant increase of *Collagen I* ($p=0.2549$) but a trend of increased *Collagen I* expression was observed. The *Collagen III* expression revealed that in addition of bleomycin vs no-injury, there was a significant increase of *Collagen III* ($p<0.05$, n=3). All statistical analysis was performed with one-way ANOVA followed by Tukey's post-hoc test (refer to section 3.3.6).

To determine whether bleomycin had 'no direct effect' on the fibroblasts, further analysis was performed. Bleomycin (5mU) was added directly onto the fibroblasts in collagen for 24 hours (without the addition of epithelial cells). The fibroblasts were extracted and quantitative RT-PCR analysis was performed. The results showed that bleomycin exposed directly on to fibroblasts revealed no difference in expression of the genes encoding *α-SMA*, *Collagen I* and *Versican* when normalised to house-keeping gene *β-actin* (Figure 13A). Overall, the gene expression for co-cultured fibroblasts in response to epithelial cell injury, revealed an increased expression of

the ECM and α-*SMA* genes, which may be via various cytokines or growth factors released by the epithelial cells (Figure 3-13 B-D). This may suggest, that the fibroblasts may have responded to epithelial injury.

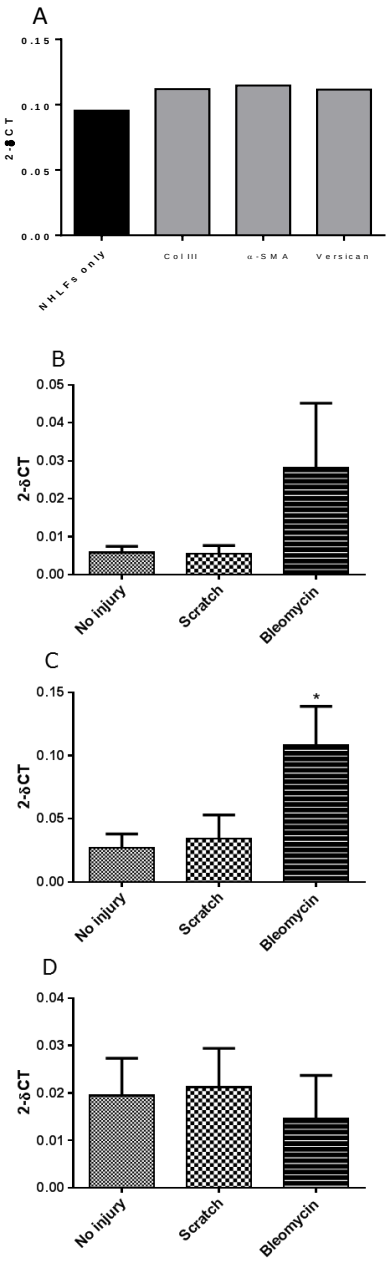


Figure 3-13: Quantitative RT-PCR analysis used to determine gene expression showing ECM components. Gene expression was determined in fibroblasts after epithelial injury. A; Monolayer of fibroblasts in collagen with no addition of; No change of expression in *Collagen type III,* α*-SMA, and Versican,* with the addition of 5mU bleomycin direct on fibroblasts (n=1). B-D; Co-cultured fibroblasts with epithelial injury. B; Expression of *Collagen I* in co-cultured fibroblasts. C; expression of *Collagen III* in co-cultured fibroblasts with $p<0.05$. D; expression of *Versican* in co-cultured fibroblasts. Data were normalised using house-keeping gene used β-*actin*. Statistical analysis performed using one-way ANOVA with Tukey's post-hoc test. The asterisk * represents $p<0.05$. Experiments were conducted in triplicate. n=3 independent biological experiments.

3.4.9 The effect of epithelial injury on apoptosis of fibroblast cells

Alveolar epithelial damage plays an important role in the pathogenesis of a fibrotic response (Uhal 2008). Persistent epithelial cell damage can provoke the migration, proliferation and activation of fibroblast cells which contribute to the initiation of fibroprolific responses (Santiago, Galindo et al. 2004). However, in fibrosis, apoptosis is reduced and contributes to the accumulation of fibroblasts, leading to fibrosis (Uhal, Joshi et al. 1998).

Studies have demonstrated that numerous apoptotic epithelial cells in the lung tissue from patients with IPF are associated with increased myofibroblast activity (Uhal 2008). Further studies have shown that apoptosis increases in damaged alveolar epithelial cells but decreases in IPF fibroblasts. These mesenchymal cells become resistant to apoptosis, and these mechanisms may play a pivotal role to the underlying pathogenesis of IPF (Kuwano 2007).

Apoptosis may participate in the development of lung disease via three different mechanisms: 1) increased apoptosis of epithelial cells leading to inefficient re-epithelialisation; 2) resistance to apoptosis of fibroblasts leading to increased fibrosis; 3) ineffective removal of apoptotic cells (Drakopanagiotakis, Xifteri et al. 2008). It is increasingly recognised that during pulmonary fibrosis, fibroblasts are not eliminated by apoptosis (Martin, Hagimoto et al. 2005).

Two signalling pathways of apoptosis known as extrinsic and intrinsic pathways are involved. The extrinsic pathway is triggered by extracellular signalling, mainly by the ligands of tumour necrosis factor receptor superfamily e.g. Fas-L and Trail. Subsequently, death receptor proteins i.e. FADD and TRADD are recruited and a Fas-associated death domain is formed, leading to the assembly of a death-inducing signalling complex and activating caspase-8. Finally, downstream caspases, especially caspase-3 and caspase-7, are activated to ultimately kill the cell (DosReis and Borges 2003). The intrinsic pathway is associated with the activation of the proapoptotic Bcl-2 family members in the mitochondria (e.g. Bax with the subsequent mitochondrial release of cytochrome c and the formation of apoptosome complex, which leads to

activating caspase-9 and then to caspase-3 and caspase-7 that induces cell apoptosis (Thannickal, Toews et al. 2004). In both pathways, the late apoptotic events take place after activation of the effector caspases, in particular, caspase 3, and include exposure of phosphatidylserine on the external surface of the plasma membrane which can be measured by cleavage of poly (ADP-ribose) polymerase (PARP) (Pagano, Pitteloud et al. 2005).

Fibroblast apoptosis is important for the resolution of fibrosis. However, the mechanisms by which the cells undergo apoptosis are not well understood. Several studies from human lung tissue and animal models have shown a variety of processes including inflammation, angiogenesis and tissue remodelling involved in apoptosis, along with cytokines and growth factors (Kuwano, Hagimoto et al. 2004). A previous study has shown apoptosis of cultured fibroblasts can be induced or suppressed by growth factors and cytokines (Santiago, Galindo et al. 2004).

A study by *Moodley et al, 2003*, reported IL-6 signalling in IPF may be anti-apoptotic in patients with pulmonary fibrosis (Moodley, Misso et al. 2003). Another molecule which induces apoptosis Fas ligand (Fas-L) is shown to induce apoptosis in cells expressing Fas antigen (Fas) in lung tissue (Kuwano, Miyazaki et al. 1999). TNF-α, a cytokine is involved in inflammatory responses and may also attenuate fibrosis by suppressing collagen synthesis (Abraham, Shiwen et al. 2000). *In vitro,* studies have shown that interferon-γ (IFN-γ) decreases the synthesis of both collagen I and III in patients with lung fibrosis (Sempowski, Derdak et al. 1996).

The aim was to investigate whether fibroblasts in the co-culture model were resistant to apoptosis when exposed to epithelial cells undergoing injury. Initially, a suitable concentration for each treatment i.e. IL-6, Fas-L, TNF-α and INF-γ, was established on the fibroblasts in collagen without epithelial cells. Fibroblasts were cultured in collagen (refer to section 2.4). The fibroblasts were exposed to various apoptosis inducers and suppressors for 24 hours (Table 3-2). Twenty four hours after the addition of various treatments, an MTT assay was performed treatments to determine cell viability.

Table 3-2: A table of apoptotic inducers and suppressors which were added to cultured fibroblasts for 24 hours

Treatments				
IL-6	**Fas-L**	**IFN-γ**	**TNF-α**	**Staurosporine**
25ng/ml	25ng/ml	5ng/ml	15ng/ml	5nM
50ng/ml	50ng/ml	10ng/ml	25ng/ml	10nM
100ng/ml	100ng/ml	15ng/ml	50ng/ml	20nM
250ng	200ng/ml	25ng/ml	75ng/ml	50nM
500nM	500ng/ml	50ng/ml		75nM
1000nM	1000ng/ml	75ng/ml		100nM
		100ng/ml		250nM
				500nM

The MTT reduction assay results revealed no trend was seen in the dose response of the fibroblasts with the various treatments used. Fibroblasts exposed to IL-6, Fas-L and Staurosporine all showed reduced cell viability significantly after 24 hours (Figure 3-14). Exposure to IL-6 decreased fibroblast cell viability at concentrations 25ng/ml, 250ng/ml and 500ng/ml. Fas-L treated fibroblasts, cell viability reduced at all concentrations and for Staurosporine exposed fibroblasts, cell viability was reduced at 50nM, 75nM, 100nM, 250nM and 500nM. An aberrant dose response of the various treatments on the fibroblasts was observed. This could be due to the fibroblast being embedded in collagen and therefore, the various treatments did not reach the fibroblasts in an uniform manner.

All these effects were significant ($p<0.05$, n=3). The statistical analysis was performed using one-way ANOVA followed by Tukey's post-hoc test. Experiments were conducted in triplicate. n=3 independent experiments (refer to section 3.3.5).

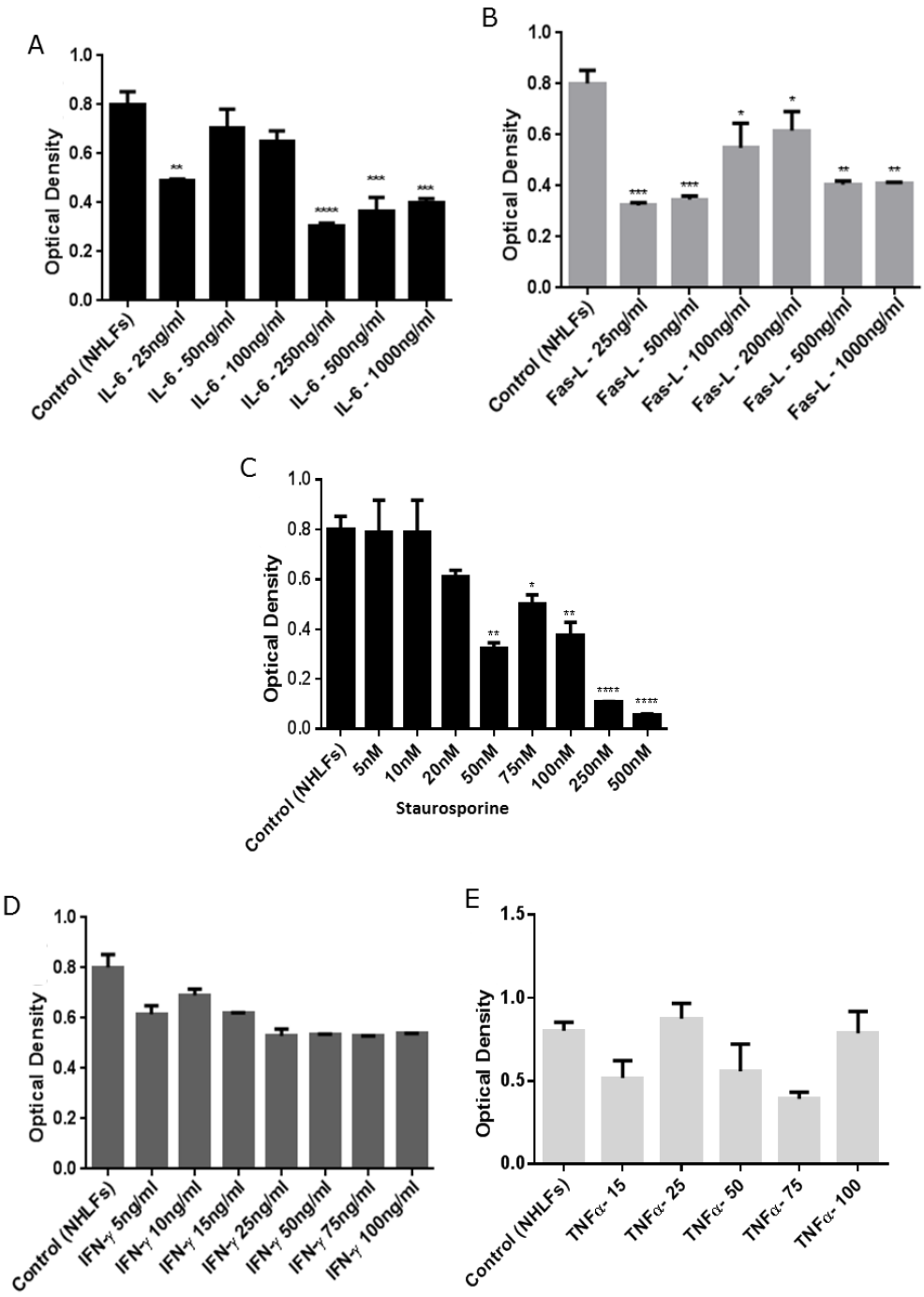


Figure 3-14: The effect of various apoptotic inducers on fibroblasts determined by MTT reduction assay. The effect of (A) IL-6, (B) Fas-L and (C) Staurosporine reduced cell viability of the fibroblasts after 24 hours of addition. (D) IFN-γ and (E) TNF-α had no effect on the cell viability of the fibroblasts after 24 hours addition. The statistical analysis was performed using a one-way ANOVA with Tukey's post-hoc test. The asterisks; *** represents *p<0.001*, ** represents *p<0.01 and* * represents *p*<0.05. Experiments were conducted in triplicate. n=3 independent biological experiments.

Apoptosis at a cellular level was determined by the expression of caspase 3 and cleavage of PARP on fibroblasts in collagen, without the addition of epithelial cells. The treatments were chosen based on the most significant effect on the fibroblasts (Table 3-3). These treatments were added to the fibroblasts in collagen for 24 hours (refer to section 2.3.4). The fibroblasts were extracted (refer to section 2.7.2), and western blot was performed to determine caspase 3 and PARP cleavage.

Table 3-3: Treatments selected for the addition on cultured fibroblasts

Lane	Treatment	Concentration
	Untreated	No addition
1	IL-6	250ng/ml
2	IL-6	500ng/ml
3	Fas-Ligand	250ng/ml
4	Fas-Ligand	500ng/ml
5	IFN-γ	50ng/ml
6	IFN-γ	100ng/ml
7	Staurosporine	250nM
8	Staurosporine	500nM

Western blot analysis confirmed that only Staurosporine at 250nM (lane 7) and 500nM (lane 8) induced the cleavage of Caspase 3 (17kDa) and PARP (89kDa) (Figure 3-15) in cultured fibroblasts after 24 hours of addition.

The activation of the caspase-3 pathway is a hallmark of apoptosis and can be used to quantify activators and inhibitors. The various treatments (Table 3-3) were used on the fibroblasts in collagen. Caspase-3 activation was investigated in fibroblasts in which the fibroblasts were exposed to various treatments to induce apoptosis. There was a suggestion that caspase-3 cleavage (17kDa) occurred, but only during staurosporine treatment of fibroblasts (7-8 lanes) as compared to the untreated fibroblasts. However, this was weak compared to PARP cleavage which is clearly seen (7-8 lanes), (Figure 3-15).

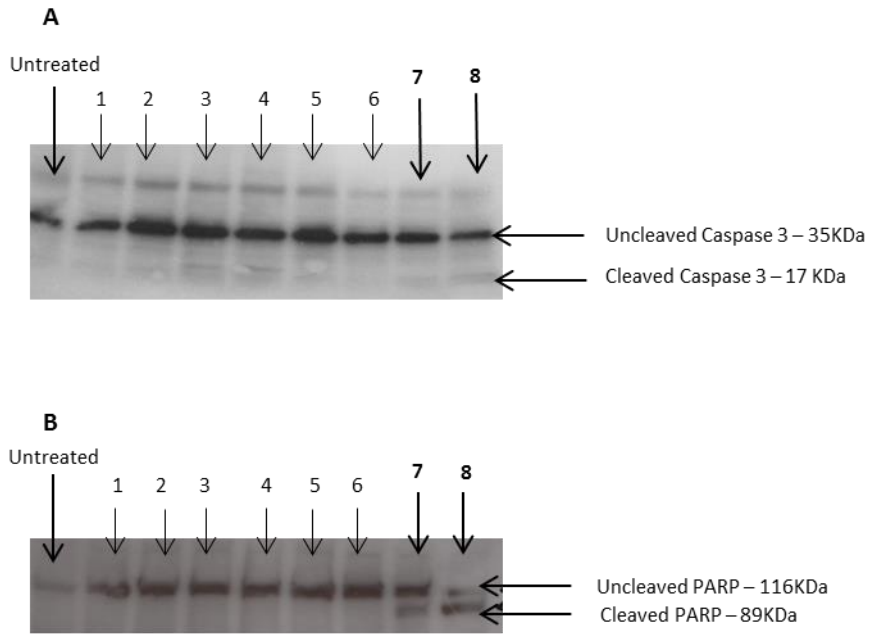


Figure 3-15: Expression of Caspase 3 in co-cultured fibroblasts with Western Blot. (A) Caspase ~ 17kDa and (B) PARP ~ 89kDa: in cultured fibroblasts only by western blotting. Lanes represents as 1. IL-6 at 250ng/ml, 2. IL-6 at 500ng/ml, 3. Fas-Ligand at 250ng/ml, 4. Fas-Ligand at 500ng/ml, 5. IFN-γ at 50ng/ml, 6, IFN-γ at 100ng/ml, 7. Staurosporine at 250nM and 8. Staurosporine at 500nM. Note: Numbers 7 and 8 are in bold to emphasize that these samples were exposed to Staurosporine.

Staurosporine was selected as a pro-apoptotic treatment in the 3D co-culture model. Fibroblasts were cultured in collagen and epithelial cells were exposed to injury, either scratch or bleomycin, for 6 days. On day 6, 500nM Staurosporine was added on the fibroblasts and left for a further 24 hours. This was to determine if the fibroblasts would be protected from apoptosis after epithelial injury. Fibroblasts were extracted from collagen and western blot was performed. The expression of PARP cleavage shown in lanes 2, 4, 6 and 8 are co-cultured fibroblasts, exposed to Staurosporine for 24 hours (Figure 3-16).

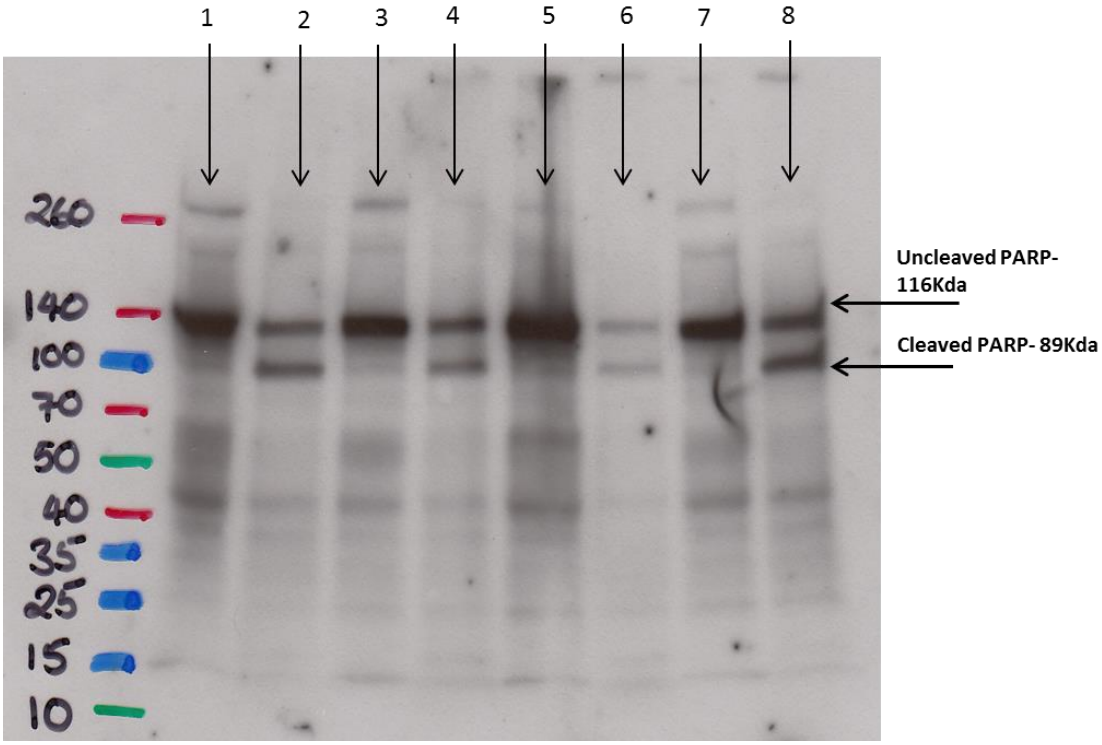


Figure 3-16: Expression of PARP with western blot. The expression of co-cultured fibroblasts after epithelial injury (various injuries inflicted) for 6 days. On day 6, there was addition of Staurosporine 500nM (only in lanes 2, 4, 6 & 8) and incubated for 24 hours. Western blotting performed after 24hours. The bands show uncleaved PARP 116Kda and Cleaved PARP 89Kda indicated by an arrow on the western blot. 1. NHLFs, 2. NHLFs with addition of staurosporine, 3. No-injury, 4. No-injury with the addition of staurosporine, 5. Scratch, 6, Scratch with the addition of staurosporine, 7. Bleomycin and 8. Bleomycin with addition of staurosporine. The expression of uncleaved PARP and Cleaved PARP were present in the fibroblasts with the addition of Staurosporine 500nM. The western blot was performed on three independent experiments (n=3). This is one representative.

Western blots were quantified by densitometry (refer to section 3.3.5). The densitometry was performed on three independent western blots. Each uncleaved and cleaved band in each lane was quantified using ImageJ. A percentage of cleaved PARP relative to uncleaved PARP for each condition was calculated and the average was plotted (Figure 3-17). Statistical analysis was performed using GraphPad Prism version 6.0. The statistics were performed using one-way analysis. The data revealed there was no significant difference in apoptosis with percentage of cleavage for either of the injuries, scratch and bleomycin compared to the no-injury (control). Therefore, the fibroblasts were not 'protected from apoptosis' when the epithelial cells were inflicted with injuries.

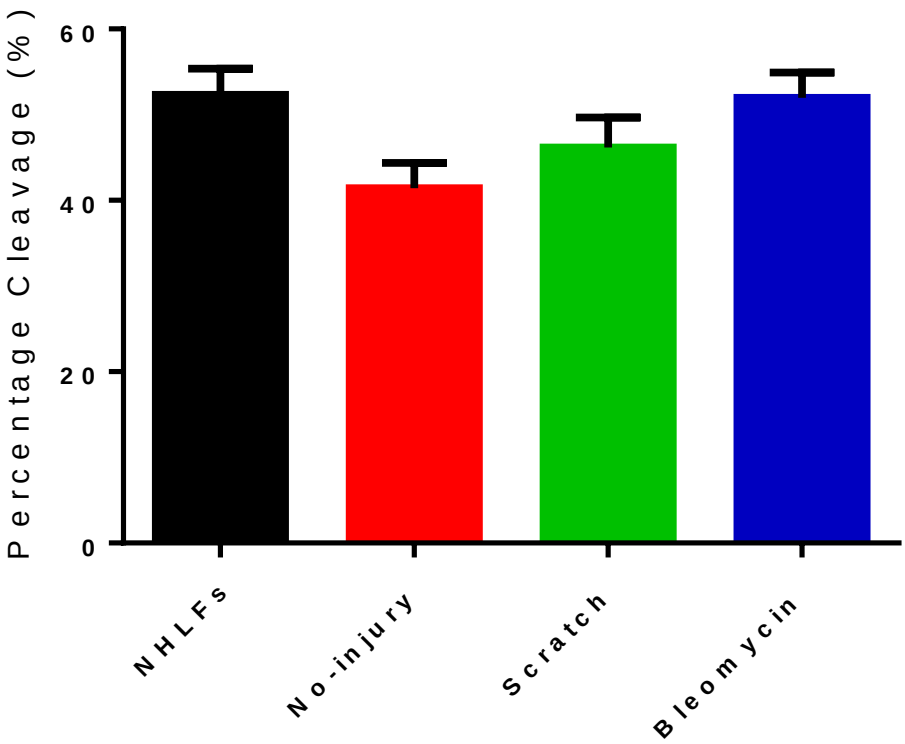


Figure 3-17: Measurement of PARP cleavage expressed as a percentage of total PARP cleavage in fibroblasts. Staurosporine at 500nM was added to the co-culture after the infliction of various injuries. Western blot was performed after 24 hours after the addition of Staurosporine at 500nM. The bands were analysed by using image J, and percentage of PARP was calculated. Bars represent means (± SEM; n=3). Statistical analysis was performed using one-way ANOVA followed by Tukey's post-hoc test, data showing no significance of injury to PARP cleavage.

3.5 Discussion

The aim of the chapter was to develop a 3D co-culture system consisting of human epithelial cells and fibroblasts using a non-direct method in a Transwell® system to study epithelial-fibroblast crosstalk in the development of pulmonary fibrosis. The effect of epithelial injury on fibroblast response was examined in the 3D co-culture model with various injuries including scratch wound, the addition of bleomycin or carbon black. Using this model, we demonstrated that in response to epithelial injury, fibroblast cells mediated responses i.e. increased cell proliferation, increased matrix gene expression and expression of cytokine production.

The 3D co-culture model consisted of small airway epithelial cells with normal human lung fibroblasts in collagen separated by a porous membrane in a Transwell® system. The use of small airway epithelial cells rather than primary alveolar type II (ATII) cells was a limitation of this model. ATII cells make up 2-5% of the population in the lung alveoli and only proliferate once the ATI cells are damaged (McElroy and Kasper 2004). Autopsy is not performed in normal healthy lung and ATII are very difficult to retrieve in the alveolus. However, given the difficulties in obtaining and maintaining primary human ATII cells in their physiological state *ex vivo*, this system provides a means to study the behaviour of cell types from normal or diseased lungs in an epithelial injury model. Therefore, commercially bought normal SAEs and normal NHLFs were purchased from Lonza.

The fibroblasts were cultured in rat tail type I collagen. Collagen is a major component of the ECM complex and is used to mimic one of the components of the basement membrane for the cells as well as to initiate signalling events between matrix and cells (Schuliga, See et al. 2009). The collagen gel provides an *in vivo* micro-environment for the fibroblasts, with a natural substrate for cellular attachment, growth and differentiation and also, promoting cellular proliferation and differentiation (Ruszczak 2003). Fibroblasts cultured in a collagen gel have distinct characteristics compared to those cultured without collagen (Mio, Adachi et al. 1996). The fibroblasts cultured in gels acquire a bipolar spindle pattern and form an

organised membrane that possess one or more broad, flattened features (Mio, Adachi et al. 1996).

Fibroblasts were co-cultured in a Transwell® system and this was to mimic a non-direct contact method, as they would in the lung. The Transwell® was acting as a basement membrane separating the epithelial cells and fibroblasts. Also, the membrane consisted of pores to potentially allow only paracrine communications through diffusible factors.

The 3D co-culture model was optimised to ensure that the model would be able to mimic some of the mechanisms and mediators released, which may be involved in the pathogenesis of IPF. Often in *in vitro* methods, to reproduce the complexity of the *in vivo* situation can be a challenge. The cell types and cell number in *in vitro* cultures are usually very limited, and may not provide the appropriate signalling molecules produced by the low volumes of cells or culture medium for production of mediators and signalling, thus cell signalling may be lost in *in vitro* systems.

Currently lung biopsy is the best form of diagnosing the disease. Previous studies have shown that disease progression in IPF patients is accompanied by fibroblast proliferation, matrix deposition, extensive scarring and alveolar destruction, leading to characteristic honeycomb lesions seen in human IPF tissue (King, Pardo et al. 2011). The limitation of a lung biopsy is that the characterisation of IPF is seen at the end of the disease. The 3D-co-culture model may provide an understanding of the initiation/early stages of the disease enabling the use of various injury methods to initiate injury response in epithelial cells and examine the response in fibroblasts. Therefore, the 3D co-culture model was validated by determining cell proliferation, gene expression of extracellular matrix genes in fibroblasts and cytokine production in epithelial cells, which may be able to provide an insight into the pathogenesis of IPF.

The approach was to optimise the cell number of the epithelial cells in a monolayer in the Transwell® insert. Also, the correct pore size on the insert was established so that

the cells did not migrate through the Transwell® membrane. It was important to establish the correct pore size, as a non-direct contact method was required to understand the independent system. A tracking probe i.e. cell tracker® was added to epithelial cells in the Transwell® insert with different pore sizes of the insert. The cell tracker dye passes through the membrane into the cell and is passed to daughter cells for multiple generations but does not transfer to neighbouring cells in contact. This dye was ideal to monitor the movement of the cells through the pores (refer to appendix 8).

After 7 days, the correct pore size was determined by observing the cells which did not migrate through. This was to determine and maintain a non-direct approach of culturing the epithelial cells with the fibroblasts. This was also to determine the suitable cell number, maintaining the monolayer of the epithelial cells without the cells detaching over the duration of the experiment.

It was important to establish the correct cell number for the fibroblasts in the collagen (section 3.4.2). This was to determine that the collagen did not contract once there was a confluent layer of fibroblasts during the 7 days, as this may have been a result of collagen degradation, which would not be suitable for the model. Previous studies have demonstrated that, cells seeded at a too high density may reach confluence, which then consequently lead to cell loss and/or cessation of proliferation (Masur, Dewal et al. 1996). So, adjusting the cell number with collagen, reassured the balance between the cell number and the collagen. This was necessary for cell to cell contact of the fibroblasts to occur in the 3D co-culture model.

Previous studies have shown repetitive damage to the airway or alveolar epithelium can result in inflammation and tissue remodelling which are common features of idiopathic pulmonary fibrosis (Meltzer and Noble 2008). Epithelial damage can be initiated directly by the inhalation of airborne toxins such as diesel exhaust particulates (Doornaert, Leblond et al. 2003) and pathogenic organisms such as Epstein-Barr virus (Tsukamoto, Hayakawa et al. 2000). This may occur indirectly via the inhalation of other environmental exposures (cigarette smoking, dust particles or

chemicals) (Meltzer and Noble 2008). Whether occurring directly or indirectly, both have the potential to cause the release of pro-inflammatory cytokines and growth factors into the airway including; IL-1, IL-6, IL-8 transforming growth factor β (TGF-β), epidermal growth factor (EGF), granulocyte macrophage-colony stimulating factor (GM-CSF) and eosinophil major basic protein (Wynn 2011).

Thus, epithelial damage has been known to cause the release of pro-inflammatory signals which pass down into the sub-mucosa to the basement membrane and initiate re-epithelisation of the surface. As a result, fibroblasts are recruited for repair, where fibroblast proliferation and ECM accumulation occur and apoptosis is disabled. The mechanisms underlying the repair process remain poorly understood.

To measure the fibrotic responses in the 3D co-culture model, it was important to establish a model in which recurrent injuries were inflicted and an inflammatory response was measured. As previously mentioned, the favoured model to understand the mechanism of pulmonary fibrosis is the bleomycin-induced pulmonary fibrosis in mice (Umezawa, Ishizuka et al. 1967). Therefore, bleomycin was used as one of the injuries. Other recurrent injury methods used were scratch wound to mimic mechanical injury (Wadsworth, Nijmeh et al. 2006) and carbon black particles (Doornaert, Leblond et al. 2003). These injuries were successfully inflicted on the epithelial cells in the 3D co-culture model over 6 days (section 3.4.6). Measurements of the inflammatory response were then determined in supernatants. A recent study measured IL-1α as a pro-inflammatory marker released by damaged epithelial cells. The study showed that IL-1α autoantibodies in serum of IPF patients were generated as a response to the inflammatory process in rapidly progressive IPF and may act as a regulatory factor for IL-1α (Ogushi, Tani et al. 2001). Another study demonstrated that IL-1α is the critical innate immune trigger released by stressed lung epithelial cells (Suwara, Green et al. 2014). In the 3D co-culture model, an inflammatory response was measured by detection of the expression of IL-1α.

In the 3D co-culture model, scratch, addition of bleomycin or addition of carbon black were inflicted on epithelial cells repeatedly. The supernatants revealed that IL-

1α response had increased over 6 days with the level of injuries (Figure 3-9). As for carbon black, there was an IL-1α response at day 2 and remained the same at day 6. There was no increase in IL-1α response over 6 days with the addition of carbon black particles. This suggested that there was no effect of carbon black on the epithelial cells. A possible reason for no IL-1α response with the addition of carbon black could be that only two cell types were used in the model. Epithelial cells alone may not amplify a response to the carbon black particles. Previous studies have shown that lung activated immune cells including neutrophils and macrophages release cytokines, reactive oxygen species (ROS), lipid mediators, and toxic proteases, which may further amplify and contribute to any DEP-induced epithelial damage (Schwarze, Totlandsdal et al. 2013). Therefore, carbon black was not used in the remainder of the study.

A histopathological feature of IPF is an increased number of pulmonary fibroblasts known as 'fibroblast foci'. The bleomycin-mouse model supports the hypothesis that during injury, epithelial cells can recruit fibroblasts to the site of injury and stimulate them to differentiate to myofibroblasts (Tanjore, Xu et al. 2009). Another study by Raghu and co-workers obtained fibroblasts from different areas of the same fibrotic lung and found higher rates of proliferation in cells derived from inflammatory areas and lower rates in fibroblasts from dense fibrotic scar tissue (Raghu 1988).

In the 3D co-culture model, scratch or bleomycin injuries to the epithelial cells increased the rate of proliferation of fibroblasts in collagen (section 3.4.7). A MTT reduction assay confirmed cell viability and the Ki-67 expressions revealed an increase in cell number. This increase in cell number could be that injured epithelial cells released soluble mediators which promoted the increased proliferation of fibroblasts. One of the growth factors which may be involved in explaining the proliferation in the model would be the effect of transforming necrosis factor alpha (TNF-α). Studies have shown that TNF-α is released from damaged epithelial cells and exerts profibrotic effects (Allen et al 2002). There are various mechanisms through which TNF-α may be involved in the development of fibrosis including induction of inflammatory cells, initiation of cytokine cascade events, regulation of

apoptosis and regulation of collagen synthesis (Lasky and Brody 2000). TNF-α may increase fibroblast proliferation, differentiation and collagen transcription indirectly via transforming growth factor-β or platelet-derived growth factor (PDGF) induction pathways (Kapanci, Desmouliere et al. 1995). Another soluble mediator which is implicated with the progression of the disease is endothelin-1 (ET-1). ET-1 is able to induce a number of growth factors through paracrine stimulation including TNF-α, TGF-β and fibronectin and enhance neovascularisation through vascular endothelial growth factor (VEGF) (Fagan, McMurtry et al. 2001). Therefore, ET-1 could be involved in the fibroblast proliferation in the 3D-co-culture model.

One particular signalling pathway, which is implicated in the initiation of fibroblast proliferation, is Sonic Hedgehog (Shh). Shh is a developmental pathway which mediates epithelial-mesenchymal communication in lungs and kidney fibrosis during embryo differentiation (Bolanos, Milla et al. 2012). The ligand Shh is mainly expressed in epithelial cells, with fibroblasts acting as responder cells (Crosby and Waters 2010). The expression/activation of Shh in the early stages of injury in the lung is an attempt of reparative mechanisms of the lung epithelium (Fernandez and Eickelberg 2012). Activation of Shh induces glioma-associated oncogene homolog (GL1), ACTA2, fibronectin and COL1A1 expression in fibroblasts (Sakai and Tager 2013), which regulates the cell cycle enabling the Shh pathway to regulate cell proliferation (Sakai and Tager 2013).

The ECM is composed of fibronectin, proteoglycans and laminins but the most abundant ECM component in the majority of tissues is collagen. The principle collagens are the interstitial types I and III, which serve to form a fibrous network in the interstitium of tissues, and these are elevated in the parenchyma of patients with IPF (Laurent, Harrison et al. 1988).

Injured epithelial cells and proliferation of fibroblasts contribute to the altered ECM in IPF, due to an imbalance between components of the matrix metalloproteinases (MMPs) family and the tissue inhibitors metalloproteinases (TIMPs). Fibroblasts play an important role in the aberrant remodelling because they are responsible for the

exaggerated secretion of most of the ECM components (Blaauboer, Boeijen et al. 2014).

Fibroblasts play central roles both in the maintenance of normal tissue function and in the wound healing response. The lung is a dynamic organ, often under varying degrees of motility and stress. By generating ECM, fibroblasts provide a scaffold for cells and a link for mediators to be able to respond to the rapid changes in the microenvironment. In the lung, fibroblasts are found in greatest numbers in the subepithelial layer of the conducting airways and the interstitium of the lung parenchyma, which puts them in a prime location to interact with the epithelial cells (Clarke, Carruthers et al. 2013).

The aim of this study was to determine whether extracellular matrix components expression in fibroblasts increased when co-cultured with epithelial cells exposed to injury (section 3.4.8). This study demonstrated that the expression *of collagen I* and *III* had significantly increased in fibroblasts with addition of bleomycin as compared to no-injury. We also found that the expression of α*-SMA* (a mesenchymal marker) had also increased in fibroblasts with addition of bleomycin (Figure 3-13).

It is increasingly recognised that the pathogenesis of IPF is directly related to the presence and activity of myofibroblasts in which there is an excessive accumulation of the matrix due to the increased proliferation of myofibroblasts (Martin, Hagimoto et al. 2005). The persistence of the fibrotic lesions that characterise IPF suggests that decreased apoptosis of these cells may play a major role in the progression of the disease. In this study, we examined the effect of cytokines IL-6, Fas-L, TNF-α and IFN-γ which have been known to have profibrotic or antifibrotic effects on fibroblast apoptosis (Santiago, Galindo et al. 2004). The aim of the study was to investigate whether epithelial injury protected fibroblasts from apoptosis.

The study identified that IL-6 and Fas-L treatments decreased cell viability of fibroblasts cultured in collagen for 24 hours without the presence of epithelial cells (Figure 3-14). The TNF-α and IFN-γ treatments revealed no significant effects on the

cell viability in fibroblasts in collagen. On the other hand, Staurosporine, a non-specific ATP-analogue which inhibits numerous Ser/Thr and Tyr kinases, is known to induce apoptosis in various cells with similar rapid kinetics as death receptor signalling (Manns, Daubrawa et al. 2011), and for this reason, staurosporine was used as a pro-apoptotic agent and showed that it also decreased cell viability in the fibroblasts (Figure 3-14).

To further observe the effect of IL-6, Fas-L, Staurosporine on cultured fibroblasts (which were exposed to injured epithelial cells), were added for 24 hours and fibroblasts were extracted to observe the expression of cleavage poly (ADP-ribose) polymerase (PARP) by western blotting. In the samples which were treated with the mediators IL-6, Fas-L and proapoptotic agent Staurosporine, only cells treated with staurosporine expressed PARP cleavage and therefore, the fibroblasts had undergone apoptosis.

Injury to epithelial cells did not protect the fibroblasts from staurosporine induced apoptosis judging by PARP cleavage in these fibroblasts. Previous studies have shown that primary cultures of fibroblasts from patients with IPF (IPF-Fb) containing significantly greater numbers of myofibroblasts, are cells which may be resistant to apoptosis compared with cultures from subjects without lung disease (normal-Fb) (Moodley, Scaffidi et al. 2003). Studies have also demonstrated that myofibroblasts are more resistant to apoptosis than fibroblasts possibly due to a large number of α-SMA positive cells expressed in IPF tissue. These constitute to the major component of the fibroblasts' foci (Budinger, Mutlu et al. 2006). This study suggests that using fibroblasts alone may not be suitable to observe the mechanism of apoptosis.

Only epithelial cells and fibroblasts were used in the 3D co-culture model. Using immune cells may have provided a more complete model to explore the mechanisms of IPF. Inflammatory and immune responses may play key roles in progression of IPF. The recruitment of macrophages, neutrophils and eosinophils has been associated with the production of chemokines and cytokines in lung injury (Todd, Luzina et al. 2012). Macrophages release chemokines including macrophage inflammatory protein

(MIP) which activates lymphocytes and granulocytes, thereby secreting TNF-α, IL-1, IL-6, and other proinflammatory cytokines in lung injury (Wynn 2011). The recruitment of eosinophils is orchestrated by a complex series of events involving antigen-presenting cells (APCs), mast cells, T cells, B cells, along with their released cytokines as immune signals. Eosinophils are a source of over 35 cytokines, chemokines, and growth factors (Davoine and Lacy 2014). All these immune cells have profound effects on the progression of immune and inflammatory responses. To improve on the current study and provide further insights of the mechanisms involved in pulmonary fibrosis, a model including the use of immune cells might be a better approach.

3.6 Summary

We have demonstrated that low level recurrent epithelial injury resulted in increased proliferation and collagen gene expression in fibroblasts. In our model, protecting fibroblasts from injury and maintaining their function could be the next step to improving the model. The 3D co-culture model may prove useful to investigate the mechanisms involved in lung injury and repair in the context of epithelial-fibroblast crosstalk that appears to be a key mechanism in early wound healing in fibrosis.

Chapter Four

Expression of Matrix Metalloproteinases in the three dimensional co-culture model and IPF serum samples

4.1 General Introduction

The paradigm of IPF suggests that fibrosis is a result of abnormal communication between the alveolar epithelial cells and the mesenchymal fibroblasts during wound healing (Selman, King et al. 2001). During the normal repair process, there is re-establishment of the fibroblast and ECM components to baseline levels, whereas in fibrosis, it has been suggested that there is uncontrolled fibroblast proliferation and accumulation of extracellular matrix components (Loffek, Schilling et al. 2011).

Extracellular matrix synthesis is regulated by cytokines and growth factors as well as matrix metalloproteinases (MMPs), which maintain the balance of ECM. MMPs are proteolytic enzymes which play a role in pulmonary fibrosis in the regulation of multiple cellular functions, including cell proliferation, adhesion, migration, differentiation, angiogenesis and apoptosis (Dancer, Wood et al. 2011).

The MMPs are a family of endopeptidases that degrade all components of the extracellular matrix and control the activity of several diverse protein functions in immunity, repair, and disease progression (Tan, Fattman et al. 2006). MMP family members have been classified into subgroups that include collagenases (MMP-1), gelatinases (MMP-2 &-9), stromelysins (MMP-3, 10 & 11) and matrilysins (MMP-7), (Pardo and Selman 2006). Studies in, *in vivo* as well as *in vitro* have demonstrated the importance of many secreted and membrane bound MMPs that contribute either directly or indirectly to the process of wound healing and repair (Loffek, Schilling et al. 2011).

MMP-1 expression is usually low in non-disease tissue and it is mainly expressed during physiological and pathological tissue remodelling *in vivo* (Pardo and Selman 2005). Studies have shown MMP-1 is localised primarily in the reactive and bronchiolar epithelial cells and lining of the honeycomb cystic spaces in IPF lung (Selman, Ruiz et al. 2000).

The biological roles for MMP-1 include processing of cytokines, pro-tumour necrosis factor (TNF)-α, interleukin (IL-1) and insulin growth factor-binding proteins, which

may aid in the regulation of cell migration, and potentially, cell growth (Limb, Matter et al. 2005). MMP-1 may play a pivotal role in epithelial migration and the movement of epithelial cells to the site of injury (Pardo and Selman 2006). A previous study has shown that the migration of epithelial cells require MMP-1 mediated degradation of type I collagen and is necessary for keratinocyte migration (Pilcher, Dumin et al. 1997). A recent study by *Herrera et al*, demonstrated that MMP-1 is involved in the activation of alveolar epithelial cells which promote migration, proliferation and resistance to apoptosis but the specific mechanisms are unknown (Herrera, Cisneros et al. 2013). The role of MMP-1 in IPF goes beyond that of digesting fibrillar collagens (Pardo and Selman 2006).

In bleomycin-induced mice, MMP-7 expression in alveolar epithelium is increased early after injury and regulates acute neutrophil influx by controlling chemokine release into the alveolar compartment (Zuo, Kaminski et al. 2002). Epithelial (E)-cadherin regulates cell-cell adhesion in epithelial cells and maintains epithelial integrity, restricts migration and proliferation and promotes differentiation (Yap, Brieher et al. 1997). E-cadherin promotes wound healing and remodelling (Pece and Gutkind 2002). Previous studies have shown that the expression of MMP-7 mediates shedding of E-cadherin from airway epithelium during repair, and from alveolar epithelium during progression of bleomycin-induced pulmonary fibrosis (McGuire, Li et al. 2003). These studies suggest that MMP-7 is pivotal to the development of IPF (McGuire, Li et al. 2003).

MMP-2 and MMP-9 are classed as gelatinases (MMP-2 gelatinase A; 72kDa and MMP-9 gelatinase B; 92kDa) and are known to degrade all basement membrane constituents, including type IV collagen, nidogen, laminins and gelatins (Corbel, Belleguic et al. 2002). MMP-2 is synthesised by a wide variety of cells, including fibroblasts, endothelial cells and alveolar epithelial cells (Fukuda, Ishizaki et al. 1998). MMP-9 is produced by inflammatory cells including neutrophils, monocytes, macrophages, eosinophils and lymphocytes (Ohno, Ohtani et al. 1997).

MMP-2 and MMP-9 expression has been found to be elevated in both human and experimental lung fibrosis (Fukuda, Ishizaki et al. 1998). In particular, MMP-9 is highly expressed in the lungs and BAL fluid of IPF patients; i.e. epithelial cells, neutrophils and alveolar macrophages (Selman, Ruiz et al. 2000).

Bleomycin-induced fibrosis in a rabbit model exhibits an early increase in MMP-9 followed by a more chronic expression of MMP-1 and MMP-2, as well as TIMP-1 and TIMP-2 (Yao, Lemjabbar et al. 1999). Studies in experimental lung silicosis, have demonstrated an increase in MMP-2 and MMP-9 with reductions in TIMP-1 and TIMP-2 (Ramos, Montano et al. 2001).

In the current study, a variety of MMPs including 1, 2, 7 and 9 expression were observed in the 3D co-culture model after injury methods i.e. supernatants or in cells. These MMPs were chosen based on the availability of methods established in the department and their importance in IPF.

4.2 Aim and Objectives

The objective of this study was to compare the expression of MMPs 1, 2, 7 and 9 in the 3D co-culture supernatants after inflicting injuries. This was to determine whether there was a correlation of MMP expression with injury. The second objective was to compare the *in vitro* MMP results (MMP-9) with those observed in serum samples of patients with IPF, to determine a mechanism of IPF in the 3D co-culture model.

4.3 Methods

4.3.1 Regulatory approvals for the serum samples

For this study, 90 serum samples and lung function data were obtained from Richard Hubbard and Vidya Navaratnam, Division of Epidemiology and Public Health, City Hospital, Nottingham, UK. In the United Kingdom, all studies with patient involvement are required to have approval from a research ethics committee, as well as the research and development department of the participating centre. This study was reviewed and approved by the Nottingham Research and Ethics Committee 1 (REC ref: 09/H0403/59).

4.3.2 Study participants

All potential participants were recruited by Vidya Navaratnam, Norma Thompson, Sheila Churchill or Susan Ledge. A standardised questionnaire, requiring information about demographic details, lifetime occupational history, previous medical history, family medical history, current medications, smoking habit and hobbies was completed by each participant. The questionnaire was compiled by Richard Hubbard, with advice from Paul Cullinan. The questions were largely taken from other validated questionnaires used in large scale epidemiological studies by Vidya Navaratnam (Navaratnam, Fogarty et al. 2014)

All participants were then contacted by Vidya Navaratnam, Norma Thompson, Susan Ledger or Faith Fordham to arrange a date for collection of the venous blood sample, which was either done at their local hospital (cases), general practice (controls), the Nottingham Respiratory Research Unit (NRRU) or in their own homes. Blood samples were collected into BD Vacutainer® tubes containing 0.109 M sodium citrate, K_2 EDTA or clot activator and gel for serum separation at room temperature by Vidya Navaratnam, Norma Thompson or Faith Fordham.

The pulmonary function tests and HRCT scans that were performed as part of routine clinical care for the cases were also collected by Vidya Navaratnam, Norma Thompson, Sheila Churchill and Susan Ledger. All cases and controls were tagged

with the NHS Information Centre to collect data on subsequent mortality, cause of death and cancer incidence.

4.3.2.1 Control definition

Controls were individuals in the general population, without a diagnosis of idiopathic pulmonary fibrosis and were matched based on age and sex. Controls were recruited from 10 general practices that were involved in the Primary Care Research Network (PCRN) in the Greater Trent Region (Navaratnam, Fogarty et al. 2014).

4.3.2.2 Case definition

Only IPF cases were recruited for the study (Navaratnam, Fogarty et al. 2014). Risk factors that may be associated with survival rather than the disease process were taken into consideration and survival bias was suggested to ensure any differences in survival amongst incident and prevalent cases of IPF were accounted (Hubbard, Johnston et al. 1998). Incident cases were diagnosed in the 6 months before the start of the study.

Diagnosis of IPF made by a respiratory physician based on ATS/ERS criteria for diagnostic criteria (Raghu, Collard et al. 2011) as well as:

a) A clinical history of cough or dyspnoea, with a chest x-ray appearance consistent with a diagnosis of IPF
b) Either a high resolution computed tomography (HRCT) scan in which the predominant pattern was of usual interstitial pneumonia (UIP) (Table 4-1) or a histological confirmation of UIP from a surgical lung biopsy.
c) Exclusion of potential cases with co-existing connective tissue disease and/or a clinical picture suggestive of extrinsic allergic alveolitis (EAA)

Histological confirmation of UIP was not essential inclusion criterion, as currently less than 10% of people with IPF in the UK have a surgical lung biopsy. In order to maintain the robust diagnosis of IPF, HRCT scans for all potential cases were reviewed by two experienced thoracic radiologists (Dr Kate Pointon and Dr Maruti Kumaran). On central review of the HRCT scans, cases were stratified into

radiological diagnoses of definite UIP, probable UIP, fibrotic non-specific interstitial pneumonitis (NSIP) or unclassified fibrotic lung disease (Table 4-1).

Table 4-1: High resolution computed tomography (HRCT) diagnostic criteria for usual interstitial pneumonia (UIP) (Raghu, Collard et al. 2011).

Definite UIP pattern	**Probable UIP pattern**
Sub pleural, basal predominance Reticular abnormality Honeycombing with or without traction bronchiectasis Absence of features listed as inconsistent with UIP pattern	Sub pleural, basal predominance Reticular abnormality Absence of features listed as inconsistent with UIP pattern

4.3.2.3 Collection of Case-control participants

Three groups were analysed, *Control* group consisted of healthy individuals with (non- IPF) (32), *Alive* group consisted of individuals who have IPF (29) and *Dead* group consisted of individual who were diagnosed with IPF and died since receiving the patient information (29). In this study, the patients were mainly male (71.1%) with a mean $\pm$SD age at diagnosis 75.7$\pm$9.7 years. The median time to death since diagnosis was 3 years.

4.3.3 3D co-culture model

As described in section 2.4

4.3.4 MMP activity assay

To investigate various MMP activities, supernatants were collected every 24 hours over 6 days in the 3D co-culture model post wounding (refer to section 2.4). MMPs are secreted as inactive zymogens, which require proteolytic cleavage for activation, therefore, the pro- and activated MMP-2 and 9 were measured in undiluted supernatants using gelatin zymography (Lowrey, Henderson et al. 2008) (Chang, Cane et al. 2012).

4.3.5 Gelatin zymography

Gelatinolytic activity of cell culture supernatants and serum was analysed by gelatin zymography (refer to section 2.5.2) (Henderson, Markwick et al. 2007) using precast Novex polyacrylamide zymogram gels (Invitrogen, Paisley, United Kingdom). Co-cultured supernatants were used undiluted; serum samples were diluted 1:40 with distilled water before to achieve a pro (92kDa) and active (82kDa) MMP-9 band. The recombinant MMP 2 was used as a standard (refer to section 2.5.2.3).

4.3.6 Quantitative analysis

The activity of MMP-2 and MMP-9 were quantified in the zymogen gels by densitometry analysis. Semi quantitative analysis of gelatinolytic activity was performed by densitometry using computer imaging software (ImageJ 1.38x; W. S. Rasband, National Institutes of Health, Bethesda, MD; http://rsbweb.nih.gov/ij/).

4.3.7 Enzyme-Linked Immuno-Sorbent Assay (ELISA)

ELISA was implemented as described in section 2.5, to investigate the expression of MMP-1 and MMP-7 in the co-culture supernatants.

4.3.8 Statistical Analysis

Data were analysed using GraphPad Prism 6.0 software (GraphPad Software, Inc.). Continuous data from independent experiments which were considered to follow a normal distribution were displayed as the mean value ± SEM, and their statistical significance was assessed by one-way ANOVA followed by Tukey's post-hoc test when comparing multiple conditions to a control or two-way ANOVA with the Bonferroni post-hoc test when comparing multiple conditions with one another. The P values which were significant were shown with asterisks. The asterisks; *** represents $p<0.001$, ** represents $p<0.01$ *and* * represents $p<0.05$. n=3 (refer to section 2.11).

4.4 Results: Expression of MMPs in 3D Co-Culture Model

4.4.1 MMP-1 expression in 3D co-culture model

In normal resting tissue, MMP-1 is not detected but expressed during injury (Brinckerhoff and Matrisian 2002). *In vivo*, studies have shown that MMP-1 is localised in the alveolar epithelial cells and alveolar macrophages and is thought to participate in collagen fibril turnover (Selman, Ruiz et al. 2000).

The aim of this experiment was to determine whether epithelial injury induced either protein or gene MMP-1 expression in the epithelial monolayer culture and 3D co-culture model. The co-culture model was performed as section 2.4. Supernatants were collected post injury over 6 days and MMP-1 expression was analysed using ELISA (refer to section 2.5.1). RNA retrieved from cells was quantified by quantitative RT-PCR (refer to section 2.8). Statistical analysis (refer to section 4.3.8).

Statistical analysis, one-way ANOVA was performed to compare the significance between the injuries in the monolayer culture and co-culture independently. The data for the epithelial cells in the monolayer revealed a trend towards the MMP-1 expression increasing with scratch and bleomycin (monolayer) vs epithelial cells with no-injury (monolayer) (Figure 4-1A). The data for cultured fibroblasts with epithelial cells revealed MMP-1 mRNA expression followed the same trend as protein expression (ELISA). However, no trend was seen when comparing injuries (Figure 4-1 B and Figure 4-2).

ELISA analysis detected protein expression of total MMP-1 in supernatants from both cell types (Figure 4-1 A & B). In the epithelial cell monolayer supernatants, there was a trend towards the MMP-1 expression increasing with injury for scratch (SAEs monolayer) vs no-injury (SAEs monolayer) and bleomycin (SAEs monolayer) vs no-injury (monolayer), both with a significant increase ($p<0.05$) (Figure 4-1A). However, the ELISA analysis for MMP-1 expression in the co-culture model supernatants revealed no particular trend with various injuries (Figure 4-1B).

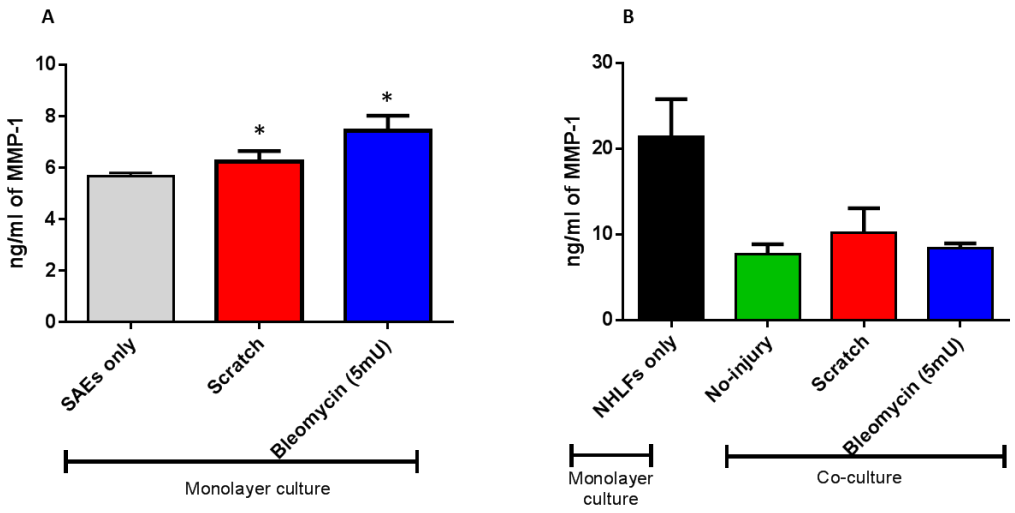


Figure 4-1: Total MMP-1 expression by ELISA. The expression of MMP-1 was determined in epithelial cells (monolayer model: consisting of epithelial cells alone) and co-culture model (Co-culture: consisting of injured epithelial cells and fibroblasts) supernatants assayed by ELISA. A; Epithelial injuries only (monolayer cell model: consisting of epithelial cells alone), data showing statistical significance of scratch ($p<0.05$) and bleomycin ($p<0.05$) injury to MMP- 1 expression for epithelial cells only. B; co-culture model (Co-culture: consisting of injured epithelial cells and fibroblasts). Statistical analysis was performed using GraphPad Prism version 6.0. One-way ANOVA was performed. The asterisk * represents $p<0.05$. Experiments were conducted in triplicate. n=3 independent biological experiments.

Quantitative RT-PCR analysis was performed to determine the gene expression of MMP-1 in co-cultured fibroblasts. The analysis suggested that epithelial injury may reduce expression of MMP-1 for mRNA and protein in the fibroblasts (Figure 4-2). The RT-PCR data confirmed that MMP-1 is predominantly expressed by fibroblasts (non-co-cultured) and the decreased expression of MMP-1 in co-cultured fibroblasts may be due to the presence of epithelial cells (Figure 4-2). The decreasing expression of MMP-1 in the co-cultured fibroblast with epithelial cells compared to non-co-cultured fibroblasts (NHLFS), may suggest that epithelial cells may be releasing a mediator which is inhibiting MMP-1 expression in fibroblasts or that culturing epithelial cells with fibroblasts reduces expression of MMP-1.

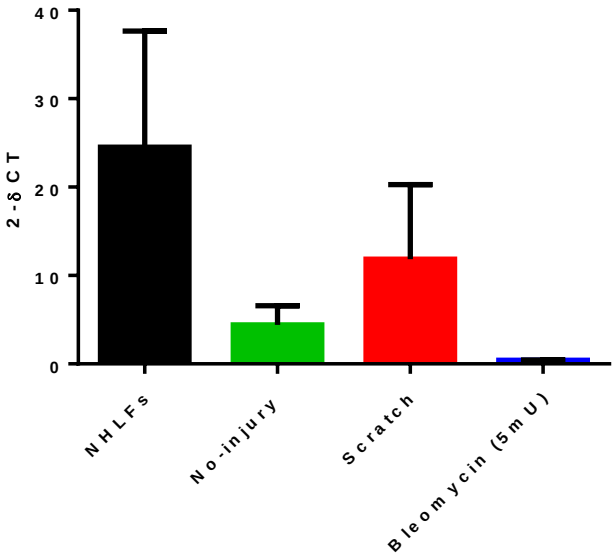


Figure 4-2: Quantitative RT-PCR analysis to determine *MMP-1* expression in co-cultured fibroblasts. Co-cultured fibroblasts consisting of injured epithelial cells and fibroblasts. Fibroblasts were extracted after 7 days in co-culture model after epithelial injury (either scratch or addition of bleomycin). Statistical analysis was performed using GraphPad Prism version 6.0. One-way ANOVA was performed. There was no significant difference. Experiments were conducted in triplicate. n=3 independent biological experiments.

4.4.2 MMP-7 expression in 3D co-culture model

Previous studies have demonstrated that MMP-7 expression is increased in epithelial injury particularly, during cell migration and in inflammatory response (McGuire, Li et al. 2003). The increased expression of MMP-7 promotes shredding of E-cadherin which mediates cell to cell adhesion in the epithelium and affects epithelial integrity, indicating migration and proliferation of other cells into the wounded area (Manicone, Huizar et al. 2009).

The aim of this experiment was to determine whether epithelial injury induced MMP-7 expression in the epithelial injury monolayer culture and 3D co-culture model. The co-culture model was performed as section 2.4. Supernatants were collected post injury over 6 days and MMP-7 expression was analysed using ELISA (refer to section 2.5.1), quantitative RT-PCR (refer to section 2.8) and statistical analysis (refer to section 4.3.8).

ELISA analysis revealed expression of total MMP-7 in both cell types. The epithelial supernatants in the monolayer culture revealed that the expression of total MMP-7 decreased with injuries, scratch (monolayer) and the addition of bleomycin (monolayer) compared to no-injury, both with a significant increase ($p<0.05$) (Figure 4-3; Monolayer). The observation for co-culture supernatants revealed there was a decreased expression of total MMP-7 with injuries, scratch (co-culture) and bleomycin (co-culture) compared to the no-injury (co-culture), both with a significant decrease ($p<0.05$) (Figure 4-3; co-culture). However, there was an increased MMP-7 expression in the non-treated fibroblasts (NHLFs). This could suggest that culturing epithelial cells with fibroblasts reduces expression of MMP-7. Quantitative RT-PCR analysis revealed expression of MMP-7 and revealed no particular trend with various injuries (Figure 4-4).

Statistical analysis, one-way ANOVA was performed to compare the significance between the injuries in the monolayer culture and co-culture independently. The data revealed that injuries of scratch and bleomycin for the epithelial cells in the monolayer culture were significant, compared to non-injured epithelial cells. The

statistical analysis for fibroblasts in monolayer culture revealed that there was a significant decrease of MMP-7 expression with injury in the co-culture model. It was difficult to perform quantitative RT-PCR analysis on epithelial cells as a sufficient amount of cells could not be retrieved.

A possible explanation as to why there was decreased expression of MMP-7 in the epithelial monolayer culture and in the 3D co-culture model could be, the epithelial cells may be inhibiting MMP-7 production. Overall, as only two cell types were used in the 3D co-culture model, MMP-7 expression was not induced as intended and possibly a differentiated model i.e. use of neutrophils may be a better approach.

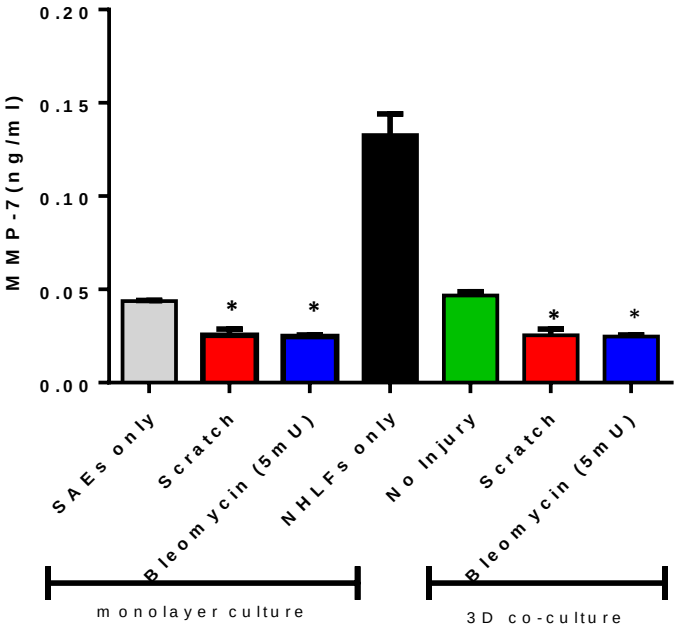


Figure 4-3: Total MMP-7 expression. The expression of MMP-7 was determined in epithelial cells (monolayer cell model: consisting of epithelial cells alone) and co-culture model (Co-culture: consisting of injured epithelial cells and fibroblasts) supernatants assayed by ELISA. Monolayer model (Monolayer cell model: consisting of epithelial cells alone). Co-culture model (Co-culture: consisting of injured epithelial cells and fibroblasts). Statistical analysis was performed using GraphPad Prism version 6.0. One-way ANOVA was performed. The asterisk * represents $p<0.05$. Analysis was based on injury vs no-injury. Experiments were conducted in triplicate. n=3 independent biological experiments.

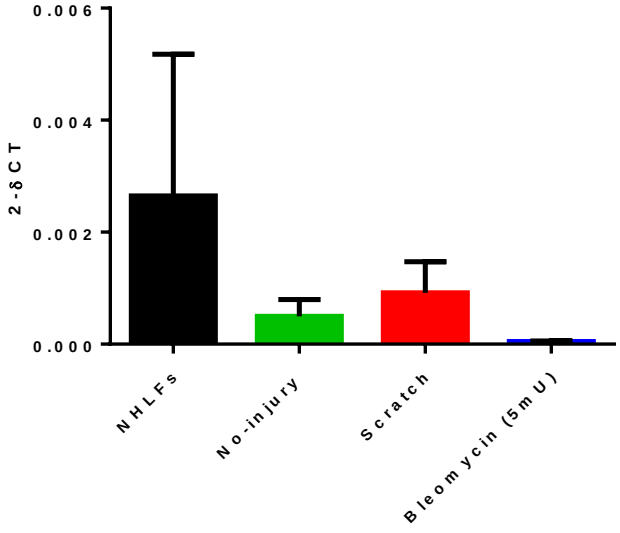


Figure 4-4: Quantitative RT-PCR analysis to determine expression of MMP-7 expression in co-cultured fibroblasts. Co-cultured fibroblasts consisting of injured epithelial cells. Fibroblasts were extracted after 7 days in co-culture model which were inflicted with epithelial injury. Statistical analysis was performed using GraphPad Prism version 6.0. One-way ANOVA was performed. There was no significant difference in the expression of MMP-7 in co-cultured fibroblasts for injuries vs no-injury. Experiments were conducted in triplicate. n=3 independent biological experiments.

4.4.3 MMP-2 expression in 3D co- culture model

MMP-2, also known as gelatinase A, degrades almost all basement membrane constituents (Corbel, Belleguic et al. 2002), which are important to maintain the integrity of the basement membrane. Studies have demonstrated elevated levels of MMP-2 in the later stages of fibrosis, in which MMP-2 expression was elevated in the areas of fibroblast foci in bleomycin-treated rats (Kim, Choeng et al. 2009). The aim of this section was to determine whether there was an increased expression of MMP-2 with various injuries in the 3D co-culture model.

Gelatin zymograms were performed to detect proteolytic enzymes capable of degrading gelatin from various injuries. In particular, to compare MMP-2 expression, MMP-2 standard was used to determine the position of pro (72kDa) - and active (62kDa) in the co-culture supernatants. The gelatin zymogram technique was performed as section 2.5.2.

The enzyme activity is measured by the degradation of the zymogram by the proteases, which is represented by a 'band' on the zymogram. The 'band width' for each condition was determined by measuring the optical density of the individual band which relates to the enzyme activity (Puthawala, Hadjiangelis et al. 2008). The largest de-stained area was selected using the region of interest with a rectangular selection tool. The same region of interest was then applied to all other bands and the mean optical density was again determined. Results were plotted as mean $\pm$ SEM and were comparable within experiments (refer to section 2.5.2.5).

The gelatin zymography results revealed expression of both pro and active MMP-2 in the co-culture supernatants (Figure 4-5). The expression of pro MMP-2 seemed to be increased in the supernatants with the addition of bleomycin.

Densitometry was performed on zymogram gels to quantify optical density of the expression of pro- and active MMP-2 as band widths (Figure 4-6). Statistical analysis was performed using one-way ANOVA. The analysis revealed there was no significant difference in the expression of active MMP-2 with the injuries in the monolayer culture and the 3D co-culture model supernatants. These data suggest that both epithelial cells and fibroblasts cleave similar amounts of active MMP-2.

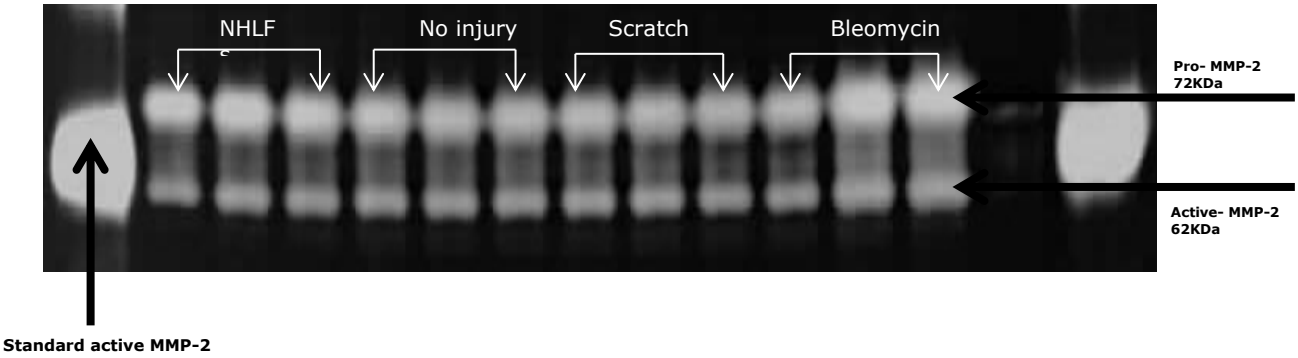


Figure 4-5: Representative gelatin zymogram of co-cultured supernatants. Co-cultured fibroblasts with epithelial injury, supernatants were taken at day 6. The conditions were fibroblasts (non-injured), no-injury, co-culture with inflicted scratch injury and co-culture with addition of bleomycin. The bands were representative of the positions of Pro- and Active MMP-2 in each condition.

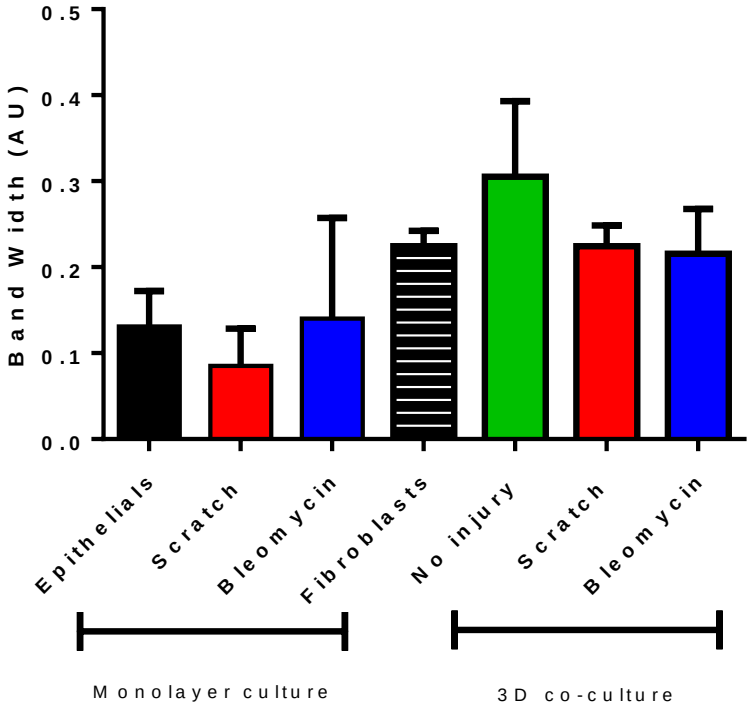


Figure 4-6: Quantification of expression of active MMP-2. The band widths were quantified using a densitometry with ImageJ software. The band widths represents the activity for each group; epithelial cells (monolayer culture), fibroblasts (3D co-culture) on day 6. Statistical analysis was performed using GraphPad Prism version 6.0. One-way ANOVA was performed. Experiments were conducted in triplicate. n=3 independent biological experiments.

4.4.4 MMP-9 expression in the 3D co-culture model

MMP-9 also known as gelatinase B is a 92kDa latent enzyme with an active product of 82kDa. MMP-9 is predominantly expressed by alveolar macrophages, neutrophils and epithelial cells. The importance of MMP-9 has been described in multiple cellular processes including proliferation, angiogenesis, migration, and host defence and cancer invasion (Dufour, Zucker et al. 2010). The aim of this study was to determine whether MMP-9 expression changed with injury in the 3D co-culture model.

Gelatin zymography was performed (refer to section 2.5.2) to determine the expression of MMP-9 in supernatants with relevance to injury. The zymogram gel revealed the position of pro-MMP-9 (92kDa) as well as a reference band of pro-MMP-2 (72kDa). Band widths were determined by measuring the optical density of the individual band (refer to section 2.5.2.5).

The gelatin zymogram confirmed there was expression of pro MMP-9, pro MMP-2 and active MMP-2 from the co-cultured fibroblast supernatants (Figure 4-7). The infliction of injuries demonstrated that pro-MMP-9 expression had increased with injury, in particular, in the bleomycin supernatants from the co-cultured fibroblasts.

Zymography was performed on supernatants from the epithelial monolayer culture (consisting of epithelial cells alone), (Figure 4-8). The results revealed that in epithelial cells injured either by scratch or administration of bleomycin alone (without the presence of fibroblasts in co-culture model), there was expression of pro-MMP-9 in supernatants.

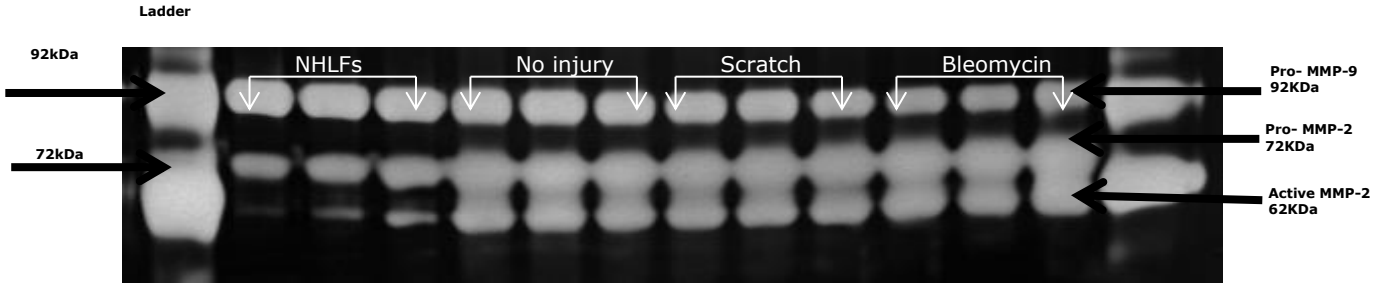


Figure 4-7: Gelatin zymogram of supernatants taken from <u>co-cultured fibroblasts</u>. Conditions were co-cultured fibroblasts with no-injury, co-culture with inflicted scratch injury and co-culture with addition of bleomycin. The supernatants for each condition were taken on day 6. The MMP-9 standard located at each end of the gel to show the band width of pro MMP-9 92kDa (n=3).

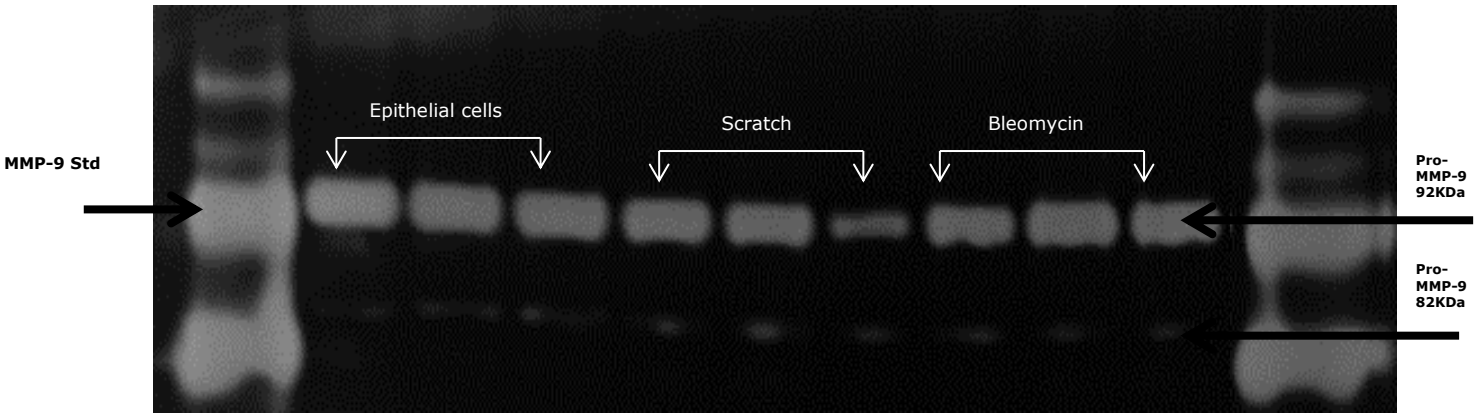


Figure 4-8: Gelatin zymogram of supernatants taken from <u>epithelial monolayer culture</u> (without co-cultured fibroblasts). Conditions were epithelial cells no-injury, scratch injury and addition of bleomycin. The supernatants for each condition were taken on day 6. MMP-9 reference standard used to identify the band. Pro-MMP-9 is 92kDa and active MMP-9 is 82kDa. A faint active band is seen directly underneath the pro-MMP-9 band. (n=3).

Densitometry was performed to quantify the expression of MMP-9 in supernatants in both cultures as band widths (refer to section 2.5). The densitometry was performed on three independent experiments with three independent zymograms. The results for co-culture model suggested that there was a decrease in pro-MMP-9 expression in the bleomycin injury as compared to non-injury with a significance of $p<0.01$, one-way ANOVA followed by Tukey's post-hoc test (Figure 4-9). As previously, shown in figure 4-7, the expression of pro-MMP-9 had increased with the addition of bleomycin. Figure 4-7 was one representative of three independent zymograms.

The results of the epithelial monolayer cultures (without fibroblasts) suggested that there was activation of MMP-9 in epithelial cells, which decreased with injury, particularly with the addition of bleomycin (Figure 4-10). Further analysis was performed using the epithelial monolayer data and revealed decreased active MMP-9 expression in the bleomycin injury was significant $p<0.01$, one-way ANOVA followed by Tukey's post-hoc test (Figure 4-11).

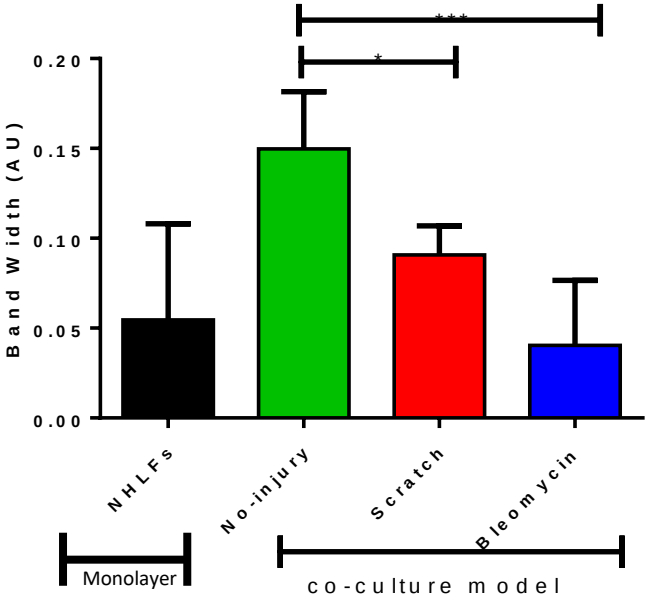


Figure 4-9: **Expression of pro-MMP-9 in the co-culture fibroblast supernatants.**
The band widths were quantified using a densitometry with ImageJ software. The band widths represents the activity for each group; epithelial cells (monolayer culture), fibroblasts (3D co-culture) on day 6. Scratch vs no-injury * p< 0.05 and Bleomycin vs no-injury (5mU) *** *p<0.001*. Statistical analysis was performed using GraphPad Prism version 6.0. The asterisks; *** represents *p<0.001*, ** represents *p<0.01 and* * represents *p*<0.05. Experiments were conducted in triplicate. n=3 independent biological experiments.

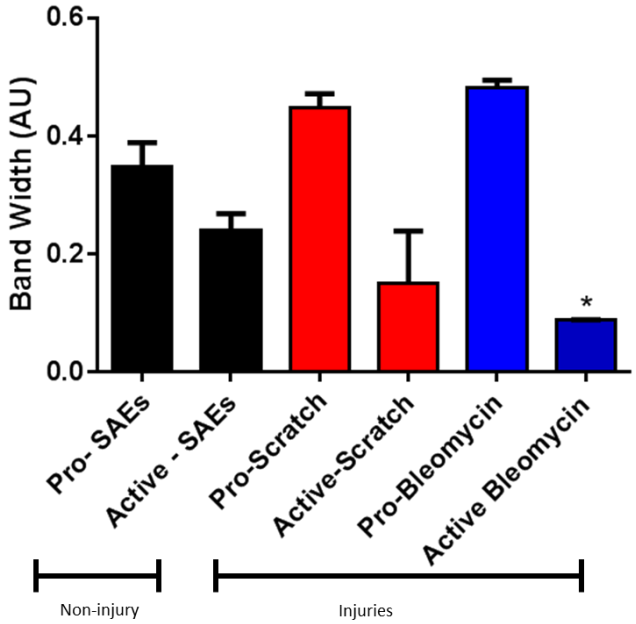


Figure 4-10: Expression of MMP-9 in the epithelial monolayer culture.
The band widths for epithelial cells. The supernatants of the epithelial cells and injuries on day 6. Pro-bleomycin vs. active bleomycin (5mU) * *p< 0.05*. Statistical analysis was performed using GraphPad Prism version 6.0. The asterisk * represents *p*<0.05. Experiments were conducted in triplicate. n=3 independent biological experiments.

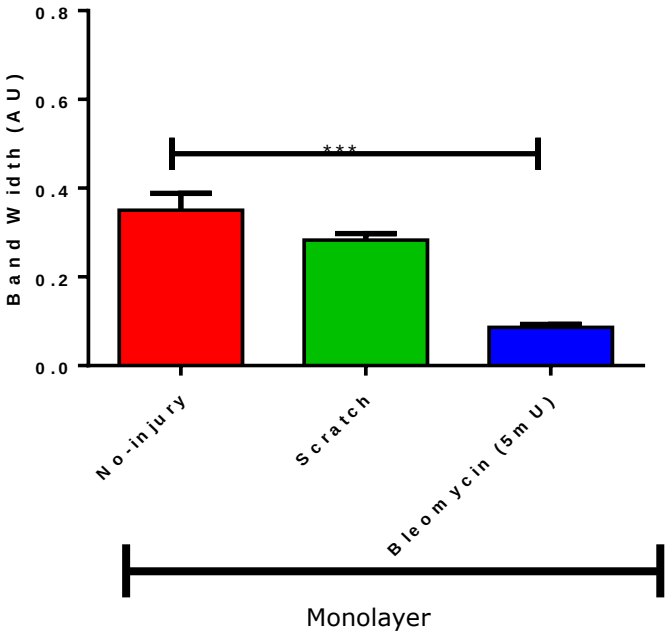


Figure 4-11: Expression of active-MMP-9 in the epithelial monolayer model. The supernatants for epithelial cells were taken on day 6. The band widths for epithelial cells were quantified using a densitometry with ImageJ software. Bleomycin (5mU) v non-injury ***, *p< 0.001.* Statistical analysis was performed using GraphPad Prism version 6.0. The asterisks; *** represents *p<0.001*. Experiments were conducted in triplicate. n=3 independent biological experiments.

As previously mentioned, pro MMP-9 expression decreased with injury in the co-culture model (Figure 4-9). This was confirmed by zymography and further analysed by densitometry. To clarify that the fibroblasts were not dying in relation to injury, the cell viability of fibroblast cells was measured using MTT reduction assay (refer to section 2.6.3). The cell viability of the fibroblasts in co-culture had increased with injury after 6 days with a significance of $p<0.01$, one-way ANOVA followed Tukey's post-hoc test (Figure 4-12).

Cell viability of epithelial cells was also measured in the epithelial monolayer model using MTT reduction assay (refer to section 2.6.3). The optical density of the epithelial cells after 6 days of post-injury had decreased with injury as compared to the non-injured epithelial cells. This may be due to the cells detaching from the well post injury (Figure 4-13).

In the co-culture supernatants, there was no MMP-9 activation detected using zymography (figure 4-8). However, in the epithelial monolayer for scratch and bleomycin injuries, there was a decrease of active-MMP-9 (Figure 4-10). There was a decrease in MMP-9 activation with bleomycin injury compared to scratch. There was a similar trend in the scratch wound which was not significant (Figure 4-11).

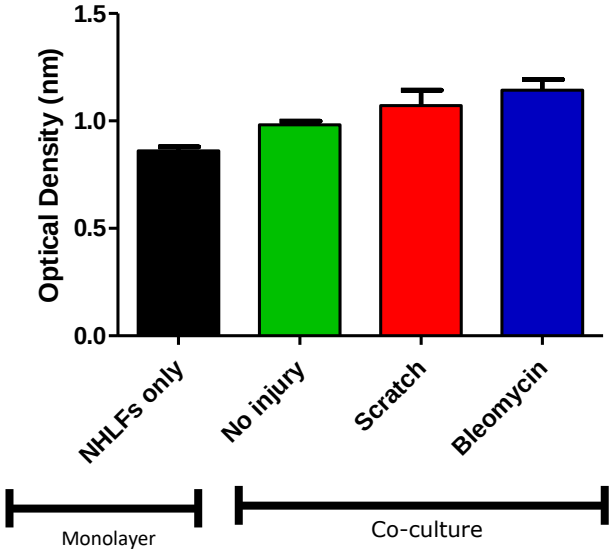


Figure 4-12: **MTT reduction assay: Fibroblasts in co-culture.**
The optical density of fibroblasts in co-culture after 6 days post injury. Statistical analysis was performed using GraphPad Prism version 6.0. One-way ANOVA was performed. Experiments were conducted in triplicate. n=3 independent biological experiments.

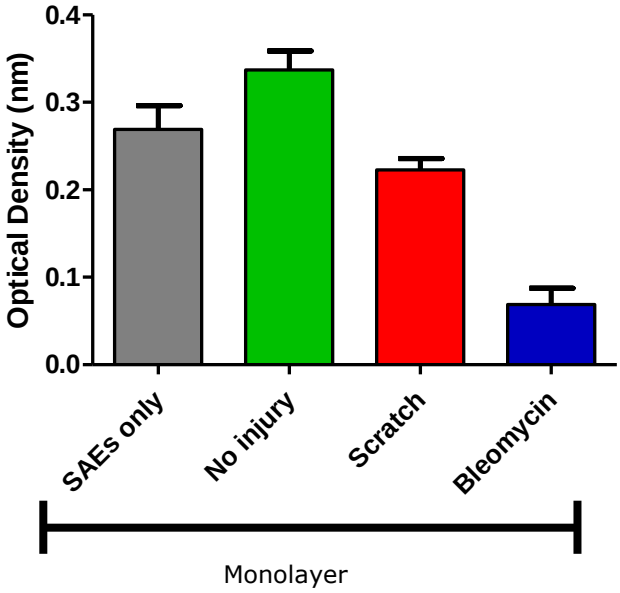


Figure 4-13: MTT reduction assay: Epithelial cells. The optical density of epithelial cells after 6 days post injury in the Transwell® in the co-culture model. Statistical analysis was performed using GraphPad Prism version 6.0. One-way ANOVA was performed. Experiments were conducted in triplicate. n=3 independent biological experiments.

4.4.5 Expression of MMP-3 and TIMP-1 in co-cultured fibroblast cells

MMP-3, also known as stromelysin-1, is induced by inflammatory stimuli by activating the release of MMP-9 to the site of injury in fibrosis (Warner, Bhagavathula et al. 2004). TIMP-1 is an inhibitor of MMP-9 and studies have shown that TIMP-1 deficiency in mice causes increased acute lung injury in response to asbestos, an effect that is associated with increased expression of MMP-9 (Kim, Burkhart et al. 2005). The aim of this study was to determine whether MMP-3 and TIMP-1 contributed to the expression of MMP-9 in the co-culture model.

To determine the mRNA expression of MMP-3, quantitative RT-PCR analysis was performed in the non-cultured fibroblasts (no addition of epithelial cells or injury) and in co-cultured fibroblasts (addition of epithelial cells with addition of injury). The analysis revealed that there was low MMP-3 expression in the non-cultured fibroblasts. In the co-cultured fibroblasts, the results revealed there was an increase of MMP-3 expression. This may suggest that epithelial cells in the co-culture model are producing MMP-3. In addition, MMP-3 expression decreased with injury and was significant with bleomycin vs no-injury ($p<0.05$), one-way ANOVA followed Tukey's post-hoc test (Figure 4-14).

The same trend was seen for TIMP-1 expression in the co-cultured fibroblasts. The results revealed there was a decrease in TIMP-1 expression with injury; bleomycin vs no-injury ($p<0.01$) (Figure 4-15). However, observing the gene expression level, TIMP-1 expression was much lower compared to MMP-3 gene expression.

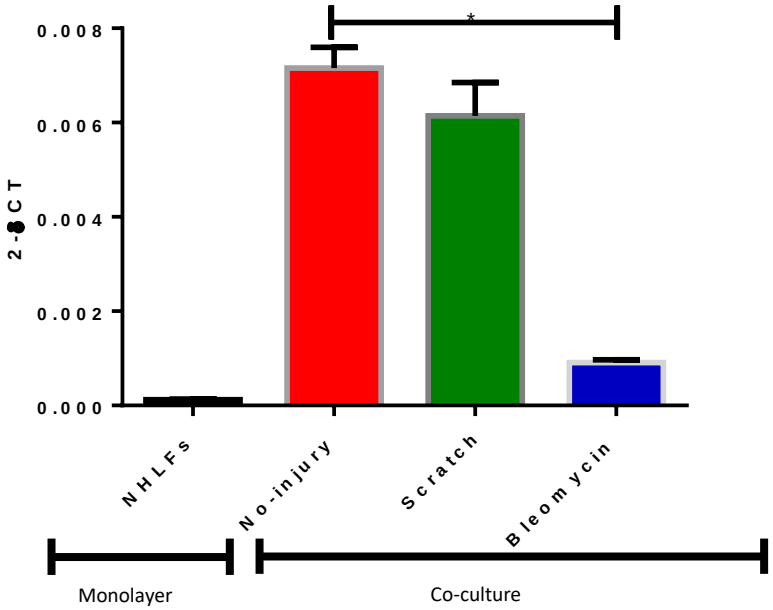


Figure 4-14: Quantitative RT-PCR analysis to determine gene expression of MMP-3 in co-cultured fibroblasts. MMP-3 expression with injury compared to no-injury in the co-culture model. Housekeeping gene β-actin was used. Bleomycin (5mU) v Non-injury * represents p< *0.05.* Statistical analysis was performed using GraphPad Prism version 6.0. One-way ANOVA was performed. Experiments were conducted in triplicate. n=3 independent biological experiments.

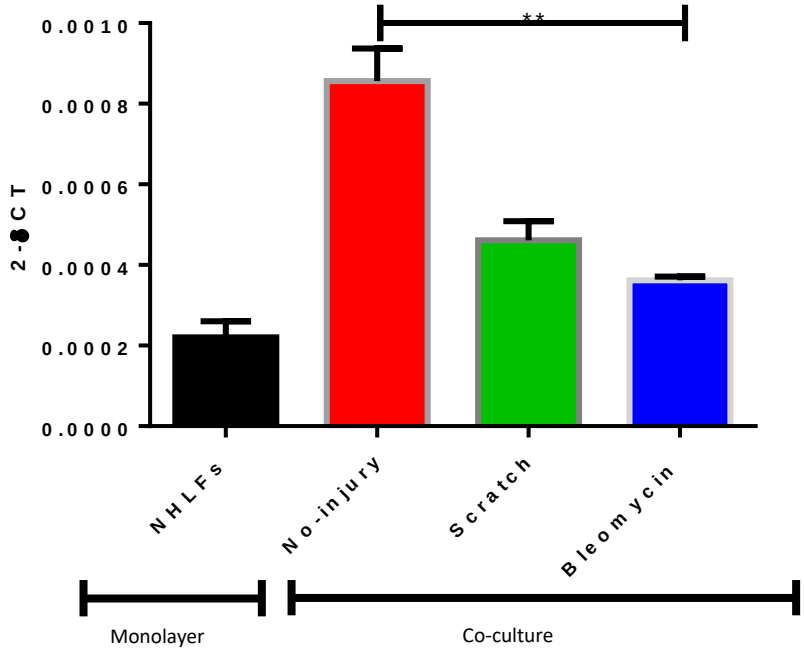


Figure 4-15: Quantitative RT-PCR analysis to determine gene expression of TIMP-1 in co-cultured fibroblasts. TIMP-1 expression with injury compared to no-injury in the co-culture model. Housekeeping gene β-actin was used. Statistical analysis was performed using GraphPad Prism version 6.0. One-way ANOVA was performed. Bleomycin (5mU) v Non-injury;** represents *p< 0.01.* Experiments were conducted in triplicate. n=3 independent biological experiments.

4.4.6 Expression of MMP-9 on IPF tissue

As previously demonstrated, both pro and active MMP-9 expression was determined in the epithelial monolayer culture and only pro-MMP-9 was expressed in the co-culture model. The aim of this section was to investigate whether the expression of MMP-9 in the lung tissue differed between the normal lung and IPF lung tissue. Samples were obtained from Nottingham BioBank. This was done with ethical approval from the Nottingham committee of the NHS National Research Ethics Service, as well as informed consent from the patients involved.

Tissue obtained from IPF patients expressed MMP-9 in the lung tissue as shown in Figure 4-16 A (x10) and B (x40)). A negative control (omitting primary antibody) had no staining; C (x10) and D (x40)). E (x10) and F (x40) normal lung was stained for MMP-9. Overall, there is MMP-9 expression in both epithelial cells and fibroblasts in the IPF tissue (Figure 4-16 A-B), but no expression of MMP-9 in the normal lung tissue (E-F).

Further staining was performed to confirm the localisation of MMP-9 in fibroblasts (Figure 4-17). Myofibroblasts/fibroblasts were identified by immunostaining with α-smooth muscle actin (α-SMA) and localisation with MMP-9 in IPF and normal lung sections. The staining of the two markers was performed on two separate sections. There was expression of MMP-9 in both epithelial cells and fibroblasts in the IPF lung section (Figure as 4-17; A (x10) and B (x40)). A negative control (omitting primary antibody), showed no staining of MMP-9 in the IPF tissue; C (x10) and D (x40). The immuno-staining of α-SMA shown in UIP tissue, E (x10) and F (x40). A negative control (omitting primary antibody), showed no staining for α-SMA in UIP tissue, G(x10) H(x40) negative. Overall it may suggest that α-SMA may be localised to the fibroblasts (Figure 4-17 (E-F). But further staining i.e. staining of adjacent sections or co-staining for the 2 markers on the same section may be required to confirm the data.

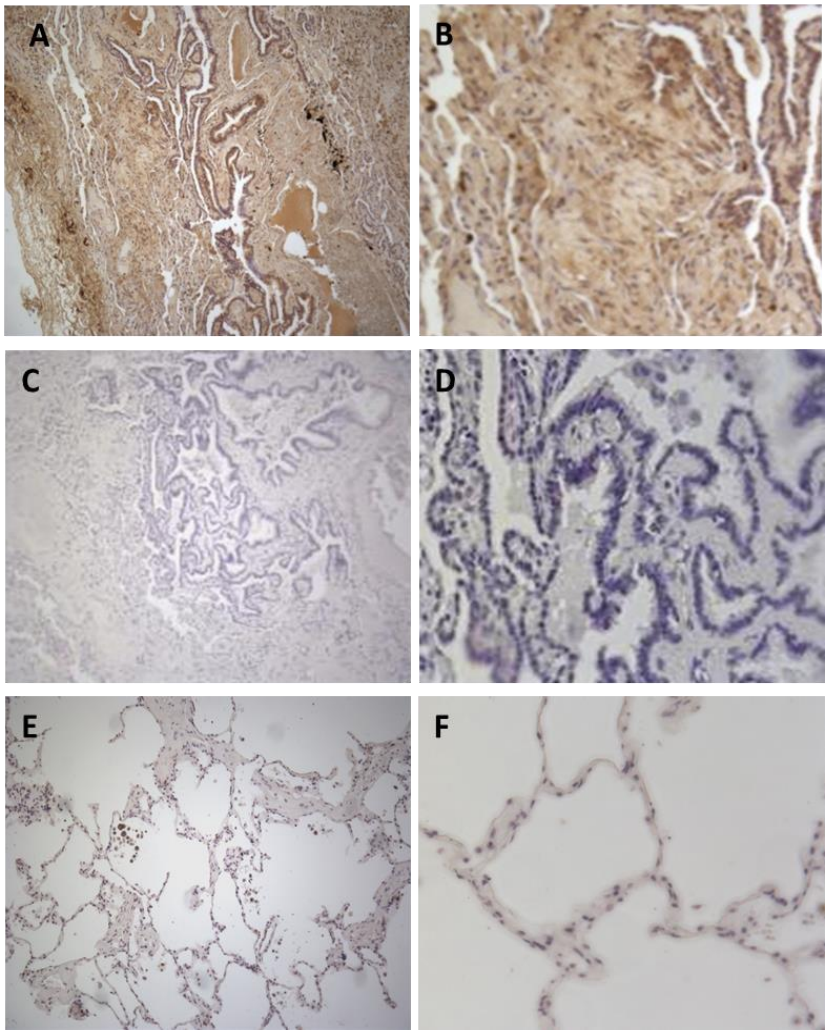


Figure 4-16: Immunohistochemistry of MMP-9 in lung tissue. Matrix Metalloprotease - 9 (MMP-9) immunolocalization in Usual Interstitial Pneumonia (UIP) and normal lung. A (x10) and B (x20): immunoreactivity for MMP-9 in UIP tissue. C(x10) and D(x20) negative control omitting primary antibody. E (x10) and F (x20) normal lung was stained for MMP-9.

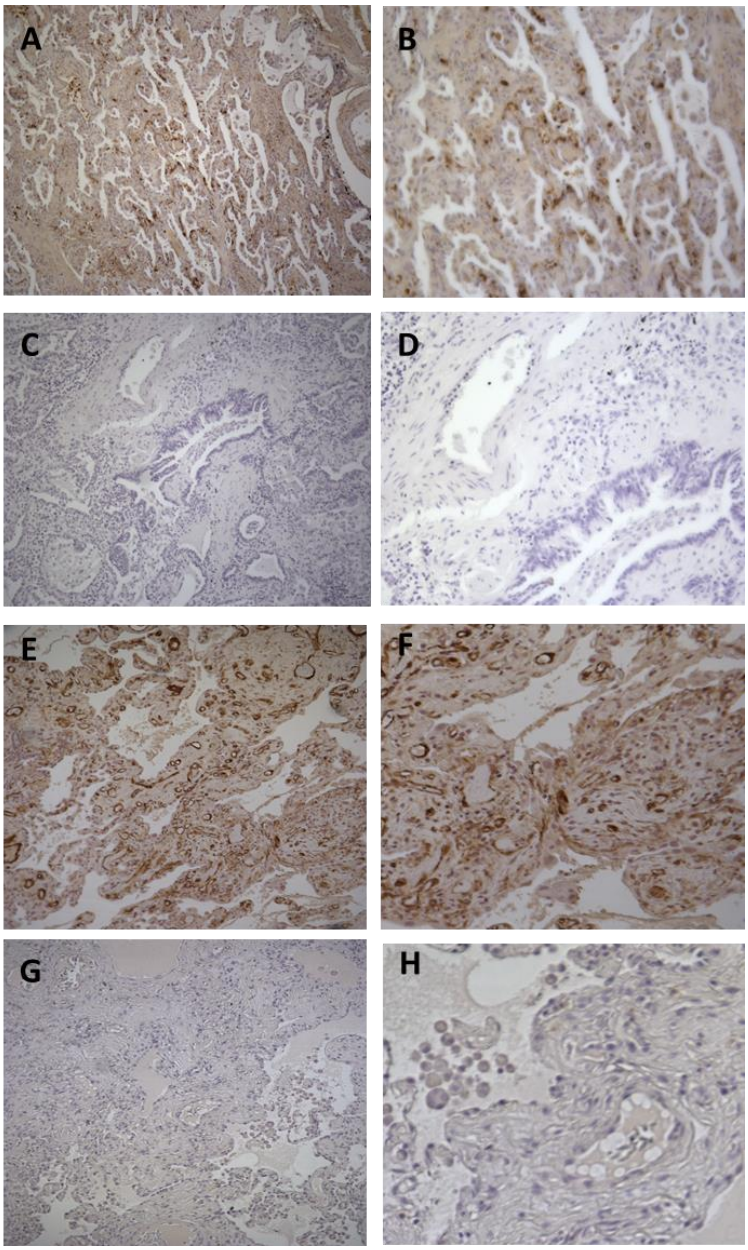


Figure 4-17: **Immunohistochemistry for MMP-9 and Alpha smooth muscle actin (α-SMA) in lung tissue**. Immunolocalization in Usual Interstitial Pneumonia (UIP) and normal lung. A (x10) and B (x20): immunoreactivity for MMP-9 in UIP tissue. C(x10) and D(x20): negative control omitting primary antibody in UIP tissue. E (x10) and F(x20): immunoreactivity for α-SMA showing in UIP tissue. G(x10) H(x20) negative control omitting primary antibody in UIP tissue.

4.5 MMP-9 expression in IPF serum samples

4.5.1 MMP-9 expression pro and active in serum samples

The zymography data from the 3D co-culture model (section 4.4.4) revealed that pro-MMP-9 expression had decreased in the co-cultured fibroblast supernatants with injury (Figure 4-9). The epithelial cells supernatants from the monolayer culture had shown a trend towards an increased expression of pro-MMP-9 with injury (Figure 4-10). However, there was no significant difference. There was a significant difference in active-MMP-9 expression from epithelial cells supernatants from the monolayer culture (Figure 4-11).

The immuno-staining revealed that MMP-9 expression was present in the epithelium layer and fibroblasts in the IPF sections. To further analyse the MMP-9 expression, IPF serum samples were used to compare MMP-9 expression in non-IPF (Healthy serum samples), alive-IPF (Serum obtained from alive IPF patients) and dead-IPF (Serum samples already obtained from IPF patients but had died since receiving patient information).

The aim of this section was to identify whether MMP-9 expression was predominant in individuals with IPF. The expression of MMP-9 was examined in the alive/dead vs non-IPF samples based on the observation of the MMP-9 expression in the epithelial monolayer and 3D co-culture supernatants following injury (Section 4.4.4). IPF serum samples were obtained from Richard Hubbard and Vidya Navaratnam, Division of Epidemiology and Public Health City hospital, Nottingham, UK (Navaratnam, Fogarty et al. 2014).

The 90 samples were divided into three groups, including *Control* group which consisted of healthy individuals (non- IPF), *Alive* group consisted of individuals who had IPF but were still *Alive* and *Dead* group consisted of individual who were diagnosed with IPF and had died since receiving the patient information (during 3 year period after diagnosis). The patients were mainly male (71.1%) and mean age $\pm$SD at diagnosis was 75.7$\pm$9.7 years. Patient information was taken over 2 years. For more information, (Table 4-2).

Table 4-2: Clinical characteristics of patients with idiopathic pulmonary fibrosis and the control group. Patient information was taken over 2 years first diagnosis 01.04.2009 to last diagnosis 29.09.10.

	Alive IPF	Dead IPF	Controls (non-IPF)
Patients	29	29	32
Females	11	6	9
Males	18	23	23
Smoker	14 (M) 6 (F)	15 (M) 2 (F)	19 (M) 4 (F)
Age Range (years)	70-89	62-93	60-89
Mean Age ± SD (years)	76.9±9.7	78.1±9.2	72.5±9.9

MMP-9 expression in the serum samples was measured by gelatin zymography (refer to section 2.5.2). The serum samples were diluted 1 in 40 to achieve a pro (92kDa) and active (82kDa) band. Samples were run in duplicate for each patient sample (Figure 4-18). The zymograms were analysed and showed that all groups: control, alive and dead serum samples expressed pro (92kDa) and active (82kDa) MMP-9, as well as pro - MMP-2 (72kDa) (Figure 4-18).

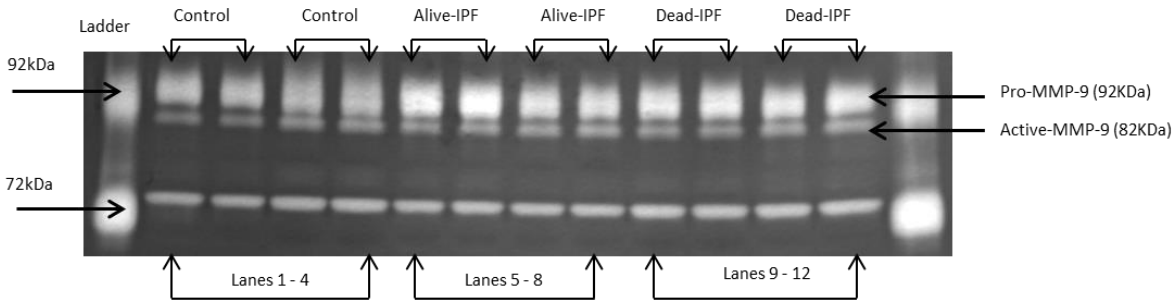


Figure: 4-18: **Gelatin zymography showing gelatinase activity of individual control and IPF serum samples.** Standard ladder showing MMP-9 at 92kDa and MMP-2 at 72kDa. The samples are run in duplicates at same dilution of 1:40, with two sets for controls (lanes 1-4), alive-IPF patients (5-8) and dead-IPF patients (9-12).

The band widths were quantified by densitometry on images of gelatin zymograms and were compared for both pro- and active MMP-9 in all serum samples (Figure 4-19). The densitometry was performed on 90 independent patient serum samples in duplicate. The zymogram is a representation of one set of data from the 90 serum samples. The results depict that there were significant differences between pro and active MMP-9 within each group ($p<0.0001$) i.e. control patients: MMP-9 pro vs active.

The bands shown in figure 4-18, in particular 'Control' expression looks weaker as compared to 'Alive-IPF' expression in figure 4-19. Each band was quantified by densitometry on images of gelatin zymograms as section 4.3.6. The difference in 'control' and 'alive' sample expression of the averaged area of each band width was calculated. For each band, an area was calculated and overall, an average was determined. Overall, 'Control' band widths were weakly expressed as shown on the representative zymogram.

Statistical analysis, one-way ANOVA was performed with a Tukey's post-hoc test. The analysis revealed that there was no significant difference in the expression of pro- and active- MMP-9 between the individual groups i.e. control, alive and dead. All three groups produced the same amount of pro and active MMP-9.

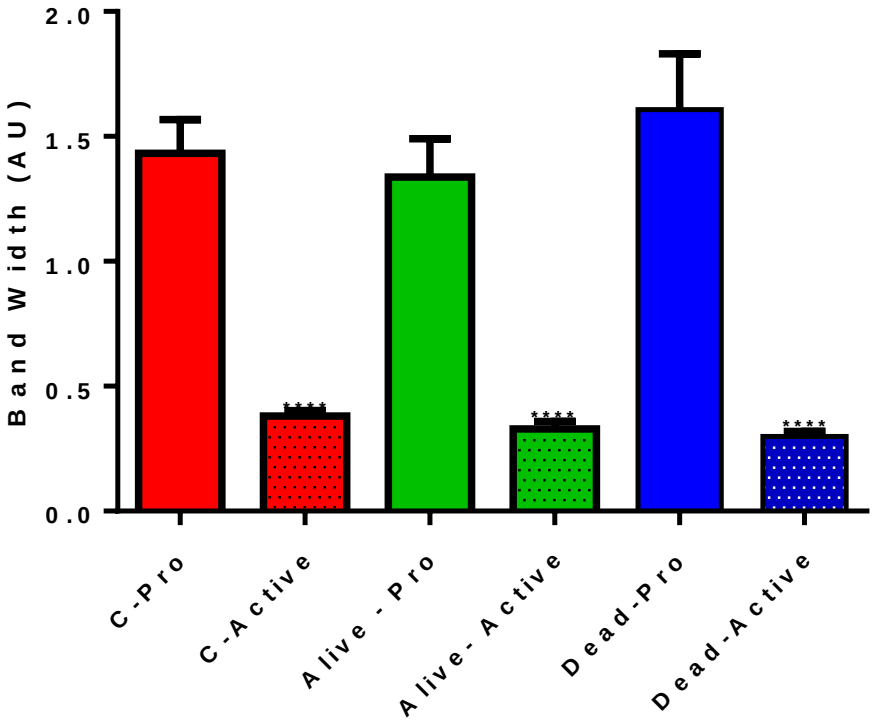


Figure 4-19: MMP-9 expression using Gelatin Zymography. The expression of pro and active MMP-9 in three groups (Control, alive and dead). The band widths were quantified using a densitometry with ImageJ software. Statistical analysis was performed using GraphPad Prism version 6.0. One-way ANOVA was performed with a Tukey's post-hoc test. The asterisks; **** represents *p<0.0001*. Experiments were conducted in triplicate. n=90 independent biological samples.

There was no significant difference between the expression of pro and active MMP-9 expression in the serum samples for individual groups; control, alive and dead patients, suggesting that all groups expressed the same amount of pro vs active. However, visually on the representative zymogram, the expression of MMP-9 in the control samples looked weaker as this was one set from 90 serum samples (Figure 4-18). Once the statistical analysis was performed for each condition for 90 samples, the results revealed that the MMP-9 expression of controls had a slightly increased expression of Pro-MMP-9 than the alive group Pro-MMP-9 expression.

However, there was a difference within the individual groups, with expression of pro and active MMP-9. As active MMP-9 expression was constant in the individual groups (Figure 4-19): the pro MMP-9 expression was determined in the individual groups. The ratio between pro and active MMP-9 expression was calculated. The calculations revealed that there was no significant difference of MMP-9 expression for each group (Figure 4-20). However, there was an insignificant increase of pro-MMP-9 in the dead IPF samples (*p<0.058*) as compared to alive samples (Table 4-3). Statistical analysis was performed using one-way ANOVA followed by Tukey's post-hoc test, (refer to section 4.3.8).

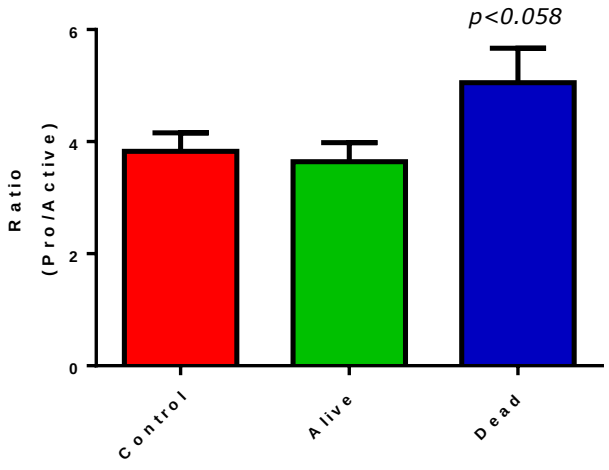


Figure 4-20: **Pro-MMP-9 expression (pro/active ratio).** The expression of pro/active MMP-9 ratio in three controls in individual patients which were analysed by densitometry and statistical analysis was performed using one-way ANOVA with Tukey's post-hoc test (*p-value= 0.058*). Each group (~n=30).

Table 4-3: **Ratios for pro and active MMP-9 expression in the groups for alive and dad compared to control patients**.

Average for each group	Band width Pro	Band Width Active	Band width Ratio	p-value of ratio
Alive	1.338	0.329	3.64	<0.938
Dead	1.607	0.295	5.05	**<0.058**

4.5.2 Total MMP-9 expression in serum samples

The total protein expression of MMP-9 was observed in 90 serum samples by two methods; zymography and ELISA. The zymogram results of pro and active MMP-9 were pooled and total MMP-9 was calculated. Total MMP-9 in serum samples was also verified by ELISA. Statistical analysis was performed using one-way ANOVA, (refer to section 4.3.8).

The results suggested that there was a small increase in total MMP-9 in serum samples of deceased IPF patients. However, comparing control with dead serum samples, there was no significance between the samples. The total MMP-9 ELISA data revealed the mean total MMP-9 in all patients was 1.5ng/ml, suggesting that there was no difference in any of the three groups (Figure 4-22).

Overall, using two methods to validate the expression of MMP-9 expression between the samples demonstrated that there was an insignificant increase in pro-MMP-9 in serum samples of the deceased IPF patients. This could suggest that the pro-MMP-9 was not activated during injury and increased with injury in the serum. Another reason could be that the immune system in patients may have been compromised and immune cells e.g. macrophages may have not released MMP-3 to activate MMP-9. Further experimental work is required to obtain conclusive results.

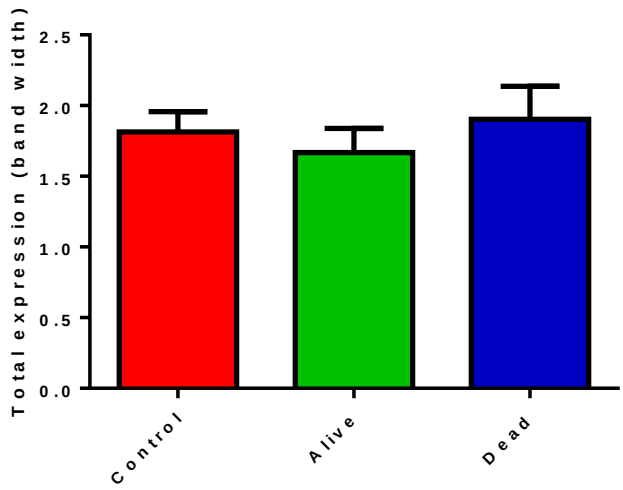


Figure 4-21: **Total MMP-9 expression in serum.** The mean expression of total MMP-9 in three groups of patients were analysed by densitometry. Statistical analysis was performed using one-way ANOVA. Experiments were conducted in triplicate. Each group (n=30 independent samples).

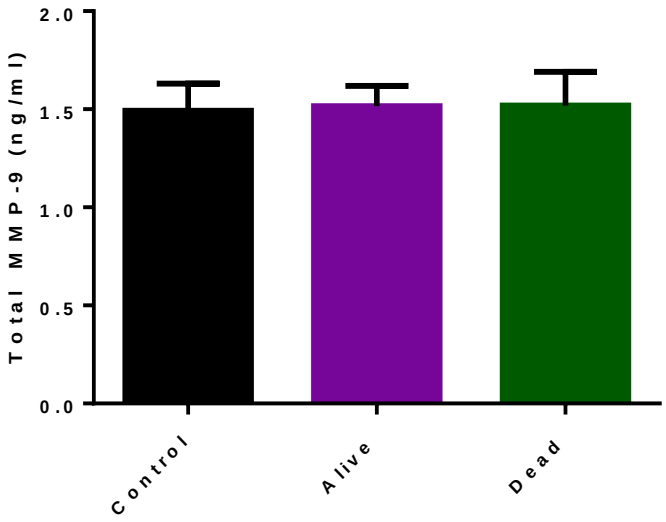


Figure 4-22: **Total MMP-9 expression using ELISA.** The mean expression of total MMP-9 in three controls in non IPF, alive IPF and dead IPF serum samples. Statistical analysis was performed using one-way ANOVA. Experiments were conducted in triplicate. Each group (n=30 independent samples).

4.5.3 Lung function and MMP-9 expression in IPF serum samples

The aim of this section was to evaluate the relationship between MMP-9 expression and pulmonary function in healthy controls and IPF patients. The MMP-9 expression was examined in serum samples and lung function data were matched for each serum sample; demographics obtained from Nottingham City Hospital (Table 4-4). The lung function data for control samples were not collected. We hypothesized that higher levels of pro-MMP-9 in serum samples would be associated with worsening lung function in patients with IPF.

Lung function measurements for the 90 patients, whose serum samples were used, were retrieved from the study by *V.Navaratnam et al, 2014*. The Transfer factor of the lung carbon monoxide (TLCO) and forced vital capacity (FVC) was evaluated in all 90 patients. The height, age and gender were all taken into consideration for each individual with IPF as per standard recommendation (Rosenberg 1996). This was calculated using a formula below:

<u>Male:</u>

FVC (l)	5.76(H)-0.026(A)-4.34	RSD=0.61
TL_{CO} (mmol min^{-1} kPa^{-1})	11.11(H)-0.066(A)-6.03	RSD=1.41

<u>Female:</u>

FVC (l)	4.43(H)-0.026(A)-2.89	RSD=0.43
TL_{CO} (mmol min^{-1} kPa^{-1})	8.18(H)-0.049(A)-2.74	RSD=1.17

H=height in metres, A=age in years.

The lung function measurements for the patients with IPF had significantly reduced TLCO %, which is an indicator of impaired transfer in both sample groups (Table 4-4). TLCO % was significantly reduced in both males and females, in particular, in the deceased IPF sample group ($p<0.05$). There was no difference in the Forced Vital capacity (FVC) of the patients with IPF in both sample groups (Figure 4-23). Usually in pulmonary function testing, steady lung decline is defined as a consistent reduction with ~80 % mortality 5 years after the initial diagnosis.

Of the 90 serum samples used for the study, 29 IPF patients died during the 3 year follow up period. The cause of death was unknown as the patient data were confidential.

Table 4-4: Baseline characteristics of serum sample subjects.

	Alive IPF	**Dead IPF**	**Controls**
Patients	29	29	32
Females	11	6	9
Males	18	23	23
Smoker	14 (M) 6 (F)	15 (M) 2 (F)	19 (M) 4 (F)
Age Range (years)	70-89	62-93	60-89
Mean Age $\pm$ SD (years)	76.9$\pm$9.7	78.1$\pm$9.2	72.5$\pm$9.9
Mean $\pm$ SD % FVC	88$\pm$18 (M) 88$\pm$30 (F)	85$\pm$18 (M) 84$\pm$43 (F)	NA
Mean $\pm$ SD % TLCO	54$\pm$18 (M) 48$\pm$18 (F)	39$\pm$20 (M) 32$\pm$17 (F)	NA
Median Death since diagnosed	NA	3 years	NA

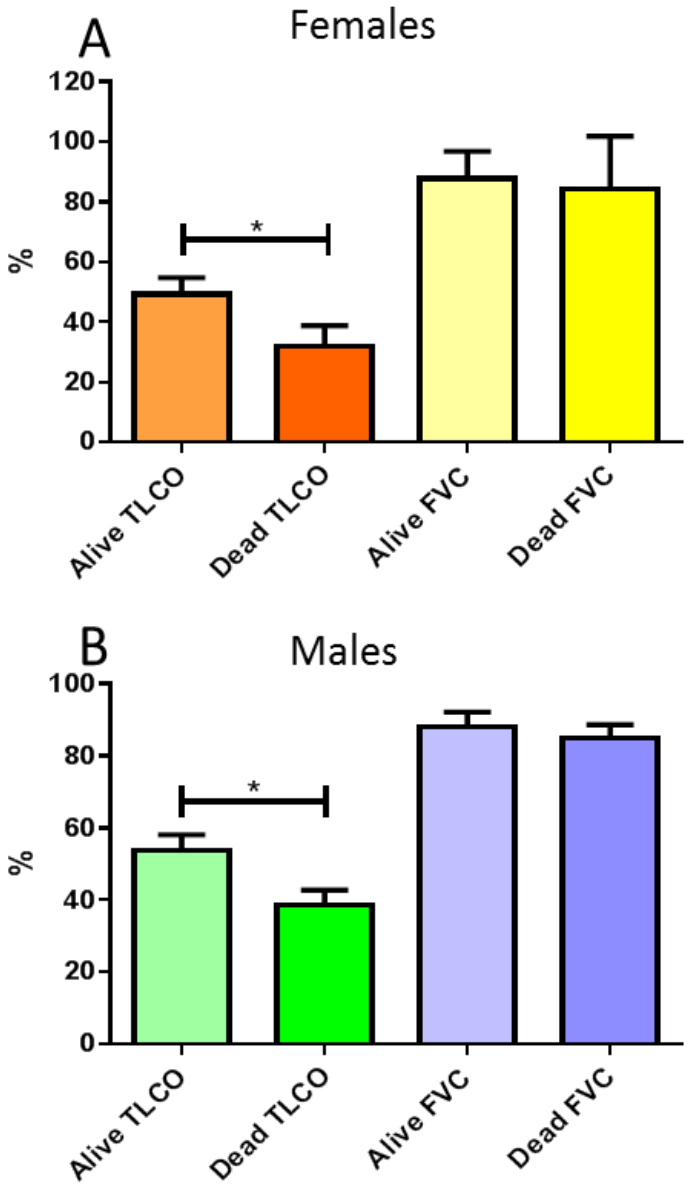


Figure 4-23: Lung function of lung capacity carbon monoxide transfer factor (TLCO) and Forced Vital capacity (FVC) of patients with IPF (alive and dead). Two groups: females (A) and in males (B) both the FVC is much higher indicating poor lung function. Statistical analysis was performed using GraphPad Prism version 6.0. One-way ANOVA was performed with a Tukey's post-hoc test. The asterisks; * represents $p<0.05$. Experiments were conducted in triplicate. n=90 Independent samples.

The next approach was to investigate the relationship between MMP-9 expression and total lung capacity information in the serum samples for both groups, dead and alive IPF patients. The results indicated that there was a positive correlation between pro-MMP-9 expression/%TLCO. However, there was no statistical difference with r^2= *0.01173* and *p=0.4448*, (Figure 4-24-(A)). There was also a positive correlation between active-MMP-9 expression/%TLCO, with statistical difference with r^2= *0.09857* and *p<0.0234*, (Figure 4-24 (B)).

Further analysis was performed to determine whether the correlation of active-MMP-9/%TLCO was effected by gender. The data revealed that active-MMP-9/ %TLCO in men-alive group with a statistical difference with r^2= *0.2211* and *p=0.0489* (Figure 4-24 (C). In summary, MMP-9 expression may be related to the lower TLCO% and a possible surrogate marker for lung function of IPF.

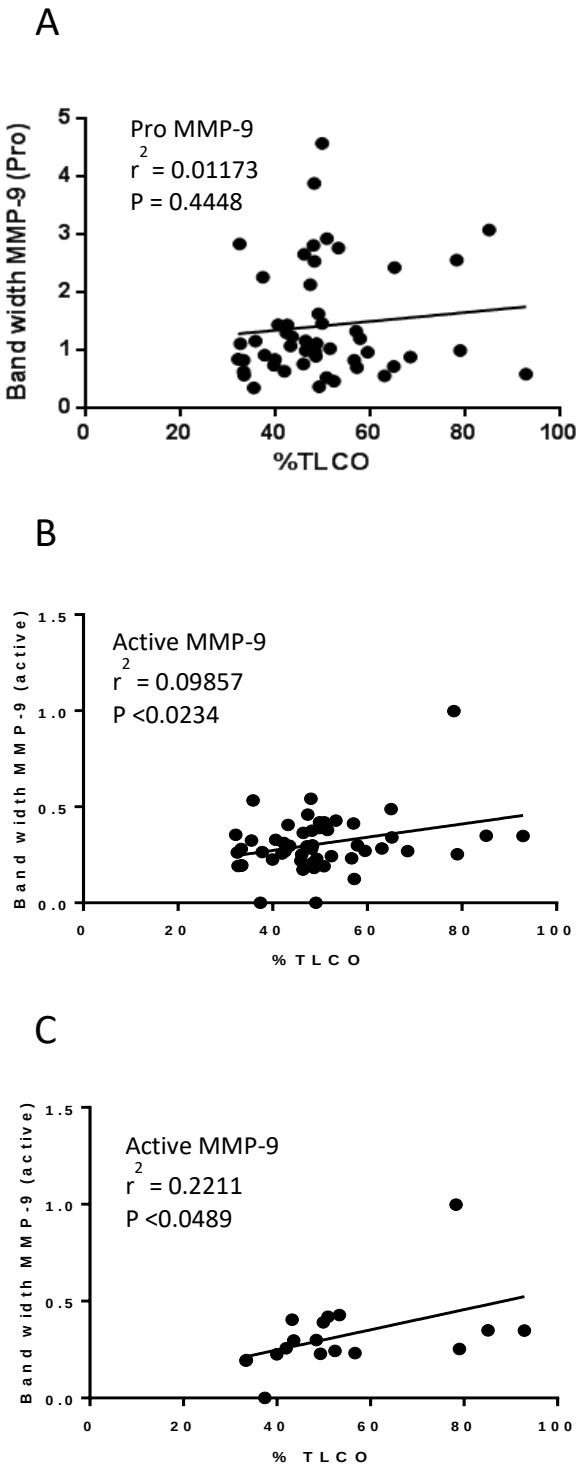


Figure 4-24: Linear regression of %TLCO and active-MMP-9. A; %TLCO of Pro-MMP-9 in both gender IPF patients. B; %TLCO of Active-MMP-9 in both gender IPF patients. C; %TLCO of Active MMP-9 for only IPF Men. Positive correlation between active-MMP-9 and lung diffusing capacity in idiopathic pulmonary fibrosis (IPF) patients (dead and alive: n=58) with r^2 = *0.09857* and *p<0.0234 (A),* in particular, active-MMP-9 and lung diffusing capacity in idiopathic pulmonary fibrosis (IPF) men patients alive group r^2= *0.2211* and *p=0.0489. U*sing linear regression analysis.

4.6 Discussion

MMPs are known to play a central role in managing the ECM substrates during tissue repair (Dancer, Wood et al. 2011), by providing resolution of inflammation, to activate and de-activate myofibroblasts, and to deposit and breakdown ECM substrates (Giannandrea and Parks 2014). In fibrosis there may be an imbalance of these MMPs leading to the accumulation of ECM substrates, impaired repair and scar formation. In this chapter, we have measured expression of MMP-1, 2, 7 and 9 as these are among the most extensively researched MMPs in fibrosis. MMP expression was measured in the epithelial monolayer culture and 3D-co-culture model with injury. The expression of MMP-9 was measured further in serum samples to determine a possible biomarker.

MMP-1 expression was measured to determine if there was a correlation with injury (section 4.4.1). The MMP-1 expression increased in epithelial cells and in non-cultured fibroblasts. The MMP-1 expression decreased with injury in the 3D co-culture model, in particular, with the scratch injury (Figure 4.1). This could be due to decreased MMP-1 activity in the fibroblasts with a possible suppressive effect coming from the epithelial cells. MMP-1 is released from various cells including fibroblasts, macrophages, endothelial cells and epithelial cells. MMP-1 is known to be absent in the interstitial compartment where collagen accumulates (Pardo and Selman 2006) suggesting it may not only function to digest fibrillar collagens. Other studies have shown that down-regulation of MMP-1 may be important for normal tissue re-modelling whereas high levels of MMP-1 have been reported in chronic non healing wounds (Pardo and Selman 2005).

MMP-7 expression decreased in epithelial cell monolayer supernatants for both injuries (Figure 4-3). Fibroblasts without injury had shown an increase of MMP-7 expression as compared to 3D co-cultured fibroblast supernatants, which decreased with injury. Previous studies have shown that MMP-7 is predominantly expressed in epithelium layer, is enhanced following injury, and is also known to regulate neutrophil influx which releases TNF-α. It could be that TNF-α is required for the expression of MMP-7. Also, the cells in the 3D co-culture model were not

differentiated and therefore there was no expression of E-cadherin, which may suggest lower MMP-7 expression.

The expression of MMP-2 by zymography revealed that there was expression of both pro and active MMP-2 in the supernatants in both models with various injuries (Figure 4-5). The results revealed that active MMP-2 expression remained the same throughout the epithelial injury model and the co-culture model. It seems that both epithelial and fibroblast cells may cleave the same amount of MMP-2 even though type II alveolar epithelial cells are known to secret MMP-2 *in vitro* (Pardo and Selman 1996) and contribute to the repairing of the epithelial cell surface. Our results may indicate that the expression of MMP-2 is produced from epithelial cells and fibroblasts suggesting that MMP-2 may play an important role in lung injury and may promote proliferation and differentiation of the fibroblasts (Pardo and Selman 2006).

In the 3D co-culture model, there was expression of only pro-MMP-9 from the fibroblasts (Figure 4-9). As for the epithelial cells (epithelial injury monolayer culture) there was expression of both pro and active MMP-9 in the supernatants. The data revealed for the co-culture model, that the pro-MMP-9 expression in fibroblasts decreased with injury compared to epithelial cells where pro-MMP-9 increased with injury. The active-MMP-9 expression decreased with injury, in particular, with administration of bleomycin. In the epithelial monolayer culture, both pro and active-MMP-9 were expressed but only pro-MMP-9 was expressed in co-cultured fibroblasts. This would suggest that MMP-9 is released by epithelial cells in the early stages of injury and aids migration of the epithelial cells to the site of injury (Kim, Choeng et al. 2009).

MMP-9 expression was determined in IPF tissue, suggesting that MMP-9 is present in both epithelial cells and fibroblasts, whereas α-SMA was co-localised to the fibroblasts (Figure 4-16 & 4-17). However, further staining i.e. staining of adjacent sections or co-staining for the 2 markers on the same section may be required to confirm the data.

Previous studies have shown that TIMP-1 may form a complex with pro-MMP-9 (Manoury, Caulet-Maugendre et al. 2006). The TIMP-1/pro-MMP-9 complex is thought to recruit MMP-3, forming a stable tertiary complex that causes MMP-3 inactivation (Stamenkovic 2003). Other work has reported a role for MMP-3, which is elevated in the IPF lung. Overexpression of MMP-3 leads to pulmonary fibrosis in the rat lung, while mice lacking MMP-3 are protected (Yamashita, Dolgonos et al. 2011). Other *in vitro* studies have suggested a role for MMP-3 in the activation of β-catenin signalling and the induction of epithelial-to-mesenchymal transition, a process thought to contribute to the pathogenesis of IPF (Chen, Lee et al. 2013).

In this study the expression of MMP-3 and TIMP-1 in co-cultured fibroblasts were measured by quantitative RT-PCR analysis and both genes had decreased with repetitive injury (Figure 4-14 & 4-15). Both genes also had low expression in fibroblasts without the presence of epithelial cells compared to cultured fibroblasts. Overall gene expression for TIMP-1 was low level. However, the decrease in gene expression of both genes with injury may be as a result of non-differentiating epithelial cells.

The decreasing expression of MMP-3 and TIMP-1 with injury may explain the decreasing expression of MMP-9 with injury (Figure 4-9). MMP-3 may play an important part in the development of fibrosis, since MMP-3 expression in epithelial cells of transgenic mice stimulates the development of fibrosis (Lindner, Zietsch et al. 2012) MMP-3 has also been implicated in the release of endostatin, an antiangiogenic collagen degradation product that can promote alveolar epithelial apoptosis, which is believed to be an important driver of ongoing fibrosis (Dancer, Wood et al. 2011). This suggests that MMP-3 expression is more dominant in epithelial cells. As the expression of MMP-3 was only measured in fibroblasts, the true expression of MMP-3 may not reflect the data. Overall, the trend does suggest MMP-3 expression may correlate to the decreasing expression of MMP-9.

Another observation is that TIMP-1 expression decreases with injury. This may also correlate to the decreasing expression of MMP-9 and possibly MMP-3. The reduced

expression of TIMP-1 may be partially related to the excess of pro-MMP-9, which is not interacting with the catalytic domain with the hemopexin domain of pro-MMP-9 (Nagase, Visse et al. 2006). In human disease, TIMP-1 is released by eosinophils, mast cells, monocytes and macrophages which are cells of the inflammatory response. The 3D co-culture model did not contain these cells and therefore, the true expression of TIMP-1 may have not been observed.

Previous studies have suggested that MMP-9 may play a dual role in the inflammatory response and migration of cells to the site of injury. A series of cytokines or growth factors could be involved to modulate the activity of MMP-9 such as CXCL8 stimulation of neutrophils to release MMP-9 (Cabrera, Gaxiola et al. 2007), or IL-13 activation of TGF-β1 *in vivo* by a MMP-9. As the 3D model was not differentiated to involve inflammatory cells, this may have affected the MMP-9 expression as well as other potential mediators released.

The expression of MMP-9 was further analysed in IPF serum samples by zymography and ELISA (section 4.5.1). The data revealed that there was expression of both pro and active MMP-9 in the serum samples. The pro-MMP-9 expression increased in the dead IPF serum samples as compared to the active MMP-9 which remained constant in the all three groups. Total MMP-9 was measured in all serum samples and revealed that there was a slight increase of total MMP-9 in dead IPF serum samples. However, there was no significance between control and dead serum samples (Figure 4-19). The ratio of pro and active MMP-9 remained the same for each group even though a slight increase was seen in the dead IPF samples, giving a $p<0.058$.

Lung function measurements were compared to MMP-9 expression to determine the relationship between lung function and MMP-9 expression. The patients with IPF (in both groups alive & dead) had significantly reduced %TLCO with increased FVC %. The active-MMP-9 expression was compared to the %TLCO of control and IPF patients. There was a positive correlation between active-MMP-9 expression and %TLCO in both dead and alive groups and in both genders, with a statistically significant difference with $r^2= 0.09857$ and $p<0.0234$. Further analysis was

performed to determine whether there was a correlation of active-MMP-9/%TLCO between men or women. The data revealed that active-MMP-9 in relation to %TLCO was more evident in males from the alive group with a statistical difference of r^2= *0.2211* and *p=0.0489,* (Figure 4-24).

Previous studies have been conducted using BALF or serum from idiopathic pulmonary fibrosis patients to investigate the presence of various MMPs and potential biomarkers i.e. MMP-1 and 7 (Rosas, Richards et al. 2008). A study by *Lemjabbar et al,* investigated the expression of MMP-9 in BALF in IPF patients and revealed that MMP-9 expression was increased in both cellular and extracellular levels (Lemjabbar, Gosset et al. 1999). Alveolar macrophages predominantly expressed MMP-9, suggesting that these cells may play a central role in releasing mediators that promote the recruitment of other inflammatory cells such as mast cells, neutrophils, and lymphocytes (Suga, Iyonaga et al. 1999). These activated inflammatory cells in the lung tissue may cause progressive injury and stimulate mesenchymal cells to accumulate (Lemjabbar, Gosset et al. 1999).

A study by *Rosas et al,* analysed forty-nine different serum markers and found two potential MMPs differentially expressed in serum from patients with IPF. MMP-1 and MMP-7 levels were most clearly increased in plasma from patients with IPF, but not in patients with sarcoidosis or COPD (Rosas, Richards et al. 2008).

As previously mentioned, MMP-9 may be a possible candidate for a biomarker along with lung function in patients with IPF. Currently, about one third of IPF patients require a surgical lung biopsy as a form of diagnosis. At times, it may not be feasible to obtain tissue samples because these procedures always carry a potential risk of serious complications (Kaarteenaho 2013). There are other methods for the diagnosis of the disease but they are not as reliable as the surgical lung biopsy. During the past decade, the research has focused on blood markers in IPF. Blood biomarkers can be easily obtained and analysed on a regular basis. Many blood biomarkers have been investigated in BAL and lung tissue, but there are very few reports describing the simultaneous examination of blood and BAL or lung tissue samples. At present, the

most widely studied blood-derived biomarkers have been KL-6 and SP-A and -D (Vij and Noth 2012).

Suga et al. investigated the role of matrix metalloproteinases (MMPs) in parenchymal remodelling in idiopathic interstitial pneumonia (IIP). MMP-2 and -9 activity was studied in bronchoalveolar lavage fluid (BALF) by zymography and the expression of MMP-2 and -9 and TIMP-2 in lung tissue by immunohistochemistry (Suga, Iyonaga et al. 2000). IPF cases showed predominant expression of MMP-9 in BALF and in lung tissue. The BALF samples revealed MMP-9 activity as well as MMP-9 in the active form. Also MMP-9 activity correlated with an increase of neutrophils in BALF, whereas the MMP-2 activity, associated with NSIP and bronchiolitis obliterans organising pneumonia (BOOP), correlated with an increase of lymphocytes. Overall the data indicated that MMP-9 was predominant in IPF-UIP and MMP-2 in NSIP and BOOP. The expression of MMP-9 in metaplastic epithelial cells was a special characteristic of UIP (Suga, Iyonaga et al. 2000).

Previous studies have shown that MMP-9 has been widely studied in IPF patients and found to be predominantly expressed by alveolar macrophages, neutrophils and epithelial cells (Dancer, Wood et al. 2011). MMP-9 gene expression and protein have been found to be elevated in both human and experimental lung fibrosis (Giannandrea and Parks 2014). Fibroblasts and alveolar macrophages extracted from IPF patient lung produced elevated MMP-9 compared with normal cells (Dancer, Wood et al. 2011). Levels of MMP-9 in BALF and MMP-9 activity are greatest in samples from rapidly progressive IPF cases (Vij and Noth 2012). Whether elevations of MMP-9 are a marker of activated neutrophils or involved in the alveolar damage in this subset of patients is unknown. However, the elevations of MMP-9 in the BALF of bleomycin induced pulmonary fibrosis model, rats have shown that MMP-9 may play an important role in the early phase of lung disease (Atkinson and Senior 2003). Lung function tests in pulmonary fibrosis have identified factors such as increase in level of dyspnoea, decrease in FVC over time or decrease in TLCO (Kolb and Collard 2014). It is common for IPF patients to have a decreasing TLCO% with progression of the disease. The median survival of patients with IPF ranges from 2.5 years to 3.5 years

(Kaarteenaho 2013). However, the clinical course of disease can vary considerably, from slow progression over many years to acute exacerbation, rapid loss of lung function and early death (Kolb and Collard 2014).

In the *in vitro* 3D co-culture model, the aim was to determine whether MMP-9 expression increased with injury in the 3D co-culture model. The data revealed a decrease in pro-MMP-9 expression in the bleomycin injury as compared to non-injury for the co-cultured fibroblasts (Figure 4-9). The data for epithelial monolayer cultures (without fibroblasts) suggested that there was activation of MMP-9 in epithelial cells, which decreased with injury, in particular, with the addition of bleomycin (Figure 4-10).

In this study, by using non-IPF and IPF serum samples, it revealed that the pro-MMP-9 expression was evident in all samples. However, there was a slight increase of pro-MMP-9 expression in the dead IPF serum compared to control samples. The reason for this could be, that under normal conditions, MMP activity is low but increases during repair or remodelling processes and in several pathological conditions (Pardo, Cabrera et al. 2016). However, the findings for pro-MMP-9 expression revealed the same for all three groups, which suggests that the understanding of MMPs may be complex as mentioned previously.

To further explore the complexity of MMPs, the relationship between MMP-9 expression and pulmonary function in healthy controls and IPF patients was compared. The data revealed a positive correlation of active-MMP-9 expression with lower %TLCO in IPF samples, in particular, in males. This may suggest before repair or remodelling processes, active MMP-9 may be present. Since these were small changes in MMP-9 expression, it is unclear if this would be a viable method to use to compare MMP expression and %TLCO in pulmonary fibrosis.

Two systems (3D co-culture model and serum samples) were used to determine the expression of MMP-9. *In vitro* data revealed expression of active MMP-9 in epithelial cells. The MMP-9 expression in serum samples revealed active-MMP-9 expression and

lower %TLCO in IPF samples. It is difficult to compare the 3D co-culture model data to the serum sample data, as the 3D model consisted of only two types of cells. In the IPF patients, MMP-9 may promote or reduce the fibrotic response depending on various stimuli and various types of cells (Dancer, Wood et al. 2011).

Therefore, using a non-invasive method may be practical but may not be appropriate as an initial diagnosis of IPF. Other factors of the disease must be taken into consideration, such as environmental factors, familial interstitial pneumonia, age or gender. However, there is no widely accepted, standardised method to combine such predictors in order to define prognosis or stage of disease.

A biomarker in IPF should be non-invasive, inexpensive, easy to repeat, and ideally blood or urine based (Ley, Brown et al. 2014). This kind of approach would be ideal as they are rapid and reliable blood-based biomarkers which have become available as part of routine procedures in clinical practice.

The metalloproteinase system is complex with activating proteinases and inhibitors interacting to regulate the overall MMP activity of different types of cells. The level of expression was evaluated by zymography and at transcriptional level by quantitative RT-PCR analysis. Further studies are required to determine whether MMP-9 activity is central to lung destruction in IPF or is a more selective target, as individual proteases or their substrates could reduce lung destruction (Atkinson and Senior 2003).

In this study, we evaluated the expression of MMPs in a non-contact method of epithelial cells and fibroblasts in an epithelial injury in the 3D co-culture model. There was expression of MMP-1 and 7 in the supernatants in the 3D co-culture model but the expression did not significantly change with injury. MMP-2 expression decreased with injury possibly suggesting the MMP-2 is inhibited by fibroblasts by a negative autocrine loop. This could be due to release of growth factors such as PGDF-BB which is involved in the inhibitory response of MMP-2 (Risinger, Updike et al. 2010).

The expression of MMPs varied suggesting that MMPs may have a role in promoting or attenuating the fibrotic responses. It seems that various activities of MMPs may impact on various cell types, location of activity, target of substrate and the level of expression of the enzyme to turn on different pathways in response to injury. Understanding the mechanisms of MMPs may be the next approach in the model.

4.7 Summary

A range of matrix metalloproteinases, 1, 2, 3, 7, and 9 were assessed in the 3D culture model. There was expression of matrix metalloproteinase 1, 2 and 7 activities which did not appear to be influenced by injury. The expression of MMP-9 decreased with injury in the 3D co-culture model. The expression of MMP-3 and TIMP-1 in fibroblasts had decreased with injury and may correlate to the decreasing expression of MMP-9 in the 3D co-culture model. MMP-9 expression was further analysed in IPF serum samples to assess correlation with the disease.

To conclude, there may be a correlation between lung function i.e. % TLCO and expression of active MMP-9. Understanding the mechanisms of pro and active MMP-9 in the model may help to gain a better understanding of the pathological mechanisms involved in IPF.

Chapter Five
Affymetrix® MicroArray Data

5.1 Introduction

Lung fibrosis is triggered by a series of micro-injuries in the epithelial cells and results in inflammation, fibroblast proliferation and extracellular matrix accumulation in the lung (Selman, Pardo et al. 2006). However, these activated fibroblasts may induce alveolar epithelial cell injury and death, thereby creating a pro-fibrotic effect of epithelial cell-fibroblast interactions, which may drive the progression of pulmonary fibrosis (Sakai and Tager 2013).

To understand IPF, studies are predominantly carried out in bleomycin-treated animals or in human lung biopsies, both having their own limitations. Another method to understand the disease in a different way is using Microarray. Microarray studies have been used as an approach in bleomycin-treated animals or patient tissues, allowing the simultaneous monitoring of the transcriptional behaviour of thousands of genes. Gene expression studies are being applied to IPF in an attempt to identify target genes that might improve the current understanding of its underlying molecular mechanisms (Kaminski, Allard et al. 2000).

Several studies have suggested that the progression of IPF is likely to be due to epithelial/fibroblast activation leading to the degradation of the lung architecture (Selman, King et al. 2001). To understand the molecular mechanisms of epithelial/ fibroblast interactions, a microarray approach was used to identify and compare the gene expression "signatures" using genome-wide, custom cDNA microarrays. Microarrays are a high throughput technology used to measure genome-wide gene expression. The concept behind microarrays is to exploit complementary base pairing to measure the amount of the different types of mRNA molecules in a cell. This indirectly measures expression levels of the genes, which defines the role of each gene and may lead to the understanding of the interactions between sets of genes in that genome (Yang and Speed 2002).

Studies have shown different gene expression profiling to understand the epithelial-fibroblast interactions. A study by *Moll et al*, has shown in, *in vitro* the direct culturing of fibroblasts in 3D collagen and epithelial cells which may control and

regulate the fibroblast differentiation and activation in the development of fibrosis (Moll, Ebeling et al. 2013). Another *in vitro* study has shown the co-culture of epithelial cells and fibroblasts in a Transwell® system. The model demonstrated epithelial injury via scratch wound injury and the fibroblasts filtering in through the Transwell® pores. This was to show whether the fibroblasts have an aberrant response to epithelial injury (Prasad, Hogaboam et al. 2014). Both *in vitro* models have shown that epithelial injury does play a role in abnormal epithelial-fibroblast crosstalk which may drive the progression of pulmonary fibrosis but the similarity with these models is that the cells have been in direct contact with one another. Our 3D co-culture model used the non-direct contact of epithelial cells and fibroblasts in the Transwell® system. This was to determine which soluble mediators may contribute to the epithelial/fibroblast crosstalk.

5.2 Aims

The aim of the work was, 1) analyse different gene expression 'signatures', in scratch and bleomycin-treated epithelial cells compared to untreated cells, as well in fibroblasts co-cultured with injured and un-injured epithelial cells. 2) Determine whether the specific signatures would provide insight regarding the divergent pathways leading to lung fibrosis.

To analyse the gene expression of epithelial cells and fibroblasts, a series of experiments were conducted using the 3D co-culture model to mimic the mechanism of epithelial and fibroblast interactions using a non-direct contact method. In particular, injuries inflicted included, mechanical disruption i.e. scratch wounding and the addition of bleomycin to inflict injuries over 6 days to epithelial cells alone. The effect was monitored on both epithelial cells and fibroblasts. The total RNA of epithelial cells and fibroblasts were harvested, quantified, and the integrity was verified by Agilent bio analyser and samples sent to Epistem, UK for Affymetrix microarray.

In this study, >300 genes were differentially expressed in injured epithelial cells between scratch and bleomycin-treated samples. Furthermore, pathway analysis was

performed by Ingenuity Systems to identify the transcription regulators that may be responsible for gene expression changes in the epithelial cells and fibroblasts. Finally, a selection of genes which were expressed in both injuries i.e. scratch and bleomycin were selected based on $p<0.05$ with a fold change > 2. The microarray data were analysed and validated by quantitative RT-PCR analysis.

5.3 Methods

5.3.1 RNA isolation of fibroblasts and epithelial cells

The experiments for each cell type epithelial cells and fibroblasts were conducted as section 2.4. Cell culture RNA was isolated from epithelial cell monolayer injured with scratch or bleomycin as well as uninjured and 3D co-cultured fibroblasts in which the epithelial cells were injured to see the effect of epithelial injury on fibroblasts. The fibroblasts were isolated for RNA.

The experiments were performed in triplicate. All these experiments were conducted independently. Table 5-0 represents the identification of the experiments conducted for each cell type. The identification number represents the independent experiment performed.

Table 5-0: This table represents the identification of the experiments conducted

Epithelial cells (monolayer culture)	**Fibroblasts (3D co-culture)**
26di	29fi
26dii	29gi
26diii	29gii

5.3.2 Agilent Bioanalysor Analysis

As section 2.10.

5.3.3 Microarray analysis of fibroblasts and epithelial cells using Affymetrix GeneChip Systems

Sample processing, microarray hybridization and gene expression analyses were carried out with the Affymetrix Genechip Systems (Affymetrix, Santa Clara, CA, USA) at Epistem, Manchester, UK. From 1μg of total RNA, complementary DNA (cDNA) was synthesized using the one-cycle cDNA synthesis kit (Epistem). Biotinylated complementary RNA (cRNA) was synthesized by the following the IVT labelling kit (Epistem) and purified using the GeneChip sample Cleanup Module (Epistem). Subsequently, Biotinylated cRNA was fragmented and hybridized to the Genechip Human Genome U133 Plus 2.0 microarrays (Epistem). After hybridization, microarrays followed the washing and staining protocol and were scanned using the Genechip Scanner 3000 (Epistem). The fluorescent signal corresponding to the intensity of hybridization intensity of each transcript was determined using the Gene Chip Operating Software (GCOS 1.4; Epistem). Intensity values were scaled such that the overall florescence intensity of each array was equivalent. Finally, probe set measurements were generated from quantified Affymetrix image (.CEL) files using the Gene chip robust Multichip average method (GC-RMA) from the Array Studio (available at http://www.omicsoft.com/software/ArrayStudio/publish.htm).

The sample processing, microarray hybridization and Affymetrix image (.CEL) files were all carried out at Epistem, Manchester, UK. The gene analysis was carried out using all 21 CEL files applied into Array Studio v 6.0 and normalised separately for each cell type using GCRMA. This was performed by GSK, Stevenage, UK.

5.3.4 Background Correction

All .CEL files were normalised using GC-RMA from the Array Studio, (Available at http://www.omicsoft.com/software/ArrayStudio/publish.htm).

The background fluorescence was corrected using GC-RMA which calculates the signal algorithm. This was used to correct the intensity reading for each probe set. Background fluorescence can arise from many sources, such as non-specific binding of labelled samples or the array surface, processing effects such as deposits left after

the wash stage or optical noise from the scanner (Dalma-Weiszhausz, Warrington et al. 2006).

'Signal' is a quantitative metric calculated for each probe set which represents the relative level of expression of a transcript. Signal was calculated using 'Tukey's Biweight Estimate' (Figure 5-1), (Mei, Hubbell et al. 2003) which yields a robust weighted mean that is relatively insensitive to outliers, even when extreme.

$$signal = \log^{-1}\left(Tukey\ Biweight\left(\log\left(PM_j - CT_j\right)\right)\right)$$

Figure 5-1: **Tukey's Biweight Estimate.** CT_j is a quantity derived from MM_j never larger than PM_j. Weights each probe intensity based on the distance from the mean.

5.3.5 Normalisation

Normalisation adjusts data for technical variation, as opposed to biological differences between the samples. The probe sets are compared to each other and analysed together. A series of assessments are performed to quantify the signal. Technical QC was performed through the MAS 5.0 analysis in the Array studio software. It ensures that the sample is of high standard and of reproducible value. It is an assessment based on signal values (Irizarry, Hobbs et al. 2003).

5.3.5.1 RawQ

RawQ is a measure of the pixel-to-pixel variation of probe cells on a GeneChip array. The two main factors that contribute to noise are electrical noise of the GeneArray scanner and sample quality. Each GeneArray Scanner has a unique inherent electrical noise associated with its probe. Since a significant portion of Noise (Raw Q) is based on electrical noise, absolute Noise (Raw Q) values among probes will vary.

5.3.5.2 Scaling Factor

Affymetrix normalises arrays by scaling them based on the median values on the array.

5.3.5.3 Background

Affymetrix average background values are usually between 20 and 100, which can be considered a good quality array.

5.3.5.4 Percent Present

The number of probe sets called "Present" relative to the total number of probe sets on the array is displayed as a percentage. Percent Present (%P) values depend on multiple factors including cell/tissue type, biological or environmental stimuli, probe array type, and overall quality of RNA. Replicate samples should have similar %P values. Extremely low %P values are a possible indication of poor sample quality. Usually the 'Percent Present' ranges from 30-60%.

5.3.5.5 Average Signal

This is brightness of the GeneChip arrays which is expressed from each probe.

5.3.5.6 ACTB 3'/5' ratio and GAPDH 3'/5' ratio

Signal intensity ratio of the 3' probe set over the 5' probe set is often referred to as the 3'/5' ratio. This ratio gives an indication of the integrity of the starting RNA and efficiency of first strand cDNA synthesis. The signal of each probe set reflects the sequence of the probes and their hybridization properties. The 1:1 molar ratio of the 3' to 5' transcript regions will not necessarily give a signal ratio of 1.

5.3.5.7 QC assessment of data (QC metrics and expression)

Following normalisation, it is necessary to do a number of quality checks which can be performed following the analysis of the raw data by the Affymetrix software. The data were based on two chip expression quality assessments: Technical Quality Control (QC) and Biological QC. Both QC parameters ensure chip quality, hybridisation, RNA quality and purity (McCall, Murakami et al. 2011).

5.3.5.8 Technical QC (MAS5.0)

Technical QC is the quantitative assessments available through the MAS 5.0 analysis in the Array studio software. It ensures that the sample is of high standard and of reproducible value.

5.3.5.9 Biological QC - Principal Component Analysis (PCA)

Biological Quality Control ensures that the biological replicates have similar gene expression profiles. The Principal component analysis is a process in the software which is used to analyse relationship between treatments, groups or cells. So if there are any outliers, they can be detected and compared to the hybridisation.

5.3.6 Summarisation

Once the back ground was corrected and the data were normalised, the intensities were summarised into expression measures showing single expression measure per probe set, per chip. The summarisation is motivated by the assumption that observed log-transformed PM values follow a linear additive model containing a probe affinity effect and a gene specific effect. A Generalised Linear Model' was used for the Statistical Modelling of the data which represented the individual cell type and treatment.

A threshold for the minimal fold change was specified with fold change >2 and *p*-value <0.05 using a Bonferroni correction. An ANOVA was performed within a class or across different classes for experiments. Principal components analysis (PCA) was used to detect any outliers and analyse relationships between treatments, groups or cells.

5.3.6.1 Ingenuity Pathway Analysis for epithelial cells and fibroblast cells.

Functional networks and pathway analyses were generated by Ingenuity Pathway Analysis (IPA) (Ingenuity Systems ®, www.ingenuity.com). Fisher's exact test was used to calculate a *P*-value determining the probability that each biological function and/ or disease assigned to that dataset and network is not due to chance alone (*P*-values $\leq$0.05 were considered as significant). Activation z-score was calculated as a

measure of functional and translational activation in Networks and Upstream regulators analysis. An absolute z-score of below (inhibited) or above (activated) 2 was considered as significant.

5.3.6.2 Measuring the efficiency of SYBR GREEN ® quantitative RT-PCR assays

The measure of the efficiency of SYBR green® was to ensure that relevant experiment assays were similar to that of the relevant house-keeping gene. Initially, standard curves were set up to determine the assay efficiency, cDNA known to express the target genes were chosen for eight cDNA dilutions, decreasing with a two-fold difference (1, 0.5, 0.25, 0.125, 0.0625, 0.03125).

Each concentration was tested in triplicate, the mean of the three values were plotted against the –log of the six cDNA concentrations (0, -0.3, -0.6, -0.9, -1.2, -1.5). The linear regression slope value was calculated, this value was then used in the equation: **(10^ (-1/ slope value) -1)*100** to calculate the primer efficiencies. A slope value of -3.3 equates to 100% primer efficiency. In these experiments, all primer efficiencies were of similar values indicating the comparative method could be used for comparison of expression levels between genes.

5.3.6.3 Validating gene expression of microarray data by Quantitative RT-PCR

Quantitative RT-PCR analysis was performed (refer to section 2.8). To validate the microarray data, a set of genes from the microarray dataset (bleomycin vs no-injury) in fibroblasts, were selected for quantitative RT-PCR analysis. This was based on the highest fold change and lowest fold change along with negative fold-change, (Table 5-2).

5.3.7 Statistical Analysis

Data were analysed using GraphPad Prism 6.0 software (GraphPad Software, Inc.). Continuous data from independent experiments, which were considered to follow a normal distribution were displayed as the mean value ± SEM, and their statistical significance was assessed by one-way ANOVA followed by Tukey's post-hoc test when comparing multiple conditions to a control or two-way ANOVA with the Bonferroni post-hoc test when comparing multiple conditions with one another. The P values, which were significant and were shown with asterisks. The asterisks; *** represents $p<0.001$, ** represents $p<0.01$ *and* * represents $p<0.05$. n=3 (refer to section 2.11).

5.4 Results

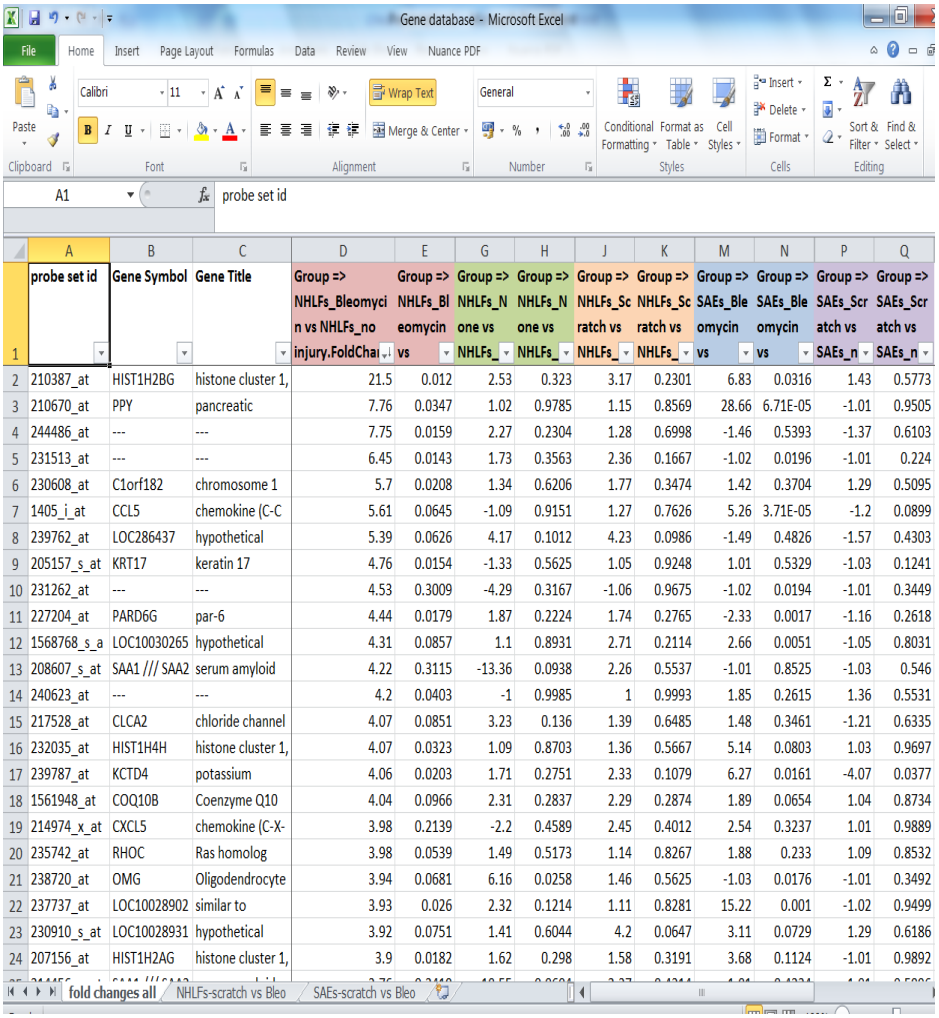
5.4.1 Array Studio Gene database

The microarray results were based on two cell types: fibroblasts and epithelial cells. In the 3D co-culture model, epithelial cells were injured with either scratch injury or administration of bleomycin, and only the fibroblasts were retrieved. In the monolayer culture, this consisted of epithelial cells only, which were injured with either scratch injury or administration of bleomycin. The arrangement of cells in the 3D co-culture model was to determine whether there was an effect of the epithelial injury on the fibroblasts. The biological experiments were independent and were conducted as n=3.

Statistical treatment of raw microarray data was done using Omicsoft TM Array Studio version 3.0 (http://www.omicsoft.com/) (refer to section 5.3.3). Microarray data were normalised (refer to section 5.3.4) using quantile normalisation and then transformed based on log2 scale. Gene lists were generated using statistical limitations on fold change in gene expression, and confidence p- values. These sets of gene lists were used for functional annotation.

The microarray gene database identified 54676 different probe sets within the different injuries with the two cell types: epithelial cells and fibroblast cells. The data were transferred into an excel spreadsheet and filters were added to divide the data

categories. The parameters for each group were added for each cell type, fibroblasts (NHLFs): bleomycin vs no-injury, NHLFs vs no-injury and scratch vs no-injury. Epithelial cells (SAEs): bleomycin vs no-injury and scratch vs no-injury. Each group was assigned with a fold change and p-value column. In total 10 columns were created with filters (Figure 5-2).



	A	B	C	D	E	G	H	J	K	M	N	P	Q
1	probe set id	Gene Symbol	Gene Title	Group => NHLFs_Bleomycin vs NHLFs_no injury.FoldChai	Group => NHLFs_Bleomycin vs	Group => NHLFs_None vs NHLFs_	Group => NHLFs_None vs NHLFs_	Group => NHLFs_Scratch vs NHLFs_	Group => NHLFs_Scratch vs NHLFs_	Group => SAEs_Bleomycin vs	Group => SAEs_Bleomycin vs	Group => SAEs_Scratch vs SAEs_n	Group => SAEs_Scratch vs SAEs_n
2	210387_at	HIST1H2BG	histone cluster 1,	21.5	0.012	2.53	0.323	3.17	0.2301	6.83	0.0316	1.43	0.5773
3	210670_at	PPY	pancreatic	7.76	0.0347	1.02	0.9785	1.15	0.8569	28.66	6.71E-05	-1.01	0.9505
4	244486_at	---	---	7.75	0.0159	2.27	0.2304	1.28	0.6998	-1.46	0.5393	-1.37	0.6103
5	231513_at	---	---	6.45	0.0143	1.73	0.3563	2.36	0.1667	-1.02	0.0196	-1.01	0.224
6	230608_at	C1orf182	chromosome 1	5.7	0.0208	1.34	0.6206	1.77	0.3474	1.42	0.3704	1.29	0.5095
7	1405_i_at	CCL5	chemokine (C-C	5.61	0.0645	-1.09	0.9151	1.27	0.7626	5.26	3.71E-05	-1.2	0.0899
8	239762_at	LOC286437	hypothetical	5.39	0.0626	4.17	0.1012	4.23	0.0986	-1.49	0.4826	-1.57	0.4303
9	205157_s_at	KRT17	keratin 17	4.76	0.0154	-1.33	0.5625	1.05	0.9248	1.01	0.5329	-1.03	0.1241
10	231262_at	---	---	4.53	0.3009	-4.29	0.3167	-1.06	0.9675	-1.02	0.0194	-1.01	0.3449
11	227204_at	PARD6G	par-6	4.44	0.0179	1.87	0.2224	1.74	0.2765	-2.33	0.0017	-1.16	0.2618
12	1568768_s_a	LOC10030265	hypothetical	4.31	0.0857	1.1	0.8931	2.71	0.2114	2.66	0.0051	-1.05	0.8031
13	208607_s_at	SAA1 /// SAA2	serum amyloid	4.22	0.3115	-13.36	0.0938	2.26	0.5537	-1.01	0.8525	-1.03	0.546
14	240623_at	---	---	4.2	0.0403	-1	0.9985	1	0.9993	1.85	0.2615	1.36	0.5531
15	217528_at	CLCA2	chloride channel	4.07	0.0851	3.23	0.136	1.39	0.6485	1.48	0.3461	-1.21	0.6335
16	232035_at	HIST1H4H	histone cluster 1,	4.07	0.0323	1.09	0.8703	1.36	0.5667	5.14	0.0803	1.03	0.9697
17	239787_at	KCTD4	potassium	4.06	0.0203	1.71	0.2751	2.33	0.1079	6.27	0.0161	-4.07	0.0377
18	1561948_at	COQ10B	Coenzyme Q10	4.04	0.0966	2.31	0.2837	2.29	0.2874	1.89	0.0654	1.04	0.8734
19	214974_x_at	CXCL5	chemokine (C-X-	3.98	0.2139	-2.2	0.4589	2.45	0.4012	2.54	0.3237	1.01	0.9889
20	235742_at	RHOC	Ras homolog	3.98	0.0539	1.49	0.5173	1.14	0.8267	1.88	0.233	1.09	0.8532
21	238720_at	OMG	Oligodendrocyte	3.94	0.0681	6.16	0.0258	1.46	0.5625	-1.03	0.0176	-1.01	0.3492
22	237737_at	LOC10028902	similar to	3.93	0.026	2.32	0.1214	1.11	0.8281	15.22	0.001	-1.02	0.9499
23	230910_s_at	LOC10028931	hypothetical	3.92	0.0751	1.41	0.6044	4.2	0.0647	3.11	0.0729	1.29	0.6186
24	207156_at	HIST1H2AG	histone cluster 1,	3.9	0.0182	1.62	0.298	1.58	0.3191	3.68	0.1124	-1.01	0.9892

Figure 5-2: MicroArray Database print screen. This print screen shows the lay out of the gene database for the epithelial cells and fibroblasts, which have been compared to their individual, control data set. Column A is the probe id, column B, is the gene symbol and column C is the gene name for each gene identified. Column D is the Fold change for the group set of bleomycin-treated fibroblasts, which have been compared to non-injured fibroblasts and Column E is the p value for the group set of fibroblasts, which have been compared to non-injured fibroblasts. Column G, is the Fold change for the group set of non-injured fibroblasts, which have been compared to non-injured fibroblasts and Column H is the p value for the group set of non-injured fibroblasts, which have been compared to non-injured fibroblasts. Column J is the Fold change for the group set of fibroblasts injured by scratch wounding, which have been compared to non-injured fibroblasts and Column K is the p value for the group set of fibroblasts injured by scratch wounding, which have been compared to non-injured fibroblasts. Column M is the Fold change for the group set of bleomycin-treated epithelial cells, which have been compared to non-injured epithelial cells and Column N is the p value for the group set of bleomycin-treated epithelial cells, which have been compared to the non-injured epithelial cells. Column P is the Fold change for the group set of the epithelial cells injured by scratch wounding, which have been compared to non-injured epithelial cells and Column Q is the p value for the group set of epithelial cells injured by scratch wounding which, have been compared to non-injured epithelial cells.

The gene database was normalised by using specific filters to identify low intensity data using a specific threshold or a relative threshold imposed according to the background intensity. The data was from 3 independent experiments which were averaged and the values generated after filtering. The differentially expressed genes were identified. The comparisons are outlined in table 5-1.

For each cell type condition, the intensity filter cut-off was set to 5 (log_2 intensity) and with a filter Max Median Intensity $\geq$5. The p-value and fold change filter were included to identify groups of genes, which were up or down regulated (Table 5-1).

Table 5-1: **This table shows the number of genes detected in each group set of fibroblasts and epithelial cells with using p-value of p≤0.05 and Max Median Intensity ≥5.**

Conditions	p-value	Genes Detected
Fibroblasts: Bleomycin vs no-injury	p≤0.05	1029
Fibroblasts: Scratch vs no-injury	p≤0.05	544
Fibroblasts: None (no epithelial cells) vs no-injury	p≤0.05	1699
Epithelial cells: Bleomycin vs no-injury	p≤0.05	5321
Epithelial cells: Scratch vs no-injury	p≤0.05	811

5.4.2 Principal Components Analysis

Principal components analysis (PCA) is a statistical technique for determining the key variables in a multidimensional data set and allows identifying the differences in the observations. The differences in the microarray data may often not be clear whether a set of experiments are measuring fundamentally different gene expression states or are measuring similar states created through different mechanisms. It is useful, therefore, to define a set of independent features for the expression and allow them to be compared directly.

In this data set, PCA was used to compare the cell types and experimental conditions to summarise the ways in, which gene responses vary. The PCA was to compare the gene changes of the individual cell types with injury and to determine if there was an effect.

This was determined by 'components' i.e. Component 1 and Component 2. Component 1 is the direction, which identifies whether the samples are variable between injuries. Component 2 allows to identify whether there is an effect between the injuries.

The samples were plotted to identify any similarities and differences between cell types or the conditions. The batches i.e. experiment 26di, 26dii and 26diii are identification number of experiments of epithelial cells from the monolayer culture; independent experiment performed. The batches 29fii, 29gi and 29gii are identification number of experiments of the fibroblasts from the 3D co-culture model, independent experiment performed.

The PCA of the expressed genes using maximum median intensity $\geq$5 for each group, identified 14755 probe sets. This indicated that no samples were outliers and each cell type i.e. epithelial cells and fibroblasts were separated by order of each condition (Figure 5-3) and by set of experiments (Figure 5-4).

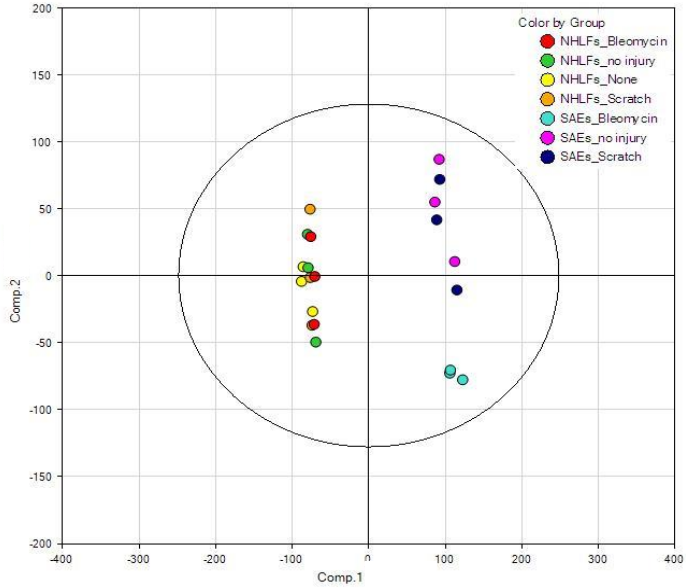


Figure 5-3: Principal Component Analysis of epithelial cells and fibroblasts. This graph shows the PCA of the condition for each cell type: epithelial cells and fibroblasts, which are within the statistical analysis of PCA. Experiments were conducted in triplicate. n=3 independent biological experiments.

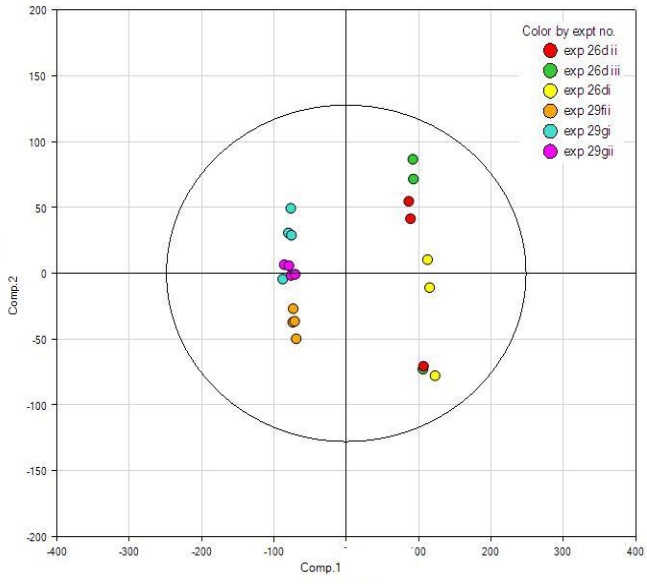


Figure 5-4: **Principal Component Analysis of each batch.** This graph shows the PCA of the experiments for each set of experiments for monolayer model epithelial cells (experiment 26d i, ii and iii) and co-culture model consisting fibroblasts (experiments 29g i, ii, and iii). Each experiment was performed in triplicate. Experiments were conducted in triplicate. n=3 independent biological experiments.

5.4.2.1 Principal Component Analysis of epithelial cells

The linear model was used to analyse the epithelial samples from the epithelial monolayer model using Log2 (intensity). Each sample was observed based on individual treatments on epithelial cells (Table 5-0). When both experiments and genes were analysed together, there was a combination of effects. The principal was to observe the relationship between the experimental batch and treatment.

The epithelial expression of the PCA revealed changes in the gene expression was largely driven by bleomycin-treatment (Figure 5-5 (blue circles)). The observation of the batch expression also revealed that experiment 26di (epithelial cells only) had a positive correlation as compared to batch 26 dii and iii (epithelial cells only) (Figure 5-6) but there was a small difference between the non-injured and scratch treated cells.

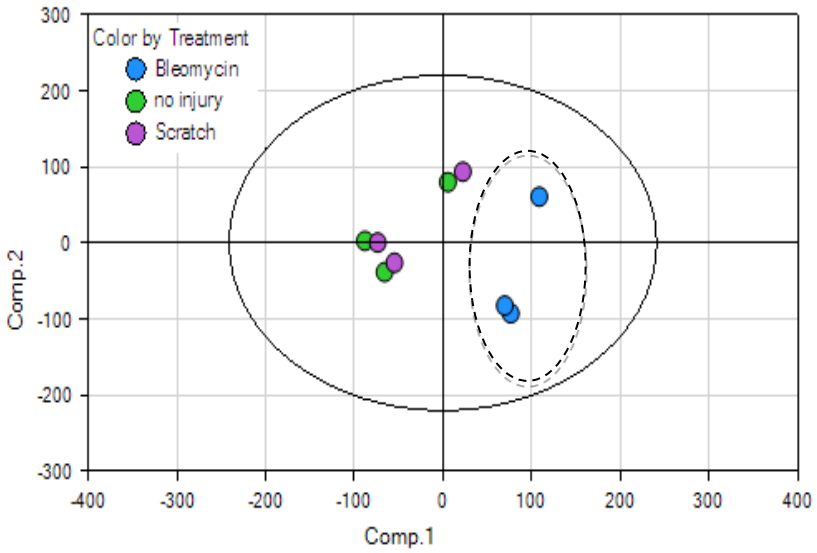


Figure 5-5: Principal component analysis of individual treatments for epithelial cells for each experiment batch. The circle cluster (blue) of sample is the epithelial cells treated with bleomycin. Experiments were conducted in triplicate. n=3 independent biological experiments.

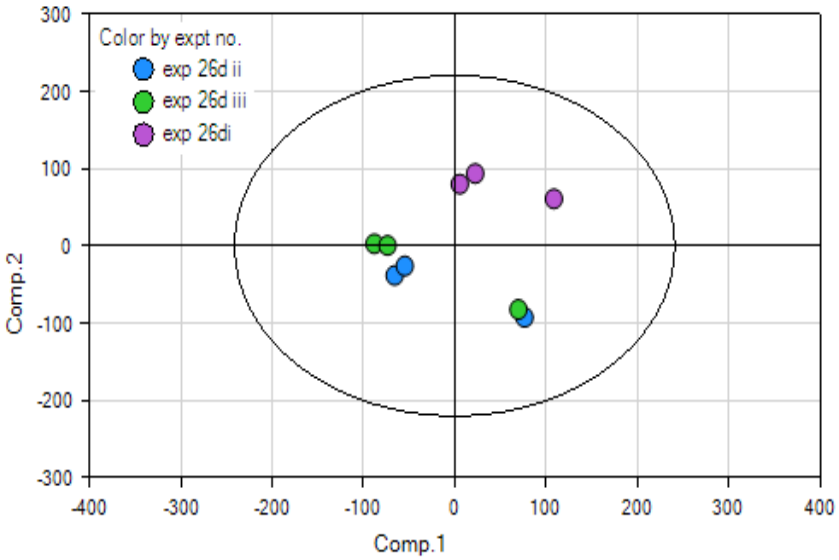


Figure 5-6: **Principal component analysis of individual experiments in epithelial cell with relevant treatments.** The experiment was conducted in the epithelial monolayer model i.e. 26di, 26dii and 26diii. Experiments were conducted in triplicate. n=3 independent biological experiments.

5.4.2.2 Comparison of gene expression for epithelial cells using Venn Diagrams

Venn diagrams are graphical ways of representing interactions among sets to display information. They are used to compare and contrast two or more relationships in the dataset.

In the microarray dataset, Venn diagrams were used to identify genes differentially expressed in both conditions i.e. bleomycin and scratch injury in epithelial cells (Table 5-1). The results revealed for epithelial cells (bleomycin vs no-injury) 5095 genes were changed ($p<0.05$) while for epithelial cells (scratch-wounding vs no-injury) 585 genes were changed ($p<0.05$). The Venn diagram identified, the number of probes sets with p<0.05 in both injury conditions were **226.** From the 226 probes sets, a list of top 25 genes was presented in Table 5-2.

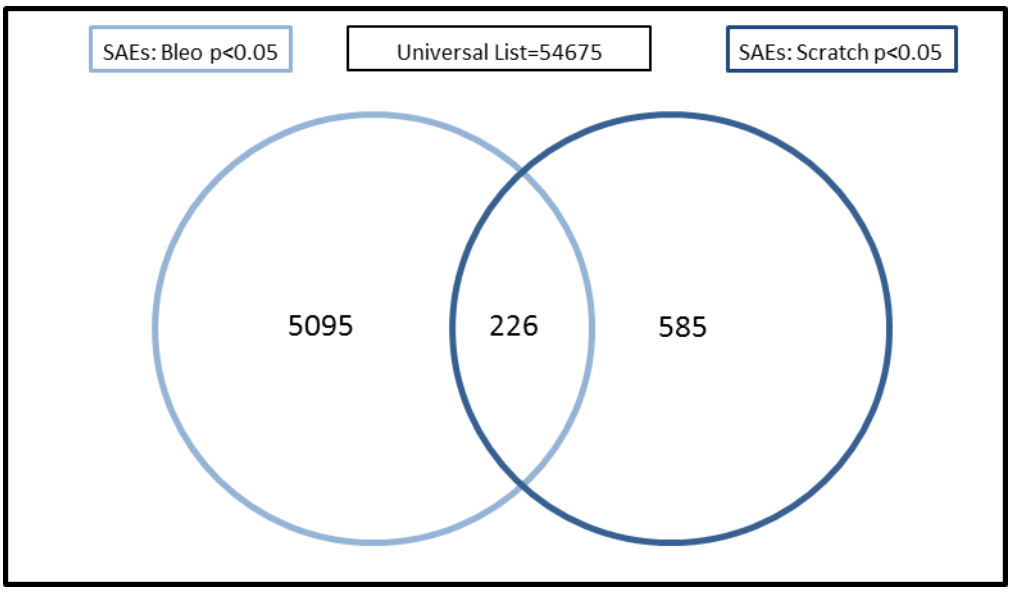


Figure 5-7: Venn diagram outlining differential expressed genes in epithelial cells. The treatments of bleomycin and scratch on epithelial cells alone. The diagram shows that there were 226 genes, which are present in both injuries ($p<0.05$).

Table 5-2: A list of top 25 genes expressed in bleomycin and scratch injuries in epithelial cells. Probe sets indicate genes, which are altered by bleomycin and scratch injuries in epithelial cells. Using the criteria fold change >2 with a p<0.05 (Bleomycin vs no-injury).

Probe set	Gene symbol	Gene title	Bleo fold change	Bleo p<0.05	Scratch fold change	Scratch p<0.05
223791_at	FAM27A	family with sequence similarity 27, member A	17.54	0.0008	2.51	0.0433
229963_at	BEX5	brain expressed, X-linked 5	10.45	0.0113	5.29	0.0343
204039_at	CEBPA	CCAAT/enhancer binding protein (C/EBP), alpha	10.24	0.0006	2.54	0.0167
236189_at	ANKRD50	ankyrin repeat domain 50	7.47	2.13E-05	1.48	0.0112
231416_at	DHDH	dihydrodiol dehydrogenase (dimeric)	6.33	8.78E-05	1.54	0.0195
239787_at	KCTD4	potassium channel tetramerisation domain containing 4	6.27	0.0161	-4.07	0.0377
228245_s_at	OVOS /// OVOS2	ovostatin /// ovostatin 2	5.77	0.0017	-3.57	0.0055
241433_at	RCOR3	REST corepressor 3	5.07	0.0002	1.54	0.0234
208188_at	KRT9	keratin 9	4.71	0.0028	2.11	0.0341
228593_at	MTMR9L	myotubularin related protein 9-like, pseudogene	4.06	0.0002	-1.61	0.0097
207980_s_at	CITED2	Cbp/p300-interacting transactivator, with Glu/Asp-rich carboxy-terminal domain, 2	4.02	0.0002	1.83	0.0042
1554830_a_at	STEAP3	STEAP family member 3	3.91	1.27E-05	1.21	0.0218
204678_s_at	KCNK1	potassium channel, subfamily K, member 1	3.85	0.0041	1.94	0.0432
222496_s_at	RBM47	RNA binding motif protein 47	3.58	0.0084	2.12	0.0467
1569303_s_at	RGS20	regulator of G-protein signalling 20	3.1	0.0004	1.4	0.0328
203713_s_at	LLGL2	lethal giant larvae homolog 2 (Drosophila)	2.88	0.0001	2.3	0.0003
219475_at	OSGIN1	oxidative stress induced growth inhibitor 1	2.84	0.002	1.67	0.0241
233030_at	PNPLA3	patatin-like phospholipase domain containing 3	2.81	0.0045	1.69	0.0435
218492_s_at	THAP7	THAP domain containing 7	2.66	0.0007	1.83	0.0044
219824_at	SLC13A4	solute carrier family 13 (sodium/sulfate symporters), member 4	2.6	0.0006	-1.57	0.0092
214091_s_at	GPX3	glutathione peroxidase 3 (plasma)	2.56	0.0036	-1.77	0.0203
209231_s_at	DCTN5	dynactin 5 (p25)	2.56	0.0004	1.61	0.0049
228846_at	MXD1	MAX dimerization protein 1	2.48	0.0004	1.33	0.0245
210790_s_at	SAR1A	SAR1 homolog A (S. cerevisiae)	2.38	0.004	1.74	0.0189
219710_at	SH3TC2	SH3 domain and tetratricopeptide repeats 2	2.37	8.00E-05	1.19	0.0278

5.4.2.3 Principal Components Analysis Fibroblast cells

The linear model was used to analyse co-cultured fibroblast samples using Log2 (intensity) in individual treatments. All the co-cultured fibroblast experiments and genes were analysed together to observe any combination effects. The principal of the PCA was to observe the relationship of the experimental batch and treatments. The results revealed that the fibroblasts with treatments, the PCA, had a variable direction and the treatments were not grouped (Figure 5-8). The batch expression PCA, showed that the experiments were grouped together in experiment 29fi, revealing a positive correlation (Figure 5-9).

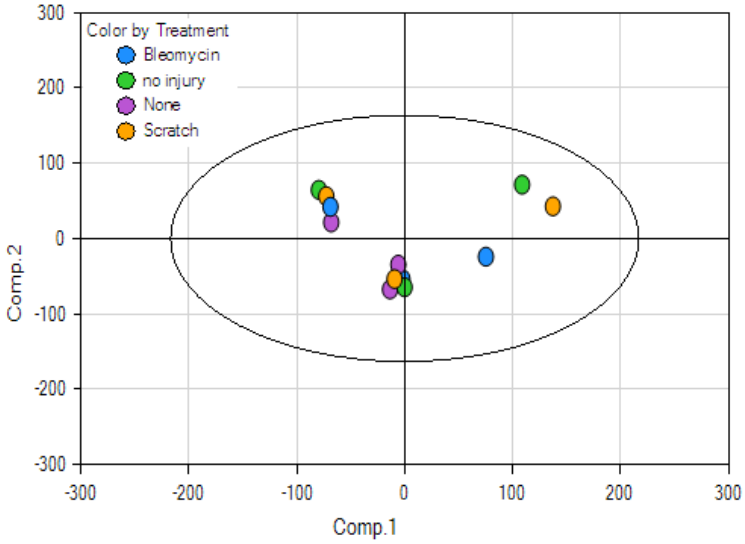


Figure 5-8: Principal component analysis of individual treatments. The PCA for co-cultured fibroblast cells after epithelial injury. The condition is represented for each experiment batch. Experiments were conducted in triplicate. n=3 independent biological experiments.

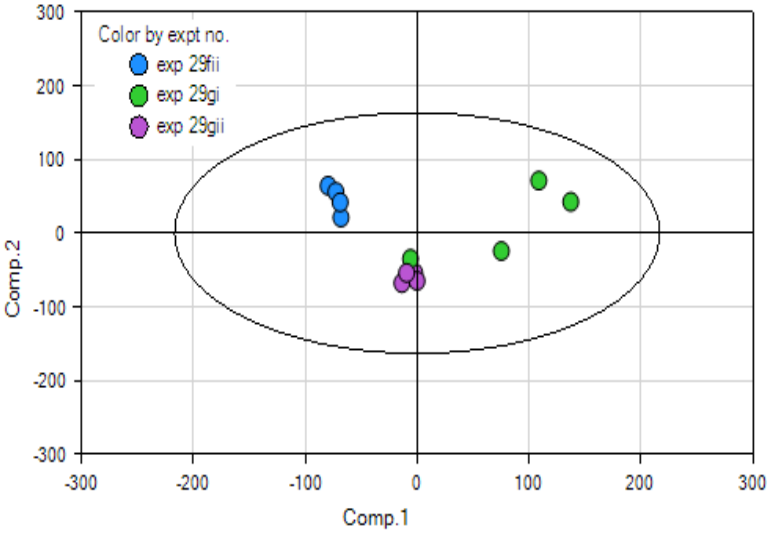


Figure 5-9: Principal component analysis of individual experiments. The PCA for co-cultured fibroblast cells with relevant treatments. The experiment was conducted in the epithelial monolayer model i.e. 29fi, 29gii and 29giii. Experiments were conducted in triplicate. n=3 independent biological experiments.

5.4.2.4 Comparison of gene expression for fibroblasts cells using Venn diagrams

Venn diagrams were used to identify differentially expressed genes in both conditions such as bleomycin and scratch injury in co-cultured fibroblasts i.e. differential expressed genes in fibroblasts in response to the different injuries. (Figure 5-10).

The results revealed that comparing fibroblast cells (bleomycin vs no-injury), 885 genes were changed (p<0.05), whilst for fibroblasts cells (scratch-wounding vs no-injury) 400 were changed (p<0.05). The number of probes sets with p<0.05 in both injuries were 144 genes. From the 144 probes sets, a list of top 25 genes was presented in Table 5-3.

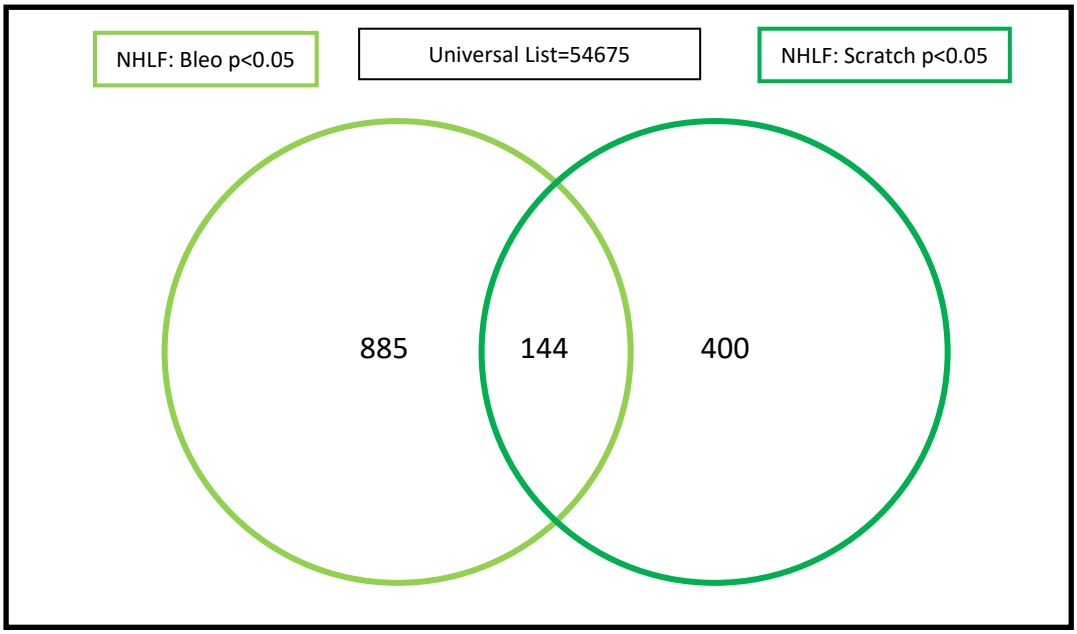


Figure 5-10: **Venn diagram outlining differential expressed genes in fibroblasts.** The genes after bleomycin and scratch treatment on co-cultured fibroblasts. The diagram shows that there were 144 genes, which are present in both injuries ($p<0.05$).

Table 5-3: The top 25 genes expressed in both bleomycin and scratch injuries in co-cultured fibroblasts. The probe sets indicate genes, which are altered by bleomycin and scratch wound in co-cultured fibroblasts. A criteria was used fold change >2 with a p<0.05 (Bleomycin vs no-injury).

Probe set	Gene symbol	Gene title	Bleo fold change	Bleo p<0.05	Scratch fold change	Scratch p<0.05
210387_at	HIST1H2BG	histone cluster 1, H2bg	21.5	0.012	3.17	0.2301
210670_at	PPY	pancreatic polypeptide	7.76	0.0347	1.15	0.8569
230608_at	C1orf182	chromosome 1 open reading frame 182	5.70	0.0208	1.77	0.3474
205157_s_at	KRT17	keratin 17	4.76	0.0154	1.05	0.9248
227204_at	PARD6G	par-6 partitioning defective 6 homolog gamma (C. elegans)	4.44	0.0179	1.74	0.2765
232035_at	HIST1H4H	histone cluster 1, H4h	4.07	0.0323	1.36	0.5667
239787_at	KCTD4	potassium channel tetramerisation domain containing 4	4.06	0.0203	2.33	0.1079
237737_at	LOC100289026	similar to hCG1744891	3.93	0.026	1.11	0.8281
207156_at	HIST1H2AG	histone cluster 1, H2ag	3.90	0.0182	1.58	0.3191
206110_at	HIST1H3H	histone cluster 1, H3h	3.75	0.0461	-1.03	0.9522
244214_at	PELI3	Pellino homolog 3 (Drosophila)	3.38	0.0368	1.84	0.2281
228575_at	IL20RB	interleukin 20 receptor beta	3.25	0.0483	2.33	0.1256
208180_s_at	HIST1H4H	histone cluster 1, H4h	3.05	0.0459	1.33	0.5491
204426_at	TMED2	transmembrane emp24 domain trafficking protein 2	3.04	0.0205	1.48	0.3151
208579_x_at	H2BFS	H2B histone family, member S	3.01	0.0299	1.20	0.6501
236076_at	LOC257396	hypothetical protein LOC257396	3.01	0.0474	1.63	0.3142
209911_x_at	HIST1H2BD	histone cluster 1, H2bd	3.00	0.0488	1.21	0.6812
207386_at	CYP7B1	cytochrome P450, family 7, subfamily B, polypeptide 1	2.92	0.0494	-1.17	0.7246
214481_at	HIST1H2AM	histone cluster 1, H2am	2.90	0.0088	-1.06	0.8307
1559252_a_at	C20orf29	Chromosome 20 open reading frame 29	2.82	0.027	2.36	0.0529
222067_x_at	HIST1H2BD	histone cluster 1, H2bd	2.75	0.0455	1.16	0.7196
205232_s_at	PAFAH2	platelet-activating factor acetylhydrolase 2	2.74	0.0339	1.05	0.8942
238575_at	OSBPL6	oxysterol binding protein-like 6	2.62	0.0359	1.59	0.2416
208490_x_at	HIST1H2BF	histone cluster 1, H2bf	2.57	0.0015	1.16	0.4124
216482_x_at	ZNF79	zinc finger protein 79	2.53	0.0146	-1.17	0.5834

5.4.2.5 Additional Gene selection

The top 25 genes, selected on the basis of fold change and p-value, whose expression was altered by both bleomycin and scratch injuries in epithelial cells (Table 5-2) or co-cultured fibroblasts (Table 5-3) did not have a known association with IPF. Although they may play a role in the disease, and would be interesting targets for future work, we were keen to validate our model using genes previously identified as having a role in IPF in order that the model could be used to further study these pathways. For this reason, a further selection of genes was made, based on their known biological function and whether they had previously been identified as potentially playing a role in pulmonary fibrosis (Table 5-4).

Table 5-4: Selection of genes based on the role they play in IPF

Probe set	Gene symbol	Gene title	Bleo fold change	Bleo p-value	Scratch fold change	Scratch p-value
229852_at	NMNAT1	nicotinamide nucleotide adenylyltransferase 1	1.62	0.01	1.74	0.01
218195_at	C6orf211	chromosome 6 open reading frame 211	1.59	0.00	1.31	0.01
226648_at	HIF1AN	hypoxia inducible factor 1, alpha subunit inhibitor	1.53	0.00	2.16	0.00
222802_at	ECN1	Endothelin 1	-1.14	0.52	1.20	0.38

5.4.3 Hierarchical clustering and Differential signature expression

In this chapter, hierarchical clustering was used to demonstrate patterns of expression between treatments for epithelial cells and co-cultured fibroblasts. Individual genes or number of genes were not identified in the hierarchical clustering. This was to compare the signature expression between treatments for each cell type. These data were of two cell types at 6 days after various treatments.

The signature expression of data was based on 7 groups, (Figure 5-11). The biological experiments were performed independently and in triplicate. The groups were: A) fibroblasts (NHLFs) in collagen (no addition of epithelial cells), B) no-injury (fibroblasts in 3D co-culture with 'no' addition of injury), C) Scratch (fibroblasts in 3D co-culture with epithelial cells-scratch injury), D) bleomycin (fibroblasts in 3D co-culture with addition of epithelial cells-bleomycin injury), (refer to section 2.4.2). Monolayer of epithelial cells with no addition of fibroblasts; E) epithelial cells with no-injury, F) epithelial cells with scratch injury and G) epithelial cells with the addition of bleomycin.

The data were presented as a ratio of the mean of the average intensities from all treatments for each condition. Gene expression levels were present at higher levels in the treated group (increased) and are shown in progressively brighter shades of red. Depending on the level of expression, genes expressed at lower levels were shown as brighter shades of green. Genes shown in black represented no change in gene expression between the individual grouped treatments. The data revealed epithelial cells, which had been treated with bleomycin had shown an increased expression as compared to epithelial cell only (non-treated cells) and epithelial cells inflicted with scratch injury (Figure 5-11).

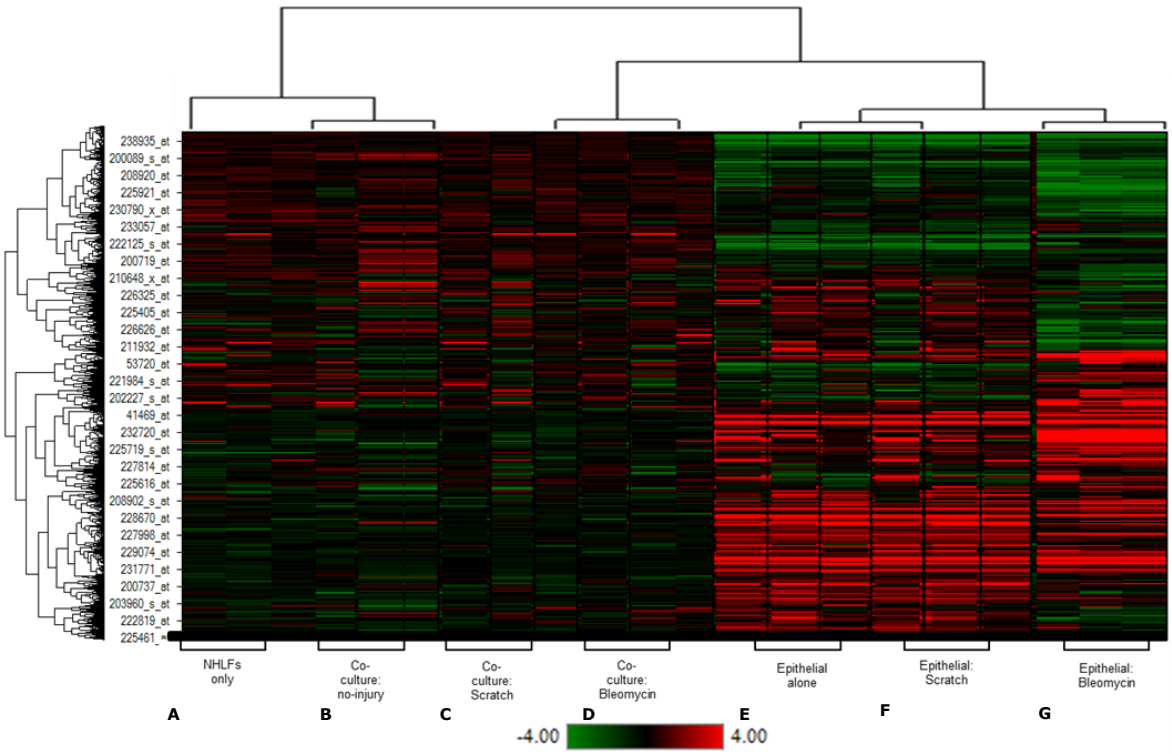


Figure 5-11: Hierarchical clustering of the differentially expressed genes in both cell types. Hierarchical clustering was performed using highly differentially expressed transcripts for epithelial cells and fibroblast cells. For each treatment, all transcripts with a statistically significant expression change were identified (adjusted $p<0.05$). The conditions were grouped by independent biological experiments (n=3 represented by the columns). The conditions were; A) NHLFs only also known as fibroblasts (no addition of epithelial cells), B) no-injury (fibroblasts in 3D co-culture with 'no' addition of injury), C) Scratch (fibroblasts in 3D co-culture with epithelial cells- scratch injury), D) bleomycin (fibroblasts in 3D co-culture with addition of epithelial cells- bleomycin injury), (refer to section 2.4.2). Monolayer of epithelial with no addition of fibroblasts; E) epithelial cells with no-injury, F) epithelial cells with scratch injury and G; epithelial cells with the addition of bleomycin. This shows that epithelial cells with the addition of bleomycin (G) expressed a high signature compared to the co-cultured fibroblasts treated with bleomycin (D). Hierarchical clustering is based is experiments conducted in triplicate. n=3 independent biological experiments.

5.4.4 Pathways involved in epithelial cells and fibroblasts

Ingenuity Pathway Analysis (IPA) software was used to determine the biological pathways and/or canonical signalling pathways, which may be involved in pulmonary fibrosis in conjunction with the gene expression from the microarray database. According to IPA, gene expression was ranked for each treatment and each cell type according to the *p*-value (*p<0.05)* and differential gene analysis. The biological processes that were significantly altered for both epithelial and fibroblast cells were related to the inflammation pathway.

The gene changes in the epithelial cells treated with bleomycin were analysed by IPA. IPA network analysis generated four well-known canonical pathways relating to the mechanism of pulmonary fibrosis, which included IL-6 signalling, TGF-β signalling, Interferon signalling and WNT- β-catenin signalling. The IPA further analysed the upstream regulators in the fibroblast cells treated with bleomycin gene set and identified that the IFN pathway matched the gene set of both cell types. The IFN pathway was common with gene sets of upstream regulators (Figure 5-12). Table 5-5, explains the function of the epithelial mediators involved in the IFN pathway.

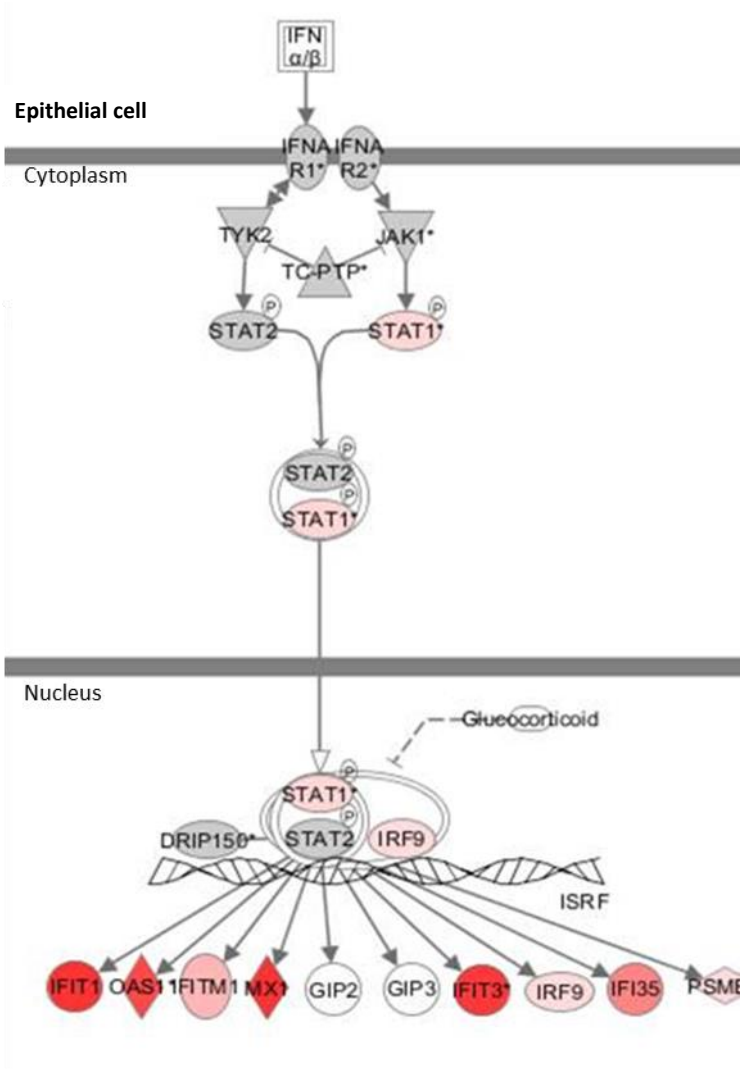


Figure 5-12: Interferon α/β Pathway in epithelial cells. The IFN α/β signalling pathway was predicted by the IPA. This was based on the epithelial cells treated with bleomycin. The pathway also shows the relevant mediators highlighted, which have been upregulated (in red).

Table 5-5: **Function of IFN α/β pathway gene altered in epithelial response to bleomycin which was upregulated (UR).**

Epithelial mediators in IFN pathway		**Function**
IFIT1 (ISG56 or P56)	UR	May inhibit viral replication and translational initiation (Fensterl and Sen 2011).
OAS1	UR	OAS1 codes for a component of the type I interferon signalling system: 2'–5' oligoadenylate synthetase (OAS) pathway of RNaseL-mediated RNA degradation. OAS enzymes catalyze the synthesis of 2'–5'-linked oligoadenylates (2–5A) from ATP, which can then bind and activate latent RNaseL resulting in the degradation of host and viral RNAs (Melchjorsen, Kristiansen et al. 2009) and (Sadler and Williams 2008).
FITM1	UR	IFITM1 can control cell proliferation. The role of IFITM1 in cell cycle progression was further studied. It is known that tumour suppressor p53 plays a pivotal role in the regulation of cell growth arrest, and mutation in p53 and inactivation of p53 through interactions with viral or cellular. Proteins are the most frequent alterations observed in tumour cells (Levine, 1997) and (Yang, Xu et al. 2007).
MX1	UR	The Mx proteins belong to the dynamin family and inhibit the replication of some RNA viruses by binding to viral ribonucleoprotein structures and preventing transcription of viral RNA or movement of viral sub particles within the cell (de Veer, Holko et al. 2001).
IFIT3	UR	Expression of IFIT3 expands acidic endolysosomal compartments and prevents fusion of endocytosed viruses, leading to their degradation. (Chesarino, McMichael et al. 2014)
IRF9	UR	Inhibits the antiproliferative activity if IFN-α among the intracellular JAK-STAT pathway factors. (Tsuno, Mejido et al. 2009).
IFI35	UR	IFI35 is a 35kDa protein. The interaction of IFI35 with Nmi (N-myc-interactor) prevents IFI35 from proteasomal degradation (Das, Dinh et al. 2014).

The interferon pathway was ranked the strongest pathway from upstream regulators in the canonical signalling pathways analysis from bleomycin epithelial differential gene expression. The IPA also identified up-stream regulators of the co-cultured fibroblasts treated with bleomycin, which connected both data sets to the IFN α/β pathway (Figure 5-13). Table 5-6 explains the function of the fibroblast mediators and how they may be involved in the IFN pathway.

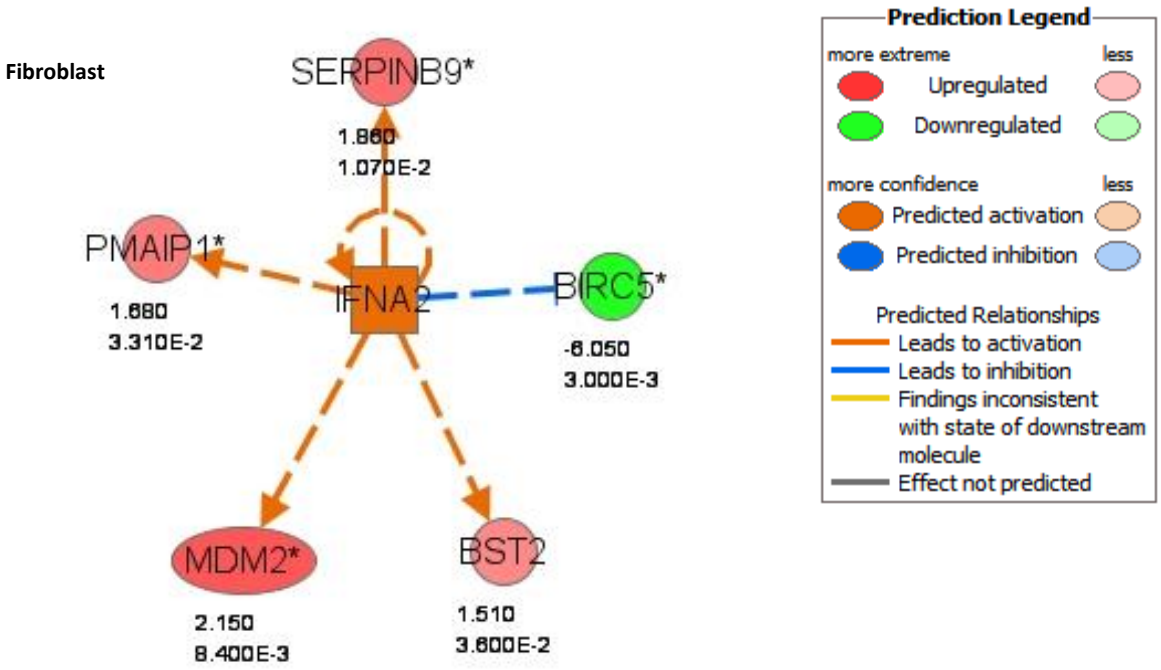


Figure 5-13: Fibroblasts treated bleomycin Upstream Mediators. Analysis identified that IFN pathway corresponded to both genes sets for both cell types. These are genes which are up-regulated and down-regulated in the IFN pathway.

Table 5-6: **Function of mediators involved in fibroblasts which may be contribute in IFN α/β pathway** (upregulated (UR) and down-regulators (DR)

Fibroblast mediators in IFN pathway		**Function**
SERPIN B9 (Sb9) (may regulatory a protein involved in fibrosis?)	UR	Serpin B9 is a protein that in humans is encoded by the *SERPINB9* gene. PI9 belongs to the large superfamily of serine proteinase inhibitors (serpins), which bind to and inactivate serine proteinases. These interactions are involved in many cellular processes, including coagulation, fibrinolysis, complement fixation, matrix remodelling, and apoptosis. SerpinB9 required for natural host defence in the lung, particularly against bacterial and viral pathogens requiring cell contact mediated killing by the immune system (Askew and Silverman 2008). Known to protect from apoptosis.
PMAIP1 (Phorbol-12-Myristate-13-Acetate-Induced Protein) Protein Noxa	UR	Promotes activation of caspases and apoptosis. Promotes mitochondrial membrane changes and efflux of apoptogenic proteins from the mitochondria. Contributes to p53/TP53-dependent apoptosis after radiation exposure (Genecard). NOXA regulated by P53 to inducing apoptosis(Kamp 2009).
BIRC5 (Survivin)	DR	ET-1 regulates myofibroblasts survival, in which increases the expressing surviving, a member of the inhibitor of apoptosis protein (IAP) family (Horowitz, Ajayi et al. 2012). Also known to accelerate cell proliferation as well as inhibit the caspase-dependent apoptotic pathways (Ungvari, Hadadi et al. 2012).
Mdm2	UR	Mdm2 cellular regulator of p53. Functions as a E3 ubiquitin ligase mediates the ubiquitination of nuclear and cytoplasmic p53 and induce the degradation of p53 protein. Mdm2 inhibits the apoptotic function of p53 mainly by targeting it for degradation (Nakashima, Kuwano et al. 2005).
BST2 (Tetherin)	UR	Bone marrow stromal cell antigen is a transmembrane that prevents virus release from infected cells (Swiecki, Wang et al. 2012). BST2 regulation can contribute to the downstream of apoptosis induction and cell proliferation (Sayeed, Luciani-Torres et al. 2013).

5.4.5 Validation of house-keeping genes via Quantitative RT-PCR

Quantitative RT-PCR analysis was used to confirm the changes in gene expression of a select number of genes. The microarray data were normalised to house-keeping genes, *β-actin* and *GAP-DH*. This was to determine, whether there was no difference due to sampling or differences in total RNA quality and quantity. A number of house-keeping genes were validated on the different sets of experiments for both epithelial and fibroblasts cells. The house keeping genes were optimised as previously (refer to section 5.3.6.2).

House-keeping genes used were *β-actin*, *Human* β_2 microglobulin (*B2M)*, *18S rRNA* and *GAP-DH* (Sigma, UK). cDNAs were generated from co-cultured fibroblasts, which had been subjected to epithelial injury such as scratch and bleomycin. Statistical analysis was performed using one-way ANOVA followed by Tukey's post-hoc test. Experiment was conducted in triplicate. n=3 independent experiments (refer to section 5.3.7).

The results showed that *β-actin* and *GAP-DH* had a very similar trend within the treatments in the samples (Figure 5-14). This determined that *β-actin* and *GAP-DH* were expressed at a constant level across the samples and that their expression did not vary in response to the experimental manipulation. However, an observation was seen that the bleomycin gene expression was much lower compared to the other injuries for all housekeeping genes. A further experiment was conducted to determine whether bleomycin had a direct effect on fibroblasts (refer to section 3.4.8). Bleomycin did not have an effect on the fibroblasts gene expression. Therefore, it would seem that the epithelial cells, which were inflicted with the administration of bleomycin in the 3D co-culture model, may have an effect on the fibroblasts through crosstalk interaction (This is discussed in section 5.5).

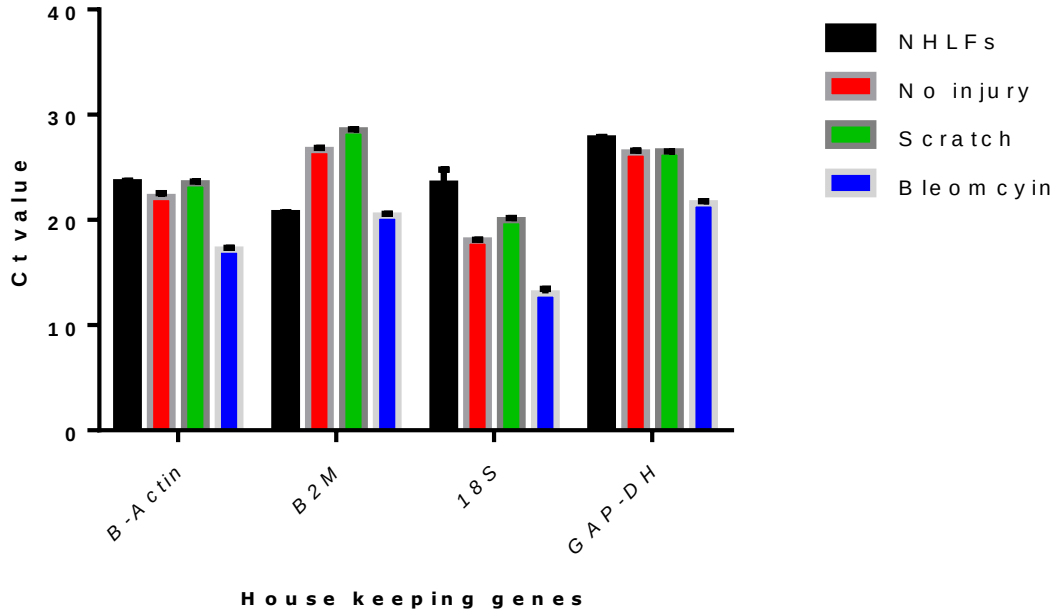


Figure 5-14: Gene expression of house-keeping genes by quantitative RT-PCR analysis of the fibroblasts in 3D co-culture model. *β-actin*, *B2M*, *18S rRNA* and *GAP-DH* were all used to determine whether expression varied in response to experimental manipulation with RT-PCR. Statistical analysis was performed using GraphPad Prism version 6.0. One-way ANOVA was performed for each data set. Experiments were conducted in triplicate. n=3 independent biological experiments.

The epithelial samples including no-injury, scratch and bleomycin in the monolayer model were also used to determine whether the expression of the different sets of house-keeping genes on the samples would differ. The experiment was conducted in triplicate for the epithelial cells (Figure 5-15). The results revealed that the housekeeping genes: β-*actin* and *GAP-DH* expression determined there was a very similar trend within the treatments. This showed that house-keeping genes were consistent for both cell types. Statistical analysis was performed using one-way ANOVA followed by Tukey's post-hoc test. The experiment was conducted in triplicate. n=3 independent experiments (refer to section 5.3.7).

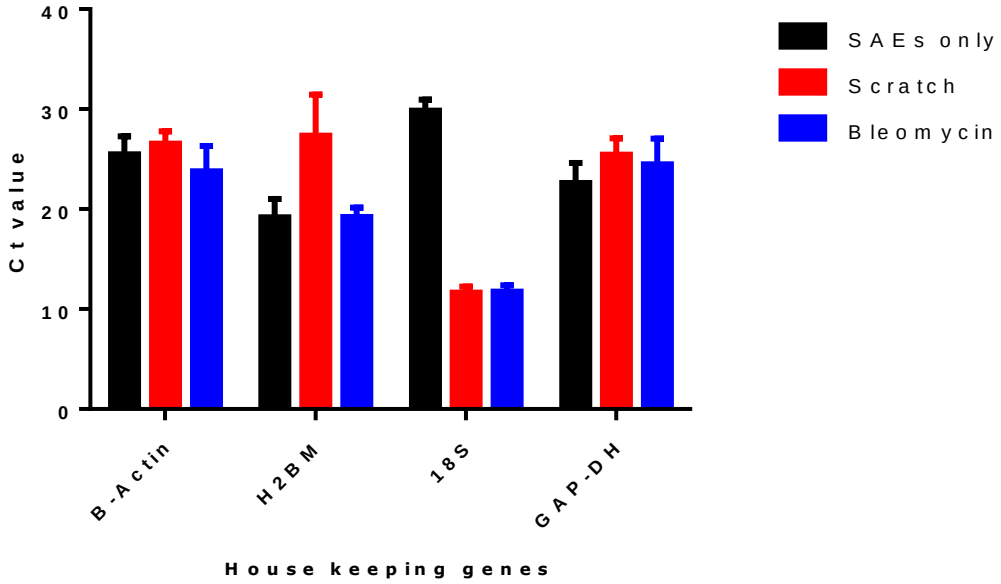


Figure 5-15: Gene expression of house-keeping genes by quantitative RT-PCR analysis in epithelial cells only. *β-actin, B2M, 18S rRNA and GAP-DH* were all used to determine whether expression varied in response to experimental manipulation with RT-PCR. Statistical analysis was performed using GraphPad Prism version 6.0. One-way ANOVA was performed for each data set. Experiments were conducted in triplicate. n=3 independent biological experiments.

5.4.6 Validation of the gene dataset

To validate the microarray expression, the two most up and down regulated genes were chosen from the microarray gene dataset. The genes were selected from co-cultured fibroblasts based on bleomycin vs no-injury (Table 5-7) and were subjected to quantitative RT-PCR analysis.

Table 5-7: Microarray data for genes selected for validation.

Gene	Fold-change	p-value
Histone cluster 1 Probe set id: 210387	21.5	0.01
Chemokine ligand 5 (CCL5) Probe set id:	5.61	0.06
Fibrillin 2 Probe set id: 215717	-4.44	0.27
SMAD7 Probe set id: 204790	-3.38	0.03

The qRT-PCR analysis revealed that genes *Histone* and *CCL5* were up-regulated in the co-cultured fibroblasts (bleomycin v no-injury), (Figure 5-16; A) with house-keeping gene β-actin. The same trend was seen with using the housekeeping gene *GAP-DH* (Figure 5-16; B). The gene expression for the selected genes confirmed the microarray dataset.

Statistical analysis was performed using one-way ANOVA followed by Tukey's post-hoc test. Experiments were conducted in triplicate, n=3 independent experiments (refer to section 5.3.7). The fold change and p-value was calculated for each gene. The analysis revealed that for *histone* the fold change was 15.3 when normalised to *β-actin*, compared to normalised *GAP-DH*, the fold change was 17.1. Gene expression of *CCL5* revealed a fold change of 1.5 when normalised to *β-actin* (Table 5-7). As compared to normalised *GAP-DH*, there was a fold change of 1.8 (Table 5-8). Overall, the results for two housekeeping genes were constant.

The analysis revealed for fibrillin *2* and *SMAD 7*, these genes were down-regulated. (Figure 5-16). Statistical analysis revealed for *fibrillin* the fold change was 1.6 when normalised to *β-actin* as compared to normalised with *GAP-DH* the fold change was 8.63 (Table 5-8). The fold change for *SMAD7* was 0.59 when normalised β-actin as compared *GAP-DH*, the fold change was 3.62 (Table 5-9).

In summary, to validate the microarray expression in the microarray dataset, the two most up and down regulated genes were chosen from the microarray gene dataset. The genes were selected from the co-cultured fibroblasts based on bleomycin vs no-injury. The analysis revealed that there was the same trend of gene expression compared to the microarray dataset.

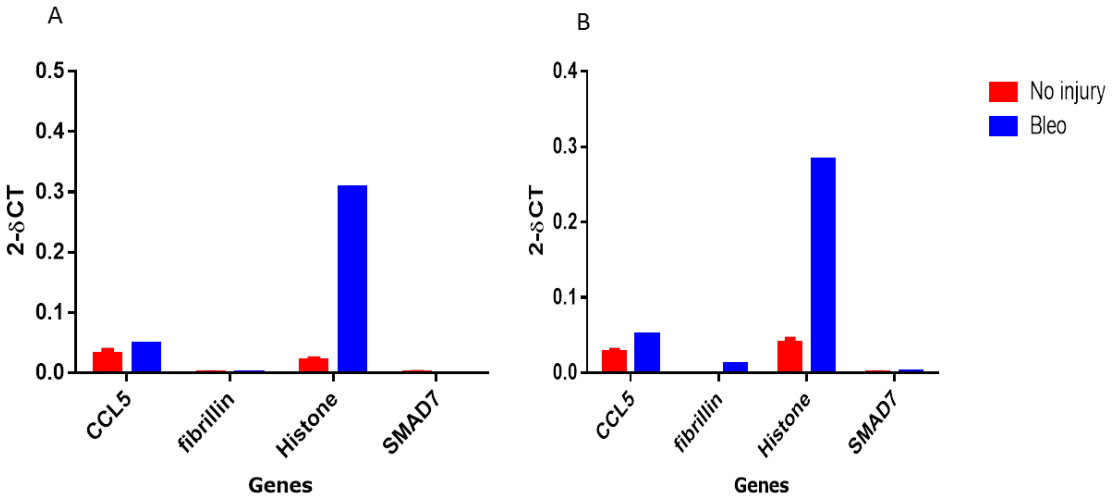


Figure 5-16: The expression of selected genes from the co-cultured fibroblasts from the microarray database analysed by RT-PCR analysis. This was to validate selected genes in the co-cultured fibroblasts (bleomycin vs no-injury) with two house-keeping genes. (A) *β-actin* was used to normalise data. (B) *GAP-DH* was used to normalise data. Statistical analysis was performed using GraphPad Prism version 6.0. One-way ANOVA was performed. Experiments were conducted in triplicate. n=3 independent biological experiments.

Table 5-8: 2-δCt values of the primers with house-keeping gene *β-actin*. The statistical analysis was performed using t-test to determine p-value.

Primers	No-injury (n=3)	Bleomycin (n=3)	Fold change	p-value
Histone	0.0201	0.3069	15.295	0.02
CCL5	0.0301	0.0474	1.577	0.01
Fibrillin 2	0.0004	0.0007	1.666	0.62
SMAD7	0.0006	0.0004	0.593	0.07

Table 5-9: 2-δCt values of the primers with house-keeping gene *GAP-DH* The statistical analysis was performed using t-test to determine p-value.

Primers	No-injury (n=3)	Bleomycin (n=3)	Fold change	p-value
Histone	0.0393	0.2826	17.184	0.02
CCL5	0.027	0.0501	1.860	0.14
Fibrillin 2	0.0003	0.0026	8.633	0.33
SMAD7	0.0004	0.0013	3.624	0.03

5.5 Discussion

The aim of the work described in this chapter was; 1) examine different gene expression 'signatures', in scratch and bleomycin treated cells in monolayer culture consisting of epithelial cells alone and 3D co-culture model consisting of cultured fibroblast cells in collagen exposed to injured epithelial cells. 2) To identify candidate genes which may play a role in the pathogenesis of fibrosis as well as to provide an insight regarding the divergent pathways involved in lung fibrosis.

Microarray analysis was performed on epithelial cells in the monolayer culture and co-cultured fibroblasts exposed to epithelial injury, a scratch wound and administration of bleomycin over 6 days. Analysis of microarray data were performed in Array Studio software and the data were normalised with two house-keeping genes *β-actin* and *GAP-DH*. The data were analysed within groups for each model i.e. 3D co-culture model: NHLFs vs no-injury, scratch vs no-injury and bleomycin vs no-injury. For the epithelial cells (no fibroblasts) i.e. scratch vs no-injury and bleomycin vs no-injury. The grouping of the data was to compare the treatments closely with differentially expressed genes for each cell type and specific treatment.

The Principal Component Analysis of the epithelial cells alone and the co-cultured fibroblasts were performed to identify the principal direction of the data (Figure 5-3). The data were grouped according to each experiment batch and specific effect of treatment for each cell type. The data for the epithelial cells alone showed, the individual treatments were within parameters in PCA. However, only bleomycin treated epithelial cells were clustered together. This suggested that the epithelial cells, exposed to bleomycin had a positive correlation within the experiments as compared to scratch injury, which showed no variance.

The PCA for co-cultured fibroblasts revealed the experiments were grouped together and showed a positive correlation within each experiment batch (Figure 5-4). However, the expression of individual treatments had a variable direction revealing that it was not consistent between the treatments. The PCA revealed the experiments were grouped together and showed a positive correlation within each experiment

batch. The PCA for epithelial cells in the monolayer culture and co-cultured fibroblasts revealed that the treatments varied in PCA direction. However, for epithelial cells the PCA showed that only bleomycin treatment had a positive correlation. This may have contributed to the bleomycin vs no-injury gene expression signature in the IPA.

Hierarchical clustering was based on the PCA for both cell types taking into consideration the differential gene expression for the individual treatments. The hierarchical clustering heat map showed that the epithelial cells treated with bleomycin revealed a stronger gene signature compared to co-cultured fibroblasts exposed to epithelial cells treated with bleomycin (Figure 5-11). This supported the PCA for the epithelial cells treated with bleomycin. To further analyse the genes expressed in the injuries, Venn diagrams were used to identify genes common to both injuries (scratch vs bleomycin).

Venn diagrams revealed that for epithelial cells scratch vs bleomycin ($p<0.05$), 226 genes were common to both injuries (Figure 5-7). Three genes were selected based on the expression in both injuries in epithelial cells and which may have some relevance to the disease pulmonary fibrosis. Many of the genes which displayed the criteria with a $p<0.05$ (Table 5-2), were not known to play a role in pulmonary fibrosis. From the list of top 25 genes only two genes; *C/EBP and KRT*, were found to play a role in pulmonary fibrosis. Therefore, the gene selection criteria of the 226 common to both injuries were expanded and endothelin -1 was chosen based on the relevant literature found and the role the gene played in pulmonary fibrosis (Table 5-4).

CCAAT/enhancer binding protein (*C/EBP*), alpha (CEBPA), CEBP-α transcriptional factor, which regulates differentiation and proliferation in the epithelium (Berg, Didon et al. 2006) and *CEBP*α mainly detected in epithelium and *CEBP*β in mesenchyme (Sato, Xu et al. 2012). Endothelin–1 (ET-1) released by epithelial cells and induce fibroblast proliferation and ECM synthesis (Boscoe, Goodwin et al. 2000). Keratin (KRT) is a known surface marker for epithelial cells, which can give rise to regenerative epithelial cells in response to lung injury (Willis, Liebler et al. 2005).

Fibroblasts differentially expressed 144 genes common to both injuries. Three genes were selected, which were common in both injuries (Table 5-3). These were nicotinamide nucleotide adenylyl transferase 1 (*NMNAT1*), Chromosome 6 open reading frame 211 (C6orf211) and Hypoxia inducible factor 1, alpha subunit inhibitor (HIF-1α), (Table 5-4).

NMNAT-1 is a central facilitator of redox reactions in the mitochondrial electron transport chain, which influences many cellular processes such as the cell cycle, and catalyses the formation of the essential cofactor nicotinamide adenine dinucleotide (NAD). Over-expression of *NMNAT-1* has been shown to extend the lifespan of cells. NMNAT-1 in HeLa cells modulates the behaviour of poly(ADPribosyl)ation protein 1 (PARP1) an enzyme essential in processes such as DNA repair and programmed cell death. This association of NMNAT-1 with activated PARP1 can also enhance the relocation of apoptosis inducing factor (AIF) from the mitochondria to the nucleus, thereby triggering apoptosis (Emblom-Callahan, Chhina et al. 2010). Chromosome 6 open reading frame 211 (C6orf211), had been associated with a proliferation metagene in tumours (Dunbier, Anderson et al. 2011). Hypoxia inducible factor 1, alpha subunit inhibitor (HIF-1α), a transcription factor that functions as a master regulator of oxygen homeostasis, has been implicated in fibrinogenesis (Ueno, Maeno et al. 2011).

To further analyse the differentially expressed genes in the epithelial cells and co-cultured fibroblasts, pathway analysis was performed on both cell types using Ingenuity Pathway Analysis (IPA). The analysis revealed that there was a stronger gene signature in the epithelial cells exposed to bleomycin. The epithelial cells treated with bleomycin revealed, the IFN pathway upregulated genes in the Ingenuity Pathway Analysis, *IFNA2, IRF7, IFNG, IFNL1, STAT1, IRF3, IRF1, IRF5, IFNA1* and *IFNA13*. For the fibroblasts, genes expressed were *SERPINB9, PMAIP1, MDM2*, *BST2* and *BIRC5*,which are downstream of *IFNA2* gene. The IFNA2 gene was strongly upregulated by epithelial cells exposed to bleomycin. The expression was driven by these epithelial cells to mediate gene expression in the co-cultured fibroblasts.

The Canonical Pathway Analysis in epithelial cells exposed to bleomycin revealed three top pathways, IL-6 signalling pathway, TGF-β pathway and interferon pathway. Co-cultured fibroblasts exposed to epithelial cells treated with bleomycin in the 3D co-culture were analysed using IPA. The upstream regulator analysis was performed and revealed activation of the interferon α/β pathway was compatible with epithelial cells exposed to bleomycin (Figure 5-12).

The microarray dataset was validated with quantitative RT-PCR analysis. Housekeeping genes *β-actin* and *GAP-DH* were used to normalise the microarray dataset (Section 5.4.5). Gene selection was chosen from the microarray dataset to determine any differences in sampling or differences in total RNA quality. A number of house-keeping genes were validated on both epithelial cells and co-cultured fibroblast cDNAs. Quantitative RT-PCR analysis confirmed that *β-actin* and *GAP-DH* revealed a similar trend within the treatments for co-cultured fibroblasts. This determined that *β-actin* and *GAP-DH* were expressed at a constant level within samples and that their expression did not vary in response to the different treatments. The quantitative real-time PCR on epithelial cells including various treatments of no-injury, scratch and bleomycin showed that *β-actin* and *GAP-DH* also had very similar trend within the treatments. The analysis revealed that these house-keeping genes were consistent for both cell types.

Array Studio gene expression analysis was validated using quantitative real-time PCR. A selection of up and down regulated genes were chosen from the microarray dataset and validated. These genes were chosen from co-cultured fibroblasts cDNAs, (bleomycin vs no-injury). The analysis revealed that *Histone* and *CCL5* were up-regulated in the co-cultured fibroblasts (bleomycin vs no-injury), whereas down regulated genes *fibrillin 2* and *SMAD 7* in the microarray data revealed that both genes were expressed at lower levels in the co-cultured fibroblasts. Overall, the results for all four genes compared with *β-actin* and *GAP-DH*, revealed the same trend in expression as shown in the microarray dataset for co-cultured fibroblasts (bleomycin vs no-injury).

The validation of the microarray dataset provides a useful insight in predicting genes and potential pathways, which may prove valuable in predicting the pathogenesis of IPF. Validating the microarray dataset gives support and confidence on the value of gene expression analysis, which has been shown to have the ability to identify new genes. In particular, gene expression has revealed that both epithelial cells and fibroblasts are involved with the IFN α/β pathway, which may be involved in mediating the inflammatory response.

The role of inflammation in the pathogenesis of IPF is controversial (Coward, Saini et al. 2010). Studies have shown that injury activates multiple inflammatory, cell signalling, and repair pathways. Activation of these cascades causes an imbalance in pro- and antifibrotic mediators. Inflammatory mediators activate multiple cell types, causing changes in cellular functioning and cell–cell interactions that ultimately result in progressive fibrosis (Maher, Wells et al. 2007). The concept of inflammation is still an evolving process as different inflammatory cell types contribute to tissue destruction and repair. Furthermore, the host's inflammatory response is determined by the concept of the initiating injury, the origin of, which remains elusive in IPF.

5.6 Summary

In summary, gene expression profiling has proven to be a useful tool for the identification of specific gene patterns. In particular, the bleomycin-mediated gene expression changes in epithelial cells only, which promote the IFN α/β pathway, have an influence on the pro or anti-fibrotic effect on fibroblasts. As the model only consisted of two cell types, epithelial cells and fibroblasts, the concept of epithelial-mesenchymal interaction may be demonstrated *in vitro*. This is a unique way to identify molecular signatures and may provide a useful understanding in this complex lung disease, without the need for animal models and lung biopsies.

Chapter Six

Candidate genes in the epithelial-mesenchymal crosstalk in the 3D co-culture model

6.1 Introduction

Idiopathic Pulmonary Fibrosis (IPF) is a poorly understood disease with an unknown aetiology. Previous studies have used advanced molecular biology approaches, such as genetically modified animals, and high-throughput transcriptional profiling approaches to provide evidence of multiple pathways, growth factors/cytokines, and systems that may be involved in fibrosis (Studer and Kaminski 2007). High-throughput technologies for gene and protein expression are becoming a popular method to simultaneously study thousands of genes; i.e. protein expression patterns between different treatments, as well as different models of disease (Kaminski and Rosas 2006). In particular, there have been many studies that have used microarray analysis to identify molecules, mechanisms, and pathways, which have further added to the understanding of the disease.

Microarray studies in animal models; Kaminski and colleagues showed that integrin β6 subunit gene ($\beta 6^{2/2}$) knockout mice developed inflammation, whilst being protected from pulmonary fibrosis. Transcriptional profiling identified two distinct groups of genes involved in the inflammatory and fibrotic responses; inflammatory cell-related genes, and extracellular matrix genes. Evidence further suggested that increased transcription of inflammatory cell-related genes also induced extracellular matrix gene expression (Kaminski, Allard et al. 2000). A second study used oligonucleotide microarrays to analyse gene expression patterns in bleomycin-induced mice. The data revealed that MMP-7 knock out mice were protected by bleomycin-induced pulmonary fibrosis (Zuo, Kaminski et al. 2002).

Microarray studies of cells isolated from lung; Choi and colleagues examined primary fibroblast lines from Idiopathic Interstitial Pneumonia (IIP) patients, with primary fibroblast lines from surgical lung biopsies (SLBs), to compare chemokine and chemokine receptor expression. Fibroblasts obtained from IIP revealed an increased gene expression of CCL7 compared to SLBs. This method could provide an early diagnostic significance in IIP (Choi, Jakubzick et al. 2004). Renzoni and colleagues analysed gene expression patterns in IPF fibroblasts and normal control fibroblasts in response to TGF-β. The data revealed that there was no substantial

difference between lung fibroblasts from two patterns of fibrotic lung disease and control lung fibroblasts, in the response to TGF-β (Renzoni, Abraham et al. 2004).

Microarray studies of whole human IPF lungs; A study by Selman and colleagues compared transcriptional signatures of IPF, hypersensitivity pneumonitis (HP), and nonspecific interstitial pneumonia (NSIP). The study revealed that IPF was characterised by the expression of genes that indicated tissue remodelling, particularly extracellular matrix genes. HP gene expression signatures were characterised by an inflammatory pattern, indicated by expression of leukocyte/lymphocyte genes, and genes encoding cytokines. In addition, NSIP gene expression did not resemble either IPF or HP gene expression (Selman, Pardo et al. 2006).

Gene expression profiling helps to speed up the understanding of the molecular mechanisms underlying IPF. This technique can identify possible candidate genes, as well as certain pathways that cause IPF, and may offer novel therapeutic targets for IPF.

6.2 Aims

The aim of the work described in this chapter was to validate gene expression signatures from the microarray dataset described in Chapter 5, with the aim of providing insights into the divergent pathways leading to lung fibrosis. We also hypothesised that specific signatures could lead to the identification of new biomarkers to aid in the diagnosis and classification of this disease.

6.3 Methods

6.3.1 Selection of candidate genes from the gene dataset

More than 54,000 transcripts were expressed in fibroblasts and epithelial cells, and a selection was chosen to determine the genes of interest i.e. which ones may have a role in IPF. Initially, the criteria for genes of interest are also known as candidate genes, were based on $p < 0.05$ with a fold change of >2. However, some genes did not match the criteria and were chosen based on their role in IPF (refer to section 6.4.1), with total of 21 genes being selected (refer to Table 6-1 and Table 6-2). The changes in the expression of the candidate genes were validated by using quantitative Real-time PCR.

6.3.2 Validation of selected microarray genes by Quantitative RT-PCR analysis.

The selected genes were validated by using quantitative RT-PCR (refer to section 2.8). Changes in expression of 21 candidate genes (Table 6-1 and Table 6-2) were validated by qRT-PCR. A selection of ECM encoding genes (*Collagen I and III)* and mesenchymal markers *(α-SMA*) was used to demonstrate activation of co-cultured fibroblasts in the model. Expression levels were normalised to the house-keeping genes *β-actin*, *2BM*, *GAP-DH* and *18s* rRNA (Table 6-3).

Table: 6-1 Genes were selected for quantitative RT-PCR for validation from the ingenuity pathway analysis

Primers	Sequence (5' to 3')
The IFN target genes	
1. IFIT1	Forward - CTGCCTAATTTACAGCAACC Reverse - TGATCCAAGACTCTGTTTTC
2. OAS1	Forward - ATTGTAAGAAGCTTGG Reverse - CAGAGTTGCTGGTAGTTTATG
3. IFITM1	Forward - CTACTCCGTGAAGTCTAGG Reverse - ATGAGGATGCCCAGAATC
4. MX1	Forward - CAGGCTTTGTGAATTACAGG Reverse - TCTTCAATTTGGACTTGGC
5. IFIT3	Forward - ATGAGTGAGGTCACCAAG Reverse - CCTTGAATAAGTTCCAGGTG
6. IRF9	Forward - CTCAGAAAGTACCATCAAAGC Reverse - TCATTATTGAGGGAGTCCTG
7. IFI35	Forward - GAAGGCTGAGATCAGGTC Reverse – GAAGTGGATCTCCAGGAC
The Fibroblast Mediators	
8. SERPINB9	Forward - TTGTCAATGCCATCTACTTC Reverse - CCTCCTGGTTTATTTTAAAGGG
9. BIRC5	Forward - CATCTCTACATTCAAGAACTGG Reverse - CCTTGAAGCAGAAGAAACAC
10. BST2	Forward - GGAGAGATCACTACATTAAAC Reverse - CTGGGTAGTACTTCTTGTC
11. MDM2	Forward - CCTTAGCTGACTATTGGAAATG Reverse - TGTTGAGTTTTCCAGTTTGG
12. PMAIP1	Forward - CAGGAGATTTGGAGACAAAC Reverse - CTCATGCAAGTTTTTGATGC

Table: 6-2 Candidate genes were selected from the microarray dataset, for quantitative RT-PCR for validation Criteria; ($p < 0.05$) with a fold change of >2.

Primers	**Sequence (5' to 3')**
Fibroblast overlap up-regulation	
1. NMNAT1	Forward – CATGGAAAATTCCAGAAGAC Reverse - TGTACCTTCCTGTTCCATTC
2. C6ORF211	Forward - GTCCACCAATCGATTACTTTG Reverse - TATCAATTGTTGCAGGTGAG
3. HIFAN	Forward - CTGTGAACTTCTGGTATAAGG Reverse - CTCATTATGGCCACTTTCTG
Epithelial overlap up regulation	
4. CEBP/α	Forward - AGCCTTGTTTGTACTGTATG Reverse - AAAATGGTGGTTTAGCAGAG
5. IL-6	Forward - GCAGAAAAAGGCAAAGAATC Reverse - CTACATTTGCCGAAGAGC
6. MAX	Forward - GAGAGAAGGGAACAAAGATG Reverse - GCAGAAAACAGTTGGAAAAG
7. PLCD1	Forward - AAGAATTCAATTGTGGACCC Reverse - GAGGCATCATAATCTTCCAC
8. GDPD5	Forward - CTTATTTTCTCAGAGATCAGCG Reverse - TGGCATATGTGTCATAACTG
9. EDN1	Forward - CAAGCAGGAAAAGAACTCAG Reverse - CTGGTTTGTCTTAGGTGTTC

Table: 6-3: Primers and house-keeping genes used to validate the candidate genes

Primers	**Sequence (5′ to 3′)**
Col 1A1	Forward – GAACGCGTGTCAATCCCTTGT Reverse - GAACGAGGTAGTCTTTCAGCAACA
Col 3A1	Forward - AACACGCAAGGCTGTGAGACT Reverse - GCCAACGTCCACACCAAATT
α-SMA	Forward - GACAATGGCTCTGGGCTCTGTAA Reverse - ATGCCATGTTCTATCGGGTACTT
Versican	Forward - CAAGCATCCTGTCTCACGAA Reverse - CAACGGAAGTCATGCTCAAA
β-actin	Forward – CCTGGCACCCAGCACAAT Reverse – GGGCCGGACTCGTCATACT
Human 2BM	Forward - TGCTGTCTCCATGTTTGATGTATCT Reverse - TCTCTGCTCCCCACCTCTAAGT
GAP-DH	Forward - GGTCTCCTCTGACTTCAACA Reverse - AGCCAAATTCGTTGTCATAC
18s	Forward - GTAACCCGTTGAACCCATT Reverse - CCATCCAATCGGTAGTAGCG

6.3.3 Quantitative real-time PCR (Q-PCR)

Quantitative real-time PCR (Q-PCR), using the SYBR green method, is a technique allowing the quantitation of gene expression with high specificity and sensitivity (Livak and Schmittgen 2001, Morey, Ryan et al. 2006). This technique was used to validate the selected genes from the microarray dataset (refer to section 2.9.3).

6.3.4 Generation of tissue and tissue processing

IPF and Normal lung tissues were obtained from The Nottingham Health Science Biobank (NHSB), University of Nottingham (Table 6-4). This was approved by the Nottingham Research and Ethics Committee (REC ref: 08/H0407/01). The paraffin embedding and sectioning was performed by Dr Emily Hodge, University of Nottingham.

Table 6-4: Tissue samples obtained from tissue bank

Tissue Sample		
Bronchus	**Normal Lung Tissue**	**IPF tissue**
T501	2004/P72	RS11008
T501	FP01	RS12022
T501	FP02	RS11011

6.3.5 Histology

6.3.5.1 Haematoxylin and eosin (H&E) staining

Haematoxylin and eosin (H&E) staining was used to identify cell structure and organisation of tissue in the IPF tissue sections. Positive control tissue was used initially to optimise the antibodies. The positive control tissues were chosen from the human protein atlas http://www.proteinatlas.org/, for the desired antibody to be optimised.

6.3.5.2 Immunohistochemistry on IPF tissue

Immunohistochemistry is a commonly used technique to investigate cell structure and organisation of tissue. It exploits the basic principles of immunology, i.e. the specific interaction of an antibody with its antigen, to allow the visualisation of specific cell or tissue constituents. Antibodies used for the immunohistochemistry along with a selection of dilutions required for the staining (Table 6-5). All immunohistochemistry conducted in studies reported in this thesis utilised the immunoperoxidase method of staining (refer to section 2.11).

Table 6-5: Antibodies used for immunohistochemistry experiments and dilutions

Antibodies	Supplier and code	Dilution
Anti CEBP-Alpha (raised in Mouse)	Abcam – ab128482	**1:200** & 1:1000
Anti-Endothelin 1 (raised in Rabbit)	Abcam - 117757	**1:500** & 1:2000
Anti-IRF9 (raised in Rabbit)	Sigma – HPA0001862	**1:50** & 1:200

6.3.6 Determining the expression of Endothelin-1 in the 3D co-culture model

The model was set up as in section 2.4. Different concentrations of the endothelin receptor antagonist, bosentan (Santa Cruz SC210957), were added to observe the effect of endothelin inhibition in epithelial cells (Table 6-6). Reduction assay was carried out as in section 2.6.3, to determine viability of the cells; ELISA was performed as in section 2.5.1, to determine the concentration of soluble EDN-1 in the supernatants and quantitative RT-PCR analysis was performed as in section 2.8.3, to determine the gene expression levels of EDN-1 in fibroblast and epithelial cells.

Table 6-6: Different concentrations of bosentan. The bosentan used in the 3D co-culture model.

Conc of bosentan
10μM
25μM
50μM
75μM
100μM
150μM

6.3.7 Statistical Analysis

Data were analysed using GraphPad Prism 6.0 software (GraphPad Software, Inc.). Continuous data from independent experiments that were considered to follow a normal distribution were displayed as the mean value ± SEM, and their statistical significance was assessed by using one-way ANOVA followed by Tukey's post-hoc test when comparing multiple conditions to a control or two-way ANOVA with the Bonferroni post-hoc test when comparing multiple conditions with one another. The *p* values, which were significant, were shown with asterisks. The asterisks; *** represents $p<0.001$, ** represents $p<0.01$ *and* * represents $p<0.05$. n=3 (refer to section 2.11).

6.4 Results

6.4.1 Gene expression changes measured by using quantitative RT-PCR analysis

Gene expression was quantified by using quantitative RT-PCR analysis to validate the microarray dataset. It was necessary to observe the gene expression at the RNA level between the cells and injuries as it would support the microarray data and show the magnitude of the change in gene expression. Over 54,000 transcripts were expressed in fibroblasts and epithelial cells. To determine the genes of interest / candidate genes, the selection was based on a criteria of $p < 0.05$ with a fold change of >2; however, some genes were selected due to their potential involvement in IPF.

For epithelial cells, the IFN pathway genes were based on the genes that were upregulated in the Ingenuity Pathway Analysis by bleomycin administration only. Epithelial cell candidate genes were chosen based on the expression in both scratch and bleomycin injuries in the microarray dataset (Table 6-7).

In fibroblasts, Ingenuity Pathway Analysis predicted five genes that may have altered expression levels after epithelial injury by bleomycin administration. The candidate genes were selected from the microarray dataset based on gene expression changes in fibroblasts after being cultured with epithelial cells inflicted with scratch and bleomycin injuries (Table 6-7).

The data shown in Table 6-8 represents the data obtained from the microarray gene dataset. The table is grouped into four sections: The IFN pathway genes, which were obtained from the IPA analysis; Epithelial cell gene expressed in both scratch and bleomycin injuries (candidate genes, relevant literature available on their role in IPF); the fibroblast mediators obtained from the IPA; and fibroblasts genes expressed in both scratch and bleomycin injuries (candidate genes, relevant literature available on their role in IPF). The data shows the *p-value* and fold change for the selected genes relevant to the injuries for the individual cell types.

Table 6-7: The selection of genes obtained from the ingenuity pathway and microarray database for epithelial cells and fibroblasts.

Primers	Probe id	Function
The IFN pathway genes (predicted from IPA)		
IFIT1	203153_at	May inhibit viral replication and translational initiation (Fensterl and Sen 2011)
OAS1	202869_at	OAS1 codes for a component of the type I interferon signalling system: 2′–5′ oligoadenylate synthetase (OAS) pathway of RNaseL-mediated RNA degradation. OAS enzymes catalyze the synthesis of 2′–5′-linked oligoadenylates (2–5A) from ATP, which can then bind and activate latent RNaseL resulting in the degradation of host and viral RNAs (Melchjorsen, Kristiansen et al. 2009) and (Sadler and Williams 2008).
IFITM1	214022_s_at	IFITM1 can control cell proliferation. The role of IFITM1 in cell cycle progression was further studied. It is known that tumour suppressor p53 plays a pivotal role in the regulation of cell growth arrest, and mutation in p53 and inactivation of p53 through interactions with viral or cellular. Proteins are the most frequent alterations observed in tumour cells (Bailey, Zhong et al. 2014) and (Yang, Xu et al. 2007).
MX1	202086_at	The Mx proteins belong to the dynamin family and inhibit the replication of some RNA viruses by binding to viral ribonucleoprotein structures and preventing transcription of viral RNA or movement of viral subparticles within the cell (de Veer, Holko et al. 2001)
IFIT3	204747_at	Expression of IFIT3 expands acidic endolysosomal compartments and prevents fusion of endocytosed viruses, leading to their degradation. (Chesarino, McMichael et al. 2014)
IRF9	203882_at	Inhibits the antiproliferative activity if IFN-α among the intracellular JAK-STAT pathway factors. (Tsuno, Mejido et al. 2009).
IFI35	209417_s_at	IFI35 is a 35kDa protein. The interaction of IFI35 with Nmi (N-myc-interactor) prevents IFI35 from proteasomal degradation (Das, Dinh et al. 2014).
Epithelial genes expressed in both scratch and bleomycin (candidate genes)		
CEBPA	204039_at	CEBP-α transcriptional factor which regulates differentiation and proliferation in the epithelium. CEBPα is a strong inhibitor of proliferation and is down regulated in proliferating cells in the normal lung development. CEBPα mainly detected in epithelium and CEBPβ in mesenchymal (Berg, Didon et al. 2006).
IL-6	205207_at	IL-6 may be involved with inflammatory processes in the lung, and its dysregulated release has been implicated in the pathogenesis of a variety of respiratory disorders. IL-6 may mediate persistent inflammation in the fibrotic lung (Saito, Tasaka et al. 2008).
MAX	214108_at	MAX is part of the MYC-MAX heterodimer. Without MAX, the MYC protein is unable to bond sufficiently to DAN and activate transcription. The heterodimer encode cell growth, differentiation and apoptosis (D'Agnano, Valentini et al. 2007).
PLCD1	205125_at	Phospholipase C, delta 1 play a role in signal transduction and it is important in cellular growth, differentiation and transformation (Hwang, Park et al. 1996).
GDPD5	32502_at	Glycerophosphodiester Phosphodiesterase Domain Containing 5 is an enzyme which hydrolyses phosphoric diester bonds ie acts on two substrates and catalyses alcohol and sn-glycerol 3-phosphate. GDPD activity inactivates the Notch activator RECK (reversion-inducing cysteine-rich protein with kazal motifs) by releasing it from the membrane through GPI-anchor cleavage. RECK release disinhibits ADAM (a disintegrin and metalloproteinase) protease-dependent shedding of the Notch ligand Delta-like 1 leading to Notch inactivation (Park, Lee et al. 2013)
EDN1	1564630_at	ET-1 via two receptors ET_A and ET_B induce fibroblast proliferation and ECM synthesis. Antagonist- bosentan which inhibits both receptors (Park, Saleh et al. 1997)

The Fibroblast Mediators (predicted from IPA)		
SERPINB9	209723_at	**Serpin B9** is a protein that in humans is encoded by the *SERPINB9* gene. PI9 belongs to the large superfamily of serine proteinase inhibitors (serpins), which bind to and inactivate serine proteinases. These interactions are involved in many cellular processes, including coagulation, fibrinolysis, complement fixation, matrix remodelling, and apoptosis. SerpinB9 required for natural host defence in the lung, particularly against bacterial and viral pathogens requiring cell contact mediated killing by the immune system (Askew and Silverman 2008). Known to protect from apoptosis.
BIRC5	202094_at	ET-1 regulates myofibroblasts survival, in which increases the expression of a member of the inhibitor of apoptosis protein (IAP) family. (Horowitz, Ajayi et al. 2012).also known to accelerate cell proliferation as well as inhibit the caspase-dependent apoptotic pathways (Ungvari, Hadadi et al. 2012).
BST2	201641_at	Bone marrow stromal cell antigen is a transmembrane that prevents virus release from infected cells (Swiecki, Wang et al. 2012). BST2 regulation can contribute to the downstream of apoptosis induction and cell proliferation (Sayeed, Luciani-Torres et al. 2013).
MDM2	217542_at	Mdm2 cellular regulator of p53. Functions as a E3 ubiquitin ligase mediates the ubiquitination of nuclear and cytoplasmic p53 and induce the degradation of p53 protein. Mdm2 inhibits the apoptotic function of p53 mainly by targeting it for degradation (Nakashima, Kuwano et al. 2005).
PMAIP1	204286_s_at	Promotes activation of caspases and apoptosis. Promotes mitochondrial membrane changes and efflux of apoptogenic proteins from the mitochondria. Contributes to p53/TP53-dependent apoptosis after radiation exposure (Genecard). NOXA regulated by P53 to inducing apoptosis(Kamp 2009).
Fibroblast genes expressed in scratch and bleomycin (injuries inflicted on epithelial cells in 3D co-culture), (candidate genes)		
NMNAT1	229852_at	Plays a central facilitator of redox reactions in the mitcondrial electron transport chain and influences cell cycle, and catalyses the formation of NAD. Over expression of NMNAT1 may extend life span of cells and promote cell survival (Emblom-Callahan, Chhina et al. 2010).
C6ORF211	218195_at	Chromosome 6 Open Reading Frame 211 is a gene that encodes proteins for proliferation and differentiation. C6ORF211, affects proliferation in cultured cells and is correlated with proliferation in breast tumours (Dunbier, Anderson et al. 2011).
HIFAN	226648_at	Hypoxia-inducible factor-1α (HIF-1α), a transcription factor that functions as a master regulator of oxygen homeostasis, has been implicated in fibrinogenesis (Greijer and van der Wall 2004).

Table 6-8: IFN genes and candidate genes which were obtained from the microarray gene database

Primers	Probe id	Bleomycin Fold change	Bleomycin p-value	Scratch Fold change	Scratch p-value
The IFN pathway genes (predicted from IPA)					
IFIT1	203153_at	32.21	0.0063	1.33	0.686
MX1	202086_at	22.12	0.0030	1.68	0.3428
OAS1	202869_at	15.01	0.0312	-1.42	0.6943
IFIT3	204747_at	12.07	0.0372	1.14	0.8823
IFI35	209417_s_at	10.03	0.0032	-1.1	0.8108
IFITM1	214022_s_at	6.02	0.0051	-1.62	0.2074
IRF9	203882_at	2.98	0.0033	1.01	0.9478
Epithelial genes expressed in both scratch and bleomycin - (candidate genes)					
CEBPA	204039_at	10.24	0.0006	2.54	0.0167
PLCD1	205125_at	1.98	0.0004	1.26	0.0205
EDN1	1564630_at	1.52	0.0049	1.3	0.0243
IL-6	205207_at	1.45	0.3219	1.03	0.9419
GDPD5	32502_at	1.49	0.0079	-1.14	0.1812
MAX	214108_at	1.24	0.368	-1.24	0.3792
The Fibroblast Mediators (predicted from IPA)					
MDM2	217542_at	2.15	0.0084	1.23	0.335
PMAIP1	204286_s_at	1.68	0.0331	1.16	0.4658
BST2	201641_at	1.51	0.036	1.06	0.7027
SERPINB9	209723_at	1.13	0.3313	1.28	0.0704
BIRC5	202094_at	1	0.5949	1	0.6063
Fibroblast genes expressed in scratch and bleomycin (injuries inflicted on epithelial cells in 3D co-culture) - (candidate genes)					
NMNAT1	229852_at	1.62	0.0092	1.74	0.005
C6ORF211	218195_at	1.59	0.0009	1.31	0.0118
HIFAN	226648_at	1.53	0.0046	2.16	0.0002

6.4.1.1 Validation of the epithelial cell candidate genes expressed in scratch and bleomycin injuries

Quantitative RT-PCR analysis was performed to validate the expression changes in epithelial cell genes that were expressed in injuries with scratch and bleomycin, which were selected from the microarray dataset. The selection of genes was determined by their potential role in pulmonary fibrosis, based on their biological function. Quantitative RT-PCR analysis was performed, and analysis revealed that all genes were expressed in epithelial cells, under all conditions: control, scratch injury, and bleomycin injury. This determined that the genes were upregulated in both injuries when the epithelial cells were exposed to injury (Figure 6-1).

The genes selected from the microarray database revealed a very similar gene expression pattern when validated by quantitative RT-PCR (Table 6-8). The validation was performed on independent experiments (n=3). The quantitative RT-PCR results revealed that: *C/EBPA* gene expression increased (fold change 18.67) in epithelial cells after injury with bleomycin compared with no injury; *C/EBPA* gene expression increased (fold change 2.09) in epithelial cells after scratch injury compared with no injury; There was a significant increase in *C/EBPA* expression in bleomycin vs no injury for epithelial cells only, ($p < 0.001$) (Figure 6-1; B).

The statistical analysis was performed using one-way ANOVA with Tukey's post-test, with a p value of < 0.05 being considered to be statistically significant. Experiments were conducted in triplicate, n=3 independent experiments (refer to section 6.3.7).

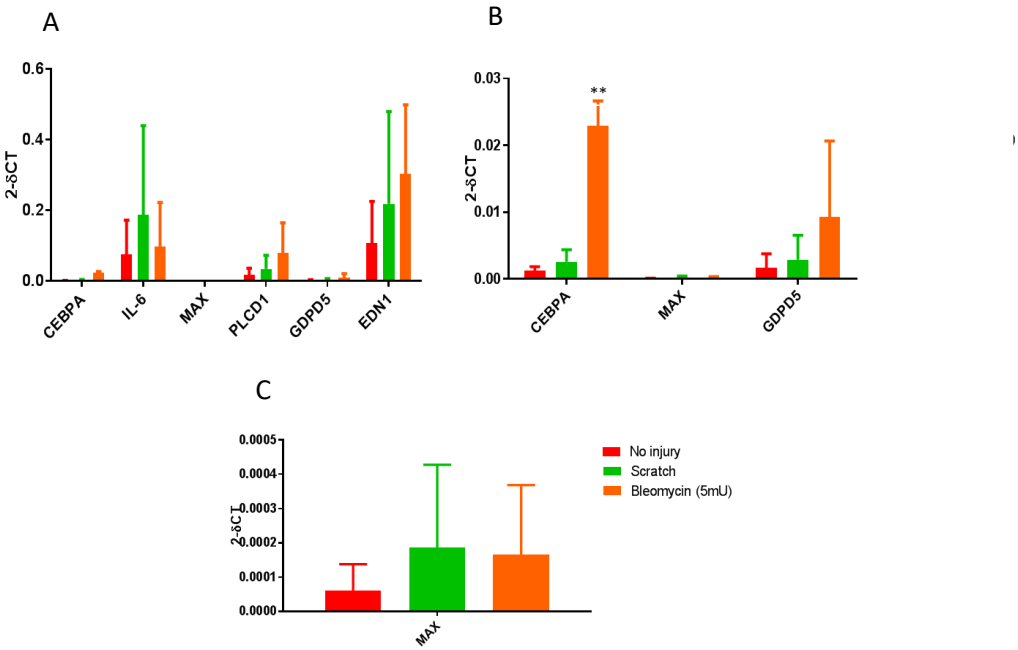


Figure 6-1: Candidate epithelial cells genes from microarray database. The epithelial genes were selected on the basis they were expressed in both scratch and bleomycin injuries. A: Expression of all candidate genes. B: Gene expression on smaller scale, *C/EBPA*, (*p<0.001*). C: Gene expression of MAX. Quantitative RT-PCR analysis was performed to validate these genes in epithelial cells with the conditions. Statistical analysis was performed using GraphPad Prism version 6.0. One-way ANOVA was performed. Data showing, statistical significance only for *C/EBPA* with bleomycin. Experiments were conducted in triplicate. n=3 independent biological experiments.

Table 6-9: The comparison of the fold change of candidate epithelial cells (bleomycin vs no-injury). The microarray gene database with fold change of **bleomycin vs no-injury** compared with quantitative RT-PCR analysis (2-ΔCT) fold change for bleomycin vs no-injury.

Epithelial genes upregulated in bleomycin vs no-injury:	Microarray: fold change	Epithelial genes upregulated in bleomycin vs no-injury:	RT-PCR: fold change
CEBPA	10.24	CEBPA	18.67
PLCD1	1.98	PLCD1	4.5165
EDN1	1.52	EDN1	2.8018
IL-6	1.45	IL-6	1.2886
GDPD5	1.49	GDPD5	5.5303
MAX	1.24	MAX	2.7251

Table 6-10: The comparison of the fold change of candidate epithelial cells (scratch vs no-injury). The microarray gene database with fold change of **scratch vs no-injury** compared with quantitative RT-PCR analysis (2-ΔCT) fold change for scratch vs no-injury.

Epithelial genes upregulated in scratch vs no-injury:	Microarray: fold change	Epithelial genes upregulated in scratch vs no-injury:	RT-PCR: fold change
CEBPA	2.54	CEBPA	2.09
PLCD1	1.26	PLCD1	1.95
EDN1	1.3	EDN1	2.02
MAX	1.24	MAX	3.06
GDPD5	1.14	GDPD5	1.71
IL-6	1.03	IL-6	2.50

6.4.1.2 Validation of IFN α/β pathway genes predicted in epithelial cells from Ingenuity Pathway analysis.

The IFN α/β pathway gene expression analysis was performed using quantitative RT-PCR analysis. The analysis confirmed that expression of the IFN α/β pathway genes were increased when the epithelial cells were exposed to bleomycin injury (Figure 6-2).

All genes showed a very similar pattern when the epithelial cells were inflicted with bleomycin injury. The gene expression measured by quantitative RT-PCR analysis revealed that the *IFIT1* gene had the highest fold change (262.57), which was consistent with the microarray dataset for the *IFIT1* gene (32.21) (Table 6-11). The *IFITM1* gene in epithelial cells (scratch vs no injury) had an increased fold change after scratch injury when measured using quantitative RT-PCR analysis (1.29), compared to the microarray dataset (1.62) (Table 6-12). However, there was no significant difference in bleomycin vs no-injury for the IFN genes expressed in the epithelial cells.

The statistical analysis was performed using one-way ANOVA with Tukey's post-test, and a *p* value of < 0.05 was considered to be statistically significant. Experiments were conducted in triplicate. n=3 independent experiments (refer to section 6.3.7).

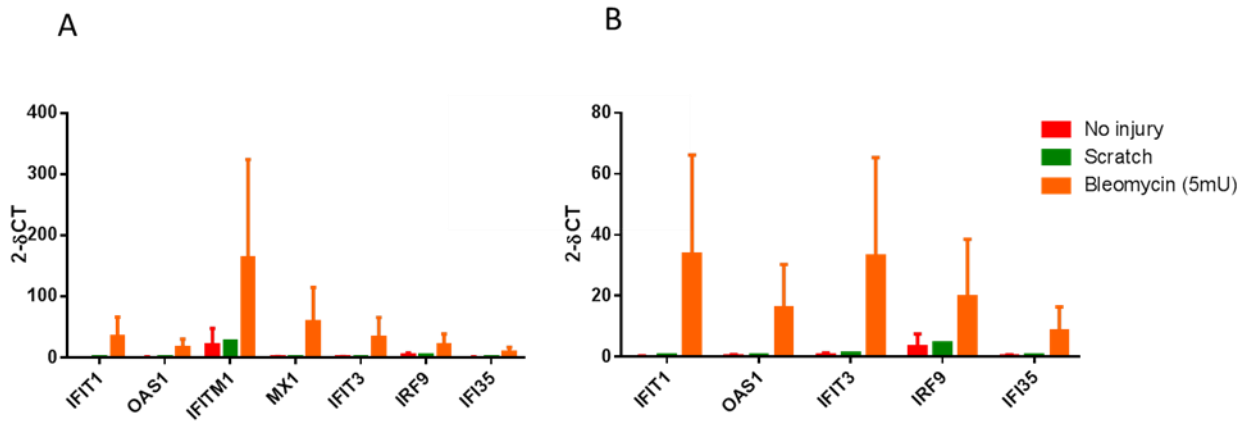


Figure 6-2: The IFN genes expressed in the epithelial cells which were chosen based on the ingenuity pathway analysis. Quantitative RT-PCR analysis was performed to validate these genes in epithelial cells with the conditions. However, there were no statistical differences with injuries vs no-injury. Statistical analysis was performed using GraphPad Prism version 6.0. One-way ANOVA was performed. Experiments were conducted in triplicate. n=3 independent biological experiments.

Table 6-11: The IFN α/β pathway gene predicted by IPA (bleomycin vs no-injury). The microarray gene database with fold change of **bleomycin vs no-injury** compared with quantitative RT-PCR analysis (2-ΔCT) fold change for bleomycin vs no-injury.

IFN genes	Microarray: fold change	IFN genes	RT-PCR: fold change
IFIT1	32.21	IFIT1	262.57
MX1	22.12	MX1	91.53
OAS1	15.01	OAS1	48.97
IFIT3	12.07	IFIT3	60.69
IFI35	10.03	IFI35	26.83
IFITM1	6.02	IFITM1	8.20
IRF9	2.98	IRF9	6.25

Table 6-12: The comparison of the fold change of IFN genes (scratch no-injury). The microarray gene database with fold change of **scratch vs no-injury** compared with quantitative RT-PCR analysis (2-ΔCT) fold change for scratch vs no-injury.

IFN genes	Microarray: fold change	IFN genes	RT-PCR: fold change
MX1	1.68	MX1	1.90
IFITM1	1.62	IFITM1	1.29
OAS1	1.42	OAS1	1.23
IFIT1	1.33	IFIT1	5.28
IFIT3	1.14	IFIT3	2.20
IFI35	1.1	IFI35	1.51
IRF9	1.01	IRF9	1.44

6.4.1.3 Validation of fibroblast candidate genes expressed in response to epithelial cell injuries scratch and bleomycin in the 3D co-culture model

Quantitative RT-PCR analysis was performed for the fibroblast candidate genes, which were selected from the microarray database using the criteria of $p<0.05$ and fold change >2. The selection was also based on their potential role in pulmonary fibrosis pathogenesis, according to background literature. The fibroblast candidate genes were selected in response to epithelial cell scratch and bleomycin injuries, which were inflicted in the 3D co-culture model.

Quantitative RT-PCR analysis was performed on the selected genes and the analysis revealed that all genes were expressed in the fibroblasts. The results also revealed that the selected genes were upregulated in both injuries (Figure 6-3). The gene expression showed a very similar trend, with increased expression when inflicted with bleomycin injury. When the microarray database analysis was compared to the fold change of the quantitative RT-PCR analysis (Table 6-13), it revealed that for bleomycin vs no-injury in fibroblast cells, the *NMNAT1* gene had the highest fold change in both the microarray data (1.62) and the quantitative RT-PCR analysis (1.88). For scratch vs no-injury in fibroblast cells, the *C6ORF211* gene had an increased expression change in the scratch-injured cells, in the microarray analysis (1.31) compared to the quantitative RT-PCR analysis (2.59) (Table 6-14).

The statistical analysis was performed using one-way ANOVA with Tukey's post-test, and a p value of < 0.05 was considered to be statistically significant. Experiments were conducted in triplicate, n=3 independent experiments (refer to section 6.3.7).

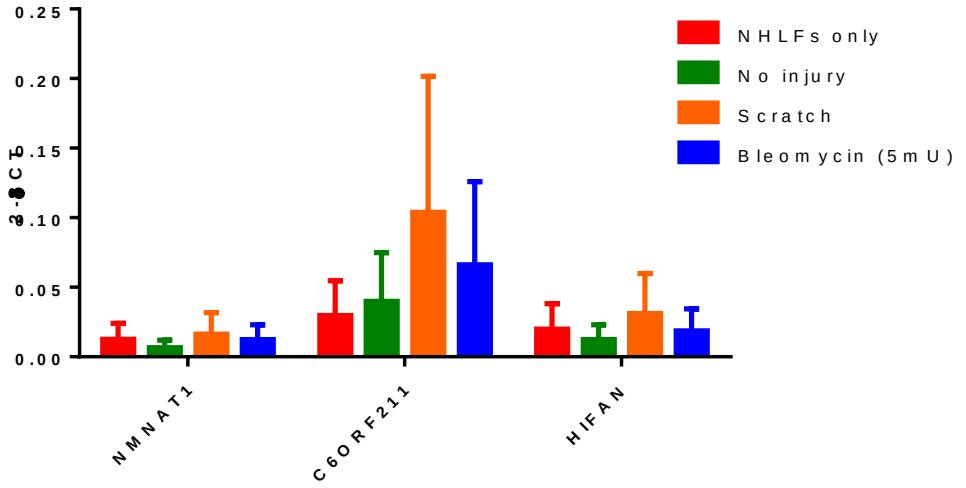


Figure 6-3: Fibroblast genes selected from the microarray database. The genes were selected on the basis that they genes were both expressed in scratch and bleomycin injuries. Quantitative RT-PCR analysis was performed to validate these genes in fibroblasts cells with the conditions. Statistical analysis was performed using GraphPad Prism version 6.0. One-way ANOVA was performed. Experiments were conducted in triplicate. n=3 independent biological experiments.

Table 6-13: The comparison of the fold change fibroblast genes (bleomycin vs no-injury). The microarray gene database with fold change of **bleomycin vs no-injury** compared with quantitative RT-PCR analysis (2-ΔCT) fold change for bleomycin vs no-injury.

Fibroblasts genes upregulated in bleomycin vs no-injury:	Microarray: fold change	Microarray: P-value	Fibroblasts genes upregulated in bleomycin vs no-injury:	RT-PCR: fold change
NMNAT1	1.62	0.0092	NMNAT1	1.88
C6ORF211	1.59	0.0009	C6ORF211	1.65
HIFAN	1.53	0.0046	HIFAN	1.49

Table 6-14: The comparison of the fold change fibroblast genes (scratch vs no-injury).The microarray gene database with fold change of **scratch vs no-injury** compared with quantitative RT-PCR analysis (2-ΔCT) fold change for scratch vs no-injury.

Fibroblasts genes upregulated in scratch vs no-injury:	Microarray: fold change	Microarray: P-value	Fibroblasts genes upregulated in scratch vs no-injury:	RT-PCR: fold change
HIFAN	2.16	0.0002	HIFAN	2.49
NMNAT1	1.74	0.005	NMNAT1	2.50
C6ORF211	1.31	0.0118	C6ORF211	2.59

6.4.1.4 Validation of the expression of fibroblast mediators predicted in the Ingenuity Pathway Analysis

The Ingenuity Pathway Analysis was performed on the microarray dataset of the epithelial cells injured with bleomycin. IPA predicted the IFN pathway as the most altered pathway in response to bleomycin injury of epithelial cells. The pathway analysis for fibroblasts in response to epithelial injury was based on the activation of the IFN pathway in epithelial cells, in particular, the *IFNA2* gene. The *IFNA2* gene was predicted to be upregulated, and contributed to the expression of the fibroblast mediator genes; MDM2, PMAIP1, BST2, SERPINB9, and BIRC5 in response to bleomycin injury of the epithelial cells.

The expression of genes was validated by quantitative RT-PCR analysis. The analysis revealed that a trend was observed in the microarray gene expression, in which there was an increased expression with bleomycin injury (Figure 6-4). The gene expression of *MDM2* revealed that the same trend of the microarray database compared to the fold change of the RT-PCR (Table 6-15). The analysis revealed that for bleomycin vs no-injury in fibroblasts, the *MDM2* gene had the highest fold change in the microarray data (2.15), and in quantitative RT-PCR analysis (4.09). For scratch vs no-injury in fibroblasts exposed to various injuries, the *MDM2* gene had increased expression with scratch injury in the microarray analysis (fold change of 1.23) and in the quantitative RT-PCR analysis (fold change of 2.46) (Table 6-16).

The statistical analysis was performed using one-way ANOVA with Tukey's post-tes, and a p value of < 0.05 was considered to be statistically significant. Experiments were conducted in triplicate, n=3 independent experiments (refer to section 6.3.7).

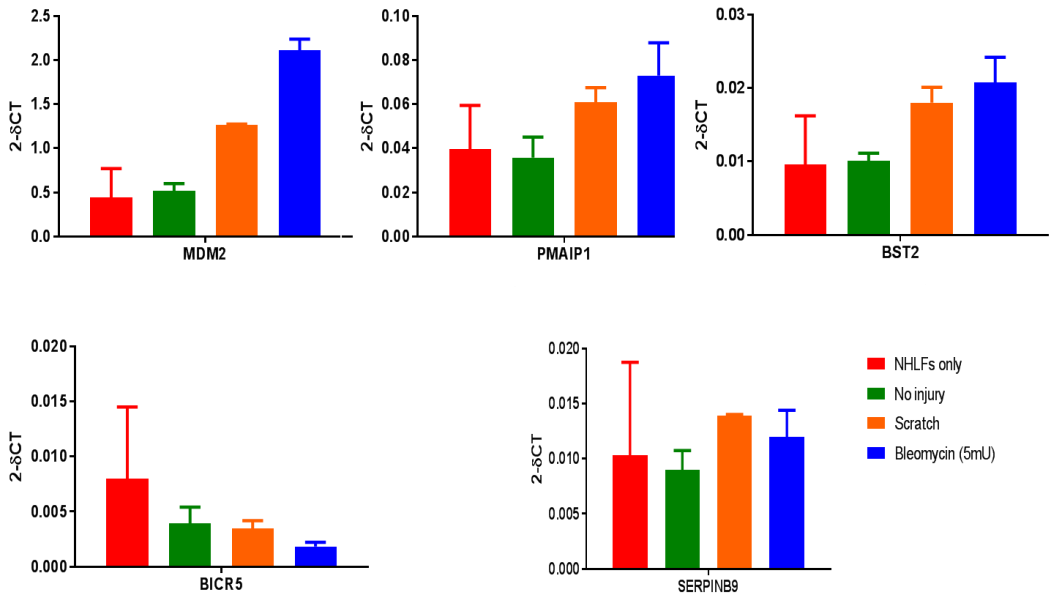


Figure 6-4: Fibroblast mediators predicted by the IPA. The genes were selected on the basis of the IFN pathway which was predominant pathway in epithelial cells and which activated the fibroblasts. These genes were validated by quantitative RT-PCR analysis of genes in co-cultured fibroblasts cells with the conditions. However, there were no statistical differences with injuries vs no-injury. Statistical analysis was performed using GraphPad Prism version 6.0. One-way ANOVA was performed. Experiments were conducted in triplicate. n=3 independent biological experiments.

Table 6-15: The comparison of the fold change of fibroblast mediators (bleomycin vs no-injury). The microarray gene database with fold change of **bleomycin vs no-injury** compared with quantitative RT-PCR analysis (2-ΔCT) fold change for bleomycin vs no-injury.

Fibroblast: IFN mediators	Microarray: fold change	Fibroblast: IFN mediators	RT-PCR: fold change
MDM2	2.15	MDM2	4.09
PMAIP1	1.68	PMAIP1	2.04
BST2	1.51	BST2	2.06
SERPINB9	1.13	SERPINB9	1.33
BIRC5	1	BIRC5	0.47

Table 6-16: The comparison of the fold change of fibroblast mediators (scratch vs no-injury). The microarray gene database with fold change of **scratch vs no-injury** compared with quantitative RT-PCR analysis (2-ΔCT) fold change for scratch vs no-injury.

Fibroblast: IFN mediators	Microarray: fold change	Fibroblast: IFN mediators	RT-PCR: fold change
SERPINB9	1.28	SERPINB9	1.54
MDM2	1.23	MDM2	2.46
PMAIP1	1.16	PMAIP1	1.70
BST2	1.06	BST2	1.79
BIRC5	1	BIRC5	0.89

6.4.2 Immunohistochemistry of selected candidate genes

The next step was to evaluate a selection of candidate genes in IPF tissue using immunohistochemistry. This was to determine whether the expression of these candidate genes would show a similar trend with injury as the microarray data. It was also to determine whether an increased expression in IPF tissue compared to normal lung tissue could be observed.

The candidate genes were selected for further evaluation in IPF tissue by immunohistochemistry, and were based on fold change gene expression between the injuries by quantitative RT-PCR analysis, and the potential role they have in pulmonary fibrosis. The genes chosen were; *C/EBP-α, endothelin-1,* and *IRF-9.*

CCAAT/ enhancer binding protein-α, (C/EBP-α) is a transcriptional factor belonging to the CCAAT/enhancer-binding protein (C/EBP) family, and plays a pivotal role in numerous cell responses, including the control of cell growth and differentiation, and immune and inflammatory processes in various diseases (Ramji and Foka 2002). Studies have shown that C/EBP-α may have an important role in the protection of the alveolar epithelium after hyperoxic injury in the adult mouse (Sato, Xu et al. 2012).

There are three isoforms of Endothelin, ET-1, ET-2, and ET-3 (Barton, Shaw et al. 1997). ET-1 is the predominant isoform, and is a potent pulmonary vasoconstrictor (Kunichika, Landsberg et al. 2004). In the lung, fibroblasts, endothelial cells, alveolar macrophages, epithelial cells, and polymorphonuclear leukocytes all secrete ET-1 (Swigris and Brown 2010). Animal studies have shown that increased levels of ET-1 can increase collagen deposition in the lungs after administration of bleomycin, and that the overexpression of ET-1 is sufficient to induce progressive pulmonary fibrosis (Kulasekaran, Scavone et al. 2009). *In vitro* studies have shown that ET-1 has profibrotic effects on lung fibroblasts, promoting proliferation, differentiation, and ECM synthesis (Shi-Wen, Denton et al. 2001).

IFN regulatory factor 9 (IRF9) is a DNA binding protein that forms a heterotrimeric transcription complex with STAT1 and STAT2, termed interferon-stimulated gene

factor 3 (ISGF3), which binds to the interferon-stimulated response element (ISRE), and promotes IFN-inducible genes (Tsuno, Mejido et al. 2009). Studies have shown that IRF-9 is important for eliciting the antiproliferative activity of IFN-α among the intracellular JAK-STAT pathway factors (Tsuno, Mejido et al. 2009).

Analysis of each candidate gene expression in the lung tissue was performed using IHC (refer to section 6.3.5). A positive control of lung bronchus tissue was used to optimise the protocol. The selection of the positive control tissue was done according to the Protein Atlas Database (http://www.proteinatlas.org/). Negative control was by omission of the primary antibody. Normal lung tissue and IPF lung tissue were obtained from the University of Nottingham, Biobank centre. This was approved by the Nottingham Research and Ethics Committee (REC ref: 08/H0407/01).

6.4.2.1 Immunohistochemistry to detect expression of C/EBP-alpha

Immunohistochemistry revealed that bronchus lung tissue sections were positive for C/EBP-α expression (Figure 6-5: A), and negative control, confirming there was no expression of the protein (Figure 6-5: B). In the normal lung tissue sections (Figure 6-5: C-E) there was expression of C/EBP-α, mainly detected in the epithelial cells. In the IPF tissue lung sections (Figure 6-5: F-H) there was also expression of C/EBP-α in all the tissue showing no difference in expression within the cell types.

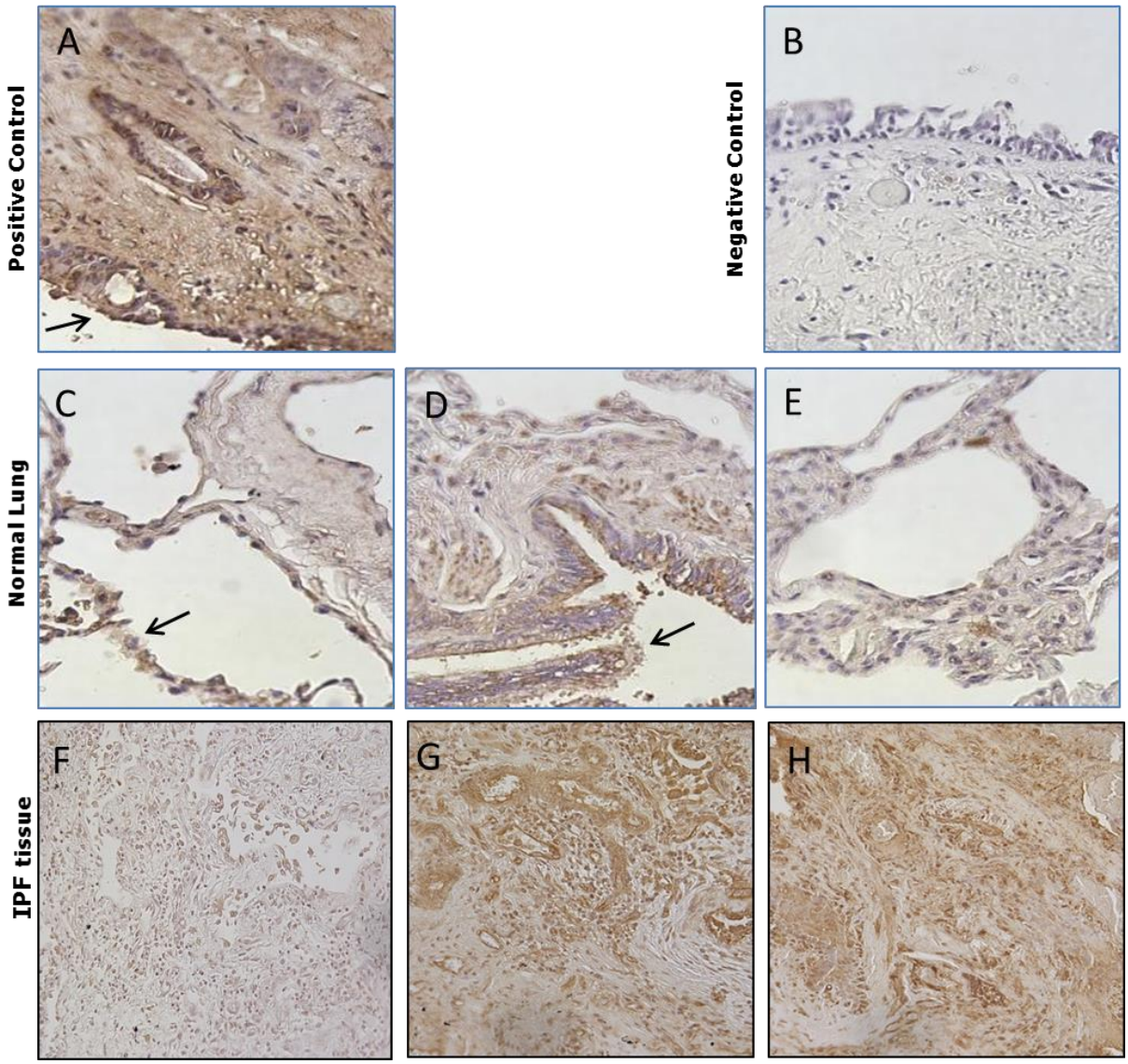


Figure 6-5: Expression of CCAAT/enhancer protein (C/EBP-α in normal and IPF lung. Immunohistochemical staining of C/EBP-α was performed in control lung section (positive for the protein), normal lung and IPF lung. The sections were counterstained with haematoxylin. (A) is positive control for C/EBP-α expression in bronchus lung tissue section T501 and (B) negative control excluding primary antibody. Normal lung tissue sections: (C)2004/P72, (D) FP01 and (E) FP02 showed expression of C/EBP-α in the epithelium (arrow indicates the epithelial cells). IPF lung tissue sections (F), RS11008 (G) RS12022 and (H) RS11011 all showed expression of C/EBP-α in all the tissue. All were photographed at x40 magnification.

6.4.2.2 Immunohistochemistry to detect expression of IRF-9

The immunohistochemistry revealed that bronchus lung tissue sections were positive for IRF-9 expression (Figure 6-6: A). Negative control, excluding the primary antibody revealed no expression of the protein (Figure 6-6: B). There was expression of IRF-9 in the epithelial cells, in the normal lung tissue section (Figure 6-6: C) but not in the other normal lung sections. In the IPF tissue lung sections, there was no expression of IRF-9 in the cell types, (Figure 6-6: F-H). This could be due to poor antibody or sub-optimal experimental conditions for detection.

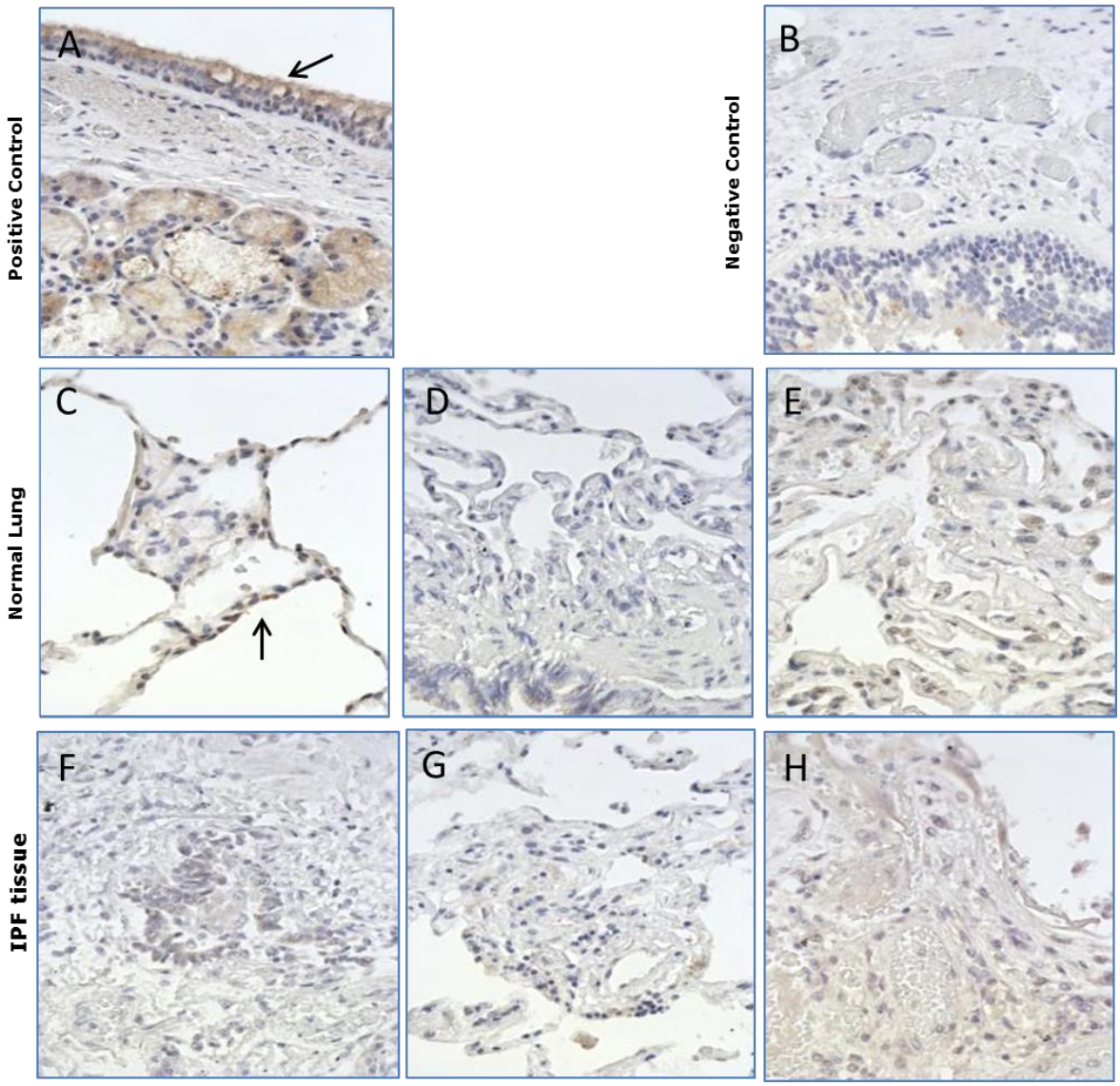


Figure 6-6: Expression of IRF-9 in normal and IPF lung. Immunohistochemical staining of IRF-9 was performed in control lung section (positive for the protein), normal lung and IPF lung. The sections were counterstained with haematoxylin. (A) Positive control for IRF-9 expression in bronchus lung tissue section T501 and (B) negative control excluding primary antibody. Normal lung tissue sections: (C) 2004/P72 detected small sears of IRF-9 expression in the epithelial cells. (indicated by the arrow). IPF lung tissue sections (F), RS11008 (G) RS12022 and (H) RS11011 all detected no expression of IRF-9 in the cell types. All were photographed at x40 magnification.

6.4.2.3 Immunohistochemistry to detect expression of Endothelin-1

The immunohistochemistry revealed that UIP lung tissue sections were positive for ET-1 expression (Figure 6-7: A). Negative control, excluding the primary antibody (Figure 6-6: B) revealed no expression of the protein. In the normal lung tissue sections there was no expression of ET-1 detected (Figure 6-7: C-E). In the IPF tissue lung sections there was expression of ET-1 in the tissue, in particular, in the epithelial cells (Figure 6-7: F-H). There was increased expression of ET-1 detected in the epithelial cells and possibly in the mesenchymal cells of the IPF tissue (Figure 6-7: F). Thus the ET-1 expression seems to be predominantly expressed in epithelial cells.

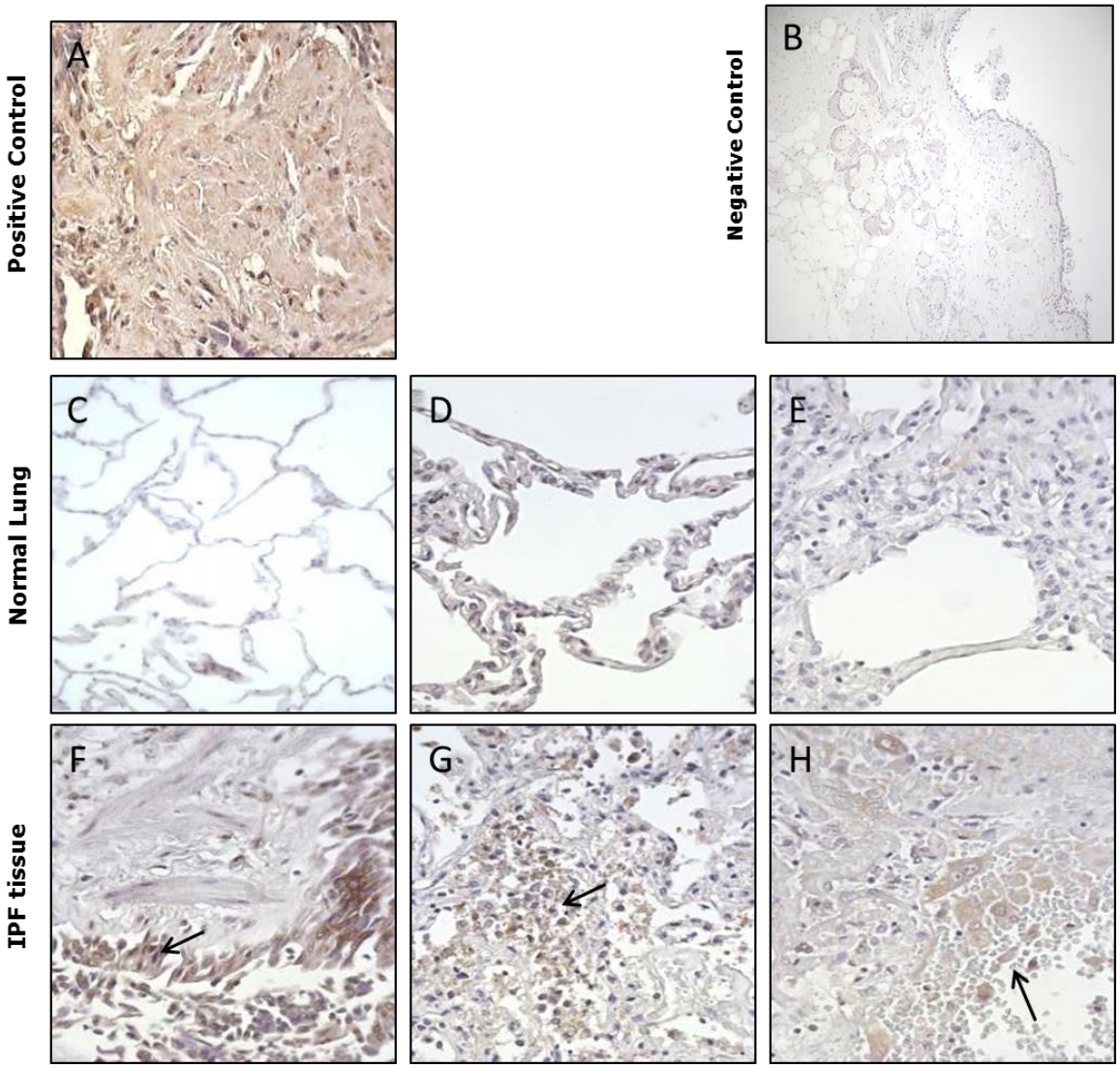


Figure 6-7: Expression of ET-1 in normal and IPF lung. Immunohistochemical staining of ET-1 was performed in control lung section (positive for the protein), normal lung and IPF lung. The sections were counterstained with haematoxylin. (A) Positive control for ET-1 expression in UIP lung tissue and (B) negative control excluding primary antibody. Normal lung tissue sections: (C) 2004/P72, (D) FP01 and (E) FP02 detected ET-1 expression in the epithelial cells. IPF lung tissue sections (F), RS11008 (G) RS12022 and (H) RS11011 all detected expression of ET-1 in the epithelial cells (indicated by arrow). All were photographed at x40 magnification.

6.4.3 The validation of upstream mediators in the IFN pathway by RT-PCR

The IFN α/β pathway was predicted in the Ingenuity Pathway Analysis, based on the expression of pathway genes in the epithelial cells exposed to bleomycin (Figure 5-12). The type I IFN family is comprised of IFN-α and IFN–β, which have a globular structure composed of five α-helices (Oritani, Kincade et al. 2001). IFN-α is produced by leukocytes while IFN-β is a fibroblast product. Studies *in vitro* have shown that IFN α/β suppresses the proliferation of many normal and transformed cells through a prolongation of the G1 phase of the cell cycle and a reduced entry into the S phase (Creasey, Bartholomew et al. 1980).

IFN-α/β share a ubiquitously expressed heterodimeric receptor, composed of two chains, IFNAR1 and IFNAR2 (Trinchieri 2010). Human IFNAR1 is composed of a 557-amino acid glycoprotein with a 21-amino acid transmembrane segment, and a 100-amino acid cytoplasmic domain. IFNAR2 consists of 515 amino acids and acts as a functional receptor for IFN α/β signalling (Oritani, Kincade et al. 2001). IFNAR1 and IFNAR2 are associated with signalling through two Janus family kinases, Tyk2 and Jak1, resulting in the recruitment of STAT1 and STAT2 leading to the formation of the heterodimer STAT1-STAT2 that dissociate from the receptors and migrate into the nucleus and activates the transcription of IFN-inducible genes (Trinchieri 2010).

The IPA predicted that the IFNA2 gene was upregulated in the IFN pathway, which predicted the expression of MDM2, PMAIP1, BST2, SERPINB9 and BIRC5 in fibroblasts exposed to injured epithelial cells in the co-culture model. The aim of this study was to validate the IFN α/β pathway in particular, the expression of IFNA1, IFNA2 and IFNB2. The IL-6 gene was also investigated as IL-6 is known to activate the IFN α/β pathway.

6.4.3.1 Validation of IFN genes in 3D co-cultured fibroblasts exposed to injured epithelial cells

The Ingenuity Pathway Analysis predicted the IFN pathway, may be initiating the injury response in epithelial cells. Further gene expression had revealed that genes, *IFNA1*, *IFNA2, IFNB1* and *IL-6*, (Figure 5-12) may be downregulated in the fibroblasts. The hypothesis was that these genes were downregulated in the fibroblasts that were exposed to injured epithelial cells.

Quantitative RT-PCR analysis was performed on fibroblasts that were cultured in the 3D co-culture model, and were exposed to injured epithelial cells. The statistical analysis was performed using one-way ANOVA with Tukey's post-test, and a *p* value of < 0.05 was considered to be statistically significant. Experiments were conducted in triplicate, n=3 independent experiments (refer to section 6.3.7).

The data revealed that *IFNA1* was expressed in the epithelial cells treated with the conditions, scratch and bleomycin but, compared to the non-injured co-culture model, there was no difference in expression with injury (Figure 6-8: A). The expression of *IFNA2* reduced significantly with both injuries; scratch ($p<0.05$) and bleomycin ($p<0.05$), compared to the non-injured control (Figure 6-8: B). The expression of *IFNB1* also decreased with the level of injuries; scratch and bleomycin but the data were insignificant compared to the non-injured co-cultured fibroblasts (Figure 6-8: C). The *IL-6* gene expression showed no consistent trend with the level of injuries as this gene was expressed in all conditions (Figure 6-8: D). However, the data did reveal that the expression of *IL-6* was ten times higher, compared to the expression of *IFNA2* and *IFNB1* genes. Overall, according to the hypothesis, only genes *IFNA2* and *IFNB1* were downregulated in the fibroblasts, which were exposed to injured epithelial cells.

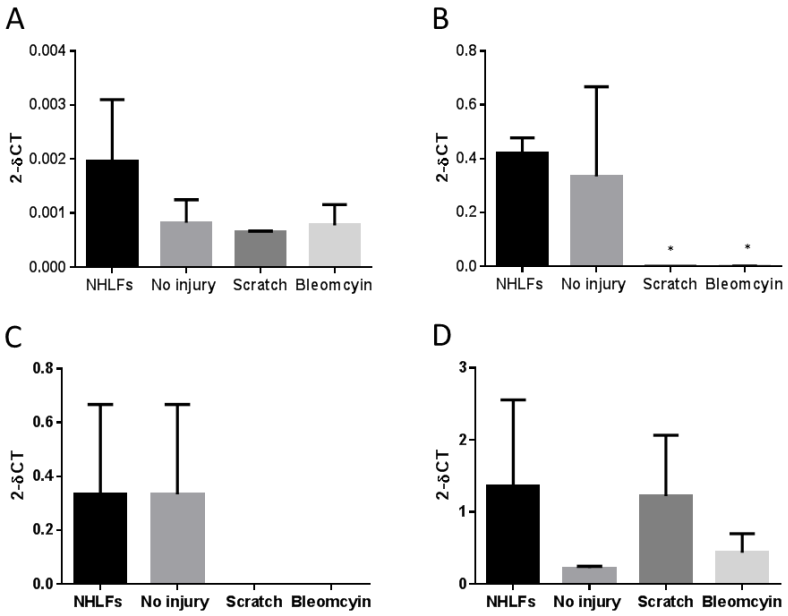


Figure 6-8: The IFN genes and IL-6 expression in 3D co-culture fibroblasts. The fibroblasts were exposed to epithelial injury for 6 days in culture. The fibroblasts were retrieved and RT-PCR was performed (A) *IFNA1* gene expression showed no consistent trend with injury. (B) *IFNA2* showed gene expression decreased with injuries i.e. scratch and bleomycin. (C) *IFNB1* showed gene expression decreased with the injury i.e. scratch and bleomycin. (D) *IL-6* gene expression showed no trend with injury. Statistical analysis was performed using a one-way ANOVA with a Tukey's post-hoc test. Experiments were conducted in triplicate. n=3 independent biological experiments.

6.4.3.2 Validation of the expression of the IFN α/β pathway genes in injured epithelial cells.

The gene expression of *IFNA1* and *IFNA2* in epithelial cells showed a trend toward an increase of expression with bleomycin injury, (Figure 6-9: A- B). However, for both genes, data were statistically insignificant. The expression of *IFNB1* revealed a significant increase in epithelial cells when treated with bleomycin ($p<0.05$), (Figure 6-9: C). *IL-6* was expressed in all conditions in the epithelial cells but again no consistent trend was seen with injury, in particular, with the administration of bleomycin. The observation revealed there was a slight decrease of *IL-6* with the addition of bleomycin but data were statistically insignificant (Figure 6-9: D). However, comparing the expression of *IL-6*, there is a ten times higher gene expression from fibroblasts as compared to the *IL-6* expression from the epithelial cells. It may seem that fibroblasts express a much higher level of *IL-6* than in epithelial cells.

The statistical analysis was performed using one-way ANOVA followed by Tukey's post-hoc test. For all data analysed statistically as described above, a *p* value of < 0.05 was considered to be statistically significant. Experiments were conducted in triplicate. n=3 independent experiments (refer to section 6.3.7).

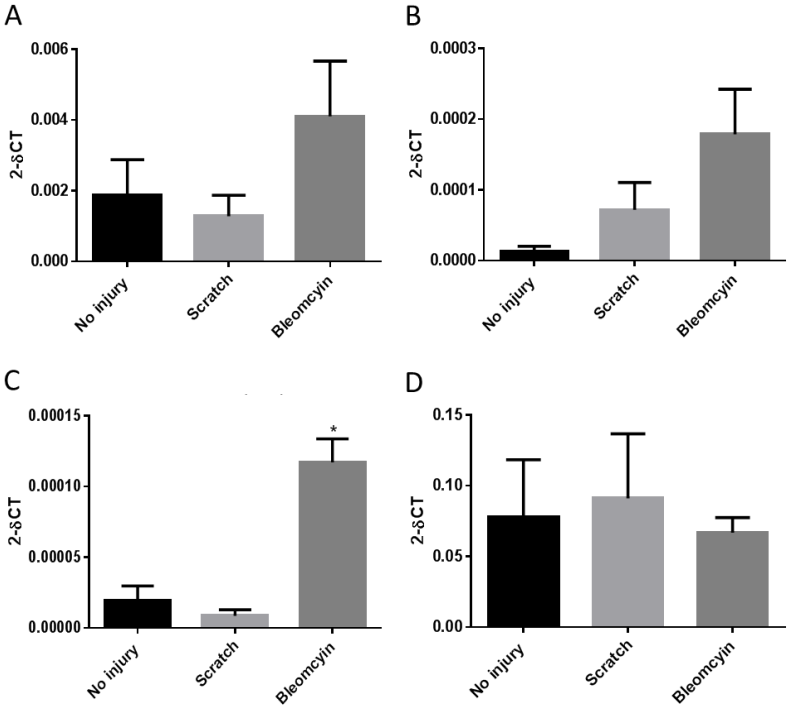


Figure 6-9: The expression of gene in injured <u>epithelial cells</u>. (A) IFNA1 gene expression showed that the expression increased with the addition of bleomycin. (B) IFNA2 showed the gene expression increased with the addition of bleomycin. (C) IFNB1 showed the gene expression increased with the addition of bleomycin ($p<0.05$). (D) IL-6 gene expression showed no trend with either injury. Statistical analysis was performed using a one-way ANOVA with a Tukey's post-hoc test. Experiments were conducted in triplicate. n=3 independent biological experiments.

6.4.4 The Effect of Endothelin-1 *in vitro*

Endothelin-1 (ET-1) is a 21 amino acid peptide, which is a potent vasoconstrictor of airway smooth muscle and may contribute to pro-fibrotic effects. Therefore, it may be considered to participate in the pathogenesis of pulmonary fibrosis and obstructive airway disease (Swigris and Brown 2010). Evidence has suggested that ET-1 is synthesised and released by different pulmonary cells including pulmonary fibroblasts and airway epithelial cells (Fagan, McMurtry et al. 2001). Studies have suggested that ET-1 may act as a proliferative stimulus in airway smooth muscle (Panettieri, Goldie et al. 1996) and fibroblasts (Gallelli, Pelaia et al. 2005). This may contribute to airway and lung remodelling processes. Although there have been several reports describing pro-fibrotic effects of ET-1 in rat and human pulmonary fibroblasts, (Gallelli, Pelaia et al. 2005) this suggests that ET-1 generates an autocrine and paracrine system that appears to be involved in the regulation of pro-fibrotic features in IPF (Ahmedat, Warnken et al. 2013).

There are three isoforms of endothelin: ET-1, ET-2 and ET-3. ET-1 is the most potent isoform and is secreted by fibroblasts, endothelial cells, alveolar macrophages and epithelial cells in the lungs (Swigris and Brown 2010). ET-1 binds to two G-protein-coupled receptors, ET receptor A (ET_A) and ET receptor B (ET_B). ET_A receptor is found primarily on mesenchymal cells i.e. fibroblasts, and plays a role in cell proliferation, vasoconstriction, proinflammatory and autocrine responses. ET_B receptor is found on the endothelium and plays an ET-1 negative feedback clearance role, airway bronchoconstriction and vascular release of nitric oxide (Fonseca, Abraham et al. 2011).

A study by *Shi-wen et al*, demonstrated *in vitro* that ET-1 promoted fibroblast activation in which there was ECM synthesis of collagen I and III by a mechanism dependant on both receptors ET_A and ET_B (Shi-Wen, Denton et al. 2001). Recent *in vitro* studies have also shown that antagonists, such as bosentan inhibit the effect of both endothelin-1 receptors (Kunichika, Landsberg et al. 2004). Bosentan is a potent dual antagonist of both endothelin receptors ET_A and ET_B. Bosentan is an orally administered drug and has been extensively studied in patients with pulmonary

hypertension (Kunichika, Landsberg et al. 2004). Studies in patients have shown an improvement in pulmonary hypertension when taking bosentan. However, little is known about the mechanism of this compound (Kunichika, Landsberg et al. 2004).

The aims of this study: Firstly, to investigate whether low levels of injury i.e. scratch and bleomycin, up-regulated ET-1 (soluble mediator) and EDN-1 (gene) in epithelial cells, which may lead to an increased, cell proliferation and matrix synthesis in the fibroblasts. Secondly, to determine whether bosentan inhibited ET-1 receptors, this may result in decreased cell proliferation and matrix synthesis in fibroblasts.

6.4.4.1 The effect of Bosentan in 3D co-culture model

The aim of this experiment was to determine a suitable concentration of bosentan, which would not be toxic and not reduce cell viability of individual cell lines; fibroblasts in collagen and epithelial cells monolayer. The fibroblasts were cultured in collagen without the addition of epithelial cells (refer to section 2.4). The epithelial cells were cultured as a monolayer (refer to section 2.4). Various concentrations of bosentan were added to each cell type and left for 24 hours (refer to section 6.3.6). A MTT reduction assay was performed in order to determine the cell viability of the fibroblasts and epithelial cells. The results revealed that fibroblasts did not decrease in viability over the range of bosentan concentrations tested, (Figure 6-10). However, for the epithelial cells there was a trend towards reduced cell viability compared to the epithelial cells with absence of bosentan. This suggested that bosentan had no effect on the fibroblasts directly but, with epithelial cells, there was an effect. The results for the addition of bosentan on the epithelial cells were insignificant. Therefore, a concentration of 100uM was used, as previously demonstrated *Bogatkevich et al 2012.*

The statistical analysis was performed using one-way ANOVA followed Tukey's post-hoc test. For all data analysed statistically as described above, a p value of < 0.05 was considered to be statistically significant. Experiments were conducted in triplicate. n=3 independent experiments (refer to section 6.3.7).

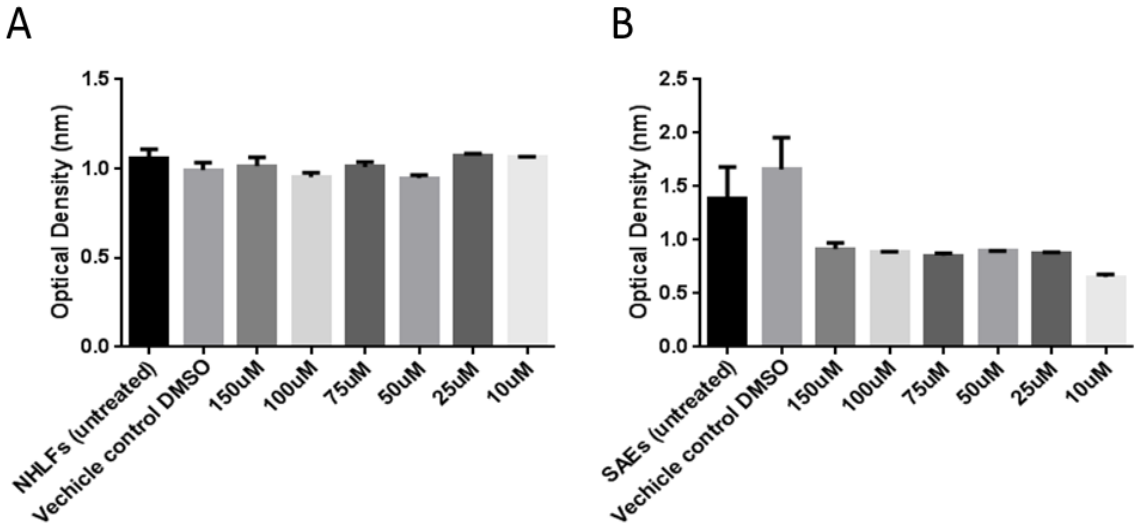


Figure 6-10: Addition of different concentrations of bosentan on fibroblasts and epithelial cells. (A). The addition of bosentan on fibroblasts in collagen for 24 hours. (B). The addition of bosentan on epithelial cells for 24 hours. Cell viability determined by MTT reduction assay. There was no reduced cell viability of the different concentration of bosentan after 24hours. Statistical analysis was performed using GraphPad Prism version 6.0. One-way ANOVA was performed. Experiments were conducted in triplicate. n=3 independent biological experiments.

The next step was to determine the effect of bosentan in the co-culture model. The model consisted of cultured fibroblasts in collagen and epithelial cells in the Transwell® insert (refer to section 2.4). Bosentan (100μM) was added to the epithelial cells only in the Transwell® insert every 48 hours for 6 days in the 3D co-culture model. The MTT reduction assay results revealed that with 'absence' of bosentan, there was an increase in cell viability. As for with 'addition' of bosentan, cell viability significantly decreased in the co-cultured fibroblasts ($p<0.05$) (Figure 6-11).

The statistical analysis was performed using one-way ANOVA followed Tukey's post-hoc test. For all data analysed statistically as described above, a p value of < 0.05 was considered to be statistically significant. Experiments were conducted in triplicate. n=3 independent experiments (refer to section 6.3.7).

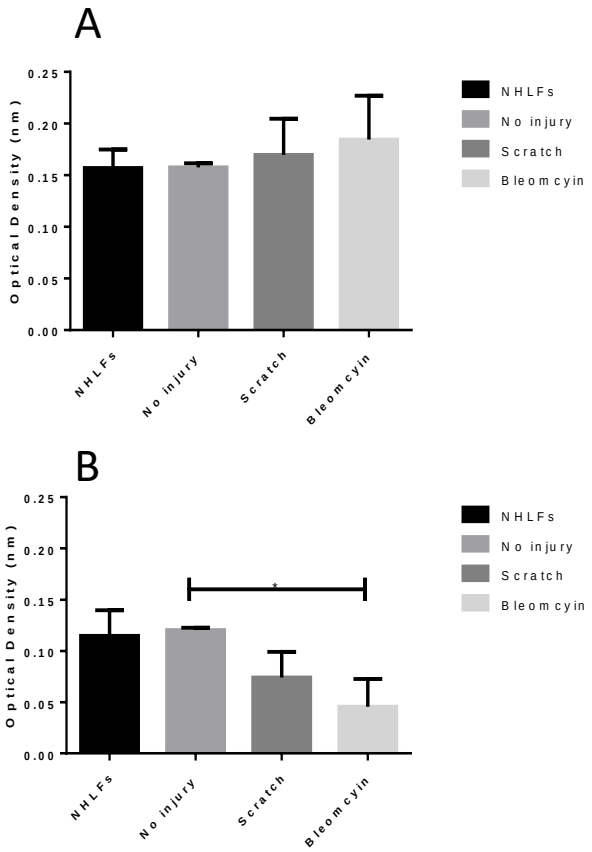


Figure 6-11: A MTT reduction assay on fibroblasts in 3D co-culture model: Absence of bosentan in the co-culture model. (B) The addition of 100μm bosentan to the co-culture model for 24 hours before a MTT reduction assay was performed. Statistical analysis was performed using a one-way ANOVA with a Tukey's post-hoc test. Experiments were conducted in triplicate. n=3 independent biological experiments.

6.4.4.2 Determination of endothelin-1 concentration in the 3D co-culture model with addition of Bosentan

The aim of this experiment was to determine the concentration of endothelin-1 in co-cultured supernatants with the addition of bosentan (100μM) and to determine whether there was a decrease in endothelin-1 concentration with the addition of bosentan. The experiment was performed on fibroblasts exposed to epithelial cells inflicted with various injuries (refer to section 2.4) and with the addition of bosentan every 48 hours on epithelial cells (refer to section 6.3.6).

The statistical analysis was performed using one-way ANOVA followed by Tukey's post-hoc test. For all data analysed statistically as described above, a *p* value of < 0.05 was considered to be statistically significant. Experiments were conducted in triplicate. n=3 independent experiments (refer to section 6.3.7).

An ELISA was used to determine the concentration of ET-1 in 3D co-culture supernatants after day 6. The results revealed in the absence of bosentan, there was an increase in the expression of endothelin-1 with scratch injury ($p<0.005$) and bleomycin ($p<0.005$) injury which was as expected (Figure 6-12: A). The addition of bosentan (100 μM) in the co-culture model (on epithelial cells), revealed a slight decrease in the expression of endothelin-1 (ng/ml), with the addition of scratch and bleomycin injury (Figure 6-12: B). The results were insignificant with injury and addition of bosentan.

In summary, the addition of bosentan revealed a significant decrease of endothelin-1 with both injuries bleomycin and scratch ($p<0.005$), (Figure 6-12: C), compared with 'absence of bosentan. This may suggest that bosentan inhibits the injury-induced increase in endothelin-1 production.

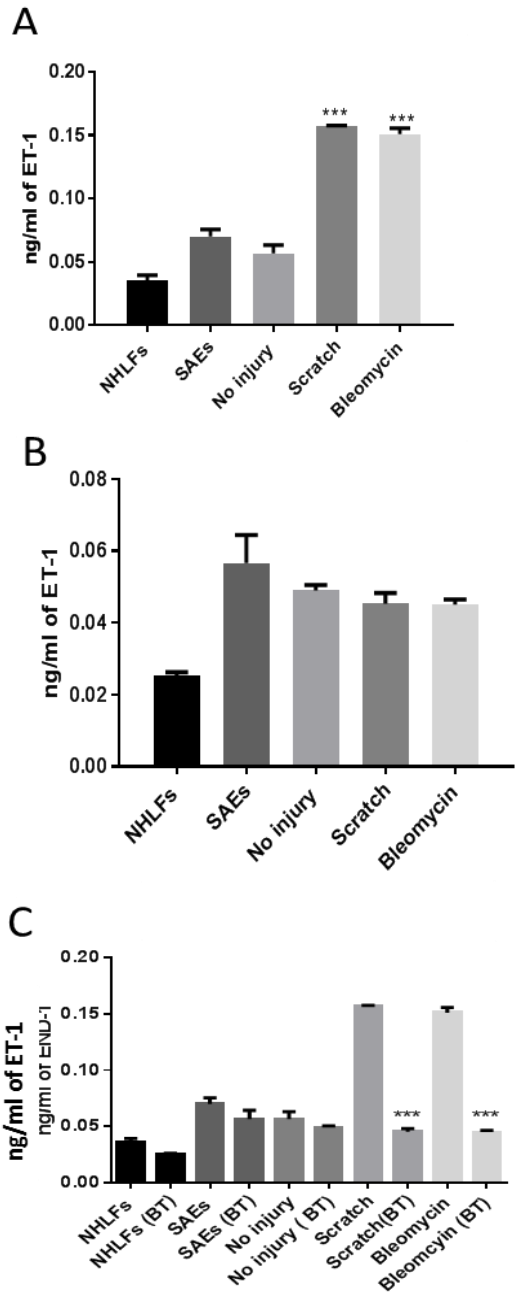


Figure 6-12: ELISA: The expression of endothelin-1 measured by ELISA in the co-cultured supernatants.(**A**) Co-culture model with the absence of bosentan over 6 days ($p<0.005$). (**B**) The addition of bosentan in the 3D co-culture model over 6 days. (**C**) Comparison of data of injuries with 'absence with 'addition of bosentan' (BT). Statistical analysis performed using one-way ANOVA followed by Tukey's post- hoc test. Experiments were conducted in triplicate. n=3 independent biological experiments.

6.4.4.3 To determine the expression of ECM genes with the addition of bosentan in co-culture model

The aim of this work was to investigate the effect of bosentan on the transcription of ECM genes and a myofibroblast marker in fibroblasts exposed to epithelial injury. The hypothesis was that induction of these genes was dependent on endothelin, and would be inhibited by the endothelin receptor antagonist bosentan. The genes selected were *collagen I* and *III* which are the most abundant collagens in fibrosis and *α-SMA*, a hallmark of fibroblast differentiation.

Gene expression was measured by quantitative RT-PCR analysis. Bosentan (100uM) was added every 24 hours in the 3D co-culture model and RNA was extracted from fibroblasts after 6 days (refer to section 2.8.1). The statistical analysis was performed using one-way ANOVA with Tukey post-test. For all data analysed statistically as described above, a *p* value of < 0.05 was considered to be statistically significant.

The data revealed that in the absence of bosentan there was a significant increase in *Collagen I, Collagen III (*$p<0.01$) and α-SMA ($p<0.05$) gene expression in fibroblasts in response to epithelial injury, (Figure 6-13). The experiment was conducted in triplicate, n=3 independent experiments (refer to section 6.3.7). However on addition of bosentan in the 3D co-culture model, the expression of *collagen I*, *collagen III* and *α-SMA* revealed no change with injury (Figure 6-14; A-C). In each case the data were normalised to NHLFs alone to provide a consistent baseline, and so represent a fold change in expression compared to NHLFs in monoculture.

Overall, it can be summarised, that the addition of bosentan inhibits the bleomycin-induced increase in ECM and α-SMA expression in fibroblasts. These data suggests that epithelial injury affects co-cultured fibroblasts response by increasing gene expression of ECM genes and smooth muscle actin, and that this induction is mediated by endothelin.

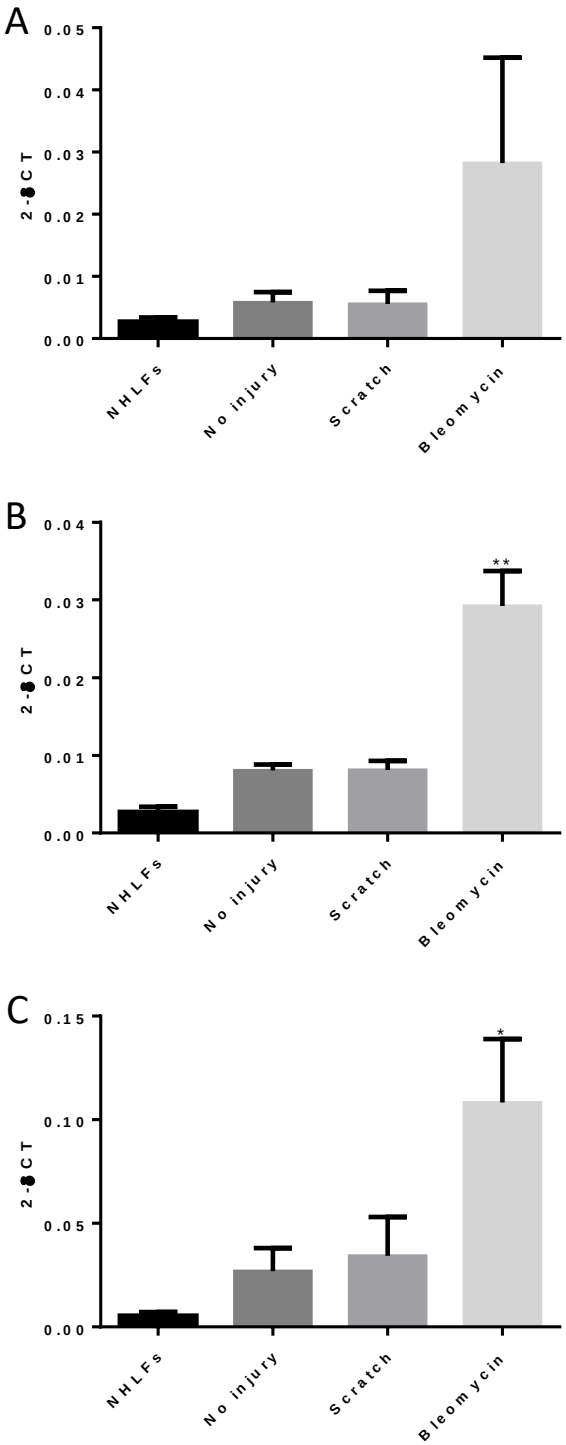


Figure 6-13: Induction of ECM genes and *α-SMA* in fibroblasts in monoculture and co-cultured with epithelial cells. Gene expression was compared injuries vs no injury. A; Expression of *Collagen I* in fibroblasts, B; expression of *Collagen III* with $p<0.005$, and C; expression of *α-SMA with* $p<0.05$. Data were normalised using house-keeping gene *β-actin*. Statistical analysis was performed by using one-way ANOVA with Tukey post-test. The asterisk * represents $p<0.05$ and ** represents $p<0.05$. Experiments were conducted in triplicate. n=3 independent biological experiments.

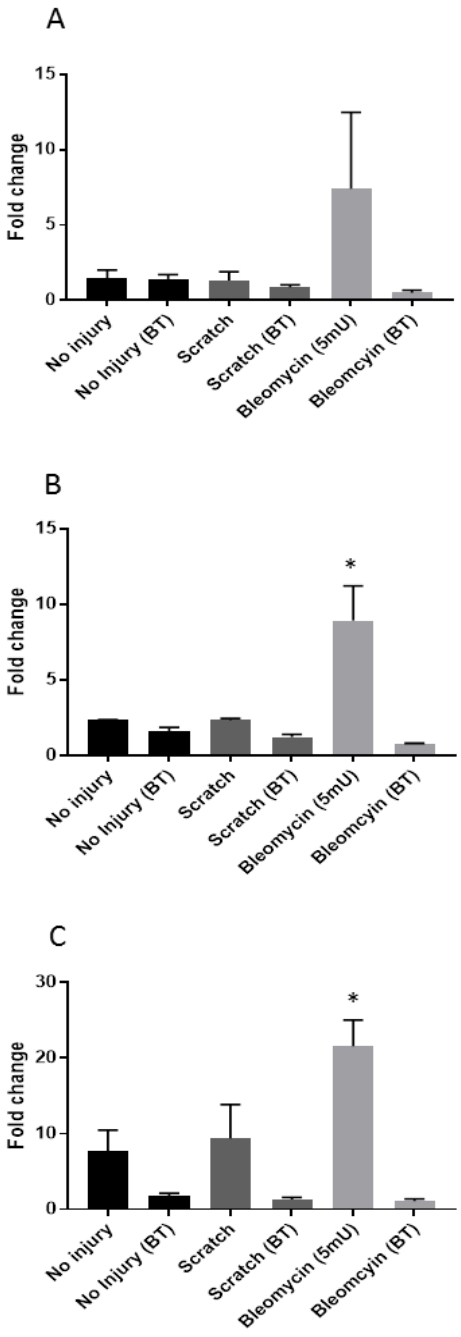


Figure 6-14: **Gene expression of *Collagen I, III* and α-*SMA* in the absence and presence (BT) of bosentan in the co-cultured fibroblasts model over 6 days.** Data were normalised to the respective untreated fibroblasts (NHLFs) for the treatments in each group. The data was compared for absence and addition of bosentan. The concentration of Bosentan 100μM. (A) Gene expression of *collagen I*, (B) Gene expression of *collagen III* and (C) Gene expression of *α-SMA*. The gene expression for *Collagen I, III and α-SMA* in the co-cultured fibroblasts showed no change of gene expression with injury on addition of bosentan (BT). The gene expression for the 'absence of bosentan', showed an increase expression for all genes. Genes; *Collagen III* and *α-SMA* both significantly increased (Bleomycin (BT) vs Bleomycin), ($p<0.05$). Statistical analysis was performed by using a one-way ANOVA with a Tukey post-test. Experiments were conducted in triplicate. n=3 independent biological experiments.

6.5 Discussion

Microarray analysis revealed over 54,000 transcripts was expressed in the epithelial cells and co-cultured fibroblasts. Initially, the criteria for selection of genes of interest, also known as candidate genes, were based on $p<0.05$ with a fold change of >2. However, some genes which did not match the criteria were chosen based on the role they played in IPF. Genes not already known to be involved in IPF may also be of interest. However, they could not be used to validate the 3D model. The candidate genes which are known to play a role in IPF were validated in the 3D-co-culture model, and later be used to identify any novel mediators which may not already be known to be involved in IPF.

The selected genes from both the epithelial monolayer culture and the co-cultured fibroblasts from the microarray dataset predicted IFN α/β pathway genes and fibroblast mediators in the IPA. These genes were all validated by quantitative RT-PCR analysis. The selection IFN α/β pathway genes were based on the genes which were predicted in the Ingenuity Pathway Analysis. For the fibroblasts in the 3D co-culture model, Ingenuity Pathway Analysis predicted five mediators which were associated with the up regulation of the IFN pathway genes in the epithelial cells exposed to bleomycin.

6.5.1 Selection of candidate genes from the microarray dataset

In the epithelial monolayer culture, epithelial cells exposed to bleomycin revealed a stronger expression of genes in the microarray analysis. A selection of candidate genes C/EBP-α, PLCD1, END-1, IL-6, GDPD5 and MAX were all expressed in the epithelial cells exposed to bleomycin. All these candidate genes played a role in IPF and were chosen based on literature. As the data from the co-culture model could be compared to the data from previous studies, this would provide a useful platform for the co-culture model and could be used to identify any novel mediators.

In the 3D co-culture model, genes NMNAT1, C6ORF211 and HIFAN were expressed in both scratch and bleomycin injuries in the fibroblasts. These were validated by quantitative RT-PCR analysis and the analysis revealed the same trend according to

the microarray dataset. The fibroblast gene selection was discarded as there was not enough evidence to support the role of each gene played in IPF.

A further gene selection was validated in tissue sections; IRF-9, END-1 and C/EBP-α. The initial gene selection was based on $p < 0.05$ with a fold change of >2. However, some genes did not match the criteria and were chosen based on the role played in IPF. Literature has also shown that these genes may play an important role in IPF. These genes were validated by quantitative RT-PCR analysis.

Immunohistochemistry was performed to determine the expression of these genes in the normal and IPF lung sections. The lung sections revealed that there was no expression of IRF-9 in normal or IPF tissue. However, this may be due to poor antibody or because the experimental conditions for detection were sub-optimal (Figure 6-6).

C/EBP-α was expressed in both normal and IPF tissue sections showing no difference in expression in both sets of tissue (Figure 6-5). C/EBP-α, is predominantly expressed in the epithelial cells whereas C/EBP-β is expressed in the mesenchymal cells (Berg, Didon et al. 2006). C/EBP-α plays an important role in the protection of the alveolar epithelium after injury (Sato, Xu et al. 2012) and its activity decreases with age (Wang, Shi et al. 2006). The lack of expression of C/EBP-α in the tissue could be due to reduced activity of the transcription factor.

Endothelin-1 is expressed by all cell types and is predominantly expressed in epithelial cells, fibroblasts and endothelial cells. During remodelling in the lung, ET-1 is secreted by epithelial cells, endothelial cells, fibroblasts, alveolar macrophages and leukocytes. This can stimulate a number of cytokines including IL-6, TNF-α, IL-1α (Liang, Yu et al. 2014), which promote cell proliferation and procollagen expression. The lung sections revealed expression for endothelin-1 in the IPF tissue section only (Figure 6-7). This was consistent with the evidence that endothelin-1 plays a role in pulmonary disease (Shi-Wen, Denton et al. 2001).

6.5.2 Pathway Analysis

IFIT1, MX1, OAS1, IFIT3, IFI35, IFITM1 and IRF-9 were genes, which were expressed in the IFN α/β pathway in the epithelial cells. In particular, IFITM1 and IRF-9 genes were of interest as they fitted with the paradigm of IPF. IFITM1 has known to be involved in the transduction of antiproliferative signals by inhibiting cell proliferation in a p53 manner (Yang, Xu et al. 2007). IRF-9 inhibits the anti-proliferative activity of IFN-α among the intracellular JAK-STAT pathway factors (Tsuno, Mejido et al. 2009).

The outcome of the IFNα/β pathway, in epithelial cells led to the proliferation of fibroblasts that was mediated by expression of MDM2, PMAIP1, BST2, SERPINB2 and BIRC5. All these genes were validated by quantitative RT-PCR to confirm the expression of the genes in both cell types. The interesting analysis was that IFNA2 gene was upregulated in both cell types, suggesting that this gene could potentially promote the expression of the fibroblast mediators, MDM2, PMAIP1, BST2, SERPINB2 and BIRC5. MDM2 is cellular regulator of p53. Overexpression of MDM2 can activate p53 and promote cell proliferation in tumour cells (Stommel and Wahl 2005).

SERPINB9 belongs to the large superfamily of serine proteinase inhibitors (serpins), which bind to and inactivate serine proteinases. It is an intracellular inhibitor of Granzyme B that protects activated cytotoxic lymphocytes from apoptosis (Rizzitelli, Meuter et al. 2012). PMAIP1, also known as Noxa, is a Bcl2 protein that is required by the intrinsic apoptotic pathway and induces apoptosis of alveolar epithelial cells (Urich, Soberanes et al. 2009). BST2 regulation can contribute to the downstream event of apoptosis induction and cell proliferation in epithelial cells (Sayeed, Luciani-Torres et al. 2013). Even though IFNA2 was upregulated in fibroblasts and fibroblast mediators were expressed in the ingenuity pathway, these results did not reflect the up-regulation of the gene in the co-culture model.

BIRC5 also known as Survivin is an important member of the inhibitor of the apoptosis protein family (Horowitz, Ajayi et al. 2012). Studies, have shown Survivin, inhibit caspase-dependent and independent apoptotic pathways and accelerate cell proliferation (Ungvari, Hadadi et al. 2012). However, the gene expression observed

in the 3D co-cultured fibroblasts did not fit in with the paradigm of IPF. The ingenuity pathway analysis showed that the gene was down-regulated in the 3D co-cultured fibroblasts.

The IPA had revealed that IFNA2 gene was upregulated in the fibroblasts, which promoted the expression of the fibroblast mediators. To confirm the expression of IFNA2, IFNA1, and IFNB1 in both cell types, quantitative RT- PCR analysis was performed in epithelial cells. The data revealed that the expression of IFNA1, IFNA2 and IFNB1 genes all increased with injury, in particular, with the addition of bleomycin. The interesting fact was that the expression of IFNA1 showed a tenfold increase in the epithelial cells with the addition of bleomycin as compared to the expression of IFNA2. In fibroblasts the IFNA1, IFNA2 and IFNB1 gene expression all decreased with injury. In particular, IFNA2 had shown a significant decrease in expression of the gene in scratch and bleomycin. But when the results were analysed further, it showed that the fibroblasts had a much higher expression of IFNA2 compared to that of epithelial cells. So this confirmed that IFNA2 can potentially promote MDM2, PMAIP1, BST2, SERPINB9 and BIRC5 expression in co-cultured fibroblasts.

6.5.3 The expression of IL-6 in the 3D co-culture model

Literature has shown that IL-6 is a known regulator of the JAK family of tyrosine kinases (JAK1, JAK2 and Tyk2) (Rincon and Irvin 2012), which mediates the phosphorylation and activation of the major transcriptional factors such as the ISGs in the interferon pathway. IL-6 is a small glycoprotein (21 kDa) produced by cells from the innate immune system (e.g. macrophages, dendritic cells, mast cells, neutrophils), as well as secreted by non-leukocytes such as endothelial cells, fibroblasts, astrocytes and epithelial cells (Rose-John, Scheller et al. 2006). IL-6 expression was also determined in epithelial cells and fibroblasts by quantitative RT-PCR analysis. The analysis revealed that there was no trend in gene expression in both injuries. However, the IL-6 gene expression was twenty times higher in the fibroblasts than in the epithelial cells. This could suggest that IL-6 may play a role in

the activation of the IFN α/β pathway. Further experiments are required to confirm the activation of IL-6 in response to IFN α/β pathway.

A recent study had shown that IL-6 activation *in vitro* enhances fibroblast proliferation and extracellular matrix protein production in mice, which are effects relevant in the progression of pulmonary fibrosis (Le, Karmouty-Quintana et al. 2014). Production of IL-6 can be induced by a variety of stimuli such as cell stress/damage, UV irradiation, microbial products, viruses, or other proinflammatory cytokines (Heinrich, Behrmann et al. 2003). Studies in inflammatory diseases have shown increased levels of IL-6 in serum and may be considered as a general marker for inflammation together with TNFα and IL-1β (Gabay 2006). However, it is becoming clear that IL-6 may not just be a pro-inflammatory marker, but an active factor that contributes to the pathogenesis of certain inflammatory diseases such as rheumatoid arthritis and a successful target for some of these diseases (Gabay 2006). IL-6 signalling is determined by binding to IL-6R and forming a complex with gp130. This leads to the activation of the JAK family of tyrosine kinases (JAK1, JAK2 and Tyk2). Activated JAKs then mediate the phosphorylation and activation of the major transcriptional factor regulated by IL-6, STAT3 and MAPK (Heinrich, Behrmann et al. 1998).

Previous studies have demonstrated that IL-6 may be involved in the activation of IRF-9 to mediate signalling of type I IFN α/β (Darnell, Kerr et al. 1994). The study showed that IRF-9 is regulated by IL-6 and is highly expressed in cells with an autocrine IL-6 loop (Erb, Langlechner et al. 2013). A study showed that IL-6 induces IRF-9 by C/EBP-α binding to the interferon-activated transcriptional element. Thus IL-6 was able to prime cells for the response to IFNA2. Stimulation of type I IFN leads to the formation of ISGF3, which consists of STAT1, STAT2 and IRF-9 (Darnell, Kerr et al. 1994). This complex moves to the nucleus where it acts as a transcriptional factor to mediate the expression of IFN stimulated genes. (Tsuno, Mejido et al. 2009) A study has shown that IRF-9 is responsible for the antiproliferative effects of IFNA2 in human ovarian adenocarcinoma. Thus, we can state that IL-6 induces the expression of IRF-9 which in turn mediates the signalling of IFNA2 which has a proliferative

effect (Erb, Langlechner et al. 2013). As there was no trend in IL-6 gene expression in both injuries, further experiments are required to confirm that activation of IL-6 may be involved in the IRF-9, to mediate signalling type I IFN α/β.

6.5.4 The expression of Endothelin-1 in the 3D co-culture model

Endothelin-1 expression increased with injury, which was validated by quantitative RT-PCR analysis. The expression was also determined by immunohistochemistry between normal lung tissue and IPF tissue, confirming increased expression in the IPF tissue. Further investigation of endothelin-1 was carried out in the 3D co-culture model and using an endothelin receptor antagonist bosentan. Bosentan inhibits two receptors of endothelin-1, ET_A and ET_B. ET_A receptors are found on mesenchymal cell types such as vascular and airway smooth muscle cells and fibroblasts. ET_B are on the endothelium (Shi-Wen, Denton et al. 2001). These two receptors work together as well as functioning independently. Bosentan was added to the co-cultured fibroblasts. This was to determine whether inhibition of ET-1 signalling reduced cell proliferation and matrix synthesis in the fibroblasts. Specific concentrations of bosentan were added to the fibroblasts in collagen to determine if the fibroblasts would die. No specific concentration affected the cell viability of fibroblasts in collagen, so 100μM was chosen based on a paper by *Bogatkevich et al 2012*. On addition of bosentan to the co-culture, the cell viability had reduced with injury in fibroblasts. The expression of endothelin-1 was measured in supernatants and it revealed that Bosentan inhibited the injury-induced increase in endothelin-1 production (Figure 6-12).

ET-1 concentration in the supernatants had decreased. This could be due to the fact that bosentan was added to the 3D co-culture model directly in the well compartments with the presence of fibroblasts in collagen. When epithelial cells underwent injury, there may have been a release of ET-1 from epithelial cells. But as the fibroblasts and epithelial cells were exposed to bosentan, no further ET-1 may have been mediated as the receptors were blocked with both cell types. The reason could be that the autocrine and paracrine routes were blocked and no ET-1 could have been released apart from the initial release of ET-1 with scratch and bleomycin injuries. However, the data suggests in the co-culture model, epithelial injury induces

an endothelin-1 mediated increase in endothelin-1 production. Further investigation is required to determine whether epithelial cells or fibroblasts were responsible for the injury-mediated increase in endothelin-1 activity.

6.5.5 Effect of Bosentan on matrix gene expression

The next step was to determine whether addition of bosentan affected matrix synthesis expression in 3D co-cultured fibroblasts (Figure 6-13). The results confirmed that the addition of bosentan inhibits the bleomycin-induced increase in ECM and α-SMA expression in fibroblasts. These data suggests that epithelial injury affects co-cultured fibroblasts response by increasing gene expression of ECM genes and smooth muscle actin, and that this induction is mediated by endothelin.

6.5.6 The role of IFN α/β, Endothelin-1 and BIRC5 in the 3D co-culture model

A study, by *Shi-wen et al*, demonstrated *in vitro* that ET-1 promoted fibroblast activation and ECM synthesis of collagen I and III by a mechanism dependant on both receptors, ET_A and ET_B (Shi-Wen, Denton et al. 2001). Additional studies have shown the relationship between BIRC5 and ET-1. Studies have also shown that BIRC5 expression is increased by endothelin-1 and that inhibition of BIRC5 reverses the anti-apoptotic effects of ET-1 (Horowitz, Ajayi et al. 2012). In our microarray study, BIRC5 was down-regulated in the fibroblasts but ET-1 expression was upregulated in the fibroblasts with both levels of injury. The data showed that when an antagonist bosentan was added to the 3D co-culture model, ET-1 expression, and collagen I and III were decreased in fibroblasts. There was also reduced expression of α-SMA in the fibroblasts confirming that there may be reduced cell proliferation with injury. Studies have shown that BIRC5 expression does play a role in IPF, particularly with the mesenchymal cells, and ET-1 mediates the up regulation of the BIRC5 through the activation of FAK and PI3K/AKT regulating cell survival (Horowitz, Ajayi et al. 2012). However, this theory did not match our data, suggesting that BIRC5 may not be regulated in the co-culture model by ET-1 and that ET-1 expression may be regulated by other mediators or by an autocrine loop which increases cell proliferation and matrix synthesis in the co-culture model.

The Ingenuity Pathway Analysis had predicted that IFNA2 inhibited the expression of BIRC5 in the 3D co-culture model with the addition of bleomycin injury. Studies have shown that BIRC5 inhibits the caspase dependant apoptotic pathways and caspase-independent apoptotic pathways which interferes with the G2-M boundary and leads to a defect of the cell cycle. This resulted in multinucleated polyploidy cells (Altznauer, Martinelli et al. 2004). BIRC5 shuttles between the nucleus and the cytoplasm where it binds to mitochondrial activator of caspase and inhibits apoptosis (Sisson, Maher et al. 2012). Studies have shown that BIRC5 acts as a link between the apoptosis machinery and the check-points that control mitotic progression. Thus deregulated expression of BIRC5 has oncogenic potential by enabling cells to overcome the G2-M checkpoint and progress through mitosis thereby providing cells with a mechanism to evade checkpoint-controlled apoptosis (Altznauer, Martinelli et al. 2004) and accelerating cell proliferation (Liu, Brouha et al. 2004).

Studies have shown that BIRC5 has been extensively over-expressed during tumorigenesis and has been identified as a candidate for cancer therapy (Altieri 2010). Previous studies have shown BIRC5 implicated in inflammatory responses (Ungvari, Hadadi et al. 2012) and pathogenesis of asthma (Ungvari, Hadadi et al. 2012) and more recently BIRC5 contributes in the pathogenesis of IPF (Sisson, Maher et al. 2012). In this study, ingenuity pathway analysis had predicted that IFNA2 inhibited the expression of BIRC5 in fibroblasts. The results showed that BIRC5 was down-regulated with injury in particular, with bleomycin. The quantitative RT-PCR data also confirmed that BIRC5 was not expressed as much as the other fibroblast mediators. There was a small expression of BIRC5 which may suggest that it may be involved in cell proliferation in fibroblasts as previous data has shown but not with inhibition of apoptosis. Further experimental work and analysis is required to conclude the relationship of BIRC5 and cell proliferation in the 3D co-culture model.

6.6 Summary

In summary, the IPA predicted a strong expression of interferon α/β pathway in the epithelial cells injured with bleomycin. A further IPA analysis predicted fibroblast mediators that may be involved in cell proliferation and matrix synthesis processes. A selection of genes in the epithelial cells was upregulated in the scratch and bleomycin injuries and expression of endothelin-1 was upregulated in the epithelial cells for both injuries. There has been extensive research on endothelin-1 in animal and human studies and it would be interesting to investigate how this molecule would play a role in our model.

In the 3D co-culture model, inhibiting endothelin-1 receptors showed down regulation of cell proliferation and matrix synthesis gene expression in co-cultured fibroblasts treated with bleomycin. The mechanism from interferon α/β pathway to the production of endothelin-1 still remains unclear but a possible theory could be that the interferon α/β pathway is activated through epithelial injury, but simultaneously endothelin-1 is released via an autocrine loop and activates cell proliferation /matrix synthesis. IPF is a multifunctional disease therefore; more than one pathway or mediator can be implemented in the disease.

Chapter Seven

Discussion

7.1 Discussion

In this study, a novel *in vitro* 3D co-culture model was developed to mimic the epithelial-mesenchymal microenvironment. The model was optimised and validated to study the crosstalk of injured epithelial cells and fibroblasts in a non-contact system. The study involved analysing mRNA expression of the epithelial cells in monolayer culture and fibroblasts in a 3D co-culture model system. This system may provide a useful insight into the potential epithelial mediators after epithelial cell wounding and the effects on fibroblasts.

The 3D co-culture model consisted of small airway epithelial cells in the Transwell® insert and normal human lung fibroblasts in collagen separated by a porous membrane in a Transwell® system. The use of SAEs rather than primary alveolar type II (ATII) cells was a limitation of this model. Using ATII cells rather than SAEs may have given an accurate approach, as ATII cells have an excellent biological function by upregulation of cytokines, chemokine, and adhesion molecule at gene and protein levels in response to stimuli i.e. TNF-α, (Mao, Wu et al. 2015). The use of ATII cells may have provided a useful tool to study inflammatory responses. However, given the difficulties in obtaining and maintaining primary human ATII cells in their physiological state *ex vivo*, this system provides a means to study the behaviour of cell types from normal lungs in the model.

It is known that ATI and ATII epithelial cells are damaged during inflammation with pulmonary fibrosis as well other diseases such as Acute Lung Injury (ALI). The use of ATII cells in *in vitro* studies have been limited and found to be difficult to retrieve and maintain. One of the limitations of ATII cells *in vitro*, is that the cells quickly transdifferentiate (i.e. lose their ATII cell–specific markers and gain "ATI-like"–specific markers) and do not proliferate in cell culture conditions (Suga, Iyonaga et al. 2000).

Previous studies have attempted to promote ATII cell proliferation *in vitro (Ley, Brown et al. 2014)*. *In vivo*, fibroblasts are located beneath the alveolar lung epithelium and during injury, interact with ATI and ATII cells through gaps within the

basement membrane (Serrano-Mollar 2012). During the interaction, fibroblasts secrete soluble factors for example; keratinocyte growth factor (KGF) that has been reported to limit trans-differentiation and to promote ATII cell proliferation (Rackley and Stripp 2012). Studies have shown that ATII cells co-cultured with human or rat fibroblasts or exposed to KGF exhibited surfactant mRNA expression *in vitro*, suggesting that KGF (added or presumably secreted by fibroblasts) was an important part for retaining ATII cell differentiation *in vitro* (de Lauretis, Veeraraghavan et al. 2011). The failure of retrieving as well as maintaining human primary ATII cells significantly limits the number of studies designed to elucidate the pathogenesis of human alveolar diseases. In this 3D co-culture model, to overcome the differentiation of the epithelial cells, the cells could have been embedded in collagen or grown on a matrix to generate aggregates comprised of polarized epithelial cells.

The fibroblasts used in the 3D co-culture model were undifferentiated. The fibroblasts were cultured in collagen type I. Collagen is a major component of the ECM complex and will mimic the basement membrane for the cells as well as initiating signalling events, 'crosstalk' between the cells (Schuliga, See et al. 2009). The advantage of culturing the fibroblasts in collagen is that collagen provides an environment similar to that of *in vivo* conditions, providing a natural substrate for cellular attachment, growth and differentiation, and also promoting cellular proliferation and differentiation (Ruszczak 2003). Fibroblasts cultured in a collagen gel (3D) have distinct characteristics compared to those cultured without collagen (2D) (Mio, Adachi et al. 1996). The fibroblasts cultured in gels acquire a bipolar spindle form, while fibroblasts without manifest a ruffled membrane that possess one or more broad, flattened features (Mio, Adachi et al. 1996).

The 3D co-culture model was designed to closely replicate *in vivo* biology of pulmonary fibrosis with basic co-culturing of two different cell lines. This was to understand the individual interactions of the injured epithelial cells and their effect on fibroblasts in the 3D co-culture model. To achieve this, both cell lines were undifferentiated and the fibroblasts were cultured in collagen. The model could have been improved by using differentiated epithelial cells and fibroblasts to screen for

more soluble mediators. The fibroblasts could had been cultured in Matrigel, which would had allowed for nutrient, gas, and signal exchanges among cells and mimic ECM conditions. Matrigel is a mixture of extracellular matrix secreted by Engelbreth-Holm-Swarm mouse sarcoma cells and contains ~1,800 proteins (Hughes, Postovit et al. 2010), which makes it a difficult to identify what is exactly responsible for maintaining cell phenotypes.

A previous study by *Prasad et al*, *2014* had developed a similar model to demonstrate the effect of fibroblast phenotype on response to epithelial injury. The model consisted of A549 (lung epithelial cells) and fibroblasts attached on either side of the Transwell® insert coated with collagen. The scratch wound was created by a usage of a sterile pipette tip across the insert. The transmigration of the fibroblasts across the Transwell® into the denuded area was assessed. The limitation of this system was that the cells were in contact with one another and therefore, an independent role in fibroblast -epithelial interaction could not be examined. The implication of using a direct contact method provided a challenge by evaluating and analysing each cell type separately in the model. Therefore, in our 3D co-culture model the cells were separated to investigate the crosstalk of epithelial-fibroblast in response to injury.

7.1.1 The type of injuries used in the 3D co-culture model

To understand the two independent responses from two cell types, it would be important to initiate an independent injury response from epithelial cells i.e. soluble mediators and what effect they may have on fibroblasts. The injuries selected were scratch wound to mimic mechanical injury and addition of bleomycin, which is a well-known drug that induces pulmonary fibrosis.

The model demonstrated that, in response to epithelial injury, fibroblast cells showed altered responses i.e. cell proliferation, matrix gene expression and cytokine production. Repetitive injury methods were established including scratch wound to mimic mechanical injury (Wadsworth, Nijmeh et al. 2006), carbon black particles (Doornaert, Leblond et al. 2003) and bleomycin to represent a well-established bleomycin-induced injury in animal models (Umezawa, Ishizuka et al. 1967).

An inflammatory response was determined using IL-1α as a pro-inflammatory marker, which was released by damaged epithelial cells. A previous study demonstrated that IL-1α is the major epithelial alarmin released from injured epithelial cells to induce inflammatory mediators in fibroblasts (Tracy, Bowman et al. 2012). A study by *Suwara et al*, *2014*, demonstrated that Interleukin-1α was a key alarmin released from endoplasmic reticulum (ER) stress-damaged epithelial cells (Suwara, Green et al. 2014). In the 3D co-culture model, repetitive injury to the epithelial cells monolayer culture by either scratch wounding or administration of bleomycin over the 7 days was able to show an increased response of IL-1α without the cells dying.

The administration of carbon black on epithelial cells revealed that the IL-1α response remained the same during the duration of the experiment. There was no increase in IL-1α response in the 3D co-culture model. The reason for this could be that the carbon particles did not penetrate epithelial cells. Previous studies have demonstrated that alveolar macrophages and bronchial epithelial cells can amplify an immune response to urban air particles (Muller et al. 2010). However, in this model, manufactured ultrafine carbon black particles were used and as the model only consisted of two cell types, epithelial cells and fibroblasts, this may not have been enough to promote an immune response.

The limitation of the usage of ultrafine carbon black particles could also because the concentrations of the ultrafine carbon black particles used may have been on a higher level compared to the concentrations that may reach these cells upon inhalation *in vivo*. Previous studies have shown that ultra-fine particles, in contrast to larger-sized particles, are less efficiently cleared from the lung, implying that there is the possibility that these particles may accumulate in the lung during prolonged exposure (Moeller et al., 2008). Furthermore, ultrafine carbon black particles are considered to be of low toxicity in comparison with ultrafine particles in the ambient air, to which several components are likely to enhance the toxicological potential in the lung (Schwarze, Totlandsdal et al. 2013).

Another reason why there may have not been an alarmin response to the addition of carbon black particles is that only two cell types were used in the model. Epithelial cells may not have amplified a response to the carbon black particles. Usually in the lung, activated immune cells including neutrophils and macrophages, release cytokines, reactive oxygen species (ROS), lipid mediators, and toxic proteases, which may amplify and contribute to any DEP-induced epithelial damage (Schwarze, Totlandsdal et al. 2013). The model could have been improved further, by expanding the selection of injuries i.e. acid to mimic gastroesophageal reflux (GER) or smoke particles to mimic cigarette smoking.

7.1.2 The effect of epithelial cell injury on fibroblasts

It is becoming increasingly recognised that IPF arises as a result of a highly aberrant wound healing response following repetitive epithelial cell injury in susceptible individuals (Selman and Pardo 2002). In turn, myofibroblasts provoke basement membrane disruption and alveolar epithelial cell (AEC) apoptosis is prevented thus perpetuating the damage and preventing appropriate re-epithelialisation. This could be termed as 'epithelial–mesenchymal crosstalk', which is a fibroproliferative disorder proceeded by alveolar epithelial cell injury and activation, with fibrotic foci at primary sites of injury and aberrant repair in IPF (Borensztajn, Crestani et al. 2013).

The underlying mechanisms leading to fibrotic foci in IPF are still unclear. The processes include, proliferation and differentiation of resident fibroblasts and myofibroblasts (Katzenstein 1985), excessive accumulation of the matrix, predominantly Collagen I and III (Laurent, Harrison et al. 1988), along with decreased fibroblast apoptosis (Uhal, Joshi et al. 1998, Kuwano, Miyazaki et al. 1999).

In this study, we demonstrated an injury response by measuring alarmins e.g. IL-1α, with repetitive injury to the epithelial cells (Refer to section 7.2.1). The effect of epithelial cell injury on fibroblasts was further analysed i.e. fibroblast proliferation and matrix synthesis (Refer section 7.1.3).

7.1.3 Fibroblasts in response to epithelial cell injury

In the 3D co-culture model, scratch and bleomycin injury to the epithelial cells increased the rate of proliferation of fibroblasts in collagen (Figure 3-2). MTT reduction assay measured cell viability and the Ki-67 expression revealed an increase of cell number and proliferation with injury (Figure 3-3). The expression of extracellular matrix genes in fibroblasts in response to epithelial cell injury was assessed and revealed that the gene expression of *collagen I* and *collagen III* had significantly increased in fibroblasts (Figure 3-13). In order to relate matrix gene expression to fibroblast differentiation, the expression of α-SMA was analysed. This revealed that α-SMA expression had also increased in fibroblasts (Figure 3-12). Previous studies have shown that myofibroblasts are highly synthetic for collagens and other ECM components, and are characterised by the *de novo* expression of α-SMA (Scotton and Chambers 2007).

The next approach was to investigate whether epithelial cell injury protected fibroblasts from apoptosis. Initially a suitable concentration of treatments on the fibroblasts was identified. A MTT reduction assay was used to measure the cell viability and a PARP cleavage assay was used as a marker for apoptosis of the fibroblasts. The study identified that IL-6 and Fas-L decreased cell viability of fibroblasts cultured in collagen in 24 hours without the presence of epithelial cells, whereas the addition of TNF-α and IFN-γ showed no significant effects on fibroblasts cultured in collagen. Staurosporine was used as a pro-apoptotic agent and revealed that cell viability had decreased in fibroblasts (Figure 3-14).

Further analysis was carried out to observe the effect of IL-6, Fas-L or Staurosporine on cultured fibroblasts (which was exposed to injured epithelial cells). IL-6, Fas-L or Staurosporine was added for 24 hours and fibroblast proteins were extracted to observe the expression of cleaved poly (ADP-ribose) polymerase (PARP) by western blotting. The cells treated with staurosporine demonstrated PARP cleavage; hence the fibroblasts were undergoing apoptosis (Figure 3-16). Overall, injury to epithelial

cells did not protect the fibroblasts from staurosporine induced apoptosis judged by PARP cleavage in fibroblasts.

A study by *Moodley et al*, *2004* demonstrated that myofibroblasts isolated from the lungs of IPF patients are capable of releasing numerous pro-fibrotic mediators, in particular, IL-6 signalling in IPF-fb may enhance the resistance to apoptosis (Moodley, Scaffidi et al. 2003). In addition, when cultured *ex vivo* they are more resistant to apoptosis (Moodley, Caterina et al. 2004).

The 3D co-culture model demonstrated proliferation and ECM expression in fibroblasts. However, the model was unable to demonstrate the protection of apoptosis in fibroblasts. The model consisted of two cells; epithelial cells and fibroblasts. The usage of two cell types alone in this model may not be suitable to observe the mechanism of apoptosis. Using a model with immune cells may have provided a more complete model to explore the mechanisms of apoptosis.

7.1.4 The expression of MMPs in the 3D Co-culture model

MMPs have a diverse set of functions. Apart from degrading components of the extracellular matrix, they are able to release, cleave and activate a wide range of growth factors, cytokines, chemokines and cell surface receptors affecting numerous cell functions including adhesion, proliferation, differentiation, recruiting and transmigration, and apoptosis. Therefore, dysregulated expression of MMPs may have a profound impact on the biological mechanisms implicated in the development of IPF (Vij and Noth 2012).

The MMPs are mostly secreted by cells as inactive precursors. The inactive form of the MMP is dependent on the 'cysteine switch' in the propeptide domain and is formed when interaction of a conserved cysteine in the propeptide with the zinc blocks the access of the catalytic site to the substrate (Greenlee, Werb et al. 2007). Although the MMPs are activated by proteases (e.g. MMP-1), several MMPs are also activated by other matrix metalloproteinases (e.g. MMP-3). The ability of MMPs to activate each other creates a complex network of proteases in the extracellular space (Greenlee,

Werb et al. 2007). Another example is that activation of MMP-2 on the cell surface depends on the binding of pro-MMP-2 to MMP-14 and TIMP-2. This complex holds the zymogen in place, allowing a second active MMP-14 to cleave the prodomain and release the activated MMP-2 (Henderson, Markwick et al. 2007).

The pathophysiological roles of MMPs in IPF have been debated but the end result always seems to be contradicted and suggests that MMPs are not a simplistic concept. In this study, a selection of MMP expressions were compared in the co-culture model after inflicting various injuries and to determine whether there was a correlation of MMP expression with injury.

MMPs were selected based on the literature and evidence. For example, studies have reported that MMP-1, -2 and -7 are elevated in the serum and MMP-3, -8 and -9 are elevated in the bronchoalveolar lavage fluid (BALF) in patients with IPF (King, Pardo et al. 2011). Immunohistochemistry studies in IPF tissues have identified most MMPs are localised in the AEC and few are in the fibrotic foci (King, Pardo et al. 2011).

The expression of MMP-1, 2, 7 and 9 (among the most highly expressed genes in IPF) were measured by ELISA and gelatin zymography. The expression of MMP-9 was measured further in serum samples to determine a possible biomarker for fibrosis. In particular, these MMPs were chosen based on a study by *Kim et al*, demonstrating MMP-2 and -9 may play important roles in the different stages of IPF (Kim, Choeng et al. 2009), and MMP-1 and -7 studied by *Rosas et al*, demonstrated these two MMPs may be potential biomarkers in IPF (Rosas, Richards et al. 2008).

MMP-1 expression was determined in the epithelial monolayer culture and 3D co-culture model with injury. This was to investigate whether MMP-1 expression increased with repetitive injury. MMP-1 expression in supernatants was measured by ELISA. In the epithelial cell monolayer supernatants, MMP-1 expression increased with the injury; scratch vs no injury and bleomycin vs no injury, both with a significant increase. In the 3D co-culture model MMP-1 expression revealed no particular trend with various injuries (Figure 4-1B). Previous studies have

demonstrated that MMP-1 is able to cleave fibrillar collagens (type I and III) which are the most abundant ECM molecules in IPF (Pardo, Selman et al. 2008). However, further studies have shown that MMP-1 is primarily localised in the reactive alveolar epithelium in IPF lungs and is virtually absent in the interstitial compartment where collagens are accumulating (Herrera, Cisneros et al. 2013). In this study, this would explain no particular trend of MMP-1 in the 3D co-culture model with a possible effect coming from the fibroblast cells. However, the specific mechanisms by which MMP-1 has an influence on cell migration, proliferation and apoptosis in IPF still remains unclear (Herrera, Cisneros et al. 2013).

MMP-7 expression was determined in the epithelial cell monolayer and co-culture model with injury. This was to investigate whether MMP-7 expression increased with repetitive injury. MMP-7 expression in supernatants was measured by ELISA. MMP-7 expression decreased with injuries; scratch vs no injury and bleomycin vs no injury with a significant decrease ($p<0.05$), (Figure 4-3). The same trend was observed for the injuries in the 3D co-culture model. However, there was an increase in expression of MMP-7 in the non- treated fibroblasts, suggesting that MMP-7 is predominantly expressed by fibroblasts. This could suggest that culturing epithelial cells with fibroblasts reduces expression of MMP-7.

The low expression of MMP-7 from the epithelial cells may be partly due to the cells not being differentiated. Previous studies have shown that MMP-7 is correlated with the increased expression of E-cadherin (McGuire, Li et al. 2003). As the epithelial cells were not differentiated in this study, there was no difference in expression of MMP-7 with injury. However, the data does reveal the independent response of the epithelial cells with no contact from the fibroblasts, suggesting fibroblast crosstalk may be necessary for epithelial cell differentiation which may initiate soluble mediators.

Furthermore, the expression of MMP-7 increased from the fibroblasts alone as compared to a decrease in expression of MMP-7 in the co-culture model. The reason for this could be that TIMP-1 may have inhibited the MMP-7 expression in the co-

culture. As previously shown TIMP-1, expression decreased with injury (refer to section 4.4.5).

The expression of MMP-2 in supernatants was measured by gelatin zymography. This was to investigate whether there was expression of MMP-2 with repetitive injury. The analysis revealed there was no significant difference in the expression of active MMP-2 with the injuries in the monolayer culture, and the 3D co-culture model supernatants. These data suggest that both epithelial cells and fibroblasts cleave similar amounts of active MMP-2 (Figure 4-6).

Previous studies have shown increased expression of MMP-2 in injured reactive epithelial cells and fibroblast foci (King, Pardo et al. 2011). Further studies have shown MMP-2 from airway epithelial cells induce the proliferation of fibroblasts (Xu, Benyon et al. 2002). The main finding in the 3D co-culture model is that active MMP-2 expression is not selective for both cell types and they express the same amount of MMP-2. Also, the results could suggest that MMP-2 may support the role of mediating crosstalk between epithelial cells and fibroblasts.

The expression of MMP-9 in supernatants was measured by gelatin zymography. In the 3D co-culture model, there was expression of only pro-MMP-9 from the fibroblasts, which decreased with injury (Figure 4-9). In epithelial cells in the monolayer culture, there was expression of both pro and active MMP-9. The expression of pro-MMP-9 increased with injury whereas active-MMP-9 decreased with injury from the epithelial cells. Previous studies have shown MMP-9 is released by epithelial cells in the early stages of injury and aids migration of the epithelial cells to the site of injury (Kim, Choeng et al. 2009). Another study has shown MMP-9 is one of the lower expressed MMPs in pulmonary fibroblasts compared to dermal fibroblasts (Lindner, Zietsch et al. 2012). Overall, the results could suggest that MMP-9 may play an important role in the early stages of injury in the 3D-co-culture model.

The gene expression analysis of *MMP-3* and *TIMP-1* in fibroblasts was measured by quantitative RT-PCR analysis. This was to determine the expression of MMP-3

(activator of MMP-9) and TIMP-1 (inhibitor of MMP-9) in the 3D co-culture model system. The data revealed that both genes *MMP-3* (Figure 4-14) and *TIMP-1* (Figure 4-15) had decreased in co-cultured fibroblasts with injury. This confirmed the decreasing pro-MMP-9 may be from the co-cultured fibroblasts (refer to section 4.4.4) and TIMP-1 may be inhibiting the effect of MMP-9. However, in epithelial cells the pro-MMP-9 had increased with injury (Figure 4-10). Previous study has shown that accumulation of pro-MMP-9 may be associated with decreasing TIMP-1, as not enough TIMP-1 is expressed for its catalytic domain to interact with the hemopexin domain of pro-MMP-9 (Nagase, Visse et al. 2006).

Another explanation could be that TIMP-1 is released by eosinophils, mast cells, monocytes and macrophage; all cells of the inflammatory response. Thus, the 3D co-culture model did not contain immune cells, hence lower TIMP-1 expression in the co-cultured fibroblasts.

Previous studies have shown that TIMP-1 may form a complex with pro-MMP-9 (Manoury, Caulet-Maugendre et al. 2006). The TIMP-1/pro-MMP-9 complex, is thought to recruit MMP-3, forming a stable ternary complex that causes MMP-3 inactivation (Stamenkovic 2003). MMP-3 is the most efficient activator of MMP-9 (Giannandrea and Parks 2014). This may have also affected the MMP-9 expression in the 3D co-culture model.

MMP-9 expression was further determined in IPF tissue, suggesting that MMP-9 is present in both epithelial cells and fibroblasts, whereas α-SMA was co-localised to the fibroblasts (Figure 4-16 & 4-17).

7.1.4.1 Expression of MMP-9 in IPF serum

Previous studies have been conducted using BALF or serum from IPF patients to investigate the presence of various MMPs and potential biomarkers (Rosas, Richards et al. 2008). A study by *Lemjabbar et al*, *1999* investigated the expression of MMP-9 in BALF in IPF patients and revealed that MMP-9 expression was increased in both the cellular and extracellular levels (Lemjabbar, Gosset et al. 1999). In this study, the

expression of MMP-9 was analysed in non-IPF and IPF serum samples by zymography and ELISA. This was to determine whether there was any correlation with MMP-9 expression in serum with non-IPF and IPF patients along with lung function data.

The zymography data revealed that there was expression of both pro and active MMP-9 from the serums samples in all three groups: alive-IPF, dead-IPF (had died since receiving the patient information) and non-IPF (control), (Figure 4-18). Total MMP-9 expression was measured in the serum and revealed that there was a slight increase of total MMP-9 in the dead-IPF serum samples but there was no significant difference between control (non-IPF) and alive-IPF serum samples (Figure 4-21). The ratio of pro to active MMP-9 was compared to determine if there was a difference of MMP-9 activation within each group (Figure 4-20). There was no significant difference of MMP-9 activation for each group even though a slight increase was seen in the dead IPF samples, $p<0.058$.

Lung function data were analysed for alive-IPF and dead-IPF patient samples correlating to the serum samples. This was to determine the relationship between lung function and MMP-9 expression of the patients with IPF (alive & dead only). The analysis revealed that %TLCO for both males and females in both groups (alive-IPF & dead-IPF), was significantly reduced. However, for dead-IPF samples there was a lower %TLCO for males (~40%) and females (~30%), (refer to section 4.5.3).

The active-MMP-9 expression was compared to the %TLCO for both alive and dead serum samples of IPF patients. The data revealed there was a positive correlation between active-MMP-9 expression (alive and dead groups) and %TLCO with statistical difference with $r^2= 0.09857$ and $p<0.0234$ (Figure 4-24;B). Further analysis was performed to determine which gender and which group may be causing a positive correlation. The data revealed that active MMP-9 was positively correlated with alive-men with IPF, with $r^2= 0.2211$ and $p<0.0489.$ Further studies will need to confirm whether TIMP-1 and MMP-9 or TIMP-1 and %TLCO correlate in the serum sample of IPF.

Overall, in this study, the expression of MMPs was evaluated in the 3D co-culture model with epithelial cells and fibroblasts. The epithelial cells were inflicted with injury and either cells or supernatant were analysed to determine the expression of various MMPs. The expression of MMPs was evaluated in the 3D co-culture model by ELISA, zymography and at transcriptional level, by quantitative RT-PCR analysis. There was expression of MMP-1 and 7 in the supernatants in the 3D co-culture model; MMP-1 expression revealed no particular trend with various injuries and MMP-7 expression revealed decreased with injuries; scratch and bleomycin.

MMP-2 expression decreased with injury possibly suggesting that MMP-2 is inhibited by fibroblasts by a negative autocrine loop. Previous studies have shown growth factors such as PGDF-BB may be involved in the inhibitory response of MMP-2 (Risinger, Updike et al. 2010). The varied expression of MMPs may have suggested that MMPs differ in the roles promoting or attenuating the fibrotic responses. They may have differing impacts from various cell types, location of activity, target of substrate or the level of expression of the enzyme to turn on different pathways in response to injury (Yao, Lemjabbar et al. 1999).

MMP-9 expression in serum between non-IPF, alive-IPF and dead-IPF patients showed no difference in expression. But there was a correlation with the MMP-9 and %TLCO. MMP-9 expression and %TLCO could possibly be used as a biomarker for predicting the disease. Using this non-invasive method as well as other patient demographic information may be a possible approach to evaluating the inflammatory tissue remodelling patterns in IPF.

Lung remodelling in IPF is a dynamic pathological process and could suggest that the activities of MMPs vary during the course of the disease as well as with different cell types. The metalloproteinase system is complex with activating proteinases and inhibitors interacting with the functions of MMPs involving non-catalytic domains and can even occur in intra-cellular locations. Further studies are required to determine whether MMP-9 activity is central to lung destruction in IPF or whether there is a more selective target as individual proteases or their substrates could reduce lung

destruction (Atkinson and Senior 2003). The knowledge of the role of MMPs is still not clear and further research is needed to understand the dynamics of MMPs in IPF.

7.1.5 Data analysis of DNA Microarray

The next step was to examine the transcriptional profiling of epithelial cells and fibroblasts. RNA was sent to Epistem, Manchester, UK for DNA microarray analysis. The microarray allowed the simultaneous determination of the mRNA levels of many genes in scratch and bleomycin treated cells i.e. epithelial cells alone and in 3D co-cultured fibroblast cells. The DNA microarray identified genes whose mRNA levels were different under biological conditions e.g. in response to treatments or in different cell types. Such genes are often considered 'candidate genes' in the biological process of interest, in this case, epithelial cell injury on fibroblasts. Array Studio software was used to perform data analysis on the microarray data to determine differential gene expression in the individual cell type.

Principal Components Analysis (PCA) was performed to determine similar patterns of the sample or treatment for each cell type. The PCA for epithelial cells revealed that the individual treatments were within the parameters in PCA, but only bleomycin treated epithelial cells were clustered together. This suggested that only epithelial cells exposed to bleomycin showed a positive correlation. The PCA for co-cultured fibroblasts revealed that the expression of individual treatments had a variable direction and were not consistent between treatments. The PCA for the experiments showed that only one experiment was clustered together (refer to section 5.4.2.1). The treatments for co-cultured fibroblasts varied in PCA direction, especially injury with bleomycin.

Hierarchical clustering was based on the PCA for both cell types and took into consideration the differential gene expression for the individual treatments. The hierarchical clustering heat map revealed that the epithelial cells treated with bleomycin had a stronger gene signature on overall gene expression. This supported the PCA for the epithelial cells treated with bleomycin as it previously shown that the treatments were clustered together (Figure 5-11).

The microarray data were transferred to a spreadsheet and were analysed within groups for each cell type using $p<0.05$ and fold change >2 as criteria (Figure 5-2). The categories for 3D co-cultured fibroblasts i.e. NHLFs vs no-injury, scratch vs no-injury vs, bleomycin vs no-injury, the same comparisons were performed for epithelial cells in the monolayer culture i.e. no-injury vs scratch and bleomycin vs no-injury. The groupings of the data were to correlate with the treatments with differentially expressed genes for each cell type. Even though there was no difference in variation with the bleomycin treated epithelial cells with co-cultured fibroblasts, the data were analysed to support the bleomycin treated epithelial cells and to determine gene expression changes with injury.

7.1.5.1 Differential genes changes for each cell type

The gene expression changes as a result of injury were displayed using Venn diagrams. For the epithelial cell altered genes; scratch vs bleomycin ($p<0.05$), 226 genes were common to both injuries (Figure 5-7). The genes were selected based on the role they may play in IPF. These genes in epithelial cells were: (1). CCAAT/enhancer binding protein (*C/EBP*), alpha (CEBPA), CEBP-α transcriptional factor which regulates differentiation and proliferation in the epithelium (Berg, Didon et al. 2006) and *CEBP*α mainly detected in the epithelium and *CEBP*β in mesenchymal cells (Sato, Xu et al. 2012). (2). Endothelin–1 (EDN-1) released by epithelial cells induces fibroblast proliferation and ECM synthesis (Boscoe, Goodwin et al. 2000). (3). Keratin (KRT) is a known surface marker for epithelial cells which can give rise to regenerative epithelial cells in response to lung injury (Willis, Liebler et al. 2005).

In fibroblasts 144 genes were differentially expressed and common to both injuries, scratch vs bleomycin ($p<0.05$) (Figure 5-10). The genes were selected based on their role in IPF. These genes in fibroblasts were: (1). Nicotinamide nucleotide adenylyl transferase 1 (*NMNAT1*). NMNAT-1 is a central facilitator of redox reactions in the mitochondrial electron transport chain, which influences many cellular processes such as the cell cycle, and catalyses the formation of the essential cofactor nicotinamide adenine dinucleotide (NAD). Over-expression of *NMNAT-1* has been shown to extend

the lifespan of cells. NMNAT-1 in HeLa cells modulates the behaviour of poly (ADP-ribose) ation protein 1 (PARP1) an enzyme essential in processes such as DNA repair and programmed cell death. This association of NMNAT-1 with activated PARP1 can also enhance the relocation of apoptosis inducing factor (AIF) from the mitochondria to the nucleus, thereby triggering apoptosis (Emblom-Callahan, Chhina et al. 2010). (2). Chromosome 6 open reading frame 211 (C6orf211), had been associated with a proliferation metagene in tumours (Dunbier, Anderson et al. 2011). (3). Hypoxia inducible factor 1, alpha subunit inhibitor (HIF1AN), a transcription factor that functions as a master regulator of oxygen homeostasis, has been implicated in fibrogenesis (Ueno, Maeno et al. 2011).

7.1.5.2 Gene Selection

In the epithelial monolayer culture, epithelial cells exposed to bleomycin revealed more genes were up-regulated in the microarray database. A selection of the genes, C/EBP-α, END-1 and Keratin, were all upregulated in the epithelial cells exposed to bleomycin. Endothelin-1 was of particular interest as a study by *Shi-wen et al*, demonstrated that endothelin-1 has profibrotic effects on lung fibroblasts, promoting proliferation, differentiation and ECM synthesis (Shi-Wen, Denton et al. 2001). In fibroblasts in the 3D co-culture model, genes NMNAT1, C6ORF211 and HIFAN were upregulated in both scratch and bleomycin injuries. These genes were validated by quantitative RT-PCR analysis, and the results revealed that these genes had similar changes in expression compared to the microarray dataset.

7.1.6 Pathway analysis

Ingenuity Pathway Analysis (IPA) allowed further insights into the mediators and pathways relevant to both cell types according to injury. The Canonical pathways analysis in epithelial cells exposed to bleomycin revealed three top pathways; IL-6 signalling pathway, TGF-β pathway and interferon pathway. To determine the predicted canonical pathway, co-cultured fibroblast gene expression data were analysed. The upstream regulator analysis was performed and revealed activation of the interferon α/β pathway was compatible with epithelial cells exposed to bleomycin.

The analysis also revealed IFN α/β pathway related upregulated genes in epithelial cells exposed to bleomycin which were *IFNA2, IRF7, IFNG, IFNL1, STAT1, IRF3, IRF1, IRF5, IFNA1* and *IFNA13*. The IPA further identified genes downstream of *IFNA2* gene; SERPINB9, PMAIP1, MDM2, BST2 and BIRC5 which were expressed in bleomycin treated co-cultured fibroblasts. According to the IPA, *IFNA2* gene was strongly upregulated by epithelial cells treated with bleomycin and was driven by these cells to mediate gene expression in the co-cultured fibroblasts (Figure 5-13).

The genes identified by IPA were validated by quantitative RT-PCR. The series of interferon stimulated genes (ISGs) data from RT-PCR analysis, revealed a similar trend of the genes; IFIT1, MX1, OAS1, IFIT3, IFI35, IFITM1 and IRF-9 in the epithelial cells exposed to bleomycin. In particular, genes IFITM1 and IRF-9 were of interest in the context of IPF. IFITM1 has known to be involved in the transduction of antiproliferative signals by inhibiting cell proliferation in a p53 dependant manner (Yang, Xu et al. 2007). IRF-9 inhibits the antiproliferative activity of IFN-α amongst the intracellular JAK-STAT pathway factors (Tsuno, Mejido et al. 2009).

The quantitative RT-PCR of MDM2, PMAIP1, BST2, SERPINB2 and BIRC5 analysis revealed that there was expression of these genes (mentioned above) in the co-cultured fibroblasts exposed to epithelial cell injury (Figure 6-4). The analysis confirmed the expression of the genes in fibroblasts and showed a similar trend of gene expression as the Ingenuity Pathway Analysis. Interestingly, *IFNA2* gene was upregulated in both epithelial cells and fibroblast cells. This could suggest that this gene could potentially have promoted the expression of the fibroblast mediators, MDM2, PMAIP1, BST2, SERPINB2 and BIRC5, in the co-cultured fibroblasts.

Further quantitative RT-PCR analysis in bleomycin treated epithelial cells confirmed the expression of the IFNA2, IFNA1, and IFNB1 (genes were selected from the IPA) (Figure 6-9). The expression of these genes increased with injury. In particular, the expression of IFNA1 increased a tenfold with the addition of bleomycin in epithelial cells compared to IFNA2 and IFNB1. In co-cultured fibroblasts the IFNA1, IFNA2 and IFNB1 gene expression all decreased with injury (Figure 6-8). In particular, IFNA2

expression showed a significant decrease in expression of the gene in scratch and bleomycin injuries. However, further observation of IFNA2 revealed that fibroblasts expressed more IFNA2 transcript compared to epithelial cells. This confirms that IFNA2 may have potentially promoted MDM2, PMAIP1, BST2, SERPINB9 and BIRC5 expression in co-cultured fibroblasts exposed to bleomycin treated epithelial cells.

The expression of MDM2, PMAIP1, BST2, SERPINB9 and BIRC5 genes in the co-cultured fibroblasts were predicted from the IPA pathway and were also related to the apoptosis pathway. In this case, apoptosis was induced in the fibroblasts. Background knowledge of the genes from previous studies revealed that overexpression of MDM2 can activate p53 and promote cell proliferation in tumour cells (Stommel and Wahl 2005). SERPINB9 belongs to the large superfamily of serine proteinase inhibitors (serpins), which bind to and inactivate serine proteinases. It is an intracellular inhibitor of Granzyme B that protects activated cytotoxic lymphocytes from apoptosis (Rizzitelli, Meuter et al. 2012). PMAIP1 also known as Noxa is a Bcl2 protein that is required in the intrinsic apoptotic pathway inducing apoptosis of alveolar epithelial cells (Urich, Soberanes et al. 2009). BST2 regulation can contribute downstream of apoptosis induction and cell proliferation in epithelial cells (Sayeed, Luciani-Torres et al. 2013). The gene expression changes promoted in the co-cultured fibroblasts were upregulated and led to the activation of the particular gene, thereby promoting apoptosis in fibroblasts.

BIRC5, also known as Survivin, is an important member of the inhibitor of the apoptosis protein family (Horowitz, Ajayi et al. 2012). Previous studies have shown Survivin inhibits caspase-dependent and independent apoptotic pathways and accelerates cell proliferation (Ungvari, Hadadi et al. 2012). However, BIRC5 expression was down-regulated in the fibroblasts and therefore, did not fit in with the context of apoptosis in IPF.

Previous studies have supported the concept that the immune response may play a role in apoptosis. Studies have identified that macrophages secrete cytokines and growth factors such as, TNF-α, IL-6, IL-10 and ISGF which stimulate tissue growth

and have also been shown to promote cell survival in the surrounding cells (Khanna, Biswas et al. 2010). These molecules initiate signals to promote a profibrotic response by mediating apoptosis resistance and promoting cell proliferation and differentiation in fibroblasts and myofibroblasts (Johnson and DiPietro 2013). The 3D co-culture model did not contain immune cells and therefore, the fibroblasts did not exhibit the profibrotic effects i.e. protection from apoptosis in the model.

7.1.6.1 The expression of IL-6

A previous *in vitro* study by *Suwara et al*, *2014* demonstrated that the release of IL-1α, from damaged epithelial cells triggered an inflammatory response in lung fibroblasts (Suwara, Green et al. 2014). Other mediators were measured in response to injury such as IL-6 and IL-8. Studies have shown that IL-6 can induce the IFN α/β pathway in epithelial cells and fibroblasts (Sansone and Bromberg 2012). Other studies have shown that IL-6 is a known regulator of the JAK family of tyrosine kinases (JAK1, JAK2 and Tyk2), which mediates the phosphorylation and activation of the major transcriptional factors such as the ISGs in the interferon pathway (Rincon and Irvin 2012). In this study, the expression of IL-6 transcript was determined in epithelial cells and co-cultured fibroblasts by quantitative RT-PCR analysis. There was no relative trend in gene expression to housekeeping genes. However, there was an increase in IL-6 expression in 3D co-cultured fibroblasts (Figure 6-8D), with no trend in the expression of IL-6. The increased expression of IL-6 compared to the IFN genes could suggest that IL-6 may play a role in the activation of the IFN α/β pathway.

Previously mentioned IL-6 (Figure 6-1), IRF-9 (Figure 6-2) and IFNA2 (Figure 6-9B) were expressed in the epithelial cells in the monolayer culture. Previous studies have shown that IL-6 may regulate IRF-9 with an autocrine IL-6 loop (Erb, Langlechner et al. 2013). IRF-9 has been demonstrated to mediate signalling of type I IFN α/β (Darnell, Kerr et al. 1994). A study by *Erb et al, 2013*, demonstrated IRF-9 mRNA and protein expression is regulated by IL-6. The study revealed that IL-6 induces IRF-9 by C/EBP-α binding to the interferon-activated transcriptional element and is able to prime cells for the response to IFNA2. Stimulation of type I IFN leads to

the formation of ISGF3, which consists of STAT1, STAT2 and IRF9 (Darnell, Kerr et al. 1994). This complex moves to the nucleus where it acts as a transcriptional factor to mediate the expression of IFN stimulated genes and showed that IRF-9 is responsible for the antiproliferative effects of IFNA2 in human ovarian adenocarcinoma (Tsuno, Mejido et al. 2009). Therefore, IL-6 induces the expression of IRF-9 which in turn mediates the signalling of IFNA2 which has a proliferative effect (Erb, Langlechner et al. 2013). In the 3D co-culture model, this may explain the increased cell proliferation of the fibroblasts induced by epithelial cells exposed to injury (refer to section 3.4.3).

7.1.6.2 Gene expression in lung sections

A selection of genes were validated by quantitative RT-PCR (refer to section 6.4.1) and candidate genes were selected for further study based on the background knowledge linked to IPF (Table 6-8). The proteins carried forward to be validated further in tissue sections were C/EBP-α, IRF-9, END-1 and by IHC (section 6.4.2).

C/EBP-α expression was visualised in both normal and IPF tissue sections showing no subjective difference in expression in both sets of tissue (Figure 6-5). Previous studies have shown C/EBP-α is predominantly expressed in epithelial cells whereas C/EBP-β is expressed in mesenchymal cells as well as in most of the developing epithelium (Berg, Didon et al. 2006). C/EBP-α plays an important role in the protection of the alveolar epithelium after injury (Sato, Xu et al. 2012) and its activity decreases with age (Wang, Shi et al. 2006). The reason why there is no subjective difference in lung tissue could be due to reduced activity of the C/EBP-α transcriptional factor.

Immunohistochemistry on lung sections revealed that there was no detectable expression of IRF-9 in normal or IPF tissue (Figure 6-6). Previous studies have shown IRF-9 is up-regulated in response to IFN-α, triggered by an inflammatory response (Tsuno, Mejido et al. 2009). However, studies using high-resolution CT have shown histopathological features of usual interstitial pneumonia consisting of temporal heterogeneity in the fibrotic areas with the presence of dense acellular collagen

alongside fibroblastic foci, whereas interstitial inflammation is mild and associated with hyperplasia of type II pneumocytes (King, Pardo et al. 2011). Therefore, IRF-9 expression was not detected in IPF tissue due to absence of inflammation.

Endothelin-1 is expressed predominantly in epithelial cells, fibroblasts and endothelial cells. Previous studies have shown that ET-1 is secreted by epithelial cells, endothelial cells, fibroblasts, alveolar macrophages and leukocytes during remodelling in the lung. On the lung sections, immunohistochemistry revealed expression of endothelin-1 in the IPF tissue section only (Figure 6-7), which was consistent with the evidence that endothelin-1 may play a role in pulmonary disease (Shi-Wen, Denton et al. 2001).

7.1.7 The effect of Bosentan on Endothelin-1 in 3D co-culture model

Endothelin-1 gene expression was upregulated by injury in epithelial cells. The expression of ET-1 was determined by immunohistochemistry in normal lung tissues and IPF tissues, confirming there was a subjective increased of ET-1 expression in the IPF tissue. Further investigation of endothelin-1 was carried out in the 3D co-culture model using an endothelin receptor antagonist bosentan.

Previous studies have shown that bosentan is a dual ET-1 receptor antagonist and known to inhibit two receptors of endothelin-1, ET_A and ET_B. ET_A receptors are found on mesenchymal cell types such as vascular and airway smooth muscle cells and fibroblasts. ET_B receptors are found on the endothelium (Shi-Wen, Denton et al. 2001). In the 3D co-culture model, bosentan was used to determine whether inhibition of ET-1 signalling reduced cell proliferation and matrix synthesis in co-cultured fibroblasts. The expression of endothelin-1 was measured in supernatants and it was found that the expression of endothelin-1 reduced with injury (Figure 6-12). This was unexpected as injury was attenuated with the addition of bosentan. This suggested that bosentan inhibited endothelin-1 production in the 3D co-culture model.

Previous studies have shown ET-1 is not stored in the cell (Nakamura, Naruse et al. 1990), but is transported through the cell in vesicles, resulting in directional secretion. Directional secretion allows ET-1 to act in an autocrine manner (Fagan, McMurtry et al. 2001). A study by *Markewitz et al*, *1995* demonstrated ET-1 is an autocrine regulator in alveolar epithelial cells. The peptide primarily binds to ET_A receptor resulting in accumulation of PGE2 and cAMP. The study suggests that ET-1 mediates inflammation through the regulation of cyclooxygenase-2 and PGE_2 (Markewitz, Kohan et al. 1995)

The next step was to investigate the effect of bosentan on the transcription of ECM genes in the fibroblasts exposed to epithelial injury. This was to determine whether the addition of bosentan would decrease the effects on fibroblast/myofibroblast differentiation and ECM genes. The genes selected were *collagen I* and *III* which are the most abundant collagens in fibrosis and α*-SMA*, a hallmark of fibroblast differentiation.

The data revealed for the 'absence of bosentan', there was a significant increase in *Collagen I, Collagen III* and α-SMA gene expression in fibroblasts in response to epithelial injury, (Figure 6-13). The data were normalised to the respective fibroblasts for the treatments for either 'absence of Bosentan' or 'addition of bosentan'. The quantitative results revealed that, with the 'addition of bosentan' in the 3D co-culture model, the expression of *collagen I*, *collagen III* and α*-SMA* revealed no change with injury (Figure 6-14; A-C). The gene expression for the 'absence of bosentan', showed an increase expression for all genes. In particular, *Collagen III* and α*-SMA* both significantly increased.

Overall, it can be summarised, that the addition of bosentan inhibits the bleomycin-induced increase in ECM and α-SMA expression in fibroblasts. These data suggests that epithelial injury affects co-cultured fibroblasts response by increasing gene expression of ECM genes and smooth muscle actin, and that this induction is mediated by endothelin.

These data show that bosentan may have an inhibitory effect on cell proliferation and matrix synthesis in the co-cultured fibroblasts exposed to injured epithelial cells. Human clinical studies have shown the effect of bosentan in IPF patients with severe pulmonary hypertension. The outcome of the study was invasive or non-invasive pulmonary hemodynamic, functional capacity and symptoms of the disease. There was no benefit of the treatment of bosentan in IPF patients (Corte, Keir et al. 2014).

7.1.8 Epithelial-fibroblast crosstalk in the 3D co-culture model

The 3D co-culture model system has provided valuable profiling data. Gene expression profiling has proven to be a useful tool for the identification of specific gene patterns in the bleomycin-mediated gene expression changes in epithelial cells which promote the IFN α/β pathway and in conjunction have an influence on the pro or anti-fibrotic effect on fibroblasts. The transcriptional study predicted that interferon α/β pathway increased with the epithelial cells injured with bleomycin, leading to a predicted activation of fibroblast mediators which may have promoted cell proliferation and matrix synthesis via a soluble mediator, Endothelin-1. A dual endothelin-1 receptor antagonist, bosentan, was used in the 3D co-culture model and revealed that there was decreased cell proliferation and matrix synthesis gene expression in fibroblasts.

There is a limited understanding of the progression of the disease whether by studies in bleomycin induced animal or in IPF human studies. In bleomycin induced mice, there is a limitation whereby the effect of bleomycin resolves and fibrosis is reversed. In human studies, the lung tissue is limited. This is due to the severe progression of the disease and only late stages of the tissue can be retrieved. Another method to utilise and maximise the cells is transcriptional profiling. In IPF, most microarray studies have been performed on lung biopsies from deceased patients (Williamson, Sadofsky et al. 2015). The disadvantage of this is that the tissue retrieved is at the last stage of the disease and virtually no information of the earlier stages of the disease can be obtained.

7.2 Recent understanding and advances of IPF

7.2.1 Current paradigm of IPF:

According to the prevailing paradigm of IPF, fibrosis is characterised by a consequence of aberrant wound healing responses to repetitive lung injury, initiation of inflammatory cascades, fibroblast activation, exaggerated pro-fibrotic cytokine expression, accumulation of extracellular matrix (ECM) deposition, and the development of fibrotic lesions known as fibroblast "foci" (Wilson and Wynn, 2009). Although much of the pathogenesis is still unknown, fibroblasts and epithelial cells are thought to be key drivers in the initiation and progression of the disease (Sakai and Tager 2013).

Currently two hypotheses remain controversial in pathogenesis of lung fibrosis. *Selman et al*, proposed the 'inflammatory theory' and *Haschek et al* proposed the "alveolar epithelial disrepair" hypothesis. The point of conflict was whether the alveolar impairment was caused by an inflammation reaction or by an abnormal repair (Zhou et al. 2016).

7.2.2 Underlying mechanisms:

Idiopathic pulmonary fibrosis is a highly heterogeneous and a complex disease resulting of alveolar epithelial cell injury characterised by migration, proliferation, and activation of fibroblasts with accumulation of matrix synthesis. This leads to scarring of the lung, architectural distortion, and irreversible loss of function of the lung (Spagnolo, Sverzellati et al. 2015). Although research has focused on the pathogenesis of pulmonary fibrosis, including mechanisms that regulate the proliferation, activation, and differentiation of collagen-secreting myofibroblasts, studies have identified new pathogenic mechanisms that are critically involved in the initiation of fibrosis (Wynn 2011).

The precise mechanisms which drive pulmonary fibrosis are unknown. However, the role of inflammation in IPF has been recently de-emphasized. Earlier findings of inflammation in fibrosis were dismissed due to poor response to anti-inflammatory therapy (Selman 2001). However, resistance to anti-inflammatory therapy may not

necessarily indicate lack of inflammatory involvement, as there are several well-established diseases in which inflammation is clearly accepted to be the predominant underlying mechanism, but which traditional anti-inflammatory therapy has been poorly effective (Todd, Luzina et al. 2012).

Inflammation plays a pivotal role in pulmonary fibrosis. A recent study has shown deregulated adaptive immune mechanisms and subsequent inflammation could have a role in the onset or progression of the disease in a subgroup of patients with IPF (Gilani 2010). There are at least two different cellular routes, the inflammatory pathway and the epithelial pathway could lead to lung fibrosis (King et al. 2011).

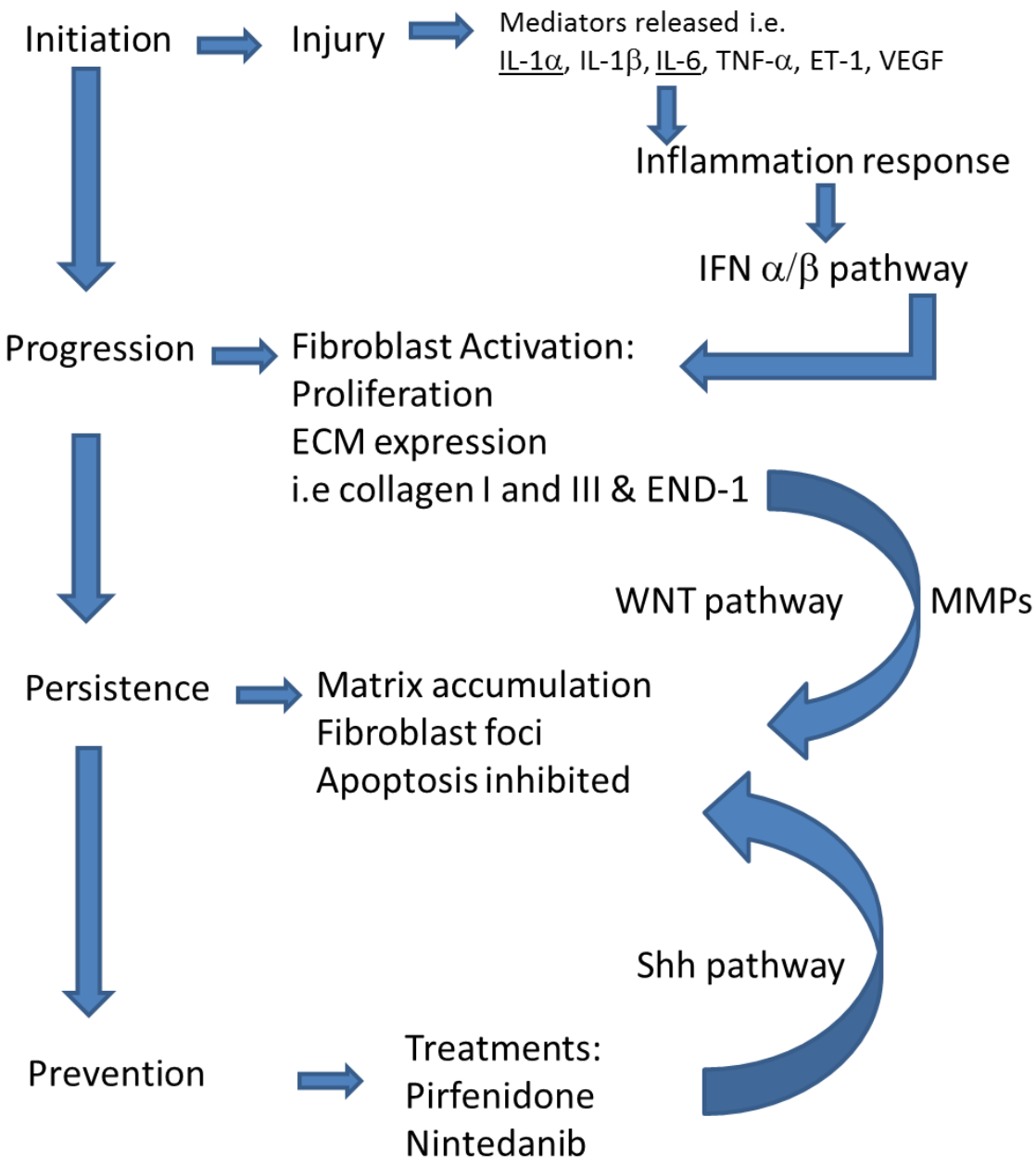


Figure 7-1: Proposed mechanism of Inflammation in pulmonary fibrosis
A diagram to show the soluble mediators and pathways, which may be involved in the mechanisms of pulmonary fibrosis. Initiation is the process in which there is repetitive injury to the epithelial cells. The progression mechanism is where the fibroblasts are activated by various growth factors and pathways, whereby there is fibroblast differentiation and migration. The persistence mechanism is where fibroblast foci are formed and there is a development of scarring. There is a development of treatments to help prevent the mechanisms of pulmonary fibrosis.

7.2.3 IPF models to understand IPF mechanisms

The pathogenesis of each form of lung fibrosis remains poorly understood. To better understand the pathogenesis of fibrotic lung disease, multiple animal models and co-culture models have been developed. This is to gain insight and a better understanding of the cell-cell and soluble mediator interactions that drive fibrotic responses in the lung.

Initiation is the process in which there is repetitive injury to the epithelial cells. The progression mechanism is where the fibroblasts are activated by various growth factors and pathways, whereby there is fibroblast differentiation and migration. The persistence mechanism is where fibroblast foci are formed and scarring is developed (Figure 7-1).

7.2.3.1 Animal models to understand IPF mechanisms

Currently animal models are a useful tool to understand the pathogenesis of IPF and other fibrotic lung diseases. Bleomycin induced lung injury animal model has been the most commonly used model to study the mechanism of lung fibrosis. The model involves a single intratracheal or intranasal delivery of bleomycin to the lung. The insult results in a dose-dependent damage to the lung, characterised by infiltrates of inflammatory cells, proliferation of fibroblasts and collagen deposition. After a single insult, the lungs are generally studied 7–14 days later. After that time, the lungs recover from injury and are back to normal and the mice don't die. While this bleomycin model may implicate many similarities to human idiopathic pulmonary fibrosis (IPF), there are also many substantial differences i.e. IPF develops over a long period of time in humans, whereas the conventional single insult bleomycin in mice is generally studied in less than a month as the progression of fibrosis is reversible in mice (Phan and Kunkel 1992). It has been suggested that IFN α/β pathway, with the recruitment of inflammatory cells, may play a role in resolving the progression of fibrosis in mice. In Figure 7-1, the diagram shows that from initiation to the persistence of IPF, many mediators are present. The mechanism of this phenomenon is yet to be understood.

7.2.3.2 Current co-culture models to understand IPF mechanisms

Development of treatments for idiopathic pulmonary fibrosis is an ongoing process. To evaluate an optimal dose of therapeutics, 3D co-culture models are being developed to understand the interactions between the cells and their microenvironment including understanding various processes, such as cell differentiation, proliferation, and gene expression in regulation of fibrosis (Datta, Scotton et al. 2011). Whilst bleomycin-induced animal experiments are necessary prior to any clinical trials, there is a large gap in the knowledge obtained between *in vitro* and *in vivo* models are needed to completely understand the therapeutic efficiency.

In vitro, 3D culture models provide a better understanding of the molecular and cellular mechanisms which are more relevant to animal and human studies, thus facilitating the development and screening of new drugs, by providing independent cell-cell interactions without the biophysical barriers such as transport of nutrients and therapeutics to different cell populations (Tatler and Jenkins 2012).

Prasad et al. 2014 demonstrated the effect of fibroblast phenotype on the response to epithelial injury in the 3D co-culture model. The model consisted of a Transwell® system with the epithelial cells seeded in the upper chamber and the fibroblasts grown on the outer side of the upper chamber. Scratch wound was applied to the upper chamber consisting of epithelial cells. The migration of the fibroblasts was monitored and growth factor profiling was performed. The study provided evidence of an altered phenotype of the IPF fibroblasts which were impaired in their response to epithelial injury as compared to normal fibroblasts. The IPF fibroblasts also expressed higher levels of PDGF-AA and bFGF which are known profibrotic growth factors. The study showed that the abnormal epithelial-fibroblast crosstalk results in the generation of a pro-fibrotic environment and impaired alveolar repair (Prasad, Hogaboam et al. 2014).

7.2.3.3 3D co-culture model to understand IPF mechanisms

Currently the paradigm of IPF still remains that the disease is initiated by repeated micro-injuries to the alveolar epithelium that leads to scarring of the lung. Studies have been unable to demonstrate the pathogenesis of IPF and other fibrotic lung disorders in animal models. Unfortunately, no animal model can exhibit the progressive disease, and most animal models do not fully determine the histologic pattern of UIP or other interstitial lung diseases.

To date, there are no ideal models to demonstrate the pathophysiology of IPF, but progress is being made to understand the mechanisms and signalling pathways in, *in vitro* co-culture models. Understanding the mechanism as well as signalling pathways involved in the pathogenesis and progression of IPF remains a critical component in discovering new therapies, providing early diagnosis, and preventing disease progression.

In the 3D co-culture *in vitro* model, we demonstrated that repeated injuries to the epithelial cells produced an inflammatory response. The model only consisted of epithelial cells and fibroblasts therefore, no other cell types such as inflammatory cells were present in the model. The injury was only inflicted to the epithelial cells and the effect on the fibroblasts was quantified. The effect of epithelial cell injury on the fibroblasts revealed increased proliferation of fibroblasts and ECM expression. The results were mimicking initiation and progression of fibrosis (Figure 7-1). It may seem that the epithelial cells may be active contributors in initiating fibrosis.

In this study, we showed that epithelial cells released IL-1α when the cells were injured. This, in turn, had an effect on fibroblasts where fibroblast proliferation was measured and ECM expression was quantified. Other mediators such as IL-1α and IL-6 were released from injured epithelial cells as shown in figure 7-1.

A study by *Aumiller et al 2013* identified two pro-inflammatory cytokines IL-1β and IL-6 as WNT/β-catenin downstream targets in mice (Xu, Porte et al. 2009). In our study, IL-1β and IL-6 may have activated the IFN α/β pathway to initiate the

inflammation response. In turn, IL-6 may have promoted TGF-β and initiated fibroblast proliferation through the WNT pathway. Understanding various mediators released by epithelial cells may provide us with basic knowledge to understand some of the mechanisms of pulmonary fibrosis.

7.2.3.4 Gene expression to understand IPF mechanisms

Gene expression profiling studies have demonstrated transcriptional changes in IPF patients (Yang 2012). These studies have identified genes and pathways that are expressed in fibrotic development such as sonic hedgehog (Stewart, Hoyne et al. 2003), fibroblast growth factor (El Agha and Bellusci 2014), platelet-derived growth factor (Zhou, Liu et al. 2012) and canonical/noncanonical WNT (Zuo, Kaminski et al. 2002).

Bleomycin induced injury in animal models have been used to understand the development of fibrosis. *Lee et al,* created an inducible lung-specific IL-13 transgenic mouse line that exhibited a variety of abnormalities resembling human allergic airway disease but also developed progressive fibrosis in the airway and lung parenchyma. The profibrotic effect of IL-13 selectively stimulated TGF-β1 which was potentially produced by profibrotic macrophages. The study also demonstrated that the activation is mediated by a plasmin/serine protease- and MMP-9–dependent and CD44-independent mechanism(s) and that the fibrogenic effect of IL-13 is mediated by TGF-β pathway (Lee, Kaminski et al. 2001).

In the 3D co-culture model, analysis revealed that there was a stronger gene signature in the epithelial cells exposed to bleomycin. The epithelial cells treated with bleomycin revealed IFNα/β pathway which also upregulated genes in the Ingenuity Pathway Analysis, *IFNA2, IRF9, IFNL1, STAT1, IRF3, IRF1, IRF5, IFNA1* and *IFNA13*. For the fibroblasts, genes expressed were *SERPINB9, PMAIP1, MDM2*, *BST2* and *BIRC5* which are downstream of *IFNA2* gene. The IFNA2 was strongly upregulated by epithelial cells exposed by bleomycin. The expression was driven by these epithelial cells to mediate gene expression in the co-cultured fibroblasts.

7.3 Future work

In this study, we utilized a novel 3D co-culture system to investigate the effect of epithelial cell injury on fibroblasts. An inflammatory response was determined using IL-1α as a pro-inflammatory marker, which was released by damaged epithelial cells with repetitive injury to the epithelial cells. Fibroblasts from normal lungs (NHLFs) responded to epithelial cell injury by promoting cell proliferation and matrix synthesis. However, we were unable to show inhibited fibroblast apoptosis. Gene expression profiling study revealed the IFNα/β pathway was upregulated in the epithelial cells exposed to bleomycin. Also, the gene expression profiling confirmed that the apoptosis mediators involved in fibroblasts were upregulated, which may explain why the fibroblasts had undergone apoptosis.

The complexity of the *in vivo* fibrosis process makes it difficult to mimic the IPF mechanisms in an *in vitro* model. However, key processes within the fibrotic pathway, such as myofibroblast differentiation, proliferation, and collagen production can be demonstrated. In our model, we displayed a non-cell contact approach Transwell system, in which we demonstrated the effect of epithelial cell injury on fibroblasts. In the *in vitro* 3D co-culture model, we may have demonstrated initiation and progression mechanisms of epithelial-fibroblast crosstalk in IPF.

There has been much emphasis on epithelial-fibroblast crosstalk in IPF, but there is a controversial paradigm that IPF is predominantly a disorder of alveolar injury and an inflammatory disorder (Selman and Pardo 2004). In IPF, interstitial inflammation is undoubtedly present and often appears minimal. It has been proposed that IPF primarily develops via an epithelial/fibroblast route (Selman and Pardo 2004). However, there is evidence that injury of the alveolar epithelium and aberrant repair itself can alter the epithelial-fibroblast crosstalk leading to the development of fibrosis (Adamson et al. 1990).

Early therapy of IPF was focused on the inflammatory hypothesis of the disease. Therapeutic immunosuppression included use of corticosteroids which was later combined with azathioprine and cyclophosphamide, although this was ineffective.

However, there is still some evidence that IPF is a disease of inflammation. IPF has emerged as a disease of aberrant repair process resulting in progressive fibrosis, with research focused on development of novel antifibrotic therapies. Since the publication of the most recent guidelines in 2011, two new agents with immense promise have been developed: pirfenidone and nintedanib.

The action of Pirfenidone, 5-methyl-1-phenyl-2-(1H)-pyridone, is thought to occur via modulation of cytokines and growth factors such as transforming growth factor-β (TGFβ) and tumour necrosis factor-α (TNFα), thereby targeting both the anti-inflammatory and antifibrotic pathways. Pirfenidone, a well-recognised early mediator of inflammation, has been shown to inhibit the production TNF-α, at the translational level. In addition, it has been shown that pirfenidone reduces fibroblast proliferation and differentiation into myofibroblasts by inhibiting key factors in the TGFβ pathway, such as the cytoplasmic Smad proteins (Aoyagi-Ikeda, Maeno et al. 2011).

Nintedanib is a small molecule that was originally designed as an ATP-competitive inhibitor of fibroblast growth factor receptor (FGFR)-1 and vascular endothelial growth factor receptor (VEGFR)-2. Both these receptors are pro-angiogenic receptor tyrosine kinases and nintedanib was designed as an anti-angiogenic drug for cancer indications. The on-going clinical development of nintedanib for cancer includes non-small cell lung cancer, colorectal cancer and ovarian cancer. As nintedanib is also an inhibitor of platelet-derived growth factor receptor (PDGFR)-α and α, it was selected for development as a potential treatment for idiopathic pulmonary fibrosis (Wollin, Wex et al. 2015).

Most of the preclinical studies investigating the effects of potential anti-fibrosis drugs have been conducted using animal models (Myllärniemi and Kaarteenaho 2015). For example, bleomycin-induced fibrosis in mice, rats or hamsters has been the most commonly used to study the mechanisms of IPF (Scotton and Chambers 2010). Although testing in animals is a popular method, it is often difficult to compare the results to the human disease. The use of our *in vitro* 3D co-culture model may provide a better understanding of the IPF mechanisms as we can modify the model

according to the disease progression. For example, to understand initiation of IPF, the model can be altered with the addition of immune cells with epithelial cells and observe the effect of epithelial cell injury on fibroblasts. The 3D co-culture may not be ideal to reflect the clinical situation of IPF but may reflect the clinical effectiveness of a pharmacological treatment in the future.

In our 3D model, gene expression data has demonstrated two distinct sets of genes induced in the 3D co-culture model; one inflammatory and the other associated with development. Out of the two current treatments, pirfenidone and nintedanib, only Pirfenidone treatment will fit in with the model as it targets TGF-β and TNF-α. It would be interesting to observe the effect of Pirfenidone once the epithelial cells are injured and whether Pirfenidone would inhibit the fibroblast proliferation and ECM synthesis in the 3D co-culture model.

7.4 Summary

This study was designed to gain insight and a better understanding of the cell-cell and soluble mediator interactions that drive fibrotic responses in the lung. The 3D co-culture model was developed using two cell lines, fibroblasts and epithelial cells as they are thought to be the key drivers in the initiation and progression of the disease (Sakai and Tager, 2013).

In the 3D co-culture *in vitro* model, we demonstrated that repeated injuries to the epithelial cells produced an inflammatory response. The model only consisted of epithelial cells and fibroblasts and therefore, no other cell types such as inflammatory cells were present in the model. The injury was only inflicted to the epithelial cells and the effect on the fibroblasts was quantified. The effect of epithelial cell injury on the fibroblasts revealed increased proliferation of fibroblasts and ECM expression.

Further microarray analysis revealed that there was a stronger gene signature in the epithelial cells exposed to bleomycin, revealing the IFN α/β pathway was upregulated in the injured epithelial cells. The expression was driven by these epithelial cells to mediate gene expression in the co-cultured fibroblasts. The data may suggest that

these were initiation and progression mechanisms of fibrosis which are important to the disease.

The advance in understanding of IPF in the 3D co-culture model is limited by using two cell lines. However, microarray analysis in this study has demonstrated that non-direct cell-cell communication can promote soluble mediators. Understanding various mediators released by epithelial cells may provide us with a basic knowledge to understand the mechanisms of pulmonary fibrosis.

To assess whether the 3D co-culture model reflects known mechanisms underlying clinical fibroproliferative disease, the model was developed to understand the interactions between the cells and their microenvironment. This included understanding various processes, such as initiation, proliferation as well as gene transcript levels for components of signalling pathways known to play a role in the pathogenesis of clinical IPF.

In our model, the effect of bosentan on the transcription of ECM genes in fibroblasts exposed to epithelial cell injury was investigated. This was to determine whether the addition of bosentan would decrease the effects on fibroblast/myofibroblast differentiation and ECM genes. The genes selected were *collagen I* and *III* which are the most abundant collagens in fibrosis and α*-SMA*, a hallmark of fibroblast differentiation.

Overall, the data demonstrated that bosentan inhibited the bleomycin-induced increase in fibroblasts ECM and α-SMA expression, suggesting bosentan may have an inhibitory effect on cell proliferation and matrix synthesis in the co-cultured fibroblasts exposed to bleomycin injured epithelial cells. Human clinical studies have shown the effect of bosentan in IPF patients with severe pulmonary hypertension. The outcome of the study was invasive or non-invasive pulmonary hemodynamic, functional capacity and symptoms of the disease. There was no benefit of the treatment of bosentan in IPF patients (Corte, Keir et al. 2014).

Whilst *in vitro* and *in vivo* models are necessary prior to any clinical trials, there is a large gap in the knowledge obtained from both types of models to completely understand the clinical fibroproliferative disease.

In summary, we have investigated the changes in gene expression associated with the development of bleomycin-induced pulmonary fibrosis in epithelial monolayer culture and 3D co-culture model. This is a unique way to identify molecular signatures and may provide a useful understanding in the complex lung disease without the need for animal models and lung biopsies. Endothelin-1 was found to be significantly modulated in the epithelial monolayer culture and 3D co-culture model. This correlated well with the histopathological expression in the diseased tissue. The profiling data will aid with understanding the underlying mechanisms involved in the development of fibrosis and will contribute to efforts aimed at identifying candidate biomarkers for fibrotic disease.

Appendices

Appendix 1: Websites and On-line resources

- NCBI (The National Centre for Biotechnology Information) public online database

  http://www.ncbi.nlm.nih.gov/

- Sigma-Aldrich - KiCqStart® SYBR® Green Primers

  http://www.sigmaaldrich.com/catalog/product/sigma/kspq12012?lang=en&region=GB

- The Human Protein Atlas

  http://www.proteinatlas.org/

Appendix 2: List of suppliers

Abcam plc: 330 Cambridge Science Park, Cambridge, CB4 0FL, UK.

AbD Serotec: Endeavour House, Langford Lane, Kidlington, OX5 1GE, UK.

Applied Biosystems/Ambion: Applied Biosystems, Lingley House, 120 Birchwood Boulevard, Warrington, WA3 7QH, UK.

ATCC/LGC Promochem: LGC Standards, Queens Road, Teddington, Middlesex, TW11 0LY, UK.

Beckman Coulter (UK) Ltd.: Oakley Court, Kingsmead Business Park, London Road, High Wycombe, HP11 1JU, UK.

Bioline Ltd.: Unit 16 The Edge Business Centre, Humber Road, London, NW2 6EW, UK.

Bio-Rad Laboratories Ltd.: Bio-Rad House, Maxted Road, Hemel Hempstead, Hertfordshire, HP2 7DX, UK.

Corning Inc.: 1 Riverfront Plaza, Corning, NY 14831, USA.

Dako UK Ltd.: Cambridge House, St Thomas Place, Ely, Cambridgeshire, CB7 4EX, UK.

ECACC: Health Protection Agency Culture Collections, Health Protection Agency, Centre for Emergency Preparedness and Response, Porton Down, Salisbury, SP4 0JG, UK.

GE Healthcare UK Ltd./Amersham: Amersham Place, Little Chalfont, Buckinghamshire, HP7 9NA, UK.

GraphPad Software, Inc.: 2236 Avenida de la Playa, La Jolla, CA 92037, USA.

IBL International GmbH: Flughafenstrasse 52a, D-22335 Hamburg, Germany.

Invitrogen/GIBCO: Invitrogen Ltd., 3 Fountain Drive, Inchinnan Business Park, Paisley, PA4 9RF, UK.

Leica Microsystems (UK) Ltd.: Davy Avenue, Knowlhill, Milton Keynes, Buckinghamshire, MK5 8LB, UK.

Lonza /Clonetics: Lonza Biologics plc, 228 Bath Road, Slough, Berkshire, SL1 4DX, UK.

Merck Biosciences/Calbiochem: Merck Chemicals Ltd., Boulevard Industrial Park, Padge Road, Beeston, Nottingham, NG9 2JR, UK.

Millipore (UK) Ltd.: Suite 3 & 5, Building 6, Croxley Green Business Park, Watford, WD18 8YH, UK.

Molecular Devices, Inc.: 1311 Orleans Drive, Sunnyvale, CA 94089-1136, USA.

New England Biolabs (NEB): New England Biolabs (UK) Ltd., 75/77 Knowl Piece, Wilbury Way, Hitchin, Herts, SG4 0TY, UK.

Nikon UK Limited: 380 Richmond Road, Kingston upon Thames, Surrey, KT2 5PR, UK.

Nunc GmbH & Co. KG: Robert-Bosch-Straße 1, D-63505 Langenselbold, Germany.

Open Biosystems/Autogen Bioclear: Autogen Bioclear UK Ltd., Holly Ditch Farm, Mile Elm, Calne, Wiltshire, SN11 0PY, UK.

Promega: Promega UK Ltd., Delta House, Southampton Science Park, Southampton, Hampshire, SO16 7NS, UK.

Qiagen: Qiagen Ltd., Qiagen House, Fleming Way, Crawley, West Sussex, RH10 9NQ, UK.

Roche Diagnostics Ltd.: Charles Avenue, Burgess Hill, RH15 9RY, UK.

Santa Cruz Biotechnology, Inc.: 2145 Delaware Avenue, Santa Cruz, CA 95060, USA.

Severn Biotech Ltd.: Unit 2, Park Lane, Kidderminster, Worcestershire, DY11 6TJ, UK.

Sigma-Aldrich: Sigma-Aldrich Company Ltd., The Old Brickyard, New Road, Gillingham, Dorset, SP8 4XT, UK.

SPOT™ Imaging Solutions: 6540 Burroughs, Sterling Heights, MI 48314, USA.

SLS (Scientific Laboratory Supplies) Ltd.: Wilford Industrial Estate, Ruddington Lane, Wilford, Nottingham, NG11 7EP, UK.

Stratagene: Agilent Technologies UK Ltd., Lakeside, Cheadle Royal Business Park, Stockport, Cheshire, SK8 3GR, UK.

Syngene: Beacon House, Nuffield Road, Cambridge, CB4 1TF, UK.

Sysmex UK Ltd.: Sysmex House, Garamonde Drive, Wymbush, Milton Keynes, MK8 8DF, UK.

Thermo/Fisher Scientific/NanoDrop Technologies: Fisher Scientific UK Ltd., Bishop Meadow Road, Loughborough, Leicestershire, LE11 5RG, UK.

Thermo Shandon Ltd.: 93-96 Chadwick Road, Runcorn, Cheshire, WA7 1PR, UK.

Vector Laboratories Ltd.: 3 Accent Park, Bakewell Road, Orton Southgate, Peterborough, PE2 6XS, UK.

VWR International Ltd./BDH: Hunter Boulevard, Magna Park, Lutterworth, Leicestershire, LE17 4XN, UK.

3H Biomedical AB: Dag Hammarskjölds väg 34A, Uppsala Science Park, SE-751 83 Uppsala, Sweden.

Appendix 3: Buffer and Reagent Information

A3.1: Western Blotting Reagents

Western Blot Gel Preparation

1.5M tris-HCL pH 8.8:90.86g Tris base was dissolved in 400ml distilled water, pH adjusted to 8.8 using 0.1M HCL and volume adjusted to 500ml using distilled water.

Western Blot running buffer

30.3g Tris-base, 144g glycine and 100ml 10% SDS were dissolved in 800ml distilled water, and made up to 1000ml using same to create 10x stock. Store at room temperature.

Western Blot transfer buffer

30.3g Tris-base and 144g glycine were dissolved in 800ml and them made up to 1000 ml using same 10x stock. The stock was diluted 1 part to 2 parts methanol andf 7 parts distilled water to prepare the 1x transfer buffer. Store at room temperature.

Western Blocking Buffer

5g marvel milk in 100ml of 0.1% PSB-T. Store at 4^{o}C.

A3.2: Zymography Reagents

Destain Solution

Add RO water 500mls, methanol 400mls and acetic acid 100mls. Store at room temperature.

Coomassie Blue Stain

Add 1g Coomassie Blue to 1 litre of Destain Solution (0.1% w/v) to make up Coomassie Stain. Store at room temperature.

Tris-Gly SDS zymogram running buffer

To make 500ml: 10x concentrate Tris-Gly SDS zymogram running buffer of Invitrogen- cat no; LC2675 ~ 50ml buffer and 450 ml deionised water. Use as required.

Tris-Gly SDS zymogram sample buffer

To make 500ml: 10x concentrate Tris-Gly SDS zymogram sample buffer- Invitrogen- cat no; LC2673 50ml buffer and 450 ml deionised water. Use as required.

Appendix 4: KiCqStart® SYBR® Green Primers

Table A4.1: KiCqStart Primers are ready-to-order, pre-designed primer pairs for quantifying gene expression by SYBR Green I RT-qPCR (Reverse Transcription Quantitative Real-Time PCR) from sigma-Aldrich. Specifications used: GC Content: 20 - 80%[2], Melting Temperature: 55.0 ± 5 ºC, Secondary Structure: None, Excessive 3′ Clamping: Minima, Homology: None. *Oligo characteristics*: Molecule: DNA (all sequences verified by mass spec QC); no modifications, Contents: 1 forward and 1 reverse primer, Length: 18 - 24 bases, Purification: RP cartridge, Format: 3 OD minimum yield, dry; 1 oligonucleotide per tube.

Table A4.1: KiCqStart Primers

Name	**Gene ID**	**Direction**	**Sequence 5'-3'**
IFIT1	3434	Forward	CTGCCTAATTTACAGCAACC
		Reverse	CTGCCTAATTTACAGCAACC
OAS1	4938	Forward	ATTGTAAGAAGCTTGG
		Reverse	CAGAGTTGCTGGTAGTTTATG
IFITM1	8519	Forward	CTACTCCGTGAAGTCTAGG
		Reverse	ATGAGGATGCCCAGAATC
MX1	4599	Forward	CAGGCTTTGTGAATTACAGG
		Reverse	TCTTCAATTTGGACTTGGC
IFIT3	3437	Forward	ATGAGTGAGGTCACCAAG
		Reverse	CCTTGAATAAGTTCCAGGTG
IRF9	10379	Forward	CTCAGAAAGTACCATCAAAGC
		Reverse	TCATTATTGAGGGAGTCCTG
IFI35	3430	Forward	GAAGGCTGAGATCAGGTC
		Reverse	GAAGTGGATCTCCAGGAC

Name	**Gene ID**	**Direction**	**Sequence 5'-3'**
SERPINB9	5272	Forward	TTGTCAATGCCATCTACTTC
		Reverse	CCTCCTGGTTTATTTTAAAGGG
BIRC5	332	Forward	CATCTCTACATTCAAGAACTGG
		Reverse	CCTTGAAGCAGAAGAAACAC
BST2	684	Forward	GGAGAGATCACTACATTAAAC
		Reverse	CTGGGTAGTACTTCTTGTC
MDM2	4193	Forward	CCTTAGCTGACTATTGGAAATG
		Reverse	TGTTGAGTTTTCCAGTTTGG
PMAIP1	5366	Forward	CAGGAGATTTGGAGACAAAC
		Reverse	CTCATGCAAGTTTTTGATGC
NMNAT1	64802	Forward	CATGGAAAATTCCAGAAGAC
		Reverse	TGTACCTTCCTGTTCCATTC
C6ORF211	79624	Forward	GTCCACCAATCGATTACTTTG
		Reverse	TATCAATTGTTGCAGGTGAG
HIFAN	3091	Forward	CTGTGAACTTCTGGTATAAGG
		Reverse	CTCATTATGGCCACTTTCTG
CEBP/α	1050	Forward	AGCCTTGTTTGTACTGTATG
		Reverse	AAAATGGTGGTTTAGCAGAG
IL-6	3569	Forward	GCAGAAAAAGGCAAAGAATC
		Reverse	CTACATTTGCCGAAGAGC
MAX	4149	Forward	GAGAGAAGGGAACAAAGATG
		Reverse	GCAGAAAACAGTTGGAAAAG
PLCD1	5333	Forward	AAGAATTCAATTGTGGACCC
		Reverse	GAGGCATCATAATCTTCCAC

Name	**Gene ID**	**Direction**	**Sequence 5'-3'**
Col1A1	1277	Forward	GAACGCGTGTCAATCCCTTGT
		Reverse	GAACGAGGTAGTCTTTCAGCAAC
versican	1462	Forward	CAAGCATCCTGTCTCACGAA
		Reverse	CAACGGAAGTCATGCTCAAA
β-actin	60	Forward	CCTGGCACCCAGCACAAT
		Reverse	GGGCCGGACTCGTCATACT
Human2BM	8342	Forward	TGCTGTCTCCATGTTTGATGT
		Reverse	TCTCTGCTCCCCACCTCTAAG
GAP-DH	2597	Forward	GGTCTCCTCTGACTTCAACA
		Reverse	AGCCAAATTCGTTGTCATAC

Table A4.2: House-keeping genes

Name	**Direction**	**Sequence 5'-3'**
18s	Forward	GTAACCCGTTGAACCCATT
	Reverse	CCATCCAATCGGTAGTAGCG
Col3A1	Forward	AACACGCAAGGCTGTGAGACT
	Reverse	GCCAACGTCCACACCAAATT
α-SMA	Forward	GACAATGGCTCTGGGCTCTGTAA
	Reverse	ATGCCATGTTCTATCGGGTACTT

Appendix 5: Bioanalyser results

Fibroblast and Small Airway Epithelial cells RNA Integrity and quality

Determining the integrity of RNA is a critical step in gene expression analysis. RNA is a thermodynamically stable molecule, which is rapidly digested in the presence of ubiquitous RNase enzymes. As a result, shorter fragments of RNA commonly occur in samples, which can potentially compromise results of downstream applications. In order to evaluate the degree of degradation, electrophoretic methods have been applied that separate the samples according to the size of the comprised molecules.

Usually, RNA integrity is evaluated using agarose gel electrophoresis stained with ethidium bromide which produces a certain pattern. As degradation proceeds, there is decrease in the 18S to 28S ribosomal band ratio. RNA is considered high quality when the ratio of the bands is about 2.0 and higher. Since this approach relies in human interpretation of gel images, it is subjective.

In order to standardize the process of RNA integrity interpretation, Aligent technologies introduced a new tool for RNA quality assessment, The RNA Integrity number (RIN), which was developed to remove individual interpretation in RNA quality control. The RIN algorithm allows for the classification of eukaryotic total RNA, based on a numbering system from 1 to 10, with 1 being the most degraded profile and 10 being the most intact.

In this way, interpretation of an electropherogram is facilitated, comparison of samples is enabled and repeatability of experiments is ensured.

The aim of this experiment was to retrieve the fibroblasts from collagen and determine a RNA integrity number, in which then the cells can go for gene expression analysis. A criteria was set for a RIN number of 7 and above.

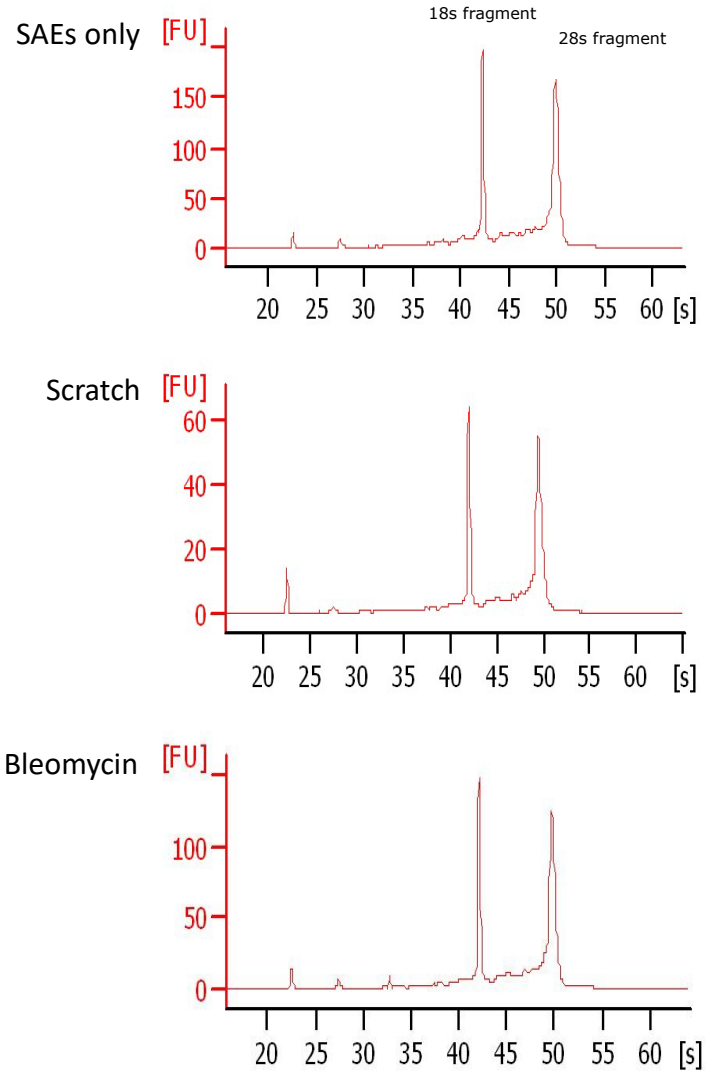


Figure A5.1: Electropherogram of the epithelial cells inflicted with injuries. There are two fragments 18 s and 28 divide the electropherogram

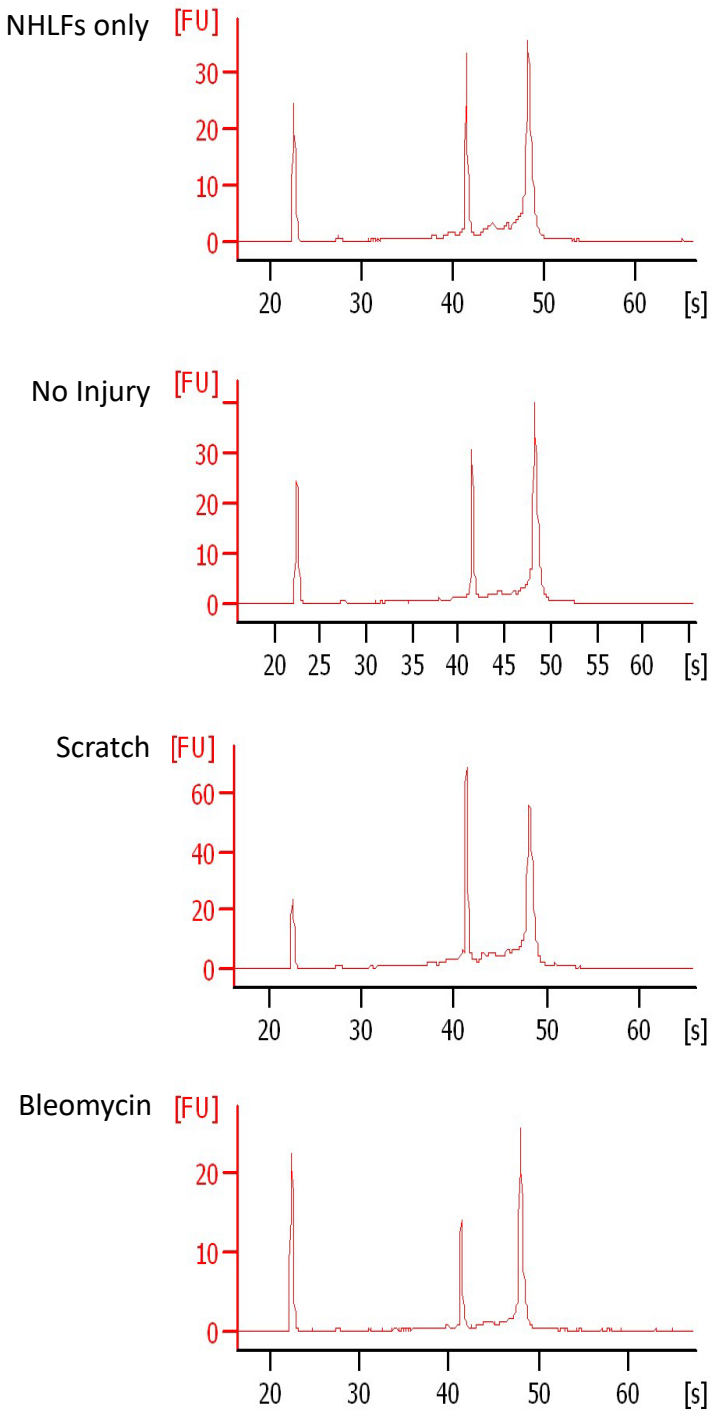


Figure A5.2: Electropherogram of the fibroblasts from 3D co-culture model. There are two fragments 18 s and 28 divide the electropherogram

Table A5.1: Table showing the RIN (RNA integrity number for the fibroblasts and epithelial cells for the 21 samples sent for analysis.

Conditions	Fibroblasts from 3D co-culture (Sample number)		
	1	2	3
NHLFs	7.8	8.6	7.2
NHLFs	9.1	9.6	7.5
NHLFs	0	9.1	8.4
No-injury	8.1	9.6	8.3
No-injury	8.4	7.4	8
No-injury	9.3	9.1	8.4
Scratch	8.4	9.2	8.5
Scratch	8.1	9.1	8
Scratch	0	9.8	8.1
Bleo (5mU)	8.3	9.3	8.1
Bleo (5mU)	8.2	8.7	8.6
Bleo (5mU)	0	0	8.9

Conditions	Epithelial cells from monolayer model (sample number)		
	1	2	3
SAEs	8.2	8.2	8.7
SAEs	8.7	8.1	8.9
SAEs	7.5	8.5	8.5
Scratch	7.6	8.4	8.6
Scratch	8.6	8.3	8.9
Scratch	7.9	8.7	8.9
Bleo (5mU)	7.5	8.4	7.8
Bleo (5mU)	7.9	9.1	7.1
Bleo (5mU)	0	0	7.7

Appendix 6: Serum samples from study

Table A6.1: Demographics information of the individual subjects used for chapter 4 studies in conjunction to the serum samples. The initial study was approved by the Nottingham Research and Ethics Committee 1 (REC ref: 09/H0403/59).

StudyID	DOB	Gender	Dateof Diagnosis	Date of Consent	Dateof Death	Dead	Smokes	Spirometry TestDate @ baseline	Height in m	TLCO	FVC	FEV1
TLFD001	18/09/1929	Female	03/09/2009	08/03/2010	13/12/2012	Y	N	03/09/2009	1.59	2.01	1.76	1.57
TLFD003	11/09/1929	Female	13/10/2009	14/04/2010		N	Y	13/08/2009	1.61	0.00	0.00	0.00
TLFD005	05/05/1947	Male	17/11/2009	10/03/2010	24/11/2011	Y	Y	01/10/2009	1.81	4.47	3.73	2.86
TLFD006	22/10/1942	Male	20/05/2009	25/02/2010	09/08/2011	Y	Y	08/06/2009	1.75	5.63	4.01	3.20
TLFD007	11/01/1941	Male	14/05/2009	10/03/2010		N	Y	01/05/2009	1.64	3.24	2.10	1.67
TLFD008	10/03/1926	Male	18/06/2009	25/03/2010	05/08/2011	Y	N	23/06/2009	1.63	2.52	2.37	1.99
TLFD015	22/04/1945	Female	23/06/2009	29/03/2010		N	Y	12/06/2009	1.54	3.18	2.25	1.76
TLFD016	03/12/1932	Male	18/11/2009	18/02/2010	08/09/2012	Y	Y	20/01/2010	1.65	4.49	3.74	2.65
TLFD017	22/11/1954	Female	26/06/2009	11/02/2010		N	N	08/07/2009	1.70	5.67	3.41	2.83
TLFD019	23/02/1945	Female	09/04/2009	25/03/2010		N	Y	21/04/2009	1.55	3.77	2.04	1.81
TLFD020	21/01/1944	Male	12/06/2009	15/03/2010	23/01/2013	Y	Y	17/06/2009	1.75	4.20	3.77	3.20
TLFD026	12/06/1925	Male	25/11/2009	15/03/2010		N	Y	25/11/2009	1.74	5.87	2.92	2.42
TLFD027	14/04/1936	Male	06/06/2009	12/04/2010		N	Y	09/12/2009	1.78	2.90	3.89	3.28
TLFD028	06/09/1939	Male	16/11/2009	27/05/2010	21/06/2011	Y	N	11/02/2010	1.66	3.60	1.83	1.62
TLFD029	17/10/1934	Female	21/08/2009	27/05/2010		N	N	19/11/2009	1.65	4.10	2.15	1.80
TLFD030	29/12/1934	Male	29/09/2010	29/04/2010		N	Y	12/08/2011	1.78	4.31	3.03	2.14
TLFD032	11/12/1942	Female	27/07/2009	23/04/2010		N	Y	09/01/2012	1.59	3.50	1.99	1.64
TLFD033	06/06/1916	Male	03/09/2009	19/02/2010		N	Y	19/02/2010	1.61	4.22	2.33	1.73
TLFD034	10/05/1924	Male	28/05/2009	23/04/2010	03/10/2011	Y	Y	23/06/2009	1.70	2.27	2.88	1.20
TLFD035	16/08/1932	Male	21/12/2009	30/04/2010	22/10/2011	Y	Y	07/01/2010	1.70	0.00	2.90	2.30
TLFD036	27/09/1940	Female	21/10/2009	29/03/2010	08/05/2012	Y	Y	28/09/2009	1.54	2.23	1.88	1.55
TLFD037	22/11/1929	Male	01/04/2009	04/03/2010		N	N	29/06/2009	1.79	3.46	4.39	3.42
TLFD039	30/11/1928	Male	21/08/2009	29/03/2010	08/09/2010	Y	N	06/08/2009	1.75	2.58	2.22	2.07
TLFD040	23/04/1943	Male	26/11/2009	08/03/2010		N	Y	11/11/2009	1.77	3.90	2.86	2.44
TLFD041	18/11/1931	Female	15/12/2009	26/04/2010	08/01/2012	Y	N	N/A	0.00	0.00	0.00	0.00
TLFD042	24/06/1934	Male	26/11/2009	12/03/2010		N	Y	25/05/2010	1.72	4.46	3.66	2.77
TLFD043	08/07/1933	Female	14/08/2009	16/03/2010		N	N	16/09/2009	1.57	3.58	1.67	1.51
TLFD044	17/08/1944	Male	14/07/2009	29/07/2010		N	Y	14/07/2009	1.71	0.00	2.56	2.10
TLFD045	16/11/1923	Male	04/11/2009	01/04/2010		N	Y	11/11/2009	1.79	3.14	3.94	3.30
TLFD052	29/04/1928	Female	01/06/2009	04/06/2010		N	Y	26/05/2009	1.56	2.72	1.77	1.48
TLFD054	13/03/1935	Male	16/09/2009	05/03/2011		N	Y	14/12/2009	1.72	4.23	2.98	2.53
TLFD056	28/01/1948	Male	03/02/2010	14/05/2010		N	N	01/04/2010	1.73	3.33	2.49	2.22
TLFD057	21/02/1938	Male	28/09/2009	20/07/2010		N	Y	27/10/2009	1.62	3.68	1.98	1.74
TLFD059	01/12/1944	Female	02/02/2010	17/05/2010		N	Y	09/03/2010	1.56	2.70	1.93	1.50
TLFD060	19/12/1952	Male	12/01/2010	11/05/2010		N	N	12/01/2010	1.82	4.89	4.16	3.08
TLFD061	15/10/1933	Male	28/01/2010	10/02/2011	09/09/2011	Y	Y	19/01/2010	1.70	4.30	3.27	2.24
TLFD062	12/08/1939	Female	16/10/2009	22/04/2010	13/11/2010	Y	N	11/06/2010	1.49	2.48	1.80	1.64
TLFD063	04/01/1932	Male	19/03/2010	22/04/2010	18/03/2011	Y	Y	30/03/2010	1.72	3.80	2.46	2.02
TLFD065	22/04/1934	Male	08/03/2010	14/05/2010		N	Y	25/03/2010	1.74	2.70	3.17	2.11
TLFD067	26/06/1952	Male	05/03/2010	18/06/2010	21/07/2010	Y	Y	09/03/2010	1.72	3.40	4.30	3.28
TLFD068	23/04/1932	Female	01/03/2010	24/06/2010		N	N	29/03/2010	1.64	4.23	2.41	1.83
TLFD070	05/03/1928	Male	11/12/2009	18/05/2010		N	N	21/12/2009	1.61	3.08	1.98	1.66
TLFD071	22/02/1932	Male	11/12/2009	24/05/2010	20/11/2011	Y	Y	02/12/2009	1.71	3.68	2.75	2.49
TLFD072	28/05/1926	Male	13/01/2010	23/06/2010	03/01/2013	Y	Y	20/01/2010	1.77	3.64	3.15	2.68
TLFD073	17/09/1934	Female	08/02/2010	16/06/2010		N	N	06/01/2010	1.52	2.80	1.90	1.75
TLFD074	24/04/1956	Male	19/03/2010	10/02/2011		N	Y	22/03/2010	1.77	4.93	3.57	2.83
TLFD075	02/04/1931	Male	09/11/2009	18/06/2010	17/12/2010	Y	Y	03/11/2009	1.72	3.25	3.09	2.27
TLFD076	20/04/1938	Male	03/07/2009	20/07/2010		N	N	07/07/2009	1.77	4.03	3.56	3.11
TLFD077	26/03/1920	Male	07/04/2010	25/05/2010	01/01/2011	Y	Y	27/04/2011	1.63	no	2.30	1.35
TLFD078	13/01/1937	Female	09/02/2010	29/06/2010	11/10/2011	Y	Y	10/03/2010	1.60	3.22	2.72	2.18
TLFD079	17/06/1937	Male	26/04/2010	23/06/2010		N	Y	25/05/2010	1.75	7.74	4.58	3.55
TLFD080	07/07/1927	Male	18/01/2010	16/06/2010		N	Y	19/11/2009	1.75	6.53	2.98	2.26
TLFD082	27/08/1924	Female	12/03/2010	13/07/2010	17/09/2011	Y	N	23/09/2010	1.57	1.85	1.77	1.65
TLFD084	11/07/1964	Male	31/12/2009	13/08/2010	28/03/2010	Y	N	30/12/2009	1.63	4.15	2.64	2.19
TLFD089	01/12/1930	Male	10/05/2010	09/08/2010	17/09/2012	Y	N	08/06/2010	1.75	4.00	2.87	2.61
TLFD090	20/05/1931	Male	23/11/2009	01/07/2010	16/06/2011	Y	N	02/12/2009	1.71	3.77	3.70	2.82
TLFD096	07/06/1943	Male	11/05/2010	20/01/2011	28/12/2011	Y	Y	10/06/2010	1.81	3.37	3.00	2.25
TLFD097	17/04/1932	Male	12/05/2010	20/01/2011	07/03/2011	Y	N	06/05/2010	1.67	no result	1.43	1.40

Appendix 7: MicroArray Database CD

Appendix 8: Epithelial cells in Transwell® insert.

8.1 Migration of epithelial cells in a Transwell® insert

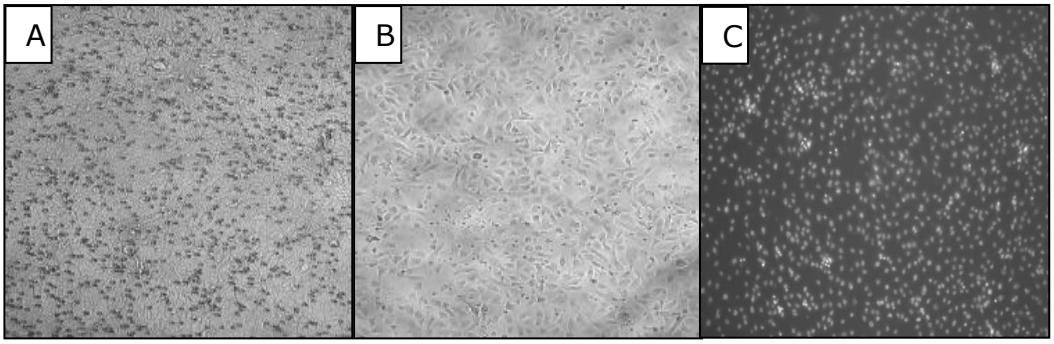


Figure A8.1: Migration of epithelial cells using a 8.0μm insert.
A; Epithelial cells in insert. B; Epithelial cells in the well below. C; DAPI stained epithelial cells.

Bibliography

Abraham, D. J., X. Shiwen, et al. (2000). "Tumor necrosis factor alpha suppresses the induction of connective tissue growth factor by transforming growth factor-beta in normal and scleroderma fibroblasts." J Biol Chem **275**(20): 15220-15225.

Adamson, I. Y. and D. H. Bowden (1974). "The pathogenesis of bleomycin-induced pulmonary fibrosis in mice." Am J Pathol **77**(2): 185-197.

Adegunsoye, A. and J. Balachandran (2015). ''Inflammatory response mechanisms exacerbating hypoxemia in coexistent pulmonary fibrosis and sleep apnea''. Mediators Inflamm. 10.1155/2015/510105.

Agostini, C. and C. Gurrieri (2006). "Chemokine/cytokine cocktail in idiopathic pulmonary fibrosis." Proc Am Thorac Soc **3**(4): 357-363.

Ahmedat, A. S., M. Warnken, et al. (2013). "Pro-fibrotic processes in human lung fibroblasts are driven by an autocrine/paracrine endothelinergic system." Br J Pharmacol **168**(2): 471-487.

Allan, G. J., J. Beattie, et al. (2008). "Epithelial injury induces an innate repair mechanism linked to cellular senescence and fibrosis involving IGF-binding protein-5." J Endocrinol **199**(2): 155-164.

Allen, J. T. and M. A. Spiteri (2002). "Growth factors in idiopathic pulmonary fibrosis: relative roles." Respir Res **3**: 13.

Altieri, D. C. (2010). "Survivin and IAP proteins in cell-death mechanisms." Biochem J **430**(2): 199-205.

Altznauer, F., S. Martinelli, et al. (2004). "Inflammation-associated cell cycle-independent block of apoptosis by survivin in terminally differentiated neutrophils." J Exp Med **199**(10): 1343-1354.

Aoyagi-Ikeda, K., T. Maeno, et al. (2011). "Notch induces myofibroblast differentiation of alveolar epithelial cells via transforming growth factor-{beta}-Smad3 pathway." Am J Respir Cell Mol Biol **45**(1): 136-144.

Aschner Y, Downey GP (2016) "Transforming Growth Factor-β: Master Regulator of the Respiratory System in Health and Disease.". Am J Respir Cell Mol Biol. 54(5):647-55.

Askew, D. J. and G. A. Silverman (2008). "Intracellular and extracellular serpins modulate lung disease." J Perinatol **28 Suppl 3**: S127-135.

Atkinson, J. J. and R. M. Senior (2003). "Matrix metalloproteinase-9 in lung remodeling." Am J Respir Cell Mol Biol **28**(1): 12-24.

Bailey, C. C., G. Zhong, et al. (2014). "IFITM-Family Proteins: The Cell's First Line of Antiviral Defense." Annu Rev Virol **1**: 261-283.

Barton, M., S. Shaw, et al. (1997). "Angiotensin II increases vascular and renal endothelin-1 and functional endothelin converting enzyme activity in vivo: role of ETA receptors for endothelin regulation." Biochem Biophys Res Commun **238**(3): 861-865.

Baumgartner, K. B., J. M. Samet, et al. (1997). "Cigarette smoking: a risk factor for idiopathic pulmonary fibrosis." Am J Respir Crit Care Med **155**(1): 242-248.

Berg, T., L. Didon, et al. (2006). "Ectopic expression of C/EBPalpha in the lung epithelium disrupts late lung development." Am J Physiol Lung Cell Mol Physiol **291**(4): L683-693.

Bergeron A, Soler P, Kambouchner M, Loiseau P, Milleron B, Valeyre D, Hance AJ, Tazi A (2003). "Cytokine profiles in idiopathic pulmonary fibrosissuggest an important role for TGF-b and IL-10." Eur Respir J 22:69–76.

Bianchi, M. E. (2007). "DAMPs, PAMPs and alarmins: all we need to know about danger." J Leukoc Biol **81**(1): 1-5.

Blaauboer, M. E., F. R. Boeijen, et al. (2014). "Extracellular matrix proteins: a positive feedback loop in lung fibrosis?" Matrix Biol **34**: 170-178.

Bogatkevich, G. S., Aktar, T. (2012). '' Inhibitory Effects of the Dual Endothelin Receptor Blocker Bosentan on Thrombin-Activated Lung Fibroblasts Isolated from Scleroderma Patients''. Rheum S1:005

Bolanos, A. L., C. M. Milla, et al. (2012). "Role of Sonic Hedgehog in idiopathic pulmonary fibrosis." Am J Physiol Lung Cell Mol Physiol **303**(11): L978-990.

Borensztajn, K., B. Crestani, et al. (2013). "Idiopathic pulmonary fibrosis: from epithelial injury to biomarkers--insights from the bench side." Respiration **86**(6): 441-452.

Boscoe, M. J., A. T. Goodwin, et al. (2000). "Endothelins and the lung." Int J Biochem Cell Biol **32**(1): 41-62.

Booth AJ, Hadley R, et al. (2012). '' Acellular normal and fibrotic human lung matrices as a culture system for in vitro investigation.'' Am J Respir Crit Care Med 1;186(9):866-76.

Brinckerhoff, C. E. and L. M. Matrisian (2002). "Matrix metalloproteinases: a tail of a frog that became a prince." Nat Rev Mol Cell Biol **3**(3): 207-214.

Budinger, G. R., G. M. Mutlu, et al. (2006). "Proapoptotic Bid is required for pulmonary fibrosis." Proc Natl Acad Sci U S A **103**(12): 4604-4609.

Bullwinkel, J., B. Baron-Luhr, et al. (2006). "Ki-67 protein is associated with ribosomal RNA transcription in quiescent and proliferating cells." J Cell Physiol **206**(3): 624-635.

Cabrera, S., M. Gaxiola, et al. (2007). "Overexpression of MMP9 in macrophages attenuates pulmonary fibrosis induced by bleomycin." Int J Biochem Cell Biol **39**(12): 2324-2338.

Chakrabarti, S.and K.D Patel. (2005). ''Matrix metalloproteinase-2 (MMP-2) and MMP-9 in pulmonary pathology''. Exp Lung Res **31**(6):599-621.

Chang, W. Y., J. L. Cane, et al. (2012). "Clinical utility of diagnostic guidelines and putative biomarkers in lymphangioleiomyomatosis." Respir Res **13**: 34.

Chapman, H. A. (2011). "Epithelial-mesenchymal interactions in pulmonary fibrosis." Annu Rev Physiol **73**: 413-435.

Checa, M., V. Ruiz, et al. (2008). "MMP-1 polymorphisms and the risk of idiopathic pulmonary fibrosis." Hum Genet **124**(5): 465-472.

Chen, Q. K., K. Lee, et al. (2013). "Extracellular matrix proteins regulate epithelial-mesenchymal transition in mammary epithelial cells." Differentiation **86**(3): 126-132.

Chesarino, N. M., T. M. McMichael, et al. (2014). "Regulation of the trafficking and antiviral activity of IFITM3 by post-translational modifications." Future Microbiol **9**(10): 1151-1163.

Choe, M. M., P. H. Sporn, et al. (2006). "Extracellular matrix remodeling by dynamic strain in a three-dimensional tissue-engineered human airway wall model." Am J Respir Cell Mol Biol **35**(3): 306-313.

Choi, E. S., C. Jakubzick, et al. (2004). "Enhanced monocyte chemoattractant protein-3/CC chemokine ligand-7 in usual interstitial pneumonia." Am J Respir Crit Care Med **170**(5): 508-515.

Chung, M. P., M. M. Monick, et al. (2003). "Role of repeated lung injury and genetic background in bleomycin-induced fibrosis." Am J Respir Cell Mol Biol **29**(3 Pt 1): 375-380.

Clarke, D. L., A. M. Carruthers, et al. (2013). "Matrix regulation of idiopathic pulmonary fibrosis: the role of enzymes." Fibrogenesis Tissue Repair **6**(1): 20.

Collard, H. R., B. B. Moore, et al. (2007). "Acute exacerbations of idiopathic pulmonary fibrosis." Am J Respir Crit Care Med **176**(7): 636-643.

Cool, C. D., S. D. Groshong, et al. (2006). "Fibroblast foci are not discrete sites of lung injury or repair: the fibroblast reticulum." Am J Respir Crit Care Med **174**(6): 654-658.

Copley, S. J., A. U. Wells, et al. (2003). "Asbestosis and idiopathic pulmonary fibrosis: comparison of thin-section CT features." Radiology **229**(3): 731-736.

Corbel, M., C. Belleguic, et al. (2002). "Involvement of gelatinases (MMP-2 and MMP-9) in the development of airway inflammation and pulmonary fibrosis." Cell Biol Toxicol **18**(1): 51-61.

Corte, T. J., G. J. Keir, et al. (2014). "Bosentan in pulmonary hypertension associated with fibrotic idiopathic interstitial pneumonia." Am J Respir Crit Care Med **190**(2): 208-217.

Cott, G. R., J. Y. Westcott, et al. (1990). "Prostaglandin and leukotriene production by alveolar type II cells in vitro." Am J Physiol **258**(4 Pt 1): L179-187.

Cottin, V. (2012). "Changing the idiopathic pulmonary fibrosis treatment approach and improving patient outcomes." Eur Respir Rev **21**(124): 161-167.

Coultas, D. B., R. E. Zumwalt, et al. (1994). "The epidemiology of interstitial lung diseases." Am J Respir Crit Care Med **150**(4): 967-972.

Coward, W. R., G. Saini, et al. (2010). "The pathogenesis of idiopathic pulmonary fibrosis." Ther Adv Respir Dis **4**(6): 367-388.

Cox, T. R. and J. T. Erler (2011). "Remodeling and homeostasis of the extracellular matrix: implications for fibrotic diseases and cancer." Dis Model Mech **4**(2): 165-178.

Creasey, A. A., J. C. Bartholomew, et al. (1980). "Role of G0-G1 arrest in the inhibition of tumor cell growth by interferon." Proc Natl Acad Sci U S A **77**(3): 1471-1475.
Fernandez, L. M. and C. M. Waters (2010). "Epithelial repair mechanisms in the lung." Am J Physiol Lung Cell Mol Physiol **298**(6): L715-731.
D'Agnano, I., A. Valentini, et al. (2007). "Oligopeptides impairing the Myc-Max heterodimerization inhibit lung cancer cell proliferation by reducing Myc transcriptional activity." J Cell Physiol **210**(1): 72-80.
Dalma-Weiszhausz, D. D., J. Warrington, et al. (2006). "The affymetrix GeneChip platform: an overview." Methods Enzymol **410**: 3-28.
Dancer, R. C., A. M. Wood, et al. (2011). "Metalloproteinases in idiopathic pulmonary fibrosis." Eur Respir J **38**(6): 1461-1467.
Darnell, J. E., Jr., I. M. Kerr, et al. (1994). "Jak-STAT pathways and transcriptional activation in response to IFNs and other extracellular signaling proteins." Science **264**(5164): 1415-1421.
Das, A., P. X. Dinh, et al. (2014). "Interferon-inducible protein IFI35 negatively regulates RIG-I antiviral signaling and supports vesicular stomatitis virus replication." J Virol **88**(6): 3103-3113.
Datta, A., C. J. Scotton, et al. (2011). "Novel therapeutic approaches for pulmonary fibrosis." Br J Pharmacol **163**(1): 141-172.
Davoine, F. and P. Lacy (2014). "Eosinophil cytokines, chemokines, and growth factors: emerging roles in immunity." Front Immunol **5**: 570.
de Lauretis, A., S. Veeraraghavan, et al. (2011). "Review series: Aspects of interstitial lung disease: connective tissue disease-associated interstitial lung disease: how does it differ from IPF? How should the clinical approach differ?" Chron Respir Dis **8**(1): 53-82.
de Veer, M. J., M. Holko, et al. (2001). "Functional classification of interferon-stimulated genes identified using microarrays." J Leukoc Biol **69**(6): 912-920.
Della Latta, V., A. Cecchettini, et al. (2015). "Bleomycin in the setting of lung fibrosis induction: From biological mechanisms to counteractions." Pharmacol Res **97**: 122-130.
Desmouliere, A. (1995). "Factors influencing myofibroblast differentiation during wound healing and fibrosis." Cell Biol Int **19**(5): 471-476.
Dinarello, C. A. (1996). "Biologic basis for interleukin-1 in disease." Blood **87**(6): 2095-2147.
Doornaert, B., V. Leblond, et al. (2003). "Negative impact of DEP exposure on human airway epithelial cell adhesion, stiffness, and repair." Am J Physiol Lung Cell Mol Physiol **284**(1): L119-132.
DosReis, G. A. and V. M. Borges (2003). "Role of Fas-ligand induced apoptosis in pulmonary inflammation and injury." Curr Drug Targets Inflamm Allergy **2**(2): 161-167.
Drakopanagiotakis, F., A. Xifteri, et al. (2008). "Apoptosis in lung injury and fibrosis." Eur Respir J **32**(6): 1631-1638.
du Bois, R. M. (2010). "Strategies for treating idiopathic pulmonary fibrosis." Nat Rev Drug Discov **9**(2): 129-140.
Dufour, A., S. Zucker, et al. (2010). "Role of matrix metalloproteinase-9 dimers in cell migration: design of inhibitory peptides." J Biol Chem **285**(46): 35944-35956.
Dunbier, A. K., H. Anderson, et al. (2011). "ESR1 is co-expressed with closely adjacent uncharacterised genes spanning a breast cancer susceptibility locus at 6q25.1." PLoS Genet **7**(4): e1001382.
El Agha, E. and S. Bellusci (2014). "Walking along the Fibroblast Growth Factor 10 Route: A Key Pathway to Understand the Control and Regulation of Epithelial and Mesenchymal Cell-Lineage Formation during Lung Development and Repair after Injury." Scientifica (Cairo) 2014: 538379.
Emblom-Callahan, M. C., M. K. Chhina, et al. (2010). "Genomic phenotype of non-cultured pulmonary fibroblasts in idiopathic pulmonary fibrosis." Genomics **96**(3): 134-145.
Erb, H. H., R. V. Langlechner, et al. (2013). "IL6 sensitizes prostate cancer to the antiproliferative effect of IFNalpha2 through IRF9." Endocr Relat Cancer **20**(5): 677-689.

Estany, S., V. Vicens-Zygmunt, et al. (2014). ''Lung fibrotic tenascin-C upregulation is associated with other extracellular matrix proteins and induced by TGFβ1. BMC **120**:14.
Fagan, K. A., I. F. McMurtry, et al. (2001). "Role of endothelin-1 in lung disease." Respir Res **2**(2): 90-101.
Fensterl, V. and G. C. Sen (2011). "The ISG56/IFIT1 gene family." J Interferon Cytokine Res **31**(1): 71-78.
Fernandez, I. E. and O. Eickelberg (2012). "The impact of TGF-beta on lung fibrosis: from targeting to biomarkers." Proc Am Thorac Soc **9**(3): 111-116.
Fernandez, I. E. and O. Eickelberg (2012). "New cellular and molecular mechanisms of lung injury and fibrosis in idiopathic pulmonary fibrosis." Lancet **380**(9842): 680-688.
Fonseca, C., D. Abraham, et al. (2011). "Endothelin in pulmonary fibrosis." Am J Respir Cell Mol Biol **44**(1): 1-10.
Fortini, M. E. (2009). '' Notch signaling: the core pathway and its posttranslational regulation. '' Dev Cell 16(5):633-47
Fujino, N., H. Kubo, et al. (2011). "Isolation of alveolar epithelial type II progenitor cells from adult human lungs." Lab Invest **91**(3): 363-378.
Fukuda, Y., M. Ishizaki, et al. (1998). "Localization of matrix metalloproteinases-1, -2, and -9 and tissue inhibitor of metalloproteinase-2 in interstitial lung diseases." Lab Invest **78**(6): 687-698.
Gabay, C. (2006). "Interleukin-6 and chronic inflammation." Arthritis Res Ther **8 Suppl 2**: S3.
Gallelli, L., G. Pelaia, et al. (2005). "Endothelin-1 induces proliferation of human lung fibroblasts and IL-11 secretion through an ET(A) receptor-dependent activation of MAP kinases." J Cell Biochem **96**(4): 858-868.
Giannandrea, M. and W. C. Parks (2014). "Diverse functions of matrix metalloproteinases during fibrosis." Dis Model Mech **7**(2): 193-203.
Gilani, S. R, Vuga, L. J, et al. (2010). ''CD28 down-regulation on circulating CD4 T-cells is associated with poor prognoses of patients with idiopathic pulmonary fibrosis.'' PLoS One 29;5(1):e8959
Greenlee, K. J, Werb Z, et al. (2007). '' Matrix metalloproteinases in lung: multiple, multifarious, and multifaceted.'' Physiol Rev 87(1):69-9.
Greijer, A. E. and E. van der Wall (2004). "The role of hypoxia inducible factor 1 (HIF-1) in hypoxia induced apoptosis." J Clin Pathol **57**(10): 1009-1014.
Gross, T. J. and G. W. Hunninghake (2001). "Idiopathic pulmonary fibrosis." N Engl J Med **345**(7): 517-525.
Habiel, D. M. and C. Hogaboam (2014). "Heterogeneity in fibroblast proliferation and survival in idiopathic pulmonary fibrosis." Front Pharmacol **5**: 2.
Hamilton, R. F., Jr., L. Li, et al. (1995). "Bleomycin induces apoptosis in human alveolar macrophages." Am J Physiol **269**(3 Pt 1): L318-325.
Harari, S. and A. Caminati (2010). "IPF: new insight on pathogenesis and treatment." Allergy **65**(5): 537-553.
Hay, E. D. (1995). "An overview of epithelio-mesenchymal transformation." Acta Anat (Basel) **154**(1): 8-20.
Heinrich, P. C., I. Behrmann, et al. (2003). "Principles of interleukin (IL)-6-type cytokine signalling and its regulation." Biochem J **374**(Pt 1): 1-20.
Heinrich, P. C., I. Behrmann, et al. (1998). "Interleukin-6-type cytokine signalling through the gp130/Jak/STAT pathway." Biochem J **334 (Pt 2)**: 297-314.
Henderson, N., L. J. Markwick, et al. (2007). "Collagen I and thrombin activate MMP-2 by MMP-14-dependent and -independent pathways: implications for airway smooth muscle migration." Am J Physiol Lung Cell Mol Physiol **292**(4): L1030-1038.
Herrera, I., J. Cisneros, et al. (2013). "Matrix metalloproteinase (MMP)-1 induces lung alveolar epithelial cell migration and proliferation, protects from apoptosis, and represses mitochondrial oxygen consumption." J Biol Chem **288**(36): 25964-25975.
Hinz, B., S. H. Phan, et al. (2007). "The myofibroblast: one function, multiple origins." Am J Pathol **170**(6): 1807-1816.
Hisatomi, K., H. Mukae, et al. (2012). "Pirfenidone inhibits TGF-beta1-induced over-expression of collagen type I and heat shock protein 47 in A549 cells." BMC Pulm Med **12**: 24.

Honeyman, L., M. Bazett, et al. (2013). "MicroRNA profiling implicates the insulin-like growth factor pathway in bleomycin-induced pulmonary fibrosis in mice." Fibrogenesis Tissue Repair **6**(1): 16.
Horan, G. S., S. Wood, et al. (2008). "Partial inhibition of integrin alpha(v)beta6 prevents pulmonary fibrosis without exacerbating inflammation." Am J Respir Crit Care Med **177**(1): 56-65.
Horowitz, J. C., I. O. Ajayi, et al. (2012). "Survivin expression induced by endothelin-1 promotes myofibroblast resistance to apoptosis." Int J Biochem Cell Biol **44**(1): 158-169.
Hsu, S. M., Raine, L., Fanger, H. (1981). '' Use of avidin-biotin-peroxidase complex (ABC) in immunoperoxidase techniques: a comparison between ABC and unlabeled antibody (PAP) procedures. J His & Cyto 29:4:577-580.

Hua, X., Liu, X., Ansari, D. O., and Lodish, H. F (1998). "Synergistic cooperation of TFE3 and smad proteins in TGF-beta-induced transcription of the plasminogen activator inhibitor-1 gene." Genes Dev. 12, 3084–3095.
Hubbard, R., I. Johnston, et al. (1998). "Survival in patients with cryptogenic fibrosing alveolitis: a population-based cohort study." Chest **113**(2): 396-400.
Hubbard, R., S. Lewis, et al. (1996). "Occupational exposure to metal or wood dust and aetiology of cryptogenic fibrosing alveolitis." Lancet **347**(8997): 284-289.
Hughes, C. S., L. M. Postovit, et al. (2010). "Matrigel: a complex protein mixture required for optimal growth of cell culture." Proteomics **10**(9): 1886-1890.
Huiping, L. (2009). "The Alveolar Epithelium and Pulmonary Fibrosis." Journal of epithelial Biology and Pharmacology **2**: 30-35.
Hwang, S. C., K. H. Park, et al. (1996). "Distribution of phospholipase C isozymes in normal human lung tissue and their immunohistochemical localization." J Korean Med Sci **11**(4): 305-313.
Hynes, R. O. (2009). '' The extracellular matrix: not just pretty fibrils.'' Science 326(5957):1216-9.
Inomata, M., K. Kamio, et al. (2014). "Pirfenidone inhibits fibrocyte accumulation in the lungs in bleomycin-induced murine pulmonary fibrosis." Respir Res **15**: 16.
Irizarry, R. A., B. Hobbs, et al. (2003). "Exploration, normalization, and summaries of high density oligonucleotide array probe level data." Biostatistics **4**(2): 249-264.
Jenkins, G. (2008). "The role of proteases in transforming growth factor-beta activation." Int J Biochem Cell Biol **40**(6-7): 1068-1078.
Jenkins, R. G., X. Su, et al. (2006). "Ligation of protease-activated receptor 1 enhances alpha(v)beta6 integrin-dependent TGF-beta activation and promotes acute lung injury." J Clin Invest **116**(6): 1606-1614.
Johnson, A. and L. A. DiPietro (2013). "Apoptosis and angiogenesis: an evolving mechanism for fibrosis." FASEB J **27**(10): 3893-3901.
Kaarteenaho, R. (2013). "The current position of surgical lung biopsy in the diagnosis of idiopathic pulmonary fibrosis." Respir Res **14**: 43.
Kalimuthu, S. and K. Se-Kwon (2013). "Cell survival and apoptosis signaling as therapeutic target for cancer: marine bioactive compounds." Int J Mol Sci **14**(2): 2334-2354.
Kalluri, R. and E. G. Neilson (2003). "Epithelial-mesenchymal transition and its implications for fibrosis." J Clin Invest **112**(12): 1776-1784.
Kaminski, N., J. D. Allard, et al. (2000). "Global analysis of gene expression in pulmonary fibrosis reveals distinct programs regulating lung inflammation and fibrosis." Proc Natl Acad Sci U S A **97**(4): 1778-1783.
Kaminski, N. and I. O. Rosas (2006). "Gene expression profiling as a window into idiopathic pulmonary fibrosis pathogenesis: can we identify the right target genes?" Proc Am Thorac Soc **3**(4): 339-344.
Kamp, D. W. (2009). "Asbestos-induced lung diseases: an update." Transl Res **153**(4): 143-152.
Kapanci, Y., A. Desmouliere, et al. (1995). "Cytoskeletal protein modulation in pulmonary alveolar myofibroblasts during idiopathic pulmonary fibrosis. Possible role of transforming growth factor beta and tumor necrosis factor alpha." Am J Respir Crit Care Med **152**(6 Pt 1): 2163-2169.

Kapuscinski, J. (1995). "DAPI: a DNA-specific fluorescent probe." Biotech Histochem **70**(5): 220-233.
Katzenstein, A. L. (1985). "Pathogenesis of "fibrosis" in interstitial pneumonia: an electron microscopic study." Hum Pathol **16**(10): 1015-1024.
Katzenstein, A. L. and J. L. Myers (1998). "Idiopathic pulmonary fibrosis: clinical relevance of pathologic classification." Am J Respir Crit Care Med **157**(4 Pt 1): 1301-1315.
Kerr, J. F. (1999). "A personal account of events leading to the definition of the apoptosis concept." Results Probl Cell Differ **23**: 1-10.
Khanna, S., S. Biswas, et al. (2010). "Macrophage dysfunction impairs resolution of inflammation in the wounds of diabetic mice." PLoS One **5**(3): e9539.
Kim, J. Y., H. C. Choeng, et al. (2009). "Early and late changes of MMP-2 and MMP-9 in bleomycin-induced pulmonary fibrosis." Yonsei Med J **50**(1): 68-77.
Kim, K. H., K. Burkhart, et al. (2005). "Tissue inhibitor of metalloproteinase-1 deficiency amplifies acute lung injury in bleomycin-exposed mice." Am J Respir Cell Mol Biol **33**(3): 271-279.
Kim, K. K., M. C. Kugler, et al. (2006). "Alveolar epithelial cell mesenchymal transition develops in vivo during pulmonary fibrosis and is regulated by the extracellular matrix." Proc Natl Acad Sci U S A **103**(35): 13180-13185.
Kim, S. J., P. Cheresh, et al. (2015). "The Role of Mitochondrial DNA in Mediating Alveolar Epithelial Cell Apoptosis and Pulmonary Fibrosis." Int J Mol Sci **16**(9): 21486-21519.
Kim K.K, Wei Y, Szekeres C, Kugler MC, Wolters PJ, Hill ML, Frank JA, Brumwell AN, Wheeler SE, Kreidberg JA, et al (2009). "Epithelial cell a3b1 integrin links b-catenin and Smad signaling to promote myofibroblast formation and pulmonary fibrosis." J Clin Invest 119:213–224.
King, T. E., Jr., A. Pardo, et al. (2011). "Idiopathic pulmonary fibrosis." Lancet **378**(9807): 1949-1961.
King, T. E., Jr., M. I. Schwarz, et al. (2001). "Idiopathic pulmonary fibrosis: relationship between histopathologic features and mortality." Am J Respir Crit Care Med **164**(6): 1025-1032.
Kolb, M. and H. R. Collard (2014). "Staging of idiopathic pulmonary fibrosis: past, present and future." Eur Respir Rev **23**(132): 220-224.
Konigshoff, M. and O. Eickelberg (2010). "WNT signaling in lung disease: a failure or a regeneration signal?" Am J Respir Cell Mol Biol **42**(1): 21-31.
Konigshoff, M., M. Kramer, et al. (2009). "WNT1-inducible signaling protein-1 mediates pulmonary fibrosis in mice and is upregulated in humans with idiopathic pulmonary fibrosis." J Clin Invest **119**(4): 772-787.
Konishi, K., K. F. Gibson, et al. (2009). "Gene expression profiles of acute exacerbations of idiopathic pulmonary fibrosis." Am J Respir Crit Care Med **180**(2): 167-175.
Krein, P. M. and B. W. Winston (2002). "Roles for insulin-like growth factor I and transforming growth factor-beta in fibrotic lung disease." Chest **122**(6 Suppl): 289S-293S.
Kugler, M. C., A. L. Joyner, et al. (2014). "Sonic Hedgehog Signaling in the Lung - from Development to Disease." Am J Respir Cell Mol Biol.
Kulasekaran, P., C. A. Scavone, et al. (2009). "Endothelin-1 and transforming growth factor-beta1 independently induce fibroblast resistance to apoptosis via AKT activation." Am J Respir Cell Mol Biol **41**(4): 484-493.
Kunichika, N., J. W. Landsberg, et al. (2004). "Bosentan inhibits transient receptor potential channel expression in pulmonary vascular myocytes." Am J Respir Crit Care Med **170**(10): 1101-1107.
Kuwano, K. (2007). "Epithelial cell apoptosis and lung remodeling." Cell Mol Immunol **4**(6): 419-429.
Kuwano, K., N. Hagimoto, et al. (2004). "The role of apoptosis in pulmonary fibrosis." Histol Histopathol **19**(3): 867-881.
Kuwano, K., R. Kunitake, et al. (2001). "Attenuation of bleomycin-induced pneumopathy in mice by a caspase inhibitor." Am J Physiol Lung Cell Mol Physiol **280**(2): L316-325.
Kuwano, K., H. Miyazaki, et al. (1999). "The involvement of Fas-Fas ligand pathway in fibrosing lung diseases." Am J Respir Cell Mol Biol **20**(1): 53-60.

Lappalainen, U., J. A. Whitsett, et al. (2005). "Interleukin-1beta causes pulmonary inflammation, emphysema, and airway remodeling in the adult murine lung." Am J Respir Cell Mol Biol **32**(4): 311-318.
Lasky, J. A. and A. R. Brody (2000). "Interstitial fibrosis and growth factors." Environ Health Perspect **108 Suppl 4**: 751-762.
Laurent, G. J., N. K. Harrison, et al. (1988). "The regulation of collagen production in normal lung and during interstitial lung disease." Postgrad Med J **64 Suppl 4**: 26-34.
Le, T. T., H. Karmouty-Quintana, et al. (2014). "Blockade of IL-6 Trans signaling attenuates pulmonary fibrosis." J Immunol **193**(7): 3755-3768.
Lee, C. G., R. J. Homer, et al. (2001). "Interleukin-13 induces tissue fibrosis by selectively stimulating and activating transforming growth factor beta(1)." J Exp Med **194**(6): 809-821.
Lee, C. M., J. W. Park, et al. (2014). "Modifiers of TGF-beta1 effector function as novel therapeutic targets of pulmonary fibrosis." Korean J Intern Med **29**(3): 281-290.
Lee, J. H., N. Kaminski, et al. (2001). "Interleukin-13 induces dramatically different transcriptional programs in three human airway cell types." Am J Respir Cell Mol Biol **25**(4): 474-485.
Lemjabbar, H., P. Gosset, et al. (1999). "Overexpression of alveolar macrophage gelatinase B (MMP-9) in patients with idiopathic pulmonary fibrosis: effects of steroid and immunosuppressive treatment." Am J Respir Cell Mol Biol **20**(5): 903-913.
Ley, B., K. K. Brown, et al. (2014). "Molecular biomarkers in idiopathic pulmonary fibrosis." Am J Physiol Lung Cell Mol Physiol **307**(9): L681-691.
Ley, B. and H. R. Collard (2013). "Epidemiology of idiopathic pulmonary fibrosis." Clin Epidemiol **5**: 483-492.
Ley, B., H. R. Collard, et al. (2011). "Clinical course and prediction of survival in idiopathic pulmonary fibrosis." Am J Respir Crit Care Med **183**(4): 431-440.
Li M, Krishnaveni MS, Li C, Zhou B, Xing Y, Banfalvi A, Li A, Lombardi V, Akbari O, Borok Z, et al (2011). "Epithelium-specific deletion of TGF-b receptor type II protects mice from bleomycin-induced pulmonary fibrosis." J Clin Invest 2011; 121:277–287
Li, Q., P.W. Park, et al. (2002). ''Matrilysin shedding of syndecan-1 regulates chemokine mobilization and transepithelial efflux of neutrophils in acute lung injury.''Cell 111(5):635-46
Li, X., R. Shu, et al. (2004). "Apoptosis in lung injury and remodeling." J Appl Physiol 97(4): 1535-1542.
Liang, L., J. Yu, et al. (2014). "Endothelin-1 stimulates proinflammatory cytokine expression in human periodontal ligament cells via mitogen-activated protein kinase pathway." J Periodontol 85(4): 618-626.
Limb, G. A., K. Matter, et al. (2005). "Matrix metalloproteinase-1 associates with intracellular organelles and confers resistance to lamin A/C degradation during apoptosis." Am J Pathol **166**(5): 1555-1563.
Lindner, D., C. Zietsch, et al. (2012). "Differential expression of matrix metalloproteases in human fibroblasts with different origins." Biochem Res Int **2012**: 875742.
Liu, L., B. Carron, et al. (2009). "Wnt pathway in pulmonary fibrosis in the bleomycin mouse model." J Environ Pathol Toxicol Oncol **28**(2): 99-108.
Liu, T., B. Brouha, et al. (2004). "Rapid induction of mitochondrial events and caspase-independent apoptosis in Survivin-targeted melanoma cells." Oncogene **23**(1): 39-48.
Livak, K. J. and T. D. Schmittgen (2001). "Analysis of relative gene expression data using real-time quantitative PCR and the 2(-Delta Delta C(T)) Method." Methods **25**(4): 402-408.
Loffek, S., O. Schilling, et al. (2011). "Series "matrix metalloproteinases in lung health and disease": Biological role of matrix metalloproteinases: a critical balance." Eur Respir J **38**(1): 191-208.
Los, M., M. Mozoluk, et al. (2002). "Activation and caspase-mediated inhibition of PARP: a molecular switch between fibroblast necrosis and apoptosis in death receptor signaling." Mol Biol Cell **13**(3): 978-988.

Lowrey, G. E., N. Henderson, et al. (2008). "MMP-9 protein level does not reflect overall MMP activity in the airways of patients with COPD." Respir Med **102**(6): 845-851.
Lung, M. L., W. K. Lam, et al. (1985). "Evidence that respiratory tract is major reservoir for Epstein-Barr virus." Lancet **1**(8434): 889-892.
Margadant, C., and Sonnenberg, A (2010). "Integrin-TGF-beta crosstalk in fibrosis, cancer and wound healing." EMBO Rep. 11, 97–105.
Maher, T. M., A. U. Wells, et al. (2007). "Idiopathic pulmonary fibrosis: multiple causes and multiple mechanisms?" Eur Respir J **30**(5): 835-839.
Manicone, A. M., I. Huizar, et al. (2009). "Matrilysin (Matrix Metalloproteinase-7) regulates anti-inflammatory and antifibrotic pulmonary dendritic cells that express CD103 (alpha(E)beta(7)-integrin)." Am J Pathol **175**(6): 2319-2331.

Manns, J., M. Daubrawa, et al. (2011). "Triggering of a novel intrinsic apoptosis pathway by the kinase inhibitor staurosporine: activation of caspase-9 in the absence of Apaf-1." FASEB J **25**(9): 3250-3261.
Manoury, B., S. Caulet-Maugendre, et al. (2006). "TIMP-1 is a key factor of fibrogenic response to bleomycin in mouse lung." Int J Immunopathol Pharmacol **19**(3): 471-487.
Mao, P., S. Wu, et al. (2015). "Human alveolar epithelial type II cells in primary culture." Physiol Rep **3**(2).
Markewitz, B. A., D. E. Kohan, et al. (1995). "Endothelin-1 synthesis, receptors, and signal transduction in alveolar epithelium: evidence for an autocrine role." Am J Physiol **268**(2 Pt 1): L192-200.
Marshall, R. P., P. Gohlke, et al. (2004). "Angiotensin II and the fibroproliferative response to acute lung injury." Am J Physiol Lung Cell Mol Physiol **286**(1): L156-164.
Martin, M. C., L. A. Allan, et al. (2005). "Protein kinase A regulates caspase-9 activation by Apaf-1 downstream of cytochrome c." J Biol Chem **280**(15): 15449-15455.
Martin, T. R., N. Hagimoto, et al. (2005). "Apoptosis and epithelial injury in the lungs." Proc Am Thorac Soc **2**(3): 214-220.
Masur, S. K., H. S. Dewal, et al. (1996). "Myofibroblasts differentiate from fibroblasts when plated at low density." Proc Natl Acad Sci U S A **93**(9): 4219-4223.
Mazzei, M. E., L. Richeldi, et al. (2015). "Nintedanib in the treatment of idiopathic pulmonary fibrosis." Ther Adv Respir Dis **9**(3): 121-129.
McCall, M. N., P. N. Murakami, et al. (2011). "Assessing affymetrix GeneChip microarray quality." BMC Bioinformatics **12**: 137.
McElroy, M. C. and M. Kasper (2004). "The use of alveolar epithelial type I cell-selective markers to investigate lung injury and repair." Eur Respir J **24**(4): 664-673.
McGuire, J. K., Q. Li, et al. (2003). "Matrilysin (matrix metalloproteinase-7) mediates E-cadherin ectodomain shedding in injured lung epithelium." Am J Pathol **162**(6): 1831-1843.
Mei, R., E. Hubbell, et al. (2003). "Probe selection for high-density oligonucleotide arrays." Proc Natl Acad Sci U S A **100**(20): 11237-11242.
Melchjorsen, J., H. Kristiansen, et al. (2009). "Differential regulation of the OASL and OAS1 genes in response to viral infections." J Interferon Cytokine Res **29**(4): 199-207.
Meltzer, E. B. and P. W. Noble (2008). "Idiopathic pulmonary fibrosis." Orphanet J Rare Dis **3**: 8.
Mio, T., Y. Adachi, et al. (1996). "Regulation of fibroblast proliferation in three-dimensional collagen gel matrix." In Vitro Cell Dev Biol Anim **32**(7): 427-433.
Moeller, A., K. Ask, et al. (2008). "The bleomycin animal model: a useful tool to investigate treatment options for idiopathic pulmonary fibrosis?" Int J Biochem Cell Biol **40**(3): 362-382.
Moll, S., M. Ebeling, et al. (2013). "Epithelial cells as active player in fibrosis: findings from an in vitro model." PLoS One **8**(2): e56575.
Moodley, Y. P., P. Caterina, et al. (2004). "Comparison of the morphological and biochemical changes in normal human lung fibroblasts and fibroblasts derived from lungs of patients with idiopathic pulmonary fibrosis during FasL-induced apoptosis." J Pathol **202**(4): 486-495.

Moodley, Y. P., N. L. Misso, et al. (2003). "Inverse effects of interleukin-6 on apoptosis of fibroblasts from pulmonary fibrosis and normal lungs." Am J Respir Cell Mol Biol **29**(4): 490-498.
Moodley, Y. P., A. K. Scaffidi, et al. (2003). "Fibroblasts isolated from normal lungs and those with idiopathic pulmonary fibrosis differ in interleukin-6/gp130-mediated cell signaling and proliferation." Am J Pathol **163**(1): 345-354.
Moore, B. B. and C. M. Hogaboam (2008). "Murine models of pulmonary fibrosis." Am J Physiol Lung Cell Mol Physiol **294**(2): L152-160.
Morey, J. S., J. C. Ryan, et al. (2006). "Microarray validation: factors influencing correlation between oligonucleotide microarrays and real-time PCR." Biol Proced Online **8**: 175-193.
Müller, L., M. Riediker et al. (2010). '' Oxidative stress and inflammation response after nanoparticle exposure: differences between human lung cell monocultures and an advanced three-dimensional model of the human epithelial airways.'' J R Soc Interface 7 Suppl 1:S27-40.
Myllärniemi M, Kaarteenaho R. (2015).''Pharmacological treatment of idiopathic pulmonary fibrosis - preclinical and clinical studies of pirfenidone, nintedanib, and N-acetylcysteine''. Eur Clin Respir J. 2015;2
Nagase, H., R. Visse, et al. (2006). "Structure and function of matrix metalloproteinases and TIMPs." Cardiovasc Res **69**(3): 562-573.
Nakagawa, S., P. Pawelek, et al. (1989). "Long-term culture of fibroblasts in contracted collagen gels: effects on cell growth and biosynthetic activity." J Invest Dermatol **93**(6): 792-798.
Nakamura, S., M. Naruse, et al. (1990). "Immunocytochemical localization of endothelin in cultured bovine endothelial cells." Histochemistry **94**(5): 475-477.
Nakashima, N., K. Kuwano, et al. (2005). "The p53-Mdm2 association in epithelial cells in idiopathic pulmonary fibrosis and non-specific interstitial pneumonia." J Clin Pathol **58**(6): 583-589.
Navaratnam, V., K. M. Fleming, et al. (2011). "The rising incidence of idiopathic pulmonary fibrosis in the U.K." Thorax **66**(6): 462-467.
Navaratnam, V., A. W. Fogarty, et al. (2014). "Presence of a prothrombotic state in people with idiopathic pulmonary fibrosis: a population-based case-control study." Thorax **69**(3): 207-215.
Nicholson, A. G., L. G. Fulford, et al. (2002). "The relationship between individual histologic features and disease progression in idiopathic pulmonary fibrosis." Am J Respir Crit Care Med **166**(2): 173-177.
Nishimura, S. L. (2009). "Integrin-mediated transforming growth factor-beta activation, a potential therapeutic target in fibrogenic disorders." Am J Pathol **175**(4): 1362-1370.
Ogushi, F., K. Tani, et al. (2001). "Autoantibodies to IL-1 alpha in sera from rapidly progressive idiopathic pulmonary fibrosis." J Med Invest **48**(3-4): 181-189.
Ohno, I., H. Ohtani, et al. (1997). "Eosinophils as a source of matrix metalloproteinase-9 in asthmatic airway inflammation." Am J Respir Cell Mol Biol **16**(3): 212-219.
Oppenheim, J. J., P. Tewary, et al. (2007). "Alarmins initiate host defense." Adv Exp Med Biol **601**: 185-194.
Oppenheim, J. J. and D. Yang (2005). "Alarmins: chemotactic activators of immune responses." Curr Opin Immunol **17**(4): 359-365.
Oritani, K., P. W. Kincade, et al. (2001). "Type I interferons and limitin: a comparison of structures, receptors, and functions." Cytokine Growth Factor Rev **12**(4): 337-348.
Pagano, A., C. Pitteloud, et al. (2005). "Poly(ADP-ribose)polymerase activation mediates lung epithelial cell death in vitro but is not essential in hyperoxia-induced lung injury." Am J Respir Cell Mol Biol **33**(6): 555-564.
Panettieri, R. A., Jr., R. G. Goldie, et al. (1996). "Endothelin-1-induced potentiation of human airway smooth muscle proliferation: an ETA receptor-mediated phenomenon." Br J Pharmacol **118**(1): 191-197.
Pardo, A. and M. Selman (1996). "Matrix metalloproteinases and lung injury." Braz J Med Biol Res **29**(9): 1109-1115.
Pardo, A. and M. Selman (2005). "MMP-1: the elder of the family." Int J Biochem Cell Biol **37**(2): 283-288.

Pardo, A. and M. Selman (2006). "Matrix metalloproteases in aberrant fibrotic tissue remodeling." Proc Am Thorac Soc **3**(4): 383-388.
Pardo, A., M. Selman, et al. (2008). "Approaching the degradome in idiopathic pulmonary fibrosis." Int J Biochem Cell Biol **40**(6-7): 1141-1155.
Park, S., C. Lee, et al. (2013). "GDE2 promotes neurogenesis by glycosylphosphatidylinositol-anchor cleavage of RECK." Science **339**(6117): 324-328.
Park, S. H., D. Saleh, et al. (1997). "Increased endothelin-1 in bleomycin-induced pulmonary fibrosis and the effect of an endothelin receptor antagonist." Am J Respir Crit Care Med **156**(2 Pt 1): 600-608.
Parks, W. C. (2003). "Matrix metalloproteinases in lung repair." Eur Respir J Suppl **44**: 36s-38s.
Parker MW, Rossi D, Peterson M, Smith K, Sikstro¨m K, White ES, Connett JE, Henke CA, Larsson O, Bitterman PB (2014). "Fibroticextracellular matrix activates a profibrotic positive feedback loop. J Clin Invest 124:1622–1635.
Pece, S. and J. S. Gutkind (2002). "E-cadherin and Hakai: signalling, remodeling or destruction?" Nat Cell Biol **4**(4): E72-74.
Peng, R., S. Sridhar, et al. (2013). "Bleomycin induces molecular changes directly relevant to idiopathic pulmonary fibrosis: a model for "active" disease." PLoS One **8**(4): e59348.
Phan, S. H. (2008). "Biology of fibroblasts and myofibroblasts." Proc Am Thorac Soc **5**(3): 334-337.
Phan, S. H. and S. L. Kunkel (1992). "Lung cytokine production in bleomycin-induced pulmonary fibrosis." Exp Lung Res **18**(1): 29-43.
Pilcher, B. K., J. A. Dumin, et al. (1997). "The activity of collagenase-1 is required for keratinocyte migration on a type I collagen matrix." J Cell Biol **137**(6): 1445-1457.
Plataki, M., A. V. Koutsopoulos, et al. (2005). "Expression of apoptotic and antiapoptotic markers in epithelial cells in idiopathic pulmonary fibrosis." Chest **127**(1): 266-274.
Pongracz, J. E. and R. A. Stockley (2006). "Wnt signalling in lung development and diseases." Respir Res **7**: 15.
Prasad, S., C. M. Hogaboam, et al. (2014). "Deficient repair response of IPF fibroblasts in a co-culture model of epithelial injury and repair." Fibrogenesis Tissue Repair **7**: 7.
Prasse, A., D. V. Pechkovsky, et al. (2006). "A vicious circle of alveolar macrophages and fibroblasts perpetuates pulmonary fibrosis via CCL18." Am J Respir Crit Care Med **173**(7): 781-792.
Puthawala, K., N. Hadjiangelis, et al. (2008). "Inhibition of integrin alpha(v)beta6, an activator of latent transforming growth factor-beta, prevents radiation-induced lung fibrosis." Am J Respir Crit Care Med **177**(1): 82-90.
Rackley, C. R. and B. R. Stripp (2012). "Building and maintaining the epithelium of the lung." J Clin Invest **122**(8): 2724-2730.
Raghu, G., K. J. Anstrom, et al. (2012). "Prednisone, azathioprine, and N-acetylcysteine for pulmonary fibrosis." N Engl J Med **366**(21): 1968-1977.
Raghu, G., S. Y. Chen, et al. (2014). "Idiopathic pulmonary fibrosis in US Medicare beneficiaries aged 65 years and older: incidence, prevalence, and survival, 2001-11." Lancet Respir Med **2**(7): 566-572.
Raghu, G., H. R. Collard, et al. (2011). "An official ATS/ERS/JRS/ALAT statement: idiopathic pulmonary fibrosis: evidence-based guidelines for diagnosis and management." Am J Respir Crit Care Med **183**(6): 788-824.
Raghu, G. and M. Selman (2015). "Nintedanib and pirfenidone. New antifibrotic treatments indicated for idiopathic pulmonary fibrosis offer hopes and raises questions." Am J Respir Crit Care Med **191**(3): 252-254.
Ramji, D. P. and P. Foka (2002). "CCAAT/enhancer-binding proteins: structure, function and regulation." Biochem J **365**(Pt 3): 561-575.
Ramos, C., M. Montano, et al. (2001). "Fibroblasts from idiopathic pulmonary fibrosis and normal lungs differ in growth rate, apoptosis, and tissue inhibitor of metalloproteinases expression." Am J Respir Cell Mol Biol **24**(5): 591-598.
Renzoni, E. A., D. J. Abraham, et al. (2004). "Gene expression profiling reveals novel TGFbeta targets in adult lung fibroblasts." Respir Res **5**: 24.
Rincon, M. and C. G. Irvin (2012). "Role of IL-6 in asthma and other inflammatory pulmonary diseases." Int J Biol Sci **8**(9): 1281-1290.

Risinger, G. M., Jr., D. L. Updike, et al. (2010). "TGF-beta suppresses the upregulation of MMP-2 by vascular smooth muscle cells in response to PDGF-BB." Am J Physiol Cell Physiol **298**(1): C191-201.
Rizzitelli, A., S. Meuter, et al. (2012). "Serpinb9 (Spi6)-deficient mice are impaired in dendritic cell-mediated antigen cross-presentation." Immunol Cell Biol **90**(9): 841-851.
Rosas, I. O., T. J. Richards, et al. (2008). "MMP1 and MMP7 as potential peripheral blood biomarkers in idiopathic pulmonary fibrosis." PLoS Med **5**(4): e93.
Rose-John, S., J. Scheller, et al. (2006). "Interleukin-6 biology is coordinated by membrane-bound and soluble receptors: role in inflammation and cancer." J Leukoc Biol **80**(2): 227-236.
Rosenberg, E. (1996). "The 1995 update of recommendations for a standard technique for measuring the single-breath carbon monoxide diffusing capacity (transfer factor)." Am J Respir Crit Care Med **154**(3 Pt 1): 827-828.
Ruszczak, Z. (2003). "Effect of collagen matrices on dermal wound healing." Adv Drug Deliv Rev **55**(12): 1595-1611.
Sadler, A. J. and B. R. Williams (2008). "Interferon-inducible antiviral effectors." Nat Rev Immunol **8**(7): 559-568.
Saito, F., S. Tasaka, et al. (2008). "Role of interleukin-6 in bleomycin-induced lung inflammatory changes in mice." Am J Respir Cell Mol Biol **38**(5): 566-571.
Sakai, N. and A. M. Tager (2013). "Fibrosis of two: Epithelial cell-fibroblast interactions in pulmonary fibrosis." Biochim Biophys Acta **1832**(7): 911-921.
Sakamaki, K. and Y. Satou (2009). "Caspases: evolutionary aspects of their functions in vertebrates." J Fish Biol **74**(4): 727-753.
Sansone, P. and J. Bromberg (2012). "Targeting the interleukin-6/Jak/stat pathway in human malignancies." J Clin Oncol **30**(9): 1005-1014.
Santiago, B., M. Galindo, et al. (2004). "Intracellular regulation of Fas-induced apoptosis in human fibroblasts by extracellular factors and cycloheximide." J Immunol **172**(1): 560-566.
Sartori, C. and M. A. Matthay (2002). "Alveolar epithelial fluid transport in acute lung injury: new insights." Eur Respir J **20**(5): 1299-1313.
Sato, A., Y. Xu, et al. (2012). "CCAAT/enhancer binding protein-alpha regulates the protease/antiprotease balance required for bronchiolar epithelium regeneration." Am J Respir Cell Mol Biol **47**(4): 454-463.
Sayeed, A., G. Luciani-Torres, et al. (2013). "Aberrant Regulation of the BST2 (Tetherin) Promoter Enhances Cell Proliferation and Apoptosis Evasion in High Grade Breast Cancer Cells." PLoS One **8**(6): e67191.
Schuliga, M. J., I. See, et al. (2009). "Fibrillar collagen clamps lung mesenchymal cells in a nonproliferative and noncontractile phenotype." Am J Respir Cell Mol Biol **41**(6): 731-741.
Schwarze, P. E., A. I. Totlandsdal, et al. (2013). "Inflammation-related effects of diesel engine exhaust particles: studies on lung cells in vitro." Biomed Res Int **2013**: 685142.
Scotton, C. J. and R. C. Chambers (2007). "Molecular targets in pulmonary fibrosis: the myofibroblast in focus." Chest **132**(4): 1311-1321.
Scotton CJ, Chambers RC (2010). Bleomycin revisited: towards a more representative model of IPF?'' Am J Physiol Lung Cell Mol Physiol. 299: L439–41.
Dancer, M., T. E. King, et al. (2001). "Idiopathic pulmonary fibrosis: prevailing and evolving hypotheses about its pathogenesis and implications for therapy." Ann Intern Med **134**(2): 136-151.
Selman, M. and A. Pardo (2002). "Idiopathic pulmonary fibrosis: an epithelial/fibroblastic cross-talk disorder." Respir Res **3**: 3.
Selman, M. and A. Pardo (2004). "Idiopathic pulmonary fibrosis: misunderstandings between epithelial cells and fibroblasts?" Sarcoidosis Vasc Diffuse Lung Dis **21**(3): 165-172.
Selman, M. and A. Pardo (2006). "Role of epithelial cells in idiopathic pulmonary fibrosis: from innocent targets to serial killers." Proc Am Thorac Soc **3**(4): 364-372.
Selman, M. and A. Pardo (2014). "Revealing the pathogenic and aging-related mechanisms of the enigmatic idiopathic pulmonary fibrosis. an integral model." Am J Respir Crit Care Med **189**(10): 1161-1172.

Selman, M., A. Pardo, et al. (2006). "Gene expression profiles distinguish idiopathic pulmonary fibrosis from hypersensitivity pneumonitis." Am J Respir Crit Care Med **173**(2): 188-198.
Selman, M., V. Ruiz, et al. (2000). "TIMP-1, -2, -3, and -4 in idiopathic pulmonary fibrosis. A prevailing nondegradative lung microenvironment?" Am J Physiol Lung Cell Mol Physiol **279**(3): L562-574.
Sempowski, G. D., S. Derdak, et al. (1996). "Interleukin-4 and interferon-gamma discordantly regulate collagen biosynthesis by functionally distinct lung fibroblast subsets." J Cell Physiol **167**(2): 290-296.
Serrano-Mollar, A. (2012). "[Alveolar epithelial cell injury as an etiopathogenic factor in pulmonary fibrosis]." Arch Bronconeumol **48 Suppl 2**: 2-6.
Sheppard, D. (2006). "Transforming growth factor beta: a central modulator of pulmonary and airway inflammation and fibrosis." Proc Am Thorac Soc **3**(5): 413-417.
Shi-Wen, X., C. P. Denton, et al. (2001). "Fibroblast matrix gene expression and connective tissue remodeling: role of endothelin-1." J Invest Dermatol **116**(3): 417-425.
Shi, W., J. Xu, et al. (2009). "Development, repair and fibrosis: what is common and why it matters." Respirology **14**(5): 656-665.
Shimbori, C., J. Gauldie, et al. (2013). "Extracellular matrix microenvironment contributes actively to pulmonary fibrosis." Curr Opin Pulm Med **19**(5): 446-452.
Singer, II, D. W. Kawka, et al. (1986). "Extensive laminin and basement membrane accumulation occurs at the onset of bleomycin-induced rodent pulmonary fibrosis." Am J Pathol **125**(2): 258-268.
Singh, S. R. and I. P. Hall (2008). "Airway myofibroblasts and their relationship with airway myocytes and fibroblasts." Proc Am Thorac Soc **5**(1): 127-132.
Sisson, T. H., T. M. Maher, et al. (2012). "Increased survivin expression contributes to apoptosis-resistance in IPF fibroblasts." Adv Biosci Biotechnol **3**(6A): 657-664.
Solovyan, V. T. and J. Keski-Oja (2006). "Proteolytic activation of latent TGF-beta precedes caspase-3 activation and enhances apoptotic death of lung epithelial cells." J Cell Physiol **207**(2): 445-453.
Spagnolo, P., G. Rossi, et al. (2014). "Pathogenesis of idiopathic pulmonary fibrosis and its clinical implications." Expert Rev Clin Immunol **10**(8): 1005-1017.
Spagnolo, P., N. Sverzellati, et al. (2015). "Idiopathic pulmonary fibrosis: an update." Ann Med **47**(1): 15-27.
Sporty, J. L., L. Horalkova, et al. (2008). "In vitro cell culture models for the assessment of pulmonary drug disposition." Expert Opin Drug Metab Toxicol **4**(4): 333-345.
Stamenkovic, I. (2003). "Extracellular matrix remodelling: the role of matrix metalloproteinases." J Pathol **200**(4): 448-464.
Stewart, G. A., G. F. Hoyne, et al. (2003). "Expression of the developmental Sonic hedgehog (Shh) signalling pathway is up-regulated in chronic lung fibrosis and the Shh receptor patched 1 is present in circulating T lymphocytes." J Pathol **199**(4): 488-495.
Stommel, J. M. and G. M. Wahl (2005). "A new twist in the feedback loop: stress-activated MDM2 destabilization is required for p53 activation." Cell Cycle **4**(3): 411-417.
Studer, S. M. and N. Kaminski (2007). "Towards systems biology of human pulmonary fibrosis." Proc Am Thorac Soc **4**(1): 85-91.
Suga, M., K. Iyonaga, et al. (1999). "Clinical significance of MCP-1 levels in BALF and serum in patients with interstitial lung diseases." Eur Respir J **14**(2): 376-382.
Suga, M., K. Iyonaga, et al. (2000). "Characteristic elevation of matrix metalloproteinase activity in idiopathic interstitial pneumonias." Am J Respir Crit Care Med **162**(5): 1949-1956.
Suwara, M. I., N. J. Green, et al. (2014). "IL-1alpha released from damaged epithelial cells is sufficient and essential to trigger inflammatory responses in human lung fibroblasts." Mucosal Immunol **7**(3): 684-693.
Swiecki, M., Y. Wang, et al. (2012). "Cutting edge: paradoxical roles of BST2/tetherin in promoting type I IFN response and viral infection." J Immunol **188**(6): 2488-2492.

Swigris, J. J. and K. K. Brown (2010). "The role of endothelin-1 in the pathogenesis of idiopathic pulmonary fibrosis." BioDrugs **24**(1): 49-54.
Tamai, K., T. Yamazaki, et al. (2011). "PDGFRalpha-positive cells in bone marrow are mobilized by high mobility group box 1 (HMGB1) to regenerate injured epithelia." Proc Natl Acad Sci U S A **108**(16): 6609-6614.
Tan, R. J., C. L. Fattman, et al. (2006). "Matrix metalloproteinases promote inflammation and fibrosis in asbestos-induced lung injury in mice." Am J Respir Cell Mol Biol **35**(3): 289-297.
Tanjore, H., X. C. Xu, et al. (2009). "Contribution of epithelial-derived fibroblasts to bleomycin-induced lung fibrosis." Am J Respir Crit Care Med **180**(7): 657-665.
Taskar, V. S. and D. B. Coultas (2006). "Is idiopathic pulmonary fibrosis an environmental disease?" Proc Am Thorac Soc **3**(4): 293-298.
Tatler, A. L. and G. Jenkins (2012). "TGF-beta activation and lung fibrosis." Proc Am Thorac Soc **9**(3): 130-136.
Thannickal, V. J., G. B. Toews, et al. (2004). "Mechanisms of pulmonary fibrosis." Annu Rev Med **55**: 395-417.
Tobin, R. W., C. E. Pope, 2nd, et al. (1998). "Increased prevalence of gastroesophageal reflux in patients with idiopathic pulmonary fibrosis." Am J Respir Crit Care Med **158**(6): 1804-1808.
Todd, N. W., I. G. Luzina, et al. (2012). "Molecular and cellular mechanisms of pulmonary fibrosis." Fibrogenesis Tissue Repair **5**(1): 11.
Tracy, E. C., M. J. Bowman, et al. (2012). "Interleukin-1alpha is the major alarmin of lung epithelial cells released during photodynamic therapy to induce inflammatory mediators in fibroblasts." Br J Cancer **107**(9): 1534-1546.
Trelstad, R. L., A. Hayashi, et al. (1982). "The epithelial-mesenchymal interface of the male rate Mullerian duct: loss of basement membrane integrity and ductal regression." Dev Biol **92**(1): 27-40.
Trinchieri, G. (2010). "Type I interferon: friend or foe?" J Exp Med **207**(10): 2053-2063.
Tsukamoto, K., H. Hayakawa, et al. (2000). "Involvement of Epstein-Barr virus latent membrane protein 1 in disease progression in patients with idiopathic pulmonary fibrosis." Thorax **55**(11): 958-961.
Tsuno, T., J. Mejido, et al. (2009). "IRF9 is a key factor for eliciting the antiproliferative activity of IFN-alpha." J Immunother **32**(8): 803-816.
Ueno, M., T. Maeno, et al. (2011). "Hypoxia-inducible factor-1alpha mediates TGF-beta-induced PAI-1 production in alveolar macrophages in pulmonary fibrosis." Am J Physiol Lung Cell Mol Physiol **300**(5): L740-752.
Uhal, B. D. (2008). "The role of apoptosis in pulmonary fibrosis." European Respiratory Review **109**(17): 138-144.
Uhal, B. D., I. Joshi, et al. (1998). "Alveolar epithelial cell death adjacent to underlying myofibroblasts in advanced fibrotic human lung." Am J Physiol **275**(6 Pt 1): L1192-1199.
Umezawa, H., M. Ishizuka, et al. (1967). "Studies on bleomycin." Cancer **20**(5): 891-895.
Ungvari, I., E. Hadadi, et al. (2012). "Implication of BIRC5 in asthma pathogenesis." Int Immunol **24**(5): 293-301.
Urich, D., S. Soberanes, et al. (2009). "Proapoptotic Noxa is required for particulate matter-induced cell death and lung inflammation." FASEB J **23**(7): 2055-2064.
Vallyathan, V., X. L. Shi, et al. (1988). "Generation of free radicals from freshly fractured silica dust. Potential role in acute silica-induced lung injury." Am Rev Respir Dis **138**(5): 1213-1219.
van Wetering, S., P. J. Sterk, et al. (1999). "Defensins: key players or bystanders in infection, injury, and repair in the lung?" J Allergy Clin Immunol **104**(6): 1131-1138.
Verrecchia, F., Chu, M. L., and Mauviel, A (2001). "Identification of novel TGF-beta/Smad gene targets in dermal fibroblasts using a combined cDNA microarray/promoter transactivation approach." J. Biol. Chem. 276, 17058–17062.
Vij, R. and I. Noth (2012). "Peripheral blood biomarkers in idiopathic pulmonary fibrosis." Transl Res **159**(4): 218-227.

Wadsworth, S. J., H. S. Nijmeh, et al. (2006). "Glucocorticoids increase repair potential in a novel in vitro human airway epithelial wounding model." J Clin Immunol **26**(4): 376-387.
Walters, D. M., H. Y. Cho, et al. (2008). "Oxidative stress and antioxidants in the pathogenesis of pulmonary fibrosis: a potential role for Nrf2." Antioxid Redox Signal **10**(2): 321-332.
Walton KL, Johnson KE, Harrison CA (2017). "Targeting TGF-β Mediated SMAD Signaling for the Prevention of Fibrosis." Front Pharmacol 14;8:461
Wang, G. L., X. Shi, et al. (2006). "Cyclin D3 maintains growth-inhibitory activity of C/EBPalpha by stabilizing C/EBPalpha-cdk2 and C/EBPalpha-Brm complexes." Mol Cell Biol **26**(7): 2570-2582.
Ward, P. A. and G. W. Hunninghake (1998). "Lung inflammation and fibrosis." Am J Respir Crit Care Med **157**(4 Pt 2): S123-129.
Warner, R. L., N. Bhagavathula, et al. (2004). "Matrix metalloproteinases in acute inflammation: induction of MMP-3 and MMP-9 in fibroblasts and epithelial cells following exposure to pro-inflammatory mediators in vitro." Exp Mol Pathol **76**(3): 189-195.
Williamson, J. D., L. R. Sadofsky, et al. (2015). "The pathogenesis of bleomycin-induced lung injury in animals and its applicability to human idiopathic pulmonary fibrosis." Exp Lung Res **41**(2): 57-73.
Willis BC, Borok Z (2007). "TGF-b-induced EMT: mechanisms and implications for fibrotic lung disease." Am J Physiol Lung Cell Mol Physiol 293:L525–L534.

Willis, B. C., J. M. Liebler, et al. (2005). "Induction of epithelial-mesenchymal transition in alveolar epithelial cells by transforming growth factor-beta1: potential role in idiopathic pulmonary fibrosis." Am J Pathol **166**(5): 1321-1332.
Wilson, M. S. and T. A. Wynn (2009). "Pulmonary fibrosis: pathogenesis, etiology and regulation." Mucosal Immunol **2**(2): 103-121.
Wollin, L., I. Maillet, et al. (2014). "Antifibrotic and anti-inflammatory activity of the tyrosine kinase inhibitor nintedanib in experimental models of lung fibrosis." J Pharmacol Exp Ther **349**(2): 209-220.
Wollin, L., E. Wex, et al. (2015). "Mode of action of nintedanib in the treatment of idiopathic pulmonary fibrosis." Eur Respir J **45**(5): 1434-1445.
Wynn, T. A. (2008). "Cellular and molecular mechanisms of fibrosis." J Pathol **214**(2): 199-210.
Wynn, T. A. (2011). "Integrating mechanisms of pulmonary fibrosis." J Exp Med **208**(7): 1339-1350.
Xu, J., R. C. Benyon, et al. (2002). "Matrix metalloproteinase-2 from bronchial epithelial cells induces the proliferation of subepithelial fibroblasts." Clin Exp Allergy **32**(6): 881-888.
Xu, M. Y., J. Porte, et al. (2009). "Lysophosphatidic acid induces alphavbeta6 integrin-mediated TGF-beta activation via the LPA2 receptor and the small G protein G alpha(q)." Am J Pathol **174**(4): 1264-1279.
Yaguchi, T., Y. Fukuda, et al. (1998). "Immunohistochemical and gelatin zymography studies for matrix metalloproteinases in bleomycin-induced pulmonary fibrosis." Pathol Int **48**(12): 954-963.
Yamashita, C. M., L. Dolgonos, et al. (2011). "Matrix metalloproteinase 3 is a mediator of pulmonary fibrosis." Am J Pathol **179**(4): 1733-1745.
Yang, D., P. Tewary, et al. "The alarmin functions of high-mobility group proteins." Biochim Biophys Acta **1799**(1-2): 157-163.
Yang, G., Y. Xu, et al. (2007). "IFITM1 plays an essential role in the antiproliferative action of interferon-gamma." Oncogene **26**(4): 594-603.
Yang, I. V. (2012). "Epigenomics of idiopathic pulmonary fibrosis." Epigenomics **4**(2): 195-203.
Yang, Y. H. and T. Speed (2002). "Design issues for cDNA microarray experiments." Nat Rev Genet **3**(8): 579-588.
Yao, P. M., H. Lemjabbar, et al. (1999). "Balance between MMP-9 and TIMP-1 expressed by human bronchial epithelial cells: relevance to asthma." Ann N Y Acad Sci **878**: 512-514.
Yap, A. S., W. M. Brieher, et al. (1997). "Molecular and functional analysis of cadherin-based adherens junctions." Annu Rev Cell Dev Biol **13**: 119-146.

Yuan, W., and Varga, J. (2001). "Transforming growth factor-beta repression of matrix metalloproteinase-1 in dermal fibroblasts involves Smad3." J. Biol. Chem. 276, 38502–38510.

Zavadil, J. and E. P. Bottinger (2005). "TGF-beta and epithelial-to-mesenchymal transitions." Oncogene **24**(37): 5764-5774.

Zhang, K., M. D. Rekhter, et al. (1994). "Myofibroblasts and their role in lung collagen gene expression during pulmonary fibrosis. A combined immunohistochemical and in situ hybridization study." Am J Pathol **145**(1): 114-125.

Zhou, B., Y. Liu, et al. (2012). "Interactions between beta-catenin and transforming growth factor-beta signaling pathways mediate epithelial-mesenchymal transition and are dependent on the transcriptional co-activator cAMP-response element-binding protein (CREB)-binding protein (CBP)." J Biol Chem **287**(10): 7026-7038.

Zhou, L. F., L. Jiang, et al. (2010). "[Change of matrix metalloproteinase-1 and matrix metalloproteinase-7 in serum and bronchoalveolar lavage fluid of patients with idiopathic pulmonary fibrosis and sarcoidosis]." Zhonghua Jie He He Hu Xi Za Zhi **33**(6): 441-444.

Zhou, Y., J. S. Hagood, et al. (2010). "Thy-1-integrin alphav beta5 interactions inhibit lung fibroblast contraction-induced latent transforming growth factor-beta1 activation and myofibroblast differentiation." J Biol Chem **285**(29): 22382-22393.

Zhou, Y., J. Y. Lee, et al. (2012). "Amphiregulin, an epidermal growth factor receptor ligand, plays an essential role in the pathogenesis of transforming growth factor-beta-induced pulmonary fibrosis." J Biol Chem **287**(50): 41991-42000.

Zhou, W. and Wang, Y. (2016) ''Candidate genes of idiopathic pulmonary fibrosis: current evidence and research.'' Appl Clin Genet 2;9:5-13.

Zuo, F., N. Kaminski, et al. (2002). "Gene expression analysis reveals matrilysin as a key regulator of pulmonary fibrosis in mice and humans." Proc Natl Acad Sci U S A **99**(9): 6292-6297.